Meiotic Regulation of Cyclin-Dependent Kinases

by

Matthew P. Miller

B.A. Biology
Carleton College, 2001

SUBMITTED TO THE DEPARTMENT OF BIOLOGY IN PARTIAL FULFILLMENT OF THE REQUIREMENTS FOR THE DEGREE OF

DOCTOR OF PHILOSOPHY IN BIOLOGY
AT THE
MASSACHUSETTS INSTITUTE OF TECHNOLOGY

FEBRUARY 2013

Signature of the Author: _____

Department of Biology
December 4, 2012

Certified by: _____

Dr. Angelika Amon
Professor of Biology
Thesis Supervisor

Accepted by: _____

Dr. Stephen P. Bell
Professor of Biology
Chair, Biology Graduate Committee

Meiotic Regulation of Cyclin-Dependent Kinases

by

Matthew P. Miller

Submitted to the Department of Biology
On December 4, 2012 in Partial Fulfillment of the
Requirements for the Degree of Doctor of Philosophy in Biology

ABSTRACT

During meiosis, a single round of DNA replication is followed by two consecutive rounds of nuclear divisions called meiosis I and meiosis II. In meiosis I, homologous chromosomes segregate, while sister chromatids remain together. Determining how this unusual chromosome segregation behavior is established is central to understanding germ cell development. Here we show that preventing microtubule-kinetochore interactions during premeiotic S phase and prophase I is essential for establishing the meiosis I chromosome segregation pattern. Premature interactions of kinetochores with microtubules transform meiosis I into a mitosis-like division by disrupting two key meiosis I events: coorientation of sister kinetochores and protection of centromeric cohesin removal from chromosomes. Furthermore we find that restricting outer kinetochore assembly contributes to preventing premature engagement of microtubules with kinetochores. We propose that inhibition of microtubule-kinetochore interactions during premeiotic S phase and prophase I is central to establishing the unique meiosis I chromosome segregation pattern.

Thesis Supervisor: Angelika Amon
Title: Professor of Biology

ACKNOWLEDGEMENTS

First, I would like to thank my advisor Angelika. Her hard work, passion and intelligence are truly inspiring. I have learned so much during my time in her lab, both scientifically and about myself. Her door was always open and she was always willing to intellectually engage with me about my science. She has taught me that you always need to ask the tough question and be your own harshest critic, lessons that I will certainly carry with me throughout my career.

I am greatly appreciative to my thesis committee, Frank Solomon and Steve Bell, for your input and interest in my science, but mostly for your advice throughout the years. I would also like to thank Andrew Murray for participating in my thesis defense.

I would like to thank a number of classmates and members of the lab, current and past, who have made the last number of years fun, challenging and rewarding. Michelle, for always being there to talk about science and about life. Elçin, for being an amazing colleague and friend. Gloria and Leon for your friendship and for mentoring me as a young student with countless hours of guidance and discussion. Jeremy, Bryce and Justin for being great friends and always willing to engage in my life. Ana, for your 'surprisingly' mature advice and moral support. Jake, for always helping me to look to the future. Luke, for our many serious conversations about life. Thomas, for helping me do the things that I love to do outside of lab. Folkert and Alexi, for always laughing with me. Nina, Heather and Luke, for always dragging me out and simply for being there for me throughout the years. You all have enriched my life in more ways than I can count.

Finally, I am forever thankful of my family. To my parents, Laura and Mike, to my brothers, Andy, Joey and Jonny, and especially to my wife, Shannon. Your unconditional love and support have shaped who I am today. Your love, willingness to listen and encouragement have helped me through past challenges and will allow me to overcome any that I meet in the future.

Shannon, I could not have made it through the last number of years without you by my side. Thank you for everything.

TABLE OF CONTENTS

Chapter 1:

Introduction

Types of Cell Division

The maintenance of cellular and organismal fitness requires the proper partitioning of genetic material during cell division. The two types of eukaryotic cell divisions, mitosis and meiosis, use common, as well as unique mechanisms to ensure accurate chromosome segregation. In mitosis, alternating rounds of DNA replication and chromosome segregation preserves the chromosome complement of the original cell. On the other hand, sexually reproducing organisms use a specialized form of cell division, termed meiosis, for the production of gametes (Figure 1). The goal of meiosis is to reduce the chromosome complement by half, such that, upon fusion of gametes, the original ploidy of the organism is restored in the zygote. A central question in sexually reproducing organisms is how to form haploid gametes from diploid progenitor cells. This feat is accomplished during the specialized meiotic cell division, in which a single round of DNA replication is followed by two consecutive rounds of nuclear division called meiosis I and meiosis II. The resulting gametes have half the genomic complement of the progenitor cell. Meiosis also results in the production of new combinations of alleles in the gametes, which promotes genetic diversity of the offspring. This chapter will discuss a number of concepts related to cell division. First, the role and regulation of cyclin-dependent kinases. Second the concept and mechanism of chromosome segregation, and third, a more detailed discussion of the meiotic program in the budding yeast, *Saccharomyces cerevisiae*.

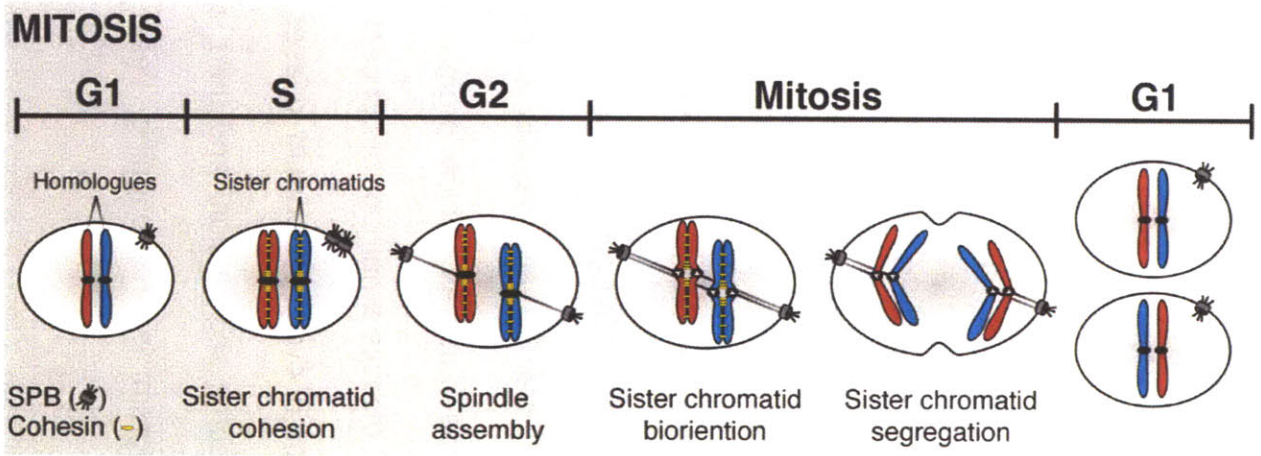
MITOSIS
G1
S
G2
Mitosis
G1
Homologues
Sister chromatids
SPB (●)
Cohesin (–)
Sister chromatid cohesion
Spindle assembly
Sister chromatid biorientation
Sister chromatid segregation

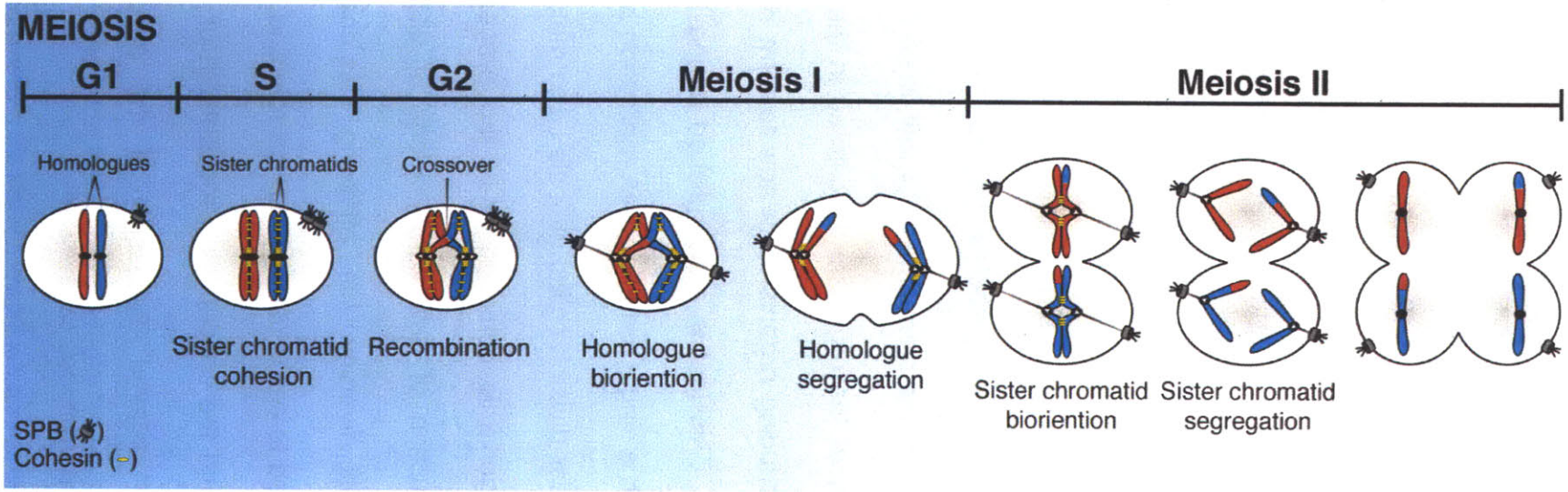
MEIOSIS
G1
S
G2
Meiosis I
Meiosis II
Homologues
Sister chromatids
Crossover
SPB (●)
Cohesin (–)
Sister chromatid cohesion
Recombination
Homologue biorientation
Homologue segregation
Sister chromatid biorientation
Sister chromatid segregation

Figure 1. Mitotic chromosome segregation versus meiotic chromosome segregation.

(top) During mitotic cell division, cohesin complexes (yellow) are loaded onto chromosomes in S phase, and provide physical linkage between sister chromatids. During metaphase sister chromatids biorient on the spindle (gray lines), and during anaphase sister chromatids segregate to opposite poles. (bottom) During meiotic cell division, cohesin complexes (yellow) are loaded onto chromosomes in pre-meiotic S phase. During meiotic prophase I, homologous chromosomes become physically linked through recombination. Homologous chromosomes are segregated away from each other during meiosis I, and sister chromatids are segregated away from each other during meiosis II.

Cyclin-Dependent Kinases – The Engines of Cell Division

The central components of cell cycle control and the major drivers of both the mitotic and meiotic cell division programs are cyclin-dependent kinases (CDKs). CDKs are serine/threonine kinases whose activity is dependent on their association with an activating subunit known as a cyclin. The oscillating activities of various cyclin-CDKs are the major drivers of many processes during cell division. For this reason, the proper control of cyclin-CDK activity is essential to ensure the proper timing of cell cycle events. The following section will discuss the regulation of CDKs as well as the cell cycle processes that are mediated by CDK activity in budding yeast mitosis and meiosis.

Regulation of cyclin-dependent kinases in yeast

Cyclin-dependent kinases in budding yeast consist of a single CDK, Cdc28 (or Cdk1). Cdc28 was first identified by Hartwell in the pioneering genetic screen for genes that control the cell division cycle in budding yeast (Hartwell, 1974; Hartwell, Mortimer, Culotti, & Culotti, 1973). CDKs are proline-directed serine and threonine kinases whose consensus target sequence is S/T-P-x-K/R, but these kinases also phosphorylate the minimal consensus sequence of S/T-P (Nigg, 1993). Cdc28 associates with and is activated by nine different cyclins, either by three G1 cyclins (Cln1-3) or by six B-type cyclins (Clb1-6). Structural work with mammalian Cdk2 revealed that binding of Cyclin A activates the kinase by inducing a large conformational change in the conserved PSTAIRE helix and T-loop. These conformational changes result in aligning active site residues and removing the T-loop, which otherwise sterically blocks the entrance of the catalytic cleft (Jeffrey et al., 1995; Pavletich, 1999). Cyclin binding results in basal kinase activity, while the phosphorylation of a threonine residue in the conserved T-loop by CDK-activating kinase (CAK) results in full activity (Mendenhall & Hodge, 1998).

During the cell cycle, cyclin-CDK activity is predominantly determined by cyclin protein levels, regulated by the balance of synthesis and degradation of the cyclin subunit. As such, a crucial mechanism for CDK regulation is at the level of cyclin transcription during the cell cycle. An additional layer of CDK regulation is mediated by CDK inhibitors (CKIs), which will be discussed in more detail in a

subsequent section. In budding yeast, transcription of *CLN3* peaks in late M-early G1 while *CLN1* and *CLN2* peak during G1-S (Hadwiger, Wittenberg, Richardson, de Barros Lopes, & Reed, 1989; Nash et al., 2001). *CLB5* and *CLB6* also peak at G1-S (Schwob & Nasmyth, 1993), followed by transcription of *CLB3* and *CLB4* near the beginning of S phase and finally *CLB1* and *CLB2* are transcribed during G2 and mitosis (Ghiara et al., 1991; Richardson, Lew, Henze, Sugimoto, & Reed, 1992; Surana et al., 1991).

Cyclins are also regulated at the level of degradation via ubiquitin-mediated degradation by the 26S proteasome. The specificity of different ubiquitin ligases for the different cyclins composes an important level of cyclin-CDK regulation during the cell cycle. Cln1 and Cln2 are targeted for degradation by the ubiquitin ligase SCF in complex with a substrate binding factor Grr1 (Barral, Jentsch, & Mann, 1995; Skowyra, Craig, Tyers, Elledge, & Harper, 1997), while SCF^{Cdc4} mediates degradation of Clb6. The adaptor protein for Cln3 is unknown but the degradation of Cln3 is also dependent on the SCF (Jackson, Reed, & Haase, 2006). A different ubiquitin ligase, the APC/C, promotes the degradation of Clb1, Clb2, Clb3 and Clb5. APC/C^{Cdc20} targets Clb5 and a subset of Clb2 for degradation at the metaphase to anaphase transition, while APC/C^{Cdh1} mediates degradation of Clb1, Clb3 and the remainder of Clb2 at mitotic exit (Irniger & Nasmyth, 1997; Schwab, Neutzner, Mocker, & Seufert, 2001; Shirayama, Toth, Galova, & Nasmyth, 1999). Clb4 is targeted for degradation by an unknown E3 ubiquitin ligase. The synthesis and degradation

cycles of the various cyclins provides the primary control of oscillations of CDK activity that drive the cell cycle. Degradation, in particular, results in non-reversible decisions as cells progress through cell division (Figure 2).

The regulation of cyclin synthesis and degradation is modulated during the meiotic cell divisions, and these changes are essential for proper progression through the meiotic program. First, the meiosis-specific kinase, Ime2, substitutes for G1 cyclin-dependent kinases to promote progression into premeiotic S-phase as the G1 cyclins are not expressed during entry into the meiotic program (Benjamin, Zhang, Shokat, & Herskowitz, 2003; Dirick, Goetsch, Ammerer, & Byers, 1998). Second, the major mitotic cyclin, Clb2, is not expressed during meiosis and the expression of the M phase cyclins, Clb1, Clb3 and Clb4 are placed under control of the meiosis-specific transcription factor *NDT80* (Figure 2) (Benjamin et al., 2003; Chu et al., 1998; Chu & Herskowitz, 1998; Dahmann & Futcher, 1995; Hepworth, Friesen, & Segall, 1998; L. Xu, Ajimura, Padmore, Klein, & Kleckner, 1995). These changes are mediated by targeted degradation of the mitosis specific transcriptional co-activator, Ndd1, during meiotic prophase I (Okaz et al., 2012). This regulation is important to maintain proper timing of meiotic events. In cells where Ndd1 is not properly degraded during prophase I, premature expression of M phase cyclins and Cdc5 result in defects in synaptonemal complex formation and recombination. Third, diverse mechanisms are employed to regulate meiotic CDK activity with the regulation of Clb1-CDK

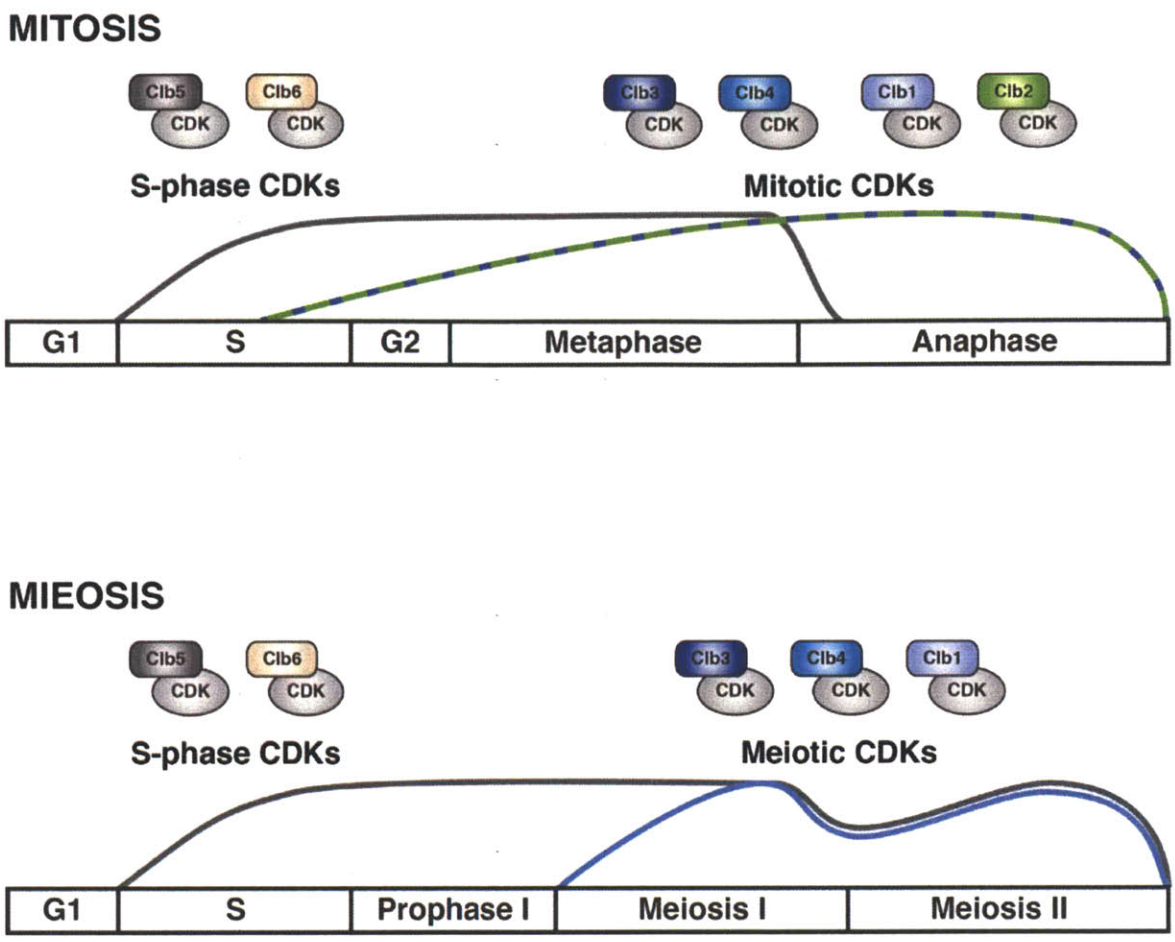

Figure 2. B-type cyclin-CDK activity during mitosis and meiosis.

(top) During the mitotic cell division, S-phase CDKs (gray line) become active at the G1-S transition, drive DNA replication and activity remains high until the metaphase-anaphase transition. M phase cyclins Clb1-4 (blue/green line) become active during late S-phase/G2. M phase CDKs are inactivated during mitotic exit.

(bottom) During the meiotic cell division, S-phase CDKs (gray line) become active at the G1-S transition, drive DNA replication and recombination and activity remains high until exit from meiosis II. M phase cyclins Clb1, Clb3, and Clb4 appear during meiosis and drive nuclear divisions. Clb-CDK activity is thought to decrease at the meiosis I-meiosis II transition.

and Clb3-CDK greatly diverging from their mitotic counterparts. Clb1-CDK activity is restricted to meiosis I while Clb3-CDK activity is restricted to meiosis II. The restriction of Clb3-CDK activity to MII occurs by 5' UTR mediated meiosis I-specific translational inhibition of the *CLB3* mRNA (Carlile & Amon, 2008). Clb1-CDK activity is regulated at the posttranslational level. Clb1 protein levels rise during meiosis I and are maintained until exit from meiosis II, while Clb1-CDK activity is largely absent during meiosis II (Carlile & Amon, 2008). Finally, a meiosis-specific APC/C co-activator, Ama1, is required to degrade both Ndd1 as well as M phase cyclins during meiotic prophase I (Okaz et al., 2012). How the APC/C is regulated to maintain proper cyclin-CDK levels at the meiosis I-meiosis II transition has not been thoroughly investigated in budding yeast.

Additional mechanisms of cyclin-CDK regulation are mediated through downregulation of CDK activity via inhibitory phosphorylation or by binding to various cyclin-dependent kinase inhibitors (CKIs). In budding yeast, phosphorylation of Cdc28 on the residues Thr18 and Tyr19 by the kinase Swe1 results in downregulation of CDK activity (Booher, Deshaies, & Kirschner, 1993). In higher eukaryotes, phosphorylation of the corresponding residues (Thr14 and Tyr15 of Cdk1 by the kinase Wee1) is important for halting the cell cycle in response to DNA damage and regulates the G2/M transition in *S. pombe*. In budding yeast, this inhibitory role is shifted to delaying the cell cycle in response to actin and septin cytoskeleton defects, known as the morphogenesis checkpoint (Enserink & Kolodner, 2010; Mendenhall & Hodge, 1998). This

inhibitory phosphorylation is counteracted by the phosphatase Mih1 in budding yeast and Cdc25 in fission yeast and higher eukaryotes (Russell, Moreno, & Reed, 1989).

The cyclin-dependent kinase inhibitors Far1 and Sic1 bind and inhibit cyclin-CDK complexes by preventing interaction with substrates (Chang & Herskowitz, 1990; Schwob, Bohm, Mendenhall, & Nasmyth, 1994). Far1 inhibits Cln-CDKs in response to mating pheromone to prevent cell cycle entry (Gartner et al., 1998; Jeoung, Oehlen, & Cross, 1998; Peter & Herskowitz, 1994; Tyers & Futcher, 1993). Sic1 binds to Clb-CDKs to restrict the G1-S transition (Mendenhall, 1993). Sic1 degradation, promoted either by Cln-CDKs or by the meiosis-specific kinase Ime2, is required to increase S-phase CDK activity which drives premitotic or premeiotic S-phase and progression into the mitotic or meiotic cell division (Mendenhall, 1993).

Control of cell cycle events by cyclin-dependent kinases

Cyclin-CDK activity drives a number of key events including entry into the cell cycle, DNA replication, spindle assembly and chromosome segregation in both mitosis and meiosis. The following section will summarize some of the major functions that cyclin-CDK activity promotes during these two cell division programs.

The G1 phase of the cell cycle is characterized as a period of low CDK activity. Cln3 accumulation in response to growth (i.e. cellular biosynthetic

capacity) triggers entry into the cell cycle as Cln3-CDK promotes the phosphorylation and nuclear exit of a G1 transcriptional inhibitor, Whi5 (Costanzo et al., 2004; de Bruin, McDonald, Kalashnikova, Yates, & Wittenberg, 2004; Wagner et al., 2009). This allows the expression of *CLN1* and *CLN2*, which promote the degradation of the CDK inhibitor Sic1 and also inhibit APC/C^{Cdh1}. This, in turn, results in a rapid increase in Clb5- and Clb6-CDK activity and entry into S-phase (Mendenhall, 1993; Nash et al., 2001). As described above, the G1 cyclins are not expressed during meiosis and the meiosis-specific kinase, Ime2, substitutes for G1 cyclin-dependent kinases to promote degradation of Sic1 and inhibition of APC/C^{Cdh1} during premeiotic S-phase (Benjamin et al., 2003; Dirick et al., 1998).

In combination with the Dbf4-dependent kinase (DDK), Cdc7, DNA replication is mediated by Clb5- and Clb6-CDK during S-phase preceding mitosis and meiosis (Figure 2). Phosphorylation of Sld2 and Sld3 promotes binding to Dpb11, the Sld2-Dpb11 complex then binds phosphorylated Sld3 at the origin and recruits the helicase activating GINS complex to origins of replication (Kamimura, Masumoto, Sugino, & Araki, 1998; Masumoto, Sugino, & Araki, 2000; Tanaka et al., 2007; Zegerman & Diffley, 2007; Muramatsu, Hirai, Tak, Kamimura, & Araki, 2010). CDK-mediated phosphorylation also prevents cells from re-replicating their DNA. Pre-RCs are disassembled after origin firing and cannot reassemble until CDK activity has dropped after mitotic exit. This control is mediated by CDK activity in a number of ways: (1) phosphorylation of Cdc6,

promoting its degradation; (2) phosphorylation of Mcm proteins to promote nuclear export; (3) phosphorylation of ORC subunits, Orc2 and Orc6, thus inhibiting Cdt1 and thus Mcm2-7 recruitment (Labib, Diffley, & Kearsey, 1999; Mimura, Seki, Tanaka, & Diffley, 2004; Nguyen, Co, Irie, & Li, 2000; Chen & Bell, 2011). These mechanisms ensure that DNA replication occurs once and only once per cell cycle. During meiosis, Clb5- and Clb6-CDK also promote DSB formation by phosphorylating a component of the recombination machinery, Mer2 (Henderson, Kee, Maleki, Santini, & Keeney, 2006).

An essential step in cell division is the assembly of a spindle to mediate chromosome segregation. Cyclin-CDK activity promotes the formation of a spindle in a number of ways: (1) through regulation of SPB duplication and separation, (2) by promoting spindle stability through microtubule bundling, and (3) through spindle elongation. In combination with the kinase Mps1, Cln-CDKs promote SPB duplication during G1 through phosphorylation of Spc42 (Haase, Winey, & Reed, 2001; Jaspersen et al., 2004). In addition, Mps1 and CDK phosphorylate the SPB component Spc110 in a cell cycle-dependent manner (Friedman et al., 2001; Friedman, Sundberg, Huang, & Davis, 1996). After SPB duplication, the old and new SPBs must separate in late S-phase to ultimately form a bipolar spindle. The exact mechanism is not known, but SPB separation is promoted by S and M-phase Clb-CDKs and is triggered by the severing of a structure known as the half bridge that connects the sister SPBs (Chee & Haase, 2010). CDK activity promotes the stability of the kinesins Cin8 and Kip1 and

Ase1, a spindle midzone component. These factors are also required for SPB separation and are thought to do so by bundling microtubules to generate force (Crasta, Huang, Morgan, Winey, & Surana, 2006).

Clb-CDKs also promote spindle stabilization and elongation. Association of Fin1, a coiled-coil protein that forms filaments between SPBs, with the mitotic spindle is controlled by CDK phosphorylation (van Hemert et al., 2002; Woodbury & Morgan, 2007a, 2007b). Additionally, components of the chromosomal passanger complex, which consists of Ipl1, Bir1, Sli15 and Nbl1 are phosphorylated by CDK. These factors localize to the mitotic spindle during anaphase and control spindle stabilization and elongation (Bouck & Bloom, 2005; Widlund et al., 2006). Finally, Clb-CDKs promote spindle elongation and anaphase by activation of APC/C^{Cdc20} (Rahal & Amon, 2008).

Each of the cyclins are individually dispensable for both mitosis and meiosis (Fitch et al., 1992). Mutational analysis of the M-phase cyclins revealed that cells carrying a deletion of *CLB2* exhibit a slight phenotype suggesting a delayed mitosis, while deletion of *CLB1*, *CLB3* or *CLB4* alone has no discernable phenotype. Cells that are *clb1Δ clb2Δ*, *clb1Δ clb2Δ clb3Δ* or *clb1Δ clb2Δ clb3Δ clb4Δ* are inviable (Fitch et al., 1992). In meiosis, Clb-CDK activity promotes exit from the pachytene stage of meiosis and entry into the meiotic divisions (Benjamin et al., 2003; Shuster & Byers, 1989). Cells carrying a deletion in either *CLB1* and *CLB3* or *CLB1* and *CLB4*, undergo a single meiotic division and form

two-spored asci (or dyads) with viable diploid spores, suggesting these cells complete meiosis I but fail to enter meiosis II (Dahmann & Futcher, 1995).

Cyclin specificity

An interesting question that remains in the field of cyclin-CDK regulation is why the cell harbors so many cyclins. As each of the cyclins are individually dispensable for both mitosis and meiosis, it is unlikely that cyclin-specific targeting of CDK activity is essential (Dahmann & Futcher, 1995; Grandin & Reed, 1993). Combinatorial mutant analysis indicates that there is significant overlap of the various cyclin-CDKs to phosphorylate different substrates (Epstein & Cross, 1992; Fisher & Nurse, 1996; Haase & Reed, 1999; Hu & Aparicio, 2005; Levine, Kiang, Jacobson, Fisher, & Cross, 1999; Tyers, 1996).

However, other experiments suggest there is specificity among cyclin targets. For example, when the S-phase cyclin Clb5 is replaced by the mitotic cyclin Clb2, the initiation of DNA replication is less effective (Cross, Yuste-Rojas, Gray, & Jacobson, 1999). In fact, a subset of CDK targets have been identified that are phosphorylated more effectively by Clb5-CDK than Clb2-CDK due to a hydrophobic patch on the Clb5 cyclin that more efficiently targets these kinase complexes to particular substrates (Cross & Jacobson, 2000; Loog & Morgan, 2005; Ubersax et al., 2003). In addition to differences between Clb5 and Clb2, work has identified proteins that specifically associate with Cln2, Clb2, Clb3 and Clb5 using co-purification mass spectrometry analysis (Archambault et al., 2004).

Furthermore, these various cyclin-CDK complexes have strikingly different abilities to phosphorylate various different targets in vitro (Koivomagi et al., 2011). Interestingly, it appears that the cyclins Clb1, Clb3 and Clb4 vary in their ability to promote biorientation of sister kinetochores (described in Chapter 2). In addition to intrinsic substrate specificity of different cyclin-CDKs, cyclin specificity can also be achieved through differential timing or levels of expression, through different subcellular localization or through the ability of various CKIs to inhibit the various complexes. To what degree each of these various regulatory mechanisms play in mediating the proper timing of cell cycle events will be an area of interesting research.

Concepts of Chromosome Segregation

How does the cell distribute its chromosomes such that each of its daughter cells will inherit a copy of every chromosome? The key to this process is the establishment of physical linkages between the chromosomes that are to be segregated (Figure 1). These linkages are formed between each pair of replicated chromosomes (or sister chromatids) and are maintained until each pair attaches to the chromosome segregation machinery from opposite poles. The linkage between sister chromatids is termed sister chromatid cohesion, and is mediated, in large part, by the cohesin complex.

A critical protein complex, known as the kinetochore, assembles on centromeric DNA to mediate attachment to the chromosome segregation machinery, comprised of spindle microtubules. By influencing and harnessing microtubule dynamics, the kinetochore-microtubule attachment results in pulling forces toward the spindle pole. When kinetochores of sister chromatids attach to microtubules emanating from opposite poles (a condition known as biorientation), the pulling forces are resisted by the linkages between sister chromatids, generating tension at the centromere (Figure 3). The resulting tension is crucial to ensuring that sister chromatids become bioriented; microtubule-kinetochore attachments that do not result in tension are selectively severed (described in more detail below). Thus, through a trial-and-error process, all kinetochores eventually become attached to microtubules from opposite poles. Once each kinetochore is stably attached to a microtubule, sister chromatid cohesion is lost

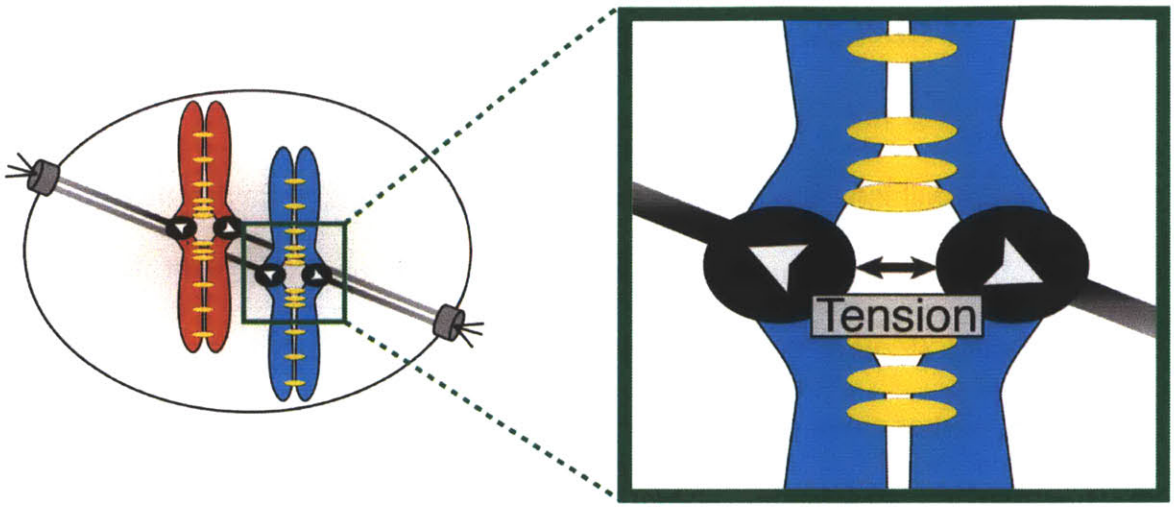

Figure 3. Diagram of tension at the centromere.

The pulling forces exerted from spindle microtubules attached to the kinetochore are resisted by linkages between sister chromatids, mediated by the cohesin complex (yellow). This results in tension across the kinetochores of sister chromatids. Arrows indicate orientation of microtubule-kinetochore attachment.

---

and the individual chromatids are pulled to opposite poles ensuring that both resulting cells get a copy of each chromosome.

Achieving this task is especially complex in meiosis as homologous chromosomes (one maternal and one paternal) must accurately partition during meiosis I and leave in place the means to properly segregate sister chromatids during meiosis II (Figure 1). The establishment of the specialized meiosis I chromosome segregation pattern requires multiple changes to the chromosome segregation machinery: (1) reciprocal recombination between homologous chromosomes provide the linkage to promote their segregation; (2) the kinetochores of replicated sister chromatids attach to microtubules from the same

pole; and (3) during anaphase I, sister-chromatid cohesion is removed from chromosomes arms to allow segregation of homologs, but maintained near centromeres to retain linkages between sister chromatids required for accurate segregation in meiosis II (described in more detail below).

Chromosome segregation and the kinetochore

The kinetochore is a protein structure that couples chromosomes to spindle microtubules during both mitosis and meiosis and, as such, is a key cell division organelle that enables accurate transmission of genetic information. The kinetochore is a protein complex that assembles on centromeric DNA and mediates chromosomes segregation by influencing and harnessing microtubule dynamics, and by utilizing motor-based motility factors. The kinetochore also serves as a signaling hub that monitors its own assembly as well as microtubule-attachment status. The following section will highlight the role of the kinetochore and spindle assembly checkpoint in promoting biorientation of sister chromatids and then will discuss the overall structure and assembly of the kinetochore and will focus on the kinetochore that is built on the budding yeast point centromere.

Promoting biorientation and spindle assemble checkpoint

The budding yeast Aurora B kinase Ipl1, in complex with the microtubule-binding protein Sli15, dock with the protein Bir1 to localize to the kinetochore (Chan & Botstein, 1993; Francisco & Chan, 1994; T. U. Tanaka et al., 2002). The

activity of Ipl1 destabilizes microtubule-kinetochore interactions that are not under tension by phosphorylating multiple kinetochore components (Biggins et al., 1999; Cheeseman et al., 2002). Chromosome biorientation is sensed by the spatial separation of Aurora B kinase, Ipl1, from kinetochore substrates (Liu, Vader, Vromans, Lampson, & Lens, 2009). The pulling forces that occur when chromosomes are bioriented, increases the spatial separation of kinetochore substrates from the inner centromere, where Aurora B is located, which reduces phosphorylation and stabilizes kinetochore-microtubules interactions (Figure 4) (Liu et al., 2009).

The spindle assembly checkpoint ensures high-fidelity chromosome segregation by monitoring interactions between chromosomes and microtubules. In budding yeast, the spindle assembly checkpoint pathway is composed of the highly conserved proteins Mad1, Mad2, Mad3, Bub1, Bub3, Mps1 and Ipl1 (Biggins et al., 1999; Hoyt, Totis, & Roberts, 1991; Li & Murray, 1991; Weiss & Winey, 1996), which prevents the onset of anaphase through inhibition of APC^{Cdc20} in the presence of unattached kinetochores (Pinsky, Kung, Shokat, & Biggins, 2006). Microtubule-kinetochore interactions that do not generate tension are severed by Aurora B, which leads to unattached kinetochores, activation of the spindle assembly checkpoint and inhibition of APC^{Cdc20}. Thus, through the activity of Aurora B and the spindle assembly checkpoint, anaphase onset does not occur until all chromosomes are properly bioriented (Musacchio & Hardwick, 2002).

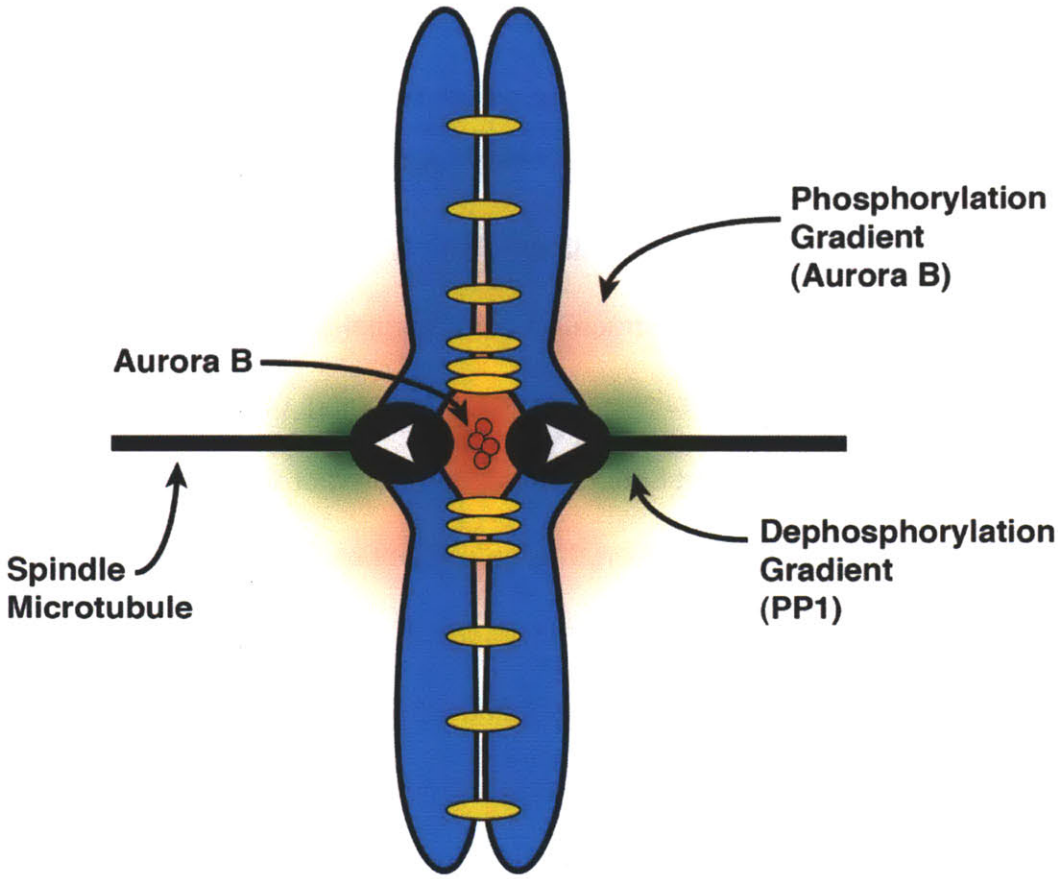

Figure 4. Tension across sister centromeres results in stable microtubule-kinetochore interactions.

Tension across sister centromeres results in stable microtubule-kinetochore interactions through spatial separation of Aurora B (concentrated at the inner centromere) from kinetochore substrates. Thus, correct attachments result in stable microtubule-kinetochore interactions by positioning/pulling the kinetochore substrates away from Aurora B. Red gradient represents Aurora B phosphorylation gradient. Recruitment of the protein phosphatase PP1 to the outer kinetochore provides a counteracting gradient of dephosphorylation (green gradient). Arrows indicate orientation of microtubule-kinetochore attachment.

Activated spindle assembly checkpoint results in the interaction of the checkpoint proteins Mad2, Mad3 and Bub3 with Cdc20 to prevent the APC/C

from targeting Securin for degradation (Chung & Chen, 2002; Fraschini et al., 2001; Hardwick, Johnston, Smith, & Murray, 2000; Hwang et al., 1998; Kim, Lin, Matsumoto, Kitazono, & Matsumoto, 1998). The exact molecular mechanism that leads to checkpoint activation is not entirely clear. Mad2 is capable of forming multimers and adopts at least two structural conformations, "open" and "closed." These conformations are distinguished by the positioning of a 50 residue C-terminal segment termed the "safety belt." Mad2 can interact with either Mad1 or with Cdc20. In the closed conformation, the safety belt of Mad2 wraps around a portion of Mad1 or Cdc20 to promote their interaction. Upon spindle assembly checkpoint activation, signaled by an unattached kinetochore, Mad2 binds Mad1 to form closed-Mad2-Mad1 complex. It is believed that this complex then serves as a template such that an open-Mad2 is recruited to the Mad2-Mad1 complex and the Mad2:Mad2 interaction enables a conformational change which allows the bound open-Mad2 to interact with and inhibit Cdc20. This cycle is repeated to propagate the checkpoint signal and inhibit anaphase onset (De Antoni et al., 2005; Hardwick, 2005).

The kinetochore itself plays a central role in this process. Nearly all checkpoint components either localize to or are recruited to the kinetochore upon microtubule detachment (Gillett, Espelin, & Sorger, 2004). Additionally, two kinetochore complexes, Cbf3 and Ndc80 (see below for more details), are required for spindle assembly checkpoint function (Gardner et al., 2001; McCleland et al., 2003). In the absence of these complexes, checkpoint signaling

is defective, perhaps due to a defect in localizing the checkpoint components to the kinetochore.

Structure and organization of the kinetochore

The kinetochore is composed of >65 proteins which assemble into multi-protein subcomplexes that range in subunit number from two to ten (De Wulf, McAinsh, & Sorger, 2003). The kinetochore is organized into three categories: (1) inner kinetochore proteins that bind directly to the centromeric DNA and provide a platform upon which the remainder of the kinetochore assembles; (2) microtubule-binding proteins that allow the harnessing of microtubule-polymer dynamics; and (3) central kinetochore proteins, which serve as linkers between the inner kinetochore and the outer microtubule binding interface (Figure 5).

The inner kinetochore is made up by the Cbf3 complex, Cbf1 and Mif2. The inner kinetochore assembles on a specialized centromeric nucleosome, in which the canonical histone H3 has been replaced by CENP-A (Cse4 in yeast) (M. M. Smith, 2002). The Cbf3 complex, including Ndc10 and Cep3, provides the majority of DNA binding activity of the inner kinetochore and, as such, is the primary determinant of kinetochore assembly in budding yeast (Espelin, Kaplan, & Sorger, 1997). The linker or central layer of the kinetochore is made up by the COMA/Ctf19 complex as well as the KMN network (composed of the KNL-1/Spc105, Mis12/Mtw1 and Ndc80 complexes) (Westermann, Drubin, & Barnes, 2007). One role of the linker layer of the kinetochore is to transmit the forces

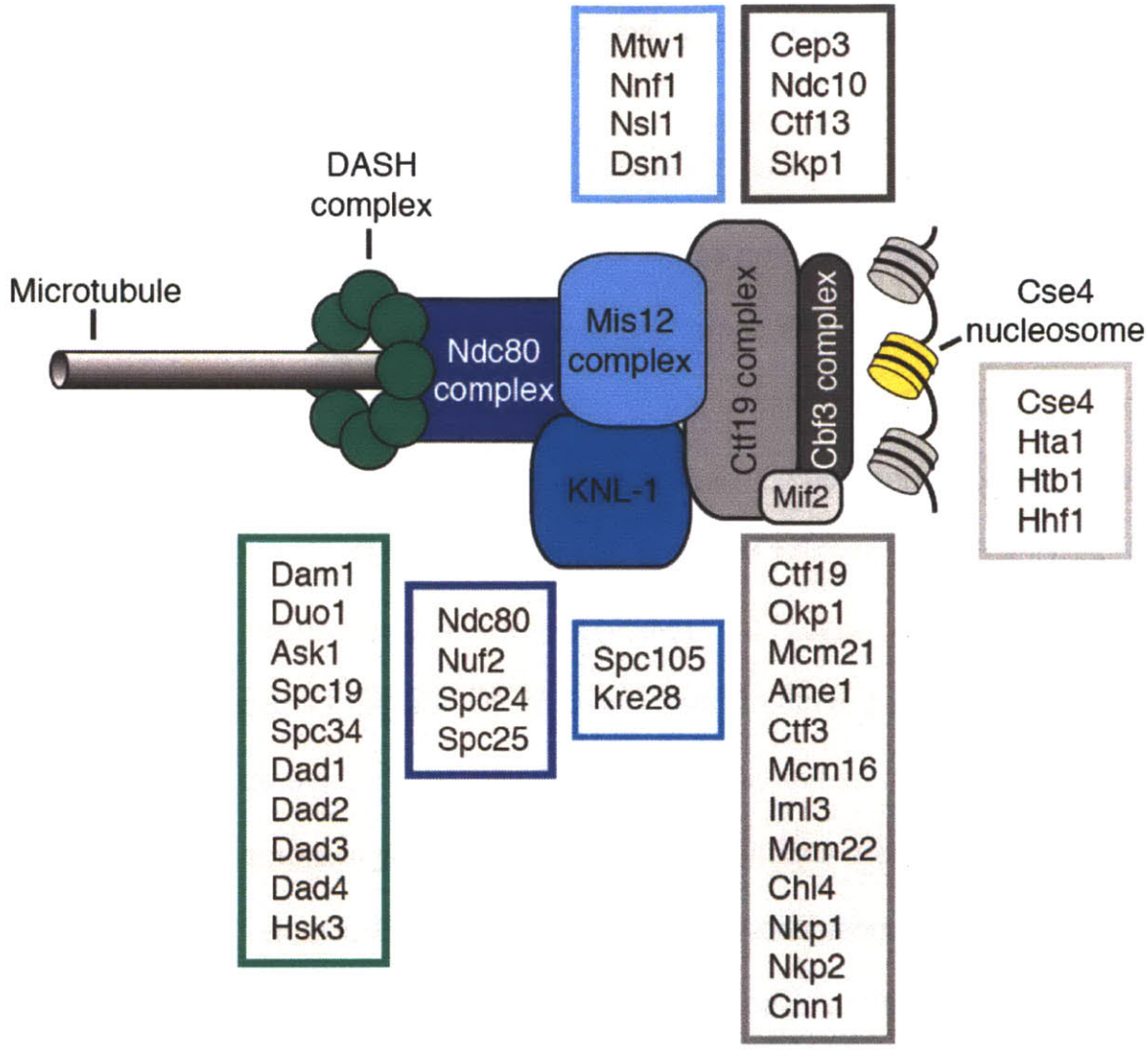

Figure 5. Diagram and organization of the budding yeast kinetochore.

The budding yeast-specific Cbf3 complex binds centromeric DNA in a sequence-specific manner and interacts with the Cse4 nucleosome. The Ctf19 complex (equivalent to the human CCAN network) and Mif2 (CENPC homolog) form the remainder of the inner kinetochore. The KMN network (KNL-1, Mis12 and Ndc80 complexes; various shades of blue) is at the core of the structure. The Ndc80 complex interacts with the DASH/Dam1 complex to form an attachment site for dynamic microtubules. Aurora B kinase, microtubule-associated proteins, motors and components of the mitotic checkpoint machinery are not shown.

generated at the outer kinetochore-microtubule interface to the inner kinetochore, thus allowing poleward chromosome movement during anaphase. However, components of the KMN network also have microtubule binding activity (Cheeseman, Chappie, Wilson-Kubalek, & Desai, 2006). Ndc80 has a calponin-homology domain that resembles the microtubule-binding site of plus-end microtubule tracking proteins, and this domain is believed to have a direct role at the kinetochore-microtubule interface (DeLuca et al., 2006; Wei et al., 2006). The outer kinetochore-microtubule interface is made up by the Dam1/DASH complex and the microtubule-associated and motor proteins Stu2, Kip3 and Cin8 (Westermann et al., 2007). The Dam1/DASH complex forms a ring around microtubules and acts as a microtubule force coupler that translates the mechanical energy associated with microtubule depolymerization into directed movement (Westermann et al., 2006). The Dam1 complex and Stu2 are believed to be primarily responsible for attaching kinetochores to microtubules and influencing microtubule dynamics, while the motor proteins modulate the organization and synchronization of chromosome movements (Tytell & Sorger, 2006). Recently, the EM structure of purified yeast kinetochore particles was visualized in the presence or absence of taxol-stabilized microtubules (Gonen et al., 2012). This work revealed that the kinetochore has multiple microtubule-attachment sites and that an overall change in kinetochore structure occurs when bound to microtubules. Future studies aimed at determining the high-resolution structure as well as mechanistic changes that occur when kinetochores are

bound to microtubules will help elucidate how this protein complex ensures proper partitioning of genetic material.

Kinetochore complex assembly and cell cycle regulation

In budding yeast, microtubules are bound to assembled kinetochores throughout the entire mitotic cell cycle, with the exception of a brief window during S-phase when the kinetochore is disassembled to allow DNA replication through the centromere (Guacci, Hogan, & Koshland, 1997; Jin, Fuchs, & Loidl, 2000; T. U. Tanaka et al., 2002; Winey & O'Toole, 2001). However, the kinetochore composition in mammalian cells is dynamic throughout the cell cycle. Inner kinetochore proteins, such as the Constitutive Centromere Associated Network (CCAN), are present and bound to the centromere throughout the cell cycle. While some outer kinetochore components such as Mis12 and KNL-1 are recruited starting in prophase (Cheeseman, Hori, Fukagawa, & Desai, 2008; Cheeseman et al., 2004). The regulatory mechanisms of kinetochore assembly have yet to be fully determined. However, post-translational modification of kinetochore components, including SUMOlation of CENP-I as well as phosphorylation of various components by CDK and Aurora B, have been implicated in this process (Emanuele et al., 2008; Mukhopadhyay, Arnaoutov, & Dasso, 2010). Whether kinetochore assembly is regulated during the meiotic cell divisions in yeast or mammalian cells has not been thoroughly examined.

Reason for a Specialized Cell Division – Meiosis

Cells have evolved elaborate mechanisms to execute proper partitioning of the genetic material during cell division. This task becomes especially difficult in meiosis, the cell division used by sexually reproducing organisms to generate gametes. As described above, the goal of meiosis is to reduce the genome content by half such that proper ploidy is maintained upon fusion of gametes. To achieve this, a single round of DNA replication is followed by two consecutive rounds of nuclear division called meiosis I and meiosis II. During meiosis I homologous chromosomes segregate. Meiosis II resembles mitosis in that sister chromatids segregate from each other. The following section first describes the asexual and sexual reproductive cycles of budding yeast and is followed by a more detailed discussion of the meiotic program of this organism.

Reproductive cycles in cell division

There are two major reproductive strategies used by organisms to transmit genetic information between generations, the asexual and sexual reproductive cycles. In asexual reproduction, an organism reproduces clonally to produce offspring that are genetically identical to the parental cell. In sexual reproduction, genetically distinct offspring are produced following the fusion of individual gametes generated by the parental organism(s). In budding yeast, cells can stably exist with either the haploid (1N) or diploid (2N) genomic complement. Both haploid and diploid yeast cells reproduce asexually, known as vegetative

growth, with daughter cells being produced by budding. Budding yeast has two mating-types, *MATa* and *MATα*. In addition to vegetative growth, haploid yeast cells are capable of mating with other haploid cells of the opposite mating type to produce diploid cells. Upon appropriate environmental cues, diploid cells can undergo a developmental program termed gametogenesis to produce four haploid gametes, called spores. These haploid spores can subsequently germinate and resume the vegetative growth cycle.

Entry into Meiotic Program

The decision to enter the meiotic developmental program varies between different organisms. In multicellular metazoans, extrinsic cues from surrounding somatic cells signal the progenitor germ cells to enter the meiotic program (Honigberg & Purnapatre, 2003). In mice for instance, retinoic acid signaling induces the initiation of meiosis through Stra8 (Anderson et al., 2008). In budding and fission yeast, poor nutrient conditions signal cells to enter the meiotic program and result in the production of stress resistant spores. In addition to being starved of key nutrients, glucose and nitrogen, budding yeast cells must also be diploid (i.e. express both *MATa* and *MATα* mating-type loci), respiration competent and grown in the presence of a non-fermentable carbon source to enter the meiotic program (reviewed in (van Werven & Amon, 2011). All of these signals appear to be integrated at the promoter of a key meiotic transcription factor and central inducer of meiosis, *IME1* (Kassir, Granot, & Simchen, 1988). In

budding yeast, the mating-type control of entry into the meiotic program is controlled by the transcription of two noncoding RNAs. The transcription of one such RNA, *IRT1*, at the *IME1* promoter, establishes a repressive chromatin domain sufficient to prevent expression of *IME1*. A second antisense transcript antagonizes the expression of an additional meiotic regulator *IME4* (Hongay, Grisafi, Galitski, & Fink, 2006; van Werven et al., 2012). These noncoding RNA-mediated regulatory events ensure that in haploid yeast cells, entry into the meiotic program is prevented.

Ime1 promotes the expression of a number of early meiotic genes, including the meiosis specific kinase Ime2, which is required for entry into premeiotic S-phase (Chu & Herskowitz, 1998; Primig et al., 2000). Ime2 substitutes for some of the functions of the G1 cyclin-dependent kinases (CDKs). The G1 cyclins repress *IME1* and, thus, their expression is repressed during meiosis (Colomina, Gari, Gallego, Herrero, & Aldea, 1999). Ime2 promotes entry into S-phase by promoting the degradation of the S-phase CDK inhibitor Sic1 (Dirick et al., 1998) as well as by inactivation of the anaphase promoting complex/cyclosome (APC/C), an ubiquitin ligase that promotes ubiquitin mediated degradation of S-phase cyclins (Bolte, Steigemann, Braus, & Irniger, 2002). These functions allow the accumulation of S-phase CDK activity and mark the transition from G1 into premeiotic S-phase.

Premeiotic S-phase

The accumulation of S-phase CDK activity (composed of the associated activity of the B-type cyclins Clb5 and Clb6) promotes DNA replication (Figure 2). The mechanism of DNA replication is similar between mitosis and meiosis, the same origins are utilized and fork progression occurs at a similar rate, although origin firing is either delayed or less efficient at the majority of origins in premeiotic S-phase (Collins & Newlon, 1994; Johnston, Williamson, Johnson, & Fennell, 1982; Blitzblau, Chan, Hochwagen, & Bell, 2012). Origin sequences are bound by the origin recognition complex (ORC), which recruits the replication factor Cdc6. This allows the Mcm2-7 helicase complex to bind and form the pre-initiation complex (preRC). Along with Clb5- and Clb6-CDK activity, Dbf4-dependent kinase (DDK) activity is required to promote DNA replication (Bell & Dutta, 2002). Interestingly, in all organisms studied to date, premeiotic S-phase is significantly longer than premitotic S-phase (Cha, Weiner, Keeney, Dekker, & Kleckner, 2000). It is possible that the longer duration of premeiotic S-phase is due to the initiation of events that are required for interactions of homologous chromosomes during prophase I. Numerous events required for proper chromosome segregation are initiated during premeiotic S-phase. The loading of meiotic cohesins (which physically tether sister chromatids together and have an essential role in recombination and homolog pairing) as well as double-strand break (DSB) formation are thought to require passage through S-phase although the explicit requirement of DNA replication on DSB formation is debated in the

field (Borde, Goldman, & Lichten, 2000; Hochwagen, Tham, Brar, & Amon, 2005).

Meiotic Prophase I

During meiotic prophase I, homologous chromosomes become physically linked through reciprocal recombination, which allows homologous chromosomes to properly orient on the meiosis I spindle. Recombination is facilitated by the formation of a protein structure established between homologous chromosomes termed the synaptonemal complex. Meiotic recombination begins with the deliberate introduction of DSB throughout the genome by the transesterase protein Spo11 (Keeney, Giroux, & Kleckner, 1997). The resulting DSBs are processed by exonuclease resection yielding single-stranded 3' overhangs, a reaction dependent on the Rad50, Mre11, Xrs2 complex (Alani, Padmore, & Kleckner, 1990; Neale, Pan, & Keeney, 2005). The 3' overhangs, bound by Rad51 and Dmc1, then invade the DNA duplex of the homologous chromosome (Bishop, 1994; Schwacha & Kleckner, 1997). In meiosis, DSBs are preferentially repaired from a homologous chromatid, as opposed to the sister chromatid as in mitosis (Kadyk & Hartwell, 1992). The unstable interaction with the homologous chromatid is then processed by one of two pathways (Figure 6); the first produces non-crossovers (NCOs) while the second results in crossovers (COs) (Allers & Lichten, 2001). For interactions that result in NCOs, the nascent 3' interaction results in synthesis-dependent strand annealing in which the 3' single

stranded tail initiates DNA replication, using the homologous chromatid as a template, before the extended end is ejected. The extended end is then annealed with its original partner and after completing DNA synthesis and ligation, the DSB

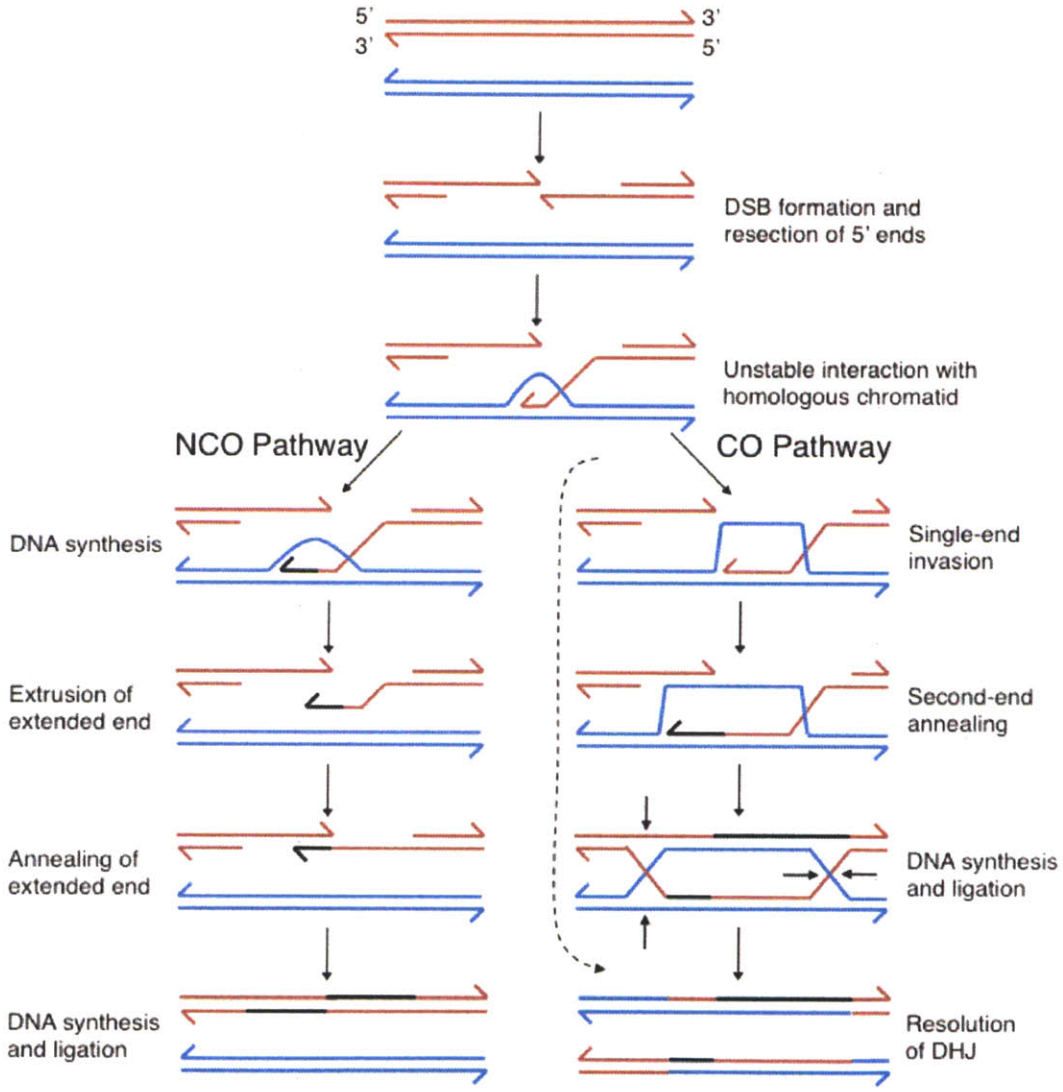

Figure 6. Repair of DSBs through CO and NCO pathways.

DSBs are processed via two pathways, resulting in the formation of two types of products, COs and NCOs. COs in the formation of recombinant molecules with a reciprocal exchange of genetic information, while NCOs repair without such a

reciprocal exchange. There is a minor CO pathway (dashed arrow) that may proceed without a DHJ intermediate. Adapted from (Bishop & Zickler, 2004).

is repaired without a reciprocal exchange of genetic information (Bishop & Zickler, 2004). Thus, a gene conversion can be observed from this type of repair.

In the CO pathway, the nascent 3' interaction is stabilized to form a single-end invasion intermediate (Hunter & Kleckner, 2001). The displaced strand of the single-end invasion then anneals with the second 3' end (second-end annealing) and after DNA synthesis and ligation, a double Holliday junction (DHJ) is formed. Resolution of the DHJ results in the formation of recombinant molecules with a reciprocal exchange of genetic information (Bishop & Zickler, 2004). This reciprocal exchange serves to produce new combinations of alleles to expand genetic diversity of the resulting gametes, but equally important, results in the formation of chiasmata, which physically links homologous chromosomes together and allows them to properly segregate during meiosis I.

CO formation is mediated by a meiosis-specific chromosome structure known as the synaptonemal complex (SC) (Page & Hawley, 2004). In early prophase I (leptotene), lateral elements (LEs) form along the length of individual chromosomes when proteins such as Hop1 and Red1 associate with chromatin (Bailis & Roeder, 1998; Hollingsworth, Goetsch, & Byers, 1990; A. V. Smith & Roeder, 1997). These associations are dependent on meiotic cohesins (Klein et al., 1999). Lateral elements (also known as axial elements) promote repair of

DSBs to occur from the homolog rather than the sister chromatid. During late prophase I (pachytene), interhomolog interactions that will become COs nucleate transverse filaments (or central elements – CEs), consisting of Zip1, to connect the LEs of homologs along their entire length and thus form the synaptonemal complex (Page & Hawley, 2004).

Since the initiation of recombination results in severe DNA damage (through DSB formation), it is essential that the initiation of the meiotic divisions does not occur until all of the damage has been repaired (Marston & Amon, 2004). In the presence of recombination intermediates, the recombination checkpoint prevents entry into meiosis I by inhibiting CDK activation in at least two ways. First, the activated checkpoint results in activation of the kinase, Swe1, which inhibits CDK activity by phosphorylating Cdc28 on Thr18 and Tyr19. Second, when activated, the checkpoint prevents expression of the meiotic transcription factor *NDT80*, which is responsible for activating transcription of a large set of meiotic genes including the meiotic (M phase) cyclins and polo-like kinase, Cdc5 (Marston & Amon, 2004; Roeder & Bailis, 2000; Shuster & Byers, 1989). The recombination checkpoint senses the presence of DNA damage and shares components with the mitotic DNA damage checkpoint, including Mec1 and Rad24. Components of the synaptonemal complex, Red1 and Hop1, are also required for recombination checkpoint signaling (Roeder & Bailis, 2000).

It was recently found that the meiosis-specific activator of the APC/C, Ama1, is required for an extended prophase I promoted by the recombination

checkpoint (Okaz et al., 2012). Cells that lack *AMA1* accumulate the mitotic transcription factor Mcm1-Fkh2-Ndd1 and prematurely express M phase cyclins and Cdc5. In addition to triggering the degradation of Ndd1, and thus preventing expression of M phase cyclins and Cdc5, APC/C^{Ama1} also promotes the degradation of these factors. Thus, APC/C^{Ama1} promotes the proper timing of meiotic events (including SC disassembly and proper recombination), by ensuring that entry into meiosis I is controlled by the recombination checkpoint sensitive transcription factor Ndt80 (Okaz et al., 2012).

Once homologous recombination is complete and all DSBs have been repaired, thus satisfying the recombination checkpoint, the meiotic transcription factor, Ndt80, drives the expression of a number of genes required to exit prophase I and enter the meiotic divisions. Among these are the M phase cyclins *CLB1*, *CLB3* and *CLB4* (Figure 2) as well as the polo-like kinase *CDC5*. The resulting increase in cyclin-CDK activity drives entry into the meiotic divisions (Chu et al., 1998; Chu & Herskowitz, 1998; Hepworth et al., 1998).

Segregation of chromosomes during meiosis I

To achieve the goal of meiosis, reducing the chromosome complement by half, cells employ a unique chromosome segregation pattern during meiosis I. In this specialized cell division, homologous chromosomes segregate from each other rather than sister chromatids. Thus, meiosis I exhibits a reductional chromosome segregation pattern (homologous chromosomes are segregated), in

contrast to the equational segregation pattern that occurs in mitosis and meiosis II (sister chromatids segregate). For this specialized segregation pattern to occur, a number of key modifications are made to the mitotic chromosome segregation machinery (Figure 7). First, homologous chromosomes

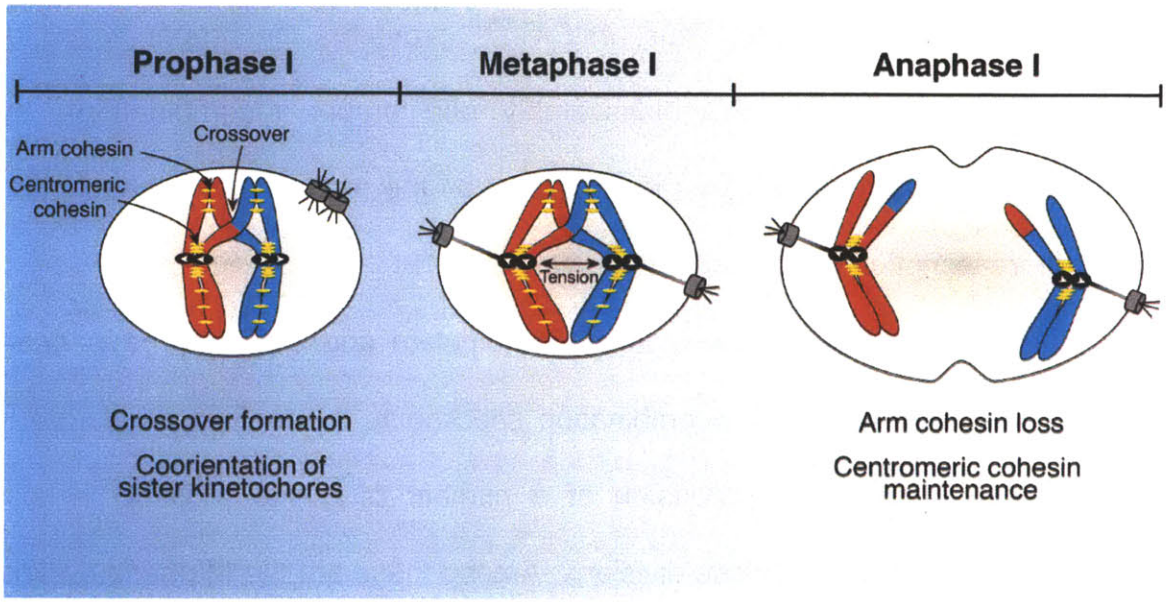

Figure 7. Meiosis specific modifications to the chromosome segregation machinery.

At least three meiosis-specific events promote the establishment of the meiosis I chromosome segregation pattern. (1) reciprocal recombination between homologous chromosomes provide the linkage to promote their segregation; (2) kinetochores of sister chromatids attach to microtubules from the same pole; (3) sister-chromatid cohesion is removed from chromosomes arms to allow segregation of homologs, but maintained near centromeres to retain linkages between sister chromatids required for accurate segregation in meiosis II. White arrows indicate orientation of microtubule-kinetochore attachment.

become physically linked through the formation of crossovers (visible as chiasmata). These linkages, along with sister chromatid cohesion on chromosome arms, allow homologous chromosomes to be properly oriented on the meiosis I spindle by resisting the pulling forces of spindle microtubules. Second, sister chromatids attach to microtubules emanating from the same spindle pole (known as coorientation), instead of from opposite poles (biorientation) as occurs during mitosis or meiosis II. The physical linkage between homologous chromosomes mediated by crossovers and the coorientation of sister chromatids leads to the biorientation of homologous chromosomes during meiosis I. Thus, the tension required to stabilize microtubule-kinetochore attachments is generated by pulling one pair of sister kinetochores toward one pole and the other pair toward the opposite pole. The pulling forces are resisted by the physical linkages between homologous chromosomes combined with arm cohesion, thus generating the tension required to stabilize microtubule attachments (Figure 8). This ensures that when cells enter anaphase I and cohesion is lost on chromosome arms, chiasmata are resolved and homologs disjoin.

The third modification to the chromosome segregation machinery is that some linkages between sister chromatids are maintained past meiosis I to prevent premature dissociation of sister chromatids and to allow proper attachment and segregation on the meiosis II spindle. The formation of crossovers was covered in the previous section; the following sections will

describe coorientation of sister chromatids as well as stepwise cohesin removal in more detail.

Coorientation of sister chromatids

Insights into the mechanism of sister chromatid coorientation came from elegant experiments carried out using grasshopper spermatocytes. These experiments revealed that coorientation of sister chromatids was a property intrinsic to the chromosome as transplantation of meiosis I chromosomes to a meiosis II spindle resulted in coorientation of sister chromatids (Paliulis & Nicklas, 2000). In fission yeast, coorientation of sister chromatids depends on cohesion of sister chromatids at the inner core of the centromere, which requires the meiotic cohesin containing the Rec8-kleisin subunit, and on a meiosis I-specific protein Moa1 (Sakuno, Tada, & Watanabe, 2009; Yokobayashi & Watanabe, 2005). Cohesion at the core centromere induces coorientation while cohesion at the pericentromere promotes sister chromatid biorientation (Sakuno et al., 2009).

In contrast, both Scc1- and Rec8-containing cohesin can support coorientation of sister chromatids during meiosis I in budding yeast (Monje-Casas, Prabhu, Lee, Boselli, & Amon, 2007; Toth et al., 2000). In budding yeast, coorientation of sister chromatids depends on the assembly and function of monopolin complex, composed of the meiosis-specific protein Mam1, the casein kinase Hrr25, and two nucleolar proteins Lrs4 and Csm1 (Petronczki et al., 2006; Rabitsch et al., 2003; Toth et al., 2000). Prior to cells entering the meiotic

divisions, the polo-like kinase, Cdc5, promotes the release of Lrs4 and Csm1 from the nucleolus. The monopolin complex then localizes to kinetochores (Rabitsch et al., 2003). The proposed function of the monopolin complex at kinetochores is to link the kinetochores of sister chromatids, effectively fusing them into a single microtubule-binding site (Corbett et al., 2010; Rabitsch et al., 2003). As in mitosis and meiosis II, it was shown using electron microscopy that in meiosis I, the linked sister kinetochores of budding yeast bind to a single microtubule, in contrast to *S. pombe* and higher eukaryotes in which kinetochores bind multiple microtubules (McDonald, O'Toole, Mastronarde, Winey, & Richard McIntosh, 1996; O'Toole et al., 1997; Winey et al., 1995; Winey, Morgan, Straight, Giddings, & Mastronarde, 2005). Thus, the monopolin complex forces sister chromatids to attach to a single microtubule emanating from one spindle pole (Figure 8). Orthologs of Csm1 and Lrs4, but not Mam1, are also present in *S. pombe* (Pcs1 and Mde4, respectively), where they bind kinetochores in mitosis and inhibit the mixed attachment of microtubules from opposite poles (merotelic attachment) (Corbett et al., 2010; Rabitsch et al., 2003).

The stable recruitment of the monopolin complex to kinetochores requires the activity of Cdc5, the meiosis-specific protein Spo13 and DDK (Matos et al., 2008). This point is exemplified by the fact that cells lacking any of these factors are defective in sister chromatid coorientation during meiosis I (Clyne et al., 2003; Katis, Matos et al., 2004; Lee & Amon, 2003; Lee, Kiburz, & Amon, 2004; Matos et al., 2008). The activity of DDK is dispensable for the assembly of the

monopolin complex, but is required for localizing the assembled complex to kinetochores (Matos et al., 2008). The exact mechanism by which these factors promote proper localization and maintenance of the monopolin complex to kinetochores will be an interesting area for future research.

The partial structure of various monopolin subcomplexes gave insight into the overall function of the monopolin complex in promoting sister kinetochore coorientation (Figure 9). Csm1 and Lrs4 form a V-shaped complex with two globular domains comprised of the C-terminus of Csm1 (Corbett et al., 2010). These globular domains are believed to bind to the kinetochore component Dsn1, thus mediating localization and kinetochore clamping by the complex (Corbett & Harrison, 2012). Mam1 binds to Csm1 as well as to Hrr25 through distinct domains. The binding interface of Mam1:Csm1 occludes one of the two Dsn1 (kinetochore component) binding sites that are present on each of the Csm1 globular domains. Additionally, it has been proposed that Mam1 binding to Hrr25

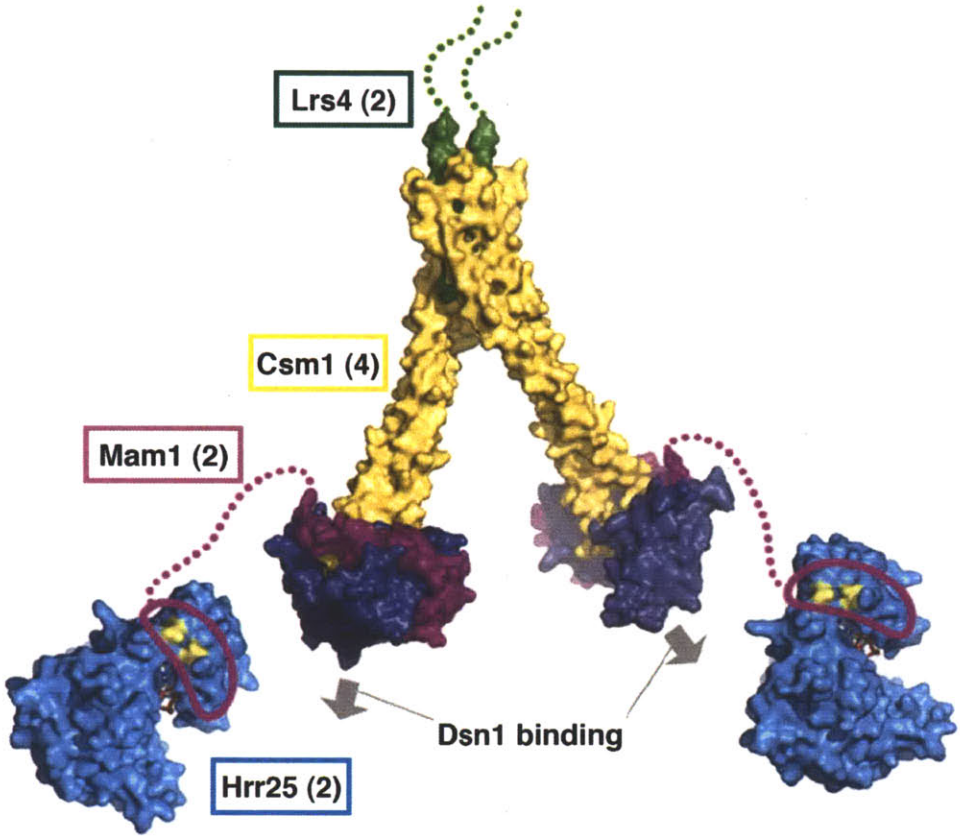

Figure 9. Structure of the monopolin complex.

The crystal structure of the monopolin complex shows a V-shaped complex that is thought to link sister kinetochores. Lrs4 = green, Csm1 = yellow and purple, Mam1 = magenta, and Hrr25 = blue. The copy number of each protein in the complex is indicated in parentheses. The location of the two available Dsn1-binding sites are indicated by arrows. Adapted from (Corbett & Harrison, 2012).

modulates its kinase activity (Corbett & Harrison, 2012). The exact mechanism by which each of these interactions, along with the kinase activity of Hrr25, lead to proper coorientation of sister chromatids remains to be elucidated.

Stepwise cohesin removal

The biorientation of homologous chromosomes in meiosis I is dependent on the activity of the kinase Aurora B (Ipl1). Analogous to its role in mitosis, Ipl1 destabilizes microtubule-kinetochore interactions that fail to promote tension across the meiosis I spindle (Monje-Casas et al., 2007). The spindle assembly checkpoint prevents the onset of chromosome segregation until this process is completed. Once each pair of homologs becomes bioriented, and thus checkpoint signaling ceases, the anaphase promoting complex/cyclosome and its specificity factor Cdc20 (APC/C^{Cdc20}) targets Securin (Pds1 in yeast) for degradation, thus relieving Separase (Esp1) inhibition (Ciosk et al., 1998; Cohen-Fix, Peters, Kirschner, & Koshland, 1996). Separase is a protease that cleaves the kleisin subunit of cohesin, the protein complex that mediates sister-chromatid cohesion (Schleiffer et al., 2003; Uhlmann, Lottspeich, & Nasmyth, 1999; Uhlmann, Wernic, Poupart, Koonin, & Nasmyth, 2000). During meiosis I, cleavage of cohesin distal to sites of crossovers allows homologs to disjoin (Buonomo et al., 2000). However, accurate segregation of sister chromatids during meiosis II requires that cohesin around centromeres be protected from cleavage during meiosis I (Figure 10).

Pathways exist to remove cohesin in a Separase-independent manner. In vertebrates, polo-like kinase promotes the removal of cohesin from chromosome arms during prophase and pro-metaphase (Losada, Hirano, & Hirano, 2002; Sumara et al., 2002) and in budding yeast, Cdc5 facilitates the removal of

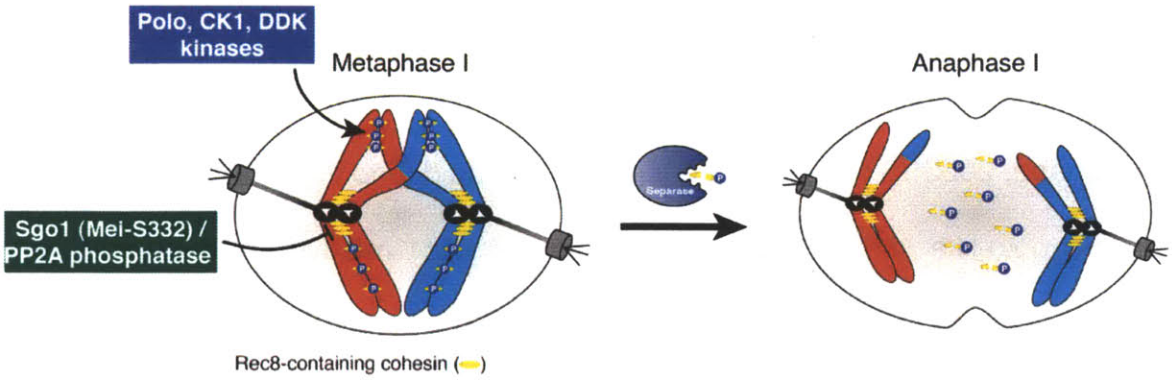

Figure 10. Protection of centromeric cohesin is accomplished by preventing phosphorylation of Rec8. This is mediated by Sgo1 (MEI-S332)-dependent recruitment of the protein phosphatase PP2A to centromeric regions where it antagonizes Rec8 phosphorylation. Rec8 is phosphorylated by a host of kinases including Polo-like kinase, Casein kinase and Dbf4-dependent kinase. Phosphorylated Rec8 (on chromosome arms) is removed by Separase promoting the onset of anaphase I.

---

cohesin from chromosome arms prior to the onset of anaphase I (Yu & Koshland, 2005). However, Separase-dependent cleavage of Rec8 is required for chromosome segregation in both meiosis I and meiosis II (Buonomo et al., 2000; Kitajima, Miyazaki, Yamamoto, & Watanabe, 2003). These results suggest that, while other pathways may play a role in the removal of cohesin during meiosis, cleavage of Rec8 near centromeres must be prevented during meiosis I.

A key factor in maintaining centromeric cohesin during meiosis I is the substitution of the kleisin subunit of the cohesin complex, Scc1/Mcd1, with the meiosis-specific subunit Rec8 (Klein et al., 1999; Watanabe, Yokobayashi, Yamamoto, & Nurse, 2001). In budding and fission yeast, expressing the mitosis-

specific kleisin, Scc1, in place of Rec8 leads to cohesin loss along the entire chromosome at anaphase I onset (Toth et al., 2000; Yokobayashi, Yamamoto, & Watanabe, 2003). This difference is thought to be due to the relative dependence on the polo-like kinase Cdc5 for cleavage of Scc1 relative to Rec8-containing cohesin. While Cdc5 promotes the cleavage of Scc1, it is absolutely required for cleavage of Rec8 (Alexandru, Uhlmann, Mechtler, Poupart, & Nasmyth, 2001; Clyne et al., 2003; Lee & Amon, 2003).

A number of factors required for the maintenance of centromeric cohesin are known. The first factor implicated in this process was the *Drosophila* protein MEI-S332 (Kerrebrock, Miyazaki, Birnby, & Orr-Weaver, 1992; Kerrebrock, Moore, Wu, & Orr-Weaver, 1995; Tang, Bickel, Young, & Orr-Weaver, 1998). Subsequent work identified homologs, termed shugoshins or Sgo1, in budding and fission yeast as well as metazoans (Katis, Galova, Rabitsch, Gregan, & Nasmyth, 2004; Kitajima, Kawashima, & Watanabe, 2004; Kitajima et al., 2006; Riedel et al., 2006). In budding yeast, Sgo1 localizes to a 50-kb region surrounding the centromere and its localization is dependent on the meiosis-specific protein Spo13, the spindle checkpoint component Bub1 and two kinetochore proteins Chl4 and Iml3 (Kiburz et al., 2005b). Cells lacking any of these factors lose centromeric cohesin prematurely during meiosis (Katis, Matos et al., 2004; Kiburz et al., 2005a; Kitajima et al., 2004; Klein et al., 1999; Lee et al., 2004; Marston, Tham, Shah, & Amon, 2004; Shonn, McCarroll, & Murray, 2002). The 50-kb centromeric domain in which Sgo1 localizes, encompasses the

region that cohesin is protected from removal in meiosis I (Kiburz et al., 2005a). These results suggest that Sgo1 forms a protective domain around centromeres to prevent cohesin removal at anaphase I onset.

The removal of cohesin is promoted by phosphorylation of the kleisin subunit Scc1 or Rec8 (Alexandru et al., 2001; Clyne et al., 2003; Hornig & Uhlmann, 2004; Lee & Amon, 2003), which is believed to make these subunits more effective Separase substrates. A number of kinases have been implicated in the phosphorylation of Rec8 during meiosis I, including Cdc5, DDK and casein kinase (Brar et al., 2006; Clyne et al., 2003; Katis et al., 2010; Lee & Amon, 2003). The protection of centromeric cohesin is accomplished by preventing phosphorylation of Rec8 (Figure 10). This occurs, at least in part, by Sgo1 (MEI-S332)-dependent recruitment of the protein phosphatase PP2A to centromeric regions where it antagonizes Rec8 phosphorylation (Katis, Galova et al., 2004; Kerrebrock et al., 1995; Kitajima et al., 2004; Kitajima et al., 2006; Riedel et al., 2006). This is supported by the fact that an Sgo1 mutant that is defective solely in the binding of PP2A, fails to protect centromeric Rec8 at anaphase I onset (Z. Xu et al., 2009). In addition, expression of an allele of Rec8 where a subset of phosphorylation sites are mutated to the phosphomimetic residue aspartate, causes premature loss of centromeric cohesin (Katis et al., 2010). Thus, recruitment of Sgo1-PP2A to centromeres establishes a protective domain in which cohesin is resistant to removal during meiosis I.

It is not entirely clear how Iml3 and Chl4 promote the protection of centromeric cohesin during meiosis I. In cells lacking these factors, Sgo1 localizes to the core centromere, but fails to localize to the surrounding pericentric regions (Kiburz et al., 2005a). Iml3 and Chl4 may serve as docking sites (at the kinetochore) for the loading of protective factors to then spread throughout the pericentromeric region. Additionally, the mechanism by which Spo13 promotes the maintenance of centromeric cohesin is not well defined. Overexpression of Spo13 during mitosis leads to inhibition of cleavage of both Rec8 and Scc1 (Lee et al., 2004; Shonn et al., 2002). These results suggest that, in addition to promoting the localization of Sgo1, Spo13 plays a role in preventing Separase from cleaving cohesin.

One key question is how centromeric cohesin is rendered resistant to cleavage in meiosis I, and then sensitive to cleavage in meiosis II? A simple explanation is that Sgo1-PP2A is maintained at kinetochores until metaphase II and is removed prior to anaphase II, thus leaving the centromeric pool of cohesin sensitive to Separase at anaphase II. However, live cell imaging showed that kinetochore associated Rts1 (a component of PP2A) levels decrease at the onset of anaphase I, but recover as cells enter metaphase II (Katis et al., 2010). What is the role of kinetochore localized Sgo1-PP2A in meiosis II? One function may be to mediate the spindle assembly checkpoint as in mitosis (Indjeian, Stern, & Murray, 2005; Z. Xu et al., 2009). Since Sgo1-PP2A appears to localize to kinetochores during mitotic anaphase as well as anaphase II, it appears that

localization of Sgo1-PP2A alone is not sufficient to promote centromeric protection of cohesin. It will be interesting to determine whether additional meiosis-specific factors (e.g. Spo13), and/or meiosis-specific changes to the centromeric chromatin structure, play an accessory role in protecting centromeric cohesin during meiosis I.

Transition between meiosis I and meiosis II

The transition between meiosis I and meiosis II is unique because two consecutive chromosome segregation phases (meiosis I and meiosis II) occur without an intervening DNA replication phase. This poses a challenge to the cell. Cyclin-CDK activity must be reduced to allow disassembly of the meiosis I spindle, however, sufficient cyclin-CDK activity must be retained to prevent relicensing of origins for DNA replication. In frog oocytes, this is accomplished by partially inhibiting cyclin-B degradation upon exit from meiosis I. Subsequently, the synthesis of cyclin-B is increased to allow entry into meiosis II (Gross et al., 2000; Hochegger et al., 2001; Taieb, Gross, Lewellyn, & Maller, 2001). In fission yeast, the small protein Mes1 functions as an inhibitor of APC/C^{Cdc20} and prevents the complete degradation of cyclins during exit from meiosis I (Izawa, Goto, Yamashita, Yamano, & Yamamoto, 2005). Mes1 appears to inhibit APC/C activity by competing with cyclins for Cdc20 binding (Kimata et al., 2008). In budding yeast, it is believed that cyclin-CDK activity must also be reduced at the meiosis I-meiosis II transition since cells expressing a non-degradable version of

Clb2 cannot exit meiosis I (Marston, Lee, & Amon, 2003). The phosphatase Cdc14 has been implicated in counteracting cyclin-CDK activity at the meiosis I-meiosis II transition. In the absence of Cdc14 or its regulatory network, the Cdc14 early anaphase release (FEAR) network, cells cannot properly exit meiosis I (Buonomo et al., 2003; Marston et al., 2003).

Segregation of chromosomes during meiosis II

Meiosis II chromosome segregation resembles mitosis in that sister chromatids segregate away from each other (Figure 1). As during meiosis I and mitosis, the kinase Aurora B (Ipl1) destabilizes microtubule-kinetochore interactions that fail to promote tension (Monje-Casas et al., 2007). The loss of monopolin at the exit from meiosis I (Toth et al., 2000) allows sister chromatids to attach to microtubules emanating from opposite poles, the default state of biorientation. Once all pairs of chromatids have properly attached to the meiosis II spindle, Separase is activated via APC/C^{Cdc20}-mediated degradation of Securin, and Separase then cleaves centromeric cohesin allowing segregation of sister chromatids.

Conclusions and Perspectives

Maintenance of cellular and organismal fitness requires the proper partitioning of genetic material during cell division. One of the key differences in transforming the mitotic cell division program to properly complete meiosis is the establishment of the specialized meiosis I chromosome segregation pattern. This requires multiple modifications to the cell cycle program and chromosome segregation machinery.

The following chapters will discuss the regulatory events that are required to establish proper chromosome segregation during meiosis. First, the proper regulation of cyclin-CDK activity is shown to be a major determinant of establishing the meiosis I chromosome segregation pattern. This occurs largely through the regulation of microtubule-kinetochore interactions. Second, the mechanism by which cyclin-CDK activity is differentially controlled during meiosis I and meiosis II is discussed. Finally, the role of Polo-like kinase in orchestrating meiosis I and meiosis II chromosome segregation is investigated. As errors in meiotic chromosome segregation are the leading cause of birth defects and miscarriages in humans (Hassold & Hunt, 2001), further insight into the mechanistic basis by which cells properly orchestrate this process will be of great interest for future investigation.

REFERENCES

Alani, E., Padmore, R., & Kleckner, N. (1990). Analysis of wild-type and rad50 mutants of yeast suggests an intimate relationship between meiotic chromosome synapsis and recombination. *Cell, 61*(3), 419-436. doi: 0092-8674(90)90524-I [pii]

Alexandru, G., Uhlmann, F., Mechtler, K., Poupart, M.A., & Nasmyth, K. (2001). Phosphorylation of the cohesin subunit Scc1 by Polo/Cdc5 kinase regulates sister chromatid separation in yeast. *Cell, 105*(4), 459-472. doi: S0092-8674(01)00362-2 [pii]

Allers, T., & Lichten, M. (2001). Differential timing and control of noncrossover and crossover recombination during meiosis. *Cell, 106*(1), 47-57. doi: S0092-8674(01)00416-0 [pii]

Anderson, E.L., Baltus, A.E., Roepers-Gajadien, H.L., Hassold, T.J., de Rooij, D.G., van Pelt, A.M. (2008). Stra8 and its inducer, retinoic acid, regulate meiotic initiation in both spermatogenesis and oogenesis in mice. *Proc Natl Acad Sci U S A, 105*(39), 14976-14980. doi: 0807297105 [pii]10.1073/pnas.0807297105

Archambault, V., Chang, E.J., Drapkin, B.J., Cross, F.R., Chait, B.T., & Rout, M.P. (2004). Targeted proteomic study of the cyclin-Cdk module. *Mol Cell, 14*(6), 699-711. doi: 10.1016/j.molcel.2004.05.025S1097276504003272 [pii]

Bailis, J.M., & Roeder, G.S. (1998). Synaptonemal complex morphogenesis and sister-chromatid cohesion require Mek1-dependent phosphorylation of a meiotic chromosomal protein. *Genes Dev, 12*(22), 3551-3563.

Barral, Y., Jentsch, S., & Mann, C. (1995). G1 cyclin turnover and nutrient uptake are controlled by a common pathway in yeast. *Genes Dev, 9*(4), 399-409.

Bell, S.P., & Dutta, A. (2002). DNA replication in eukaryotic cells. *Annu Rev Biochem, 71*, 333-374. doi: 10.1146/annurev.biochem.71.110601.135425110601.135425 [pii]

Benjamin, K.R., Zhang, C., Shokat, K.M., & Herskowitz, I. (2003). Control of landmark events in meiosis by the CDK Cdc28 and the meiosis-specific kinase Ime2. *Genes & development, 17*(12), 1524-1539. doi: 10.1101/gad.1101503

Biggins, S., Severin, F.F., Bhalla, N., Sassoon, I., Hyman, A.A., & Murray, A.W. (1999). The conserved protein kinase Ipl1 regulates microtubule binding to kinetochores in budding yeast. *Genes & development, 13*(5), 532-544.

Bishop, D.K. (1994). RecA homologs Dmc1 and Rad51 interact to form multiple nuclear complexes prior to meiotic chromosome synapsis. *Cell, 79*(6), 1081-1092. doi: 0092-8674(94)90038-8 [pii]

Bishop, D.K., & Zickler, D. (2004). Early decision; meiotic crossover interference prior to stable strand exchange and synapsis. *Cell, 117*(1), 9-15. doi: S0092867404002971 [pii]

Blitzblau, H.G., Chan, C.S., Hochwagen, A., & Bell, S.P. (2012). Separation of DNA replication from the assembly of break-competent meiotic chromosomes. *PLoS Genet, 8*(5), e1002643. doi: 10.1371/journal.pgen.1002643PGENETICS-D-11-02760 [pii]

Bolte, M., Steigemann, P., Braus, G.H., & Irniger, S. (2002). Inhibition of APC-mediated proteolysis by the meiosis-specific protein kinase Ime2. *Proc Natl Acad Sci U S A, 99*(7), 4385-4390. doi: 10.1073/pnas.072385099072385099 [pii]

Booher, R.N., Deshaies, R.J., & Kirschner, M.W. (1993). Properties of Saccharomyces cerevisiae wee1 and its differential regulation of p34CDC28 in response to G1 and G2 cyclins. *EMBO J, 12*(9), 3417-3426.

Borde, V., Goldman, A.S., & Lichten, M. (2000). Direct coupling between meiotic DNA replication and recombination initiation. *Science, 290*(5492), 806-809. doi: 8941 [pii]

Bouck, D.C., & Bloom, K.S. (2005). The kinetochore protein Ndc10p is required for spindle stability and cytokinesis in yeast. *Proc Natl Acad Sci U S A, 102*(15), 5408-5413. doi: 0405925102 [pii]10.1073/pnas.0405925102

Brar, G.A., Kiburz, B.M., Zhang, Y., Kim, J.E., White, F., & Amon, A. (2006). Rec8 phosphorylation and recombination promote the step-wise loss of cohesins in meiosis. *Nature, 441*(7092), 532-536. doi: 10.1038/nature04794

Buonomo, S.B., Clyne, R.K., Fuchs, J., Loidl, J., Uhlmann, F., & Nasmyth, K. (2000). Disjunction of homologous chromosomes in meiosis I depends on proteolytic cleavage of the meiotic cohesin Rec8 by separin. *Cell, 103*(3), 387-398.

Buonomo, S.B., Rabitsch, K.P., Fuchs, J., Gruber, S., Sullivan, M., Uhlmann, F. (2003). Division of the nucleolus and its release of CDC14 during anaphase of meiosis I depends on separase, SPO12, and SLK19. *Dev Cell, 4*(5), 727-739. doi: S1534580703001291 [pii]

Carlile, T.M., & Amon, A. (2008). Meiosis I is established through division-specific translational control of a cyclin. *Cell, 133*(2), 280-291. doi: S0092-8674(08)00283-3 [pii]10.1016/j.cell.2008.02.032

Cha, R.S., Weiner, B.M., Keeney, S., Dekker, J., & Kleckner, N. (2000). Progression of meiotic DNA replication is modulated by interchromosomal interaction proteins, negatively by Spo11p and positively by Rec8p. *Genes Dev, 14*(4), 493-503.

Chan, C.S., & Botstein, D. (1993). Isolation and characterization of chromosome-gain and increase-in-ploidy mutants in yeast. *Genetics, 135*(3), 677-691.

Chang, F., & Herskowitz, I. (1990). Identification of a gene necessary for cell cycle arrest by a negative growth factor of yeast: FAR1 is an inhibitor of a G1 cyclin, CLN2. *Cell, 63*(5), 999-1011. doi: 0092-8674(90)90503-7 [pii]

Chee, M.K., & Haase, S.B. (2010). B-cyclin/CDKs regulate mitotic spindle assembly by phosphorylating kinesins-5 in budding yeast. *PLoS Genet, 6*(5), e1000935. doi: 10.1371/journal.pgen.1000935

Cheeseman, I.M., Anderson, S., Jwa, M., Green, E.M., Kang, J., Yates, J.R., 3rd. (2002). Phospho-regulation of kinetochore-microtubule attachments by the Aurora kinase Ipl1p. *Cell, 111*(2), 163-172.

Cheeseman, I.M., Chappie, J.S., Wilson-Kubalek, E.M., & Desai, A. (2006). The conserved KMN network constitutes the core microtubule-binding site of the kinetochore. *Cell, 127*(5), 983-997. doi: S0092-8674(06)01345-6 [pii]10.1016/j.cell.2006.09.039

Cheeseman, I.M., Hori, T., Fukagawa, T., & Desai, A. (2008). KNL1 and the CENP-H/I/K complex coordinately direct kinetochore assembly in vertebrates. *Mol Biol Cell, 19*(2), 587-594. doi: E07-10-1051 [pii]10.1091/mbc.E07-10-1051

Cheeseman, I.M., Niessen, S., Anderson, S., Hyndman, F., Yates, J.R., 3rd, Oegema, K. (2004). A conserved protein network controls assembly of the outer kinetochore and its ability to sustain tension. *Genes Dev, 18*(18), 2255-2268. doi: 10.1101/gad.123410418/18/2255 [pii]

Chen, S., & Bell, S.P. (2011). CDK prevents Mcm2-7 helicase loading by inhibiting Cdt1 interaction with Orc6. *Genes Dev, 25*(4), 363-372. doi: gad.2011511 [pii]10.1101/gad.2011511

Chu, S., DeRisi, J., Eisen, M., Mulholland, J., Botstein, D., Brown, P.O. (1998). The transcriptional program of sporulation in budding yeast. *Science, 282*(5389), 699-705.

Chu, S., & Herskowitz, I. (1998). Gametogenesis in yeast is regulated by a transcriptional cascade dependent on Ndt80. *Molecular cell, 1*(5), 685-696.

Chung, E., & Chen, R.H. (2002). Spindle checkpoint requires Mad1-bound and Mad1-free Mad2. *Mol Biol Cell, 13*(5), 1501-1511. doi: 10.1091/mbc.02-01-0003

Ciosk, R., Zachariae, W., Michaelis, C., Shevchenko, A., Mann, M., & Nasmyth, K. (1998). An ESP1/PDS1 complex regulates loss of sister chromatid cohesion at the metaphase to anaphase transition in yeast. *Cell, 93*(6), 1067-1076.

Clyne, R.K., Katis, V.L., Jessop, L., Benjamin, K.R., Herskowitz, I., Lichten, M. (2003). Polo-like kinase Cdc5 promotes chiasmata formation and cosegregation of sister centromeres at meiosis I. *Nature cell biology, 5*(5), 480-485. doi: 10.1038/ncb977

Cohen-Fix, O., Peters, J.M., Kirschner, M.W., & Koshland, D. (1996). Anaphase initiation in Saccharomyces cerevisiae is controlled by the APC-dependent degradation of the anaphase inhibitor Pds1p. *Genes & development, 10*(24), 3081-3093.

Collins, I., & Newlon, C.S. (1994). Chromosomal DNA replication initiates at the same origins in meiosis and mitosis. *Mol Cell Biol, 14*(5), 3524-3534.

Colomina, N., Gari, E., Gallego, C., Herrero, E., & Aldea, M. (1999). G1 cyclins block the Ime1 pathway to make mitosis and meiosis incompatible in budding yeast. *EMBO J, 18*(2), 320-329. doi: 10.1093/emboj/18.2.320

Corbett, K.D., & Harrison, S.C. (2012). Molecular architecture of the yeast monopolin complex. *Cell Rep, 1*(6), 583-589. doi: S2211-1247(12)00137-4 [pii]10.1016/j.celrep.2012.05.012

Corbett, K.D., Yip, C.K., Ee, L.S., Walz, T., Amon, A., & Harrison, S.C. (2010). The monopolin complex crosslinks kinetochore components to regulate chromosome-microtubule attachments. *Cell, 142*(4), 556-567. doi: 10.1016/j.cell.2010.07.017

Costanzo, M., Nishikawa, J.L., Tang, X., Millman, J.S., Schub, O., Breitkreuz, K. (2004). CDK activity antagonizes Whi5, an inhibitor of G1/S transcription in yeast. *Cell, 117*(7), 899-913. doi: 10.1016/j.cell.2004.05.024S0092867404004994 [pii]

Crasta, K., Huang, P., Morgan, G., Winey, M., & Surana, U. (2006). Cdk1 regulates centrosome separation by restraining proteolysis of microtubule-associated proteins. *EMBO J, 25*(11), 2551-2563. doi: 7601136 [pii]10.1038/sj.emboj.7601136

Cross, F.R., & Jacobson, M.D. (2000). Conservation and function of a potential substrate-binding domain in the yeast Clb5 B-type cyclin. *Mol Cell Biol, 20*(13), 4782-4790.

Cross, F.R., Yuste-Rojas, M., Gray, S., & Jacobson, M.D. (1999). Specialization and targeting of B-type cyclins. *Mol Cell, 4*(1), 11-19. doi: S1097-2765(00)80183-5 [pii]

Dahmann, C., & Futcher, B. (1995). Specialization of B-type cyclins for mitosis or meiosis in S. cerevisiae. *Genetics, 140*(3), 957-963.

De Antoni, A., Pearson, C.G., Cimini, D., Canman, J.C., Sala, V., Nezi, L. (2005). The Mad1/Mad2 complex as a template for Mad2 activation in the spindle assembly checkpoint. *Curr Biol, 15*(3), 214-225. doi: S0960982205000734 [pii]10.1016/j.cub.2005.01.038

de Bruin, R.A., McDonald, W.H., Kalashnikova, T.I., Yates, J., 3rd, & Wittenberg, C. (2004). Cln3 activates G1-specific transcription via phosphorylation of the SBF bound repressor Whi5. *Cell, 117*(7), 887-898. doi: 10.1016/j.cell.2004.05.025S009286740400532X [pii]

De Wulf, P., McAinsh, A.D., & Sorger, P.K. (2003). Hierarchical assembly of the budding yeast kinetochore from multiple subcomplexes. *Genes Dev, 17*(23), 2902-2921. doi: 10.1101/gad.11444031144403 [pii]

DeLuca, J.G., Gall, W.E., Ciferri, C., Cimini, D., Musacchio, A., & Salmon, E.D. (2006). Kinetochore microtubule dynamics and attachment stability are regulated by Hec1. *Cell, 127*(5), 969-982. doi: S0092-8674(06)01408-5 [pii]10.1016/j.cell.2006.09.047

Dirick, L., Goetsch, L., Ammerer, G., & Byers, B. (1998). Regulation of meiotic S phase by Ime2 and a Clb5,6-associated kinase in Saccharomyces cerevisiae. *Science, 281*(5384), 1854-1857.

Emanuele, M.J., Lan, W., Jwa, M., Miller, S.A., Chan, C.S., & Stukenberg, P.T. (2008). Aurora B kinase and protein phosphatase 1 have opposing roles in modulating kinetochore assembly. *J Cell Biol, 181*(2), 241-254. doi: jcb.200710019 [pii]10.1083/jcb.200710019

Enserink, J.M., & Kolodner, R.D. (2010). An overview of Cdk1-controlled targets and processes. *Cell Div, 5*, 11. doi: 1747-1028-5-11 [pii]10.1186/1747-1028-5-11

Epstein, C.B., & Cross, F.R. (1992). CLB5: a novel B cyclin from budding yeast with a role in S phase. *Genes Dev, 6*(9), 1695-1706.

Espelin, C.W., Kaplan, K.B., & Sorger, P.K. (1997). Probing the architecture of a simple kinetochore using DNA-protein crosslinking. *J Cell Biol, 139*(6), 1383-1396.

Fisher, D.L., & Nurse, P. (1996). A single fission yeast mitotic cyclin B p34cdc2 kinase promotes both S-phase and mitosis in the absence of G1 cyclins. *EMBO J, 15*(4), 850-860.

Fitch, I., Dahmann, C., Surana, U., Amon, A., Nasmyth, K., Goetsch, L. (1992). Characterization of four B-type cyclin genes of the budding yeast Saccharomyces cerevisiae. *Molecular biology of the cell, 3*(7), 805-818.

Francisco, L., & Chan, C.S. (1994). Regulation of yeast chromosome segregation by Ipl1 protein kinase and type 1 protein phosphatase. *Cell Mol Biol Res, 40*(3), 207-213.

Fraschini, R., Beretta, A., Sironi, L., Musacchio, A., Lucchini, G., & Piatti, S. (2001). Bub3 interaction with Mad2, Mad3 and Cdc20 is mediated by WD40 repeats and does not require intact kinetochores. *EMBO J, 20*(23), 6648-6659. doi: 10.1093/emboj/20.23.6648

Friedman, D.B., Kern, J.W., Huneycutt, B.J., Vinh, D.B., Crawford, D.K., Steiner, E. (2001). Yeast Mps1p phosphorylates the spindle pole component Spc110p in the N-terminal domain. *J Biol Chem, 276*(21), 17958-17967. doi: 10.1074/jbc.M010461200M010461200 [pii]

Friedman, D.B., Sundberg, H.A., Huang, E.Y., & Davis, T.N. (1996). The 110-kD spindle pole body component of Saccharomyces cerevisiae is a phosphoprotein that is modified in a cell cycle-dependent manner. *J Cell Biol, 132*(5), 903-914.

Gardner, R.D., Poddar, A., Yellman, C., Tavormina, P.A., Monteagudo, M.C., & Burke, D.J. (2001). The spindle checkpoint of the yeast Saccharomyces cerevisiae requires kinetochore function and maps to the CBF3 domain. *Genetics, 157*(4), 1493-1502.

Gartner, A., Jovanovic, A., Jeoung, D.I., Bourlat, S., Cross, F.R., & Ammerer, G. (1998). Pheromone-dependent G1 cell cycle arrest requires Far1 phosphorylation, but may not involve inhibition of Cdc28-Cln2 kinase, in vivo. *Mol Cell Biol, 18*(7), 3681-3691.

Ghiara, J.B., Richardson, H.E., Sugimoto, K., Henze, M., Lew, D.J., Wittenberg, C. (1991). A cyclin B homolog in S. cerevisiae: chronic activation of the Cdc28 protein kinase by cyclin prevents exit from mitosis. *Cell, 65*(1), 163-174. doi: 0092-8674(91)90417-W [pii]

Gillett, E.S., Espelin, C.W., & Sorger, P.K. (2004). Spindle checkpoint proteins and chromosome-microtubule attachment in budding yeast. *J Cell Biol, 164*(4), 535-546. doi: 10.1083/jcb.200308100jcb.200308100 [pii]

Gonen, S., Akiyoshi, B., Iadanza, M.G., Shi, D., Duggan, N., Biggins, S. (2012). The structure of purified kinetochores reveals multiple microtubule-attachment sites. *Nat Struct Mol Biol, 19*(9), 925-929. doi: 10.1038/nsmb.2358nsmb.2358 [pii]

Grandin, N., & Reed, S.I. (1993). Differential function and expression of Saccharomyces cerevisiae B-type cyclins in mitosis and meiosis. *Molecular and cellular biology, 13*(4), 2113-2125.

Gross, S.D., Schwab, M.S., Taieb, F.E., Lewellyn, A.L., Qian, Y.W., & Maller, J.L. (2000). The critical role of the MAP kinase pathway in meiosis II in Xenopus oocytes is mediated by p90(Rsk). *Curr Biol, 10*(8), 430-438. doi: S0960-9822(00)00425-5 [pii]

Guacci, V., Hogan, E., & Koshland, D. (1997). Centromere position in budding yeast: evidence for anaphase A. *Mol Biol Cell, 8*(6), 957-972.

Haase, S.B., & Reed, S.I. (1999). Evidence that a free-running oscillator drives G1 events in the budding yeast cell cycle. *Nature, 401*(6751), 394-397. doi: 10.1038/43927

Haase, S.B., Winey, M., & Reed, S.I. (2001). Multi-step control of spindle pole body duplication by cyclin-dependent kinase. *Nat Cell Biol, 3*(1), 38-42. doi: 10.1038/35050543

Hadwiger, J.A., Wittenberg, C., Richardson, H.E., de Barros Lopes, M., & Reed, S.I. (1989). A family of cyclin homologs that control the G1 phase in yeast. *Proc Natl Acad Sci U S A, 86*(16), 6255-6259.

Hardwick, K.G. (2005). Checkpoint signalling: Mad2 conformers and signal propagation. *Curr Biol, 15*(4), R122-124. doi: S0960982205001478 [pii]10.1016/j.cub.2005.02.008

Hardwick, K.G., Johnston, R.C., Smith, D.L., & Murray, A.W. (2000). MAD3 encodes a novel component of the spindle checkpoint which interacts with Bub3p, Cdc20p, and Mad2p. *J Cell Biol, 148*(5), 871-882.

Hartwell, L.H. (1974). Saccharomyces cerevisiae cell cycle. *Bacteriol Rev, 38*(2), 164-198.

Hartwell, L.H., Mortimer, R.K., Culotti, J., & Culotti, M. (1973). Genetic Control of the Cell Division Cycle in Yeast: V. Genetic Analysis of cdc Mutants. *Genetics, 74*(2), 267-286.

Hassold, T., & Hunt, P. (2001). To err (meiotically) is human: the genesis of human aneuploidy. *Nature reviews. Genetics, 2*(4), 280-291. doi: 10.1038/35066065

Henderson, K.A., Kee, K., Maleki, S., Santini, P.A., & Keeney, S. (2006). Cyclin-dependent kinase directly regulates initiation of meiotic recombination. *Cell, 125*(7), 1321-1332. doi: S0092-8674(06)00636-2 [pii]10.1016/j.cell.2006.04.039

Hepworth, S.R., Friesen, H., & Segall, J. (1998). NDT80 and the meiotic recombination checkpoint regulate expression of middle sporulation-specific genes in Saccharomyces cerevisiae. *Mol Cell Biol, 18*(10), 5750-5761.

Hochegger, H., Klotzbucher, A., Kirk, J., Howell, M., le Guellec, K., Fletcher, K. (2001). New B-type cyclin synthesis is required between meiosis I and II during Xenopus oocyte maturation. *Development, 128*(19), 3795-3807.

Hochwagen, A., Tham, W.H., Brar, G.A., & Amon, A. (2005). The FK506 binding protein Fpr3 counteracts protein phosphatase 1 to maintain meiotic recombination checkpoint activity. *Cell, 122*(6), 861-873. doi: S0092-8674(05)00703-8 [pii]10.1016/j.cell.2005.07.010

Hollingsworth, N.M., Goetsch, L., & Byers, B. (1990). The HOP1 gene encodes a meiosis-specific component of yeast chromosomes. *Cell, 61*(1), 73-84. doi: 0092-8674(90)90216-2 [pii]

Hongay, C.F., Grisafi, P.L., Galitski, T., & Fink, G.R. (2006). Antisense transcription controls cell fate in Saccharomyces cerevisiae. *Cell, 127*(4), 735-745. doi: S0092-8674(06)01300-6 [pii]10.1016/j.cell.2006.09.038

Honigberg, S.M., & Purnapatre, K. (2003). Signal pathway integration in the switch from the mitotic cell cycle to meiosis in yeast. *J Cell Sci, 116*(Pt 11), 2137-2147. doi: 10.1242/jcs.00460116/11/2137 [pii]

Hornig, N.C., & Uhlmann, F. (2004). Preferential cleavage of chromatin-bound cohesin after targeted phosphorylation by Polo-like kinase. *EMBO J, 23*(15), 3144-3153. doi: 10.1038/sj.emboj.76003037600303 [pii]

Hoyt, M.A., Totis, L., & Roberts, B.T. (1991). S. cerevisiae genes required for cell cycle arrest in response to loss of microtubule function. *Cell, 66*(3), 507-517. doi: 0092-8674(81)90014-3 [pii]

Hu, F., & Aparicio, O.M. (2005). Swe1 regulation and transcriptional control restrict the activity of mitotic cyclins toward replication proteins in Saccharomyces cerevisiae. *Proc Natl Acad Sci U S A, 102*(25), 8910-8915. doi: 0406987102 [pii]10.1073/pnas.0406987102

Hunter, N., & Kleckner, N. (2001). The single-end invasion: an asymmetric intermediate at the double-strand break to double-holliday junction transition of meiotic recombination. *Cell, 106*(1), 59-70. doi: S0092-8674(01)00430-5 [pii]

Hwang, L.H., Lau, L.F., Smith, D.L., Mistrot, C.A., Hardwick, K.G., Hwang, E.S. (1998). Budding yeast Cdc20: a target of the spindle checkpoint. *Science, 279*(5353), 1041-1044.

Indjeian, V.B., Stern, B.M., & Murray, A.W. (2005). The centromeric protein Sgo1 is required to sense lack of tension on mitotic chromosomes. *Science, 307*(5706), 130-133. doi: 307/5706/130 [pii]10.1126/science.1101366

Irniger, S., & Nasmyth, K. (1997). The anaphase-promoting complex is required in G1 arrested yeast cells to inhibit B-type cyclin accumulation and to prevent uncontrolled entry into S-phase. *J Cell Sci, 110 (Pt 13)*, 1523-1531.

Izawa, D., Goto, M., Yamashita, A., Yamano, H., & Yamamoto, M. (2005). Fission yeast Mes1p ensures the onset of meiosis II by blocking degradation of cyclin Cdc13p. *Nature, 434*(7032), 529-533. doi: nature03406 [pii]10.1038/nature03406

Jackson, L.P., Reed, S.I., & Haase, S.B. (2006). Distinct mechanisms control the stability of the related S-phase cyclins Clb5 and Clb6. *Mol Cell Biol, 26*(6), 2456-2466. doi: 26/6/2456 [pii]10.1128/MCB.26.6.2456-2466.2006

Jaspersen, S.L., Huneycutt, B.J., Giddings, T.H., Jr., Resing, K.A., Ahn, N.G., & Winey, M. (2004). Cdc28/Cdk1 regulates spindle pole body duplication through phosphorylation of Spc42 and Mps1. *Dev Cell, 7*(2), 263-274. doi: 10.1016/j.devcel.2004.07.006S1534580704002424 [pii]

Jeffrey, P.D., Russo, A.A., Polyak, K., Gibbs, E., Hurwitz, J., Massague, J. (1995). Mechanism of CDK activation revealed by the structure of a cyclinA-CDK2 complex. *Nature, 376*(6538), 313-320. doi: 10.1038/376313a0

Jeoung, D.I., Oehlen, L.J., & Cross, F.R. (1998). Cln3-associated kinase activity in Saccharomyces cerevisiae is regulated by the mating factor pathway. *Mol Cell Biol, 18*(1), 433-441.

Jin, Q.W., Fuchs, J., & Loidl, J. (2000). Centromere clustering is a major determinant of yeast interphase nuclear organization. *J Cell Sci, 113 (Pt 11)*, 1903-1912.

Johnston, L.H., Williamson, D.H., Johnson, A.L., & Fennell, D.J. (1982). On the mechanism of premeiotic DNA synthesis in the yeast Saccharomyces cerevisiae. *Exp Cell Res, 141*(1), 53-62. doi: 0014-4827(82)90067-2 [pii]

Kadyk, L.C., & Hartwell, L.H. (1992). Sister chromatids are preferred over homologs as substrates for recombinational repair in Saccharomyces cerevisiae. *Genetics, 132*(2), 387-402.

Kamimura, Y., Masumoto, H., Sugino, A., & Araki, H. (1998). Sld2, which interacts with Dpb11 in Saccharomyces cerevisiae, is required for chromosomal DNA replication. *Mol Cell Biol, 18*(10), 6102-6109.

Kassir, Y., Granot, D., & Simchen, G. (1988). IME1, a positive regulator gene of meiosis in S. cerevisiae. *Cell, 52*(6), 853-862. doi: 0092-8674(88)90427-8 [pii]

Katis, V.L., Galova, M., Rabitsch, K.P., Gregan, J., & Nasmyth, K. (2004). Maintenance of cohesin at centromeres after meiosis I in budding yeast requires a kinetochore-associated protein related to MEI-S332. *Current biology : CB, 14*(7), 560-572. doi: 10.1016/j.cub.2004.03.001

Katis, V.L., Lipp, J.J., Imre, R., Bogdanova, A., Okaz, E., Habermann, B. (2010). Rec8 phosphorylation by casein kinase 1 and Cdc7-Dbf4 kinase regulates cohesin cleavage by separase during meiosis. *Developmental cell, 18*(3), 397-409. doi: 10.1016/j.devcel.2010.01.014

Katis, V.L., Matos, J., Mori, S., Shirahige, K., Zachariae, W., & Nasmyth, K. (2004). Spo13 facilitates monopolin recruitment to kinetochores and regulates maintenance of centromeric cohesion during yeast meiosis. *Current biology : CB, 14*(24), 2183-2196. doi: 10.1016/j.cub.2004.12.020

Keeney, S., Giroux, C.N., & Kleckner, N. (1997). Meiosis-specific DNA double-strand breaks are catalyzed by Spo11, a member of a widely conserved protein family. *Cell, 88*(3), 375-384. doi: S0092-8674(00)81876-0 [pii]

Kerrebrock, A.W., Miyazaki, W.Y., Birnby, D., & Orr-Weaver, T.L. (1992). The Drosophila mei-S332 gene promotes sister-chromatid cohesion in meiosis following kinetochore differentiation. *Genetics, 130*(4), 827-841.

Kerrebrock, A.W., Moore, D.P., Wu, J.S., & Orr-Weaver, T.L. (1995). Mei-S332, a Drosophila protein required for sister-chromatid cohesion, can localize to meiotic centromere regions. *Cell, 83*(2), 247-256.

Kiburz, B.M., Reynolds, D.B., Megee, P.C., Marston, A.L., Lee, B.H., Lee, T.I. (2005a). The core centromere and Sgo1 establish a 50-kb cohesin-protected domain around centromeres during meiosis I. *Genes & development, 19*(24), 3017-3030. doi: 10.1101/gad.1373005

Kiburz, B.M., Reynolds, D.B., Megee, P.C., Marston, A.L., Lee, B.H., Lee, T.I. (2005b). The core centromere and Sgo1 establish a 50-kb cohesin-protected domain around centromeres during meiosis I. *Genes Dev, 19*(24), 3017-3030. doi: 19/24/3017 [pii]10.1101/gad.1373005

Kim, S.H., Lin, D.P., Matsumoto, S., Kitazono, A., & Matsumoto, T. (1998). Fission yeast Slp1: an effector of the Mad2-dependent spindle checkpoint. *Science, 279*(5353), 1045-1047.

Kimata, Y., Trickey, M., Izawa, D., Gannon, J., Yamamoto, M., & Yamano, H. (2008). A mutual inhibition between APC/C and its substrate Mes1 required for meiotic progression in fission yeast. *Dev Cell, 14*(3), 446-454. doi: S1534-5807(07)00487-X [pii]10.1016/j.devcel.2007.12.010

Kitajima, T.S., Kawashima, S.A., & Watanabe, Y. (2004). The conserved kinetochore protein shugoshin protects centromeric cohesion during meiosis. *Nature, 427*(6974), 510-517. doi: 10.1038/nature02312

Kitajima, T.S., Miyazaki, Y., Yamamoto, M., & Watanabe, Y. (2003). Rec8 cleavage by separase is required for meiotic nuclear divisions in fission yeast. *EMBO J, 22*(20), 5643-5653. doi: 10.1093/emboj/cdg527

Kitajima, T.S., Sakuno, T., Ishiguro, K., Iemura, S., Natsume, T., Kawashima, S.A. (2006). Shugoshin collaborates with protein phosphatase 2A to protect cohesin. *Nature, 441*(7089), 46-52. doi: 10.1038/nature04663

Klein, F., Mahr, P., Galova, M., Buonomo, S.B., Michaelis, C., Nairz, K. (1999). A central role for cohesins in sister chromatid cohesion, formation of axial elements, and recombination during yeast meiosis. *Cell, 98*(1), 91-103. doi: 10.1016/S0092-8674(00)80609-1

Koivomagi, M., Valk, E., Venta, R., Iofik, A., Lepiku, M., Morgan, D.O. (2011). Dynamics of Cdk1 substrate specificity during the cell cycle. *Mol Cell, 42*(5), 610-623. doi: S1097-2765(11)00383-2 [pii]10.1016/j.molcel.2011.05.016

Labib, K., Diffley, J.F., & Kearsey, S.E. (1999). G1-phase and B-type cyclins exclude the DNA-replication factor Mcm4 from the nucleus. *Nat Cell Biol, 1*(7), 415-422. doi: 10.1038/15649

Lee, B.H., & Amon, A. (2003). Role of Polo-like kinase CDC5 in programming meiosis I chromosome segregation. *Science, 300*(5618), 482-486. doi: 10.1126/science.10818461081846 [pii]

Lee, B.H., Kiburz, B.M., & Amon, A. (2004). Spo13 maintains centromeric cohesion and kinetochore coorientation during meiosis I. *Current biology : CB, 14*(24), 2168-2182. doi: 10.1016/j.cub.2004.12.033

Levine, K., Kiang, L., Jacobson, M.D., Fisher, R.P., & Cross, F.R. (1999). Directed evolution to bypass cyclin requirements for the Cdc28p cyclin-dependent kinase. *Mol Cell, 4*(3), 353-363. doi: S1097-2765(00)80337-8 [pii]

Li, R., & Murray, A.W. (1991). Feedback control of mitosis in budding yeast. *Cell, 66*(3), 519-531. doi: 0092-8674(81)90015-5 [pii]

Liu, D., Vader, G., Vromans, M.J., Lampson, M.A., & Lens, S.M. (2009). Sensing chromosome bi-orientation by spatial separation of aurora B kinase from kinetochore substrates. *Science, 323*(5919), 1350-1353. doi: 1167000 [pii]10.1126/science.1167000

Loog, M., & Morgan, D.O. (2005). Cyclin specificity in the phosphorylation of cyclin-dependent kinase substrates. *Nature, 434*(7029), 104-108. doi: nature03329 [pii]10.1038/nature03329

Losada, A., Hirano, M., & Hirano, T. (2002). Cohesin release is required for sister chromatid resolution, but not for condensin-mediated compaction, at the onset of mitosis. *Genes Dev, 16*(23), 3004-3016. doi: 10.1101/gad.249202

Marston, A.L., & Amon, A. (2004). Meiosis: cell-cycle controls shuffle and deal. *Nature reviews. Molecular cell biology, 5*(12), 983-997. doi: 10.1038/nrm1526

Marston, A.L., Lee, B.H., & Amon, A. (2003). The Cdc14 phosphatase and the FEAR network control meiotic spindle disassembly and chromosome segregation. *Dev Cell, 4*(5), 711-726. doi: S1534580703001308 [pii]

Marston, A.L., Tham, W.H., Shah, H., & Amon, A. (2004). A genome-wide screen identifies genes required for centromeric cohesion. *Science, 303*(5662), 1367-1370. doi: 10.1126/science.1094220

Masumoto, H., Sugino, A., & Araki, H. (2000). Dpb11 controls the association between DNA polymerases alpha and epsilon and the autonomously replicating sequence region of budding yeast. *Mol Cell Biol, 20*(8), 2809-2817.

Matos, J., Lipp, J.J., Bogdanova, A., Guillot, S., Okaz, E., Junqueira, M. (2008). Dbf4-dependent CDC7 kinase links DNA replication to the segregation of homologous chromosomes in meiosis I. *Cell, 135*(4), 662-678. doi: 10.1016/j.cell.2008.10.026

McCleland, M.L., Gardner, R.D., Kallio, M.J., Daum, J.R., Gorbsky, G.J., Burke, D.J. (2003). The highly conserved Ndc80 complex is required for kinetochore assembly, chromosome congression, and spindle checkpoint activity. *Genes Dev, 17*(1), 101-114. doi: 10.1101/gad.1040903

McDonald, K., O'Toole, E.T., Mastronarde, D.N., Winey, M., & Richard McIntosh, J. (1996). Mapping the three-dimensional organization of microtubules in mitotic spindles of yeast. *Trends Cell Biol, 6*(6), 235-239. doi: 0962-8924(96)40003-4 [pii]

Mendenhall, M.D. (1993). An inhibitor of p34CDC28 protein kinase activity from Saccharomyces cerevisiae. *Science, 259*(5092), 216-219.

Mendenhall, M.D., & Hodge, A.E. (1998). Regulation of Cdc28 cyclin-dependent protein kinase activity during the cell cycle of the yeast Saccharomyces cerevisiae. *Microbiology and molecular biology reviews : MMBR, 62*(4), 1191-1243.

Mimura, S., Seki, T., Tanaka, S., & Diffley, J.F. (2004). Phosphorylation-dependent binding of mitotic cyclins to Cdc6 contributes to DNA replication control. *Nature, 431*(7012), 1118-1123. doi: nature03024 [pii]10.1038/nature03024

Monje-Casas, F., Prabhu, V.R., Lee, B.H., Boselli, M., & Amon, A. (2007). Kinetochore orientation during meiosis is controlled by Aurora B and the monopolin complex. *Cell, 128*(3), 477-490. doi: 10.1016/j.cell.2006.12.040

Mukhopadhyay, D., Arnaoutov, A., & Dasso, M. (2010). The SUMO protease SENP6 is essential for inner kinetochore assembly. *J Cell Biol, 188*(5), 681-692. doi: jcb.200909008 [pii]10.1083/jcb.200909008

Muramatsu, S., Hirai, K., Tak, Y.S., Kamimura, Y., & Araki, H. (2010). CDK-dependent complex formation between replication proteins Dpb11, Sld2, Pol (epsilon}, and GINS in budding yeast. *Genes Dev, 24*(6), 602-612. doi: 24/6/602 [pii]10.1101/gad.1883410

Musacchio, A., & Hardwick, K.G. (2002). The spindle checkpoint: structural insights into dynamic signalling. *Nat Rev Mol Cell Biol, 3*(10), 731-741. doi: 10.1038/nrm929nrm929 [pii]

Nash, P., Tang, X., Orlicky, S., Chen, Q., Gertler, F.B., Mendenhall, M.D. (2001). Multisite phosphorylation of a CDK inhibitor sets a threshold for the onset of DNA replication. *Nature, 414*(6863), 514-521. doi: 10.1038/3510700935107009 [pii]

Neale, M.J., Pan, J., & Keeney, S. (2005). Endonucleolytic processing of covalent protein-linked DNA double-strand breaks. *Nature, 436*(7053), 1053-1057. doi: nature03872 [pii]10.1038/nature03872

Nguyen, V.Q., Co, C., Irie, K., & Li, J.J. (2000). Clb/Cdc28 kinases promote nuclear export of the replication initiator proteins Mcm2-7. *Curr Biol, 10*(4), 195-205. doi: S0960-9822(00)00337-7 [pii]

Nigg, E.A. (1993). Cellular substrates of p34(cdc2) and its companion cyclin-dependent kinases. *Trends Cell Biol, 3*(9), 296-301. doi: 096289249390011O [pii]

O'Toole, E.T., Mastronarde, D.N., Giddings, T.H., Jr., Winey, M., Burke, D.J., & McIntosh, J.R. (1997). Three-dimensional analysis and ultrastructural design of mitotic spindles from the cdc20 mutant of Saccharomyces cerevisiae. *Mol Biol Cell, 8*(1), 1-11.

Okaz, E., Arguello-Miranda, O., Bogdanova, A., Vinod, P.K., Lipp, J.J., Markova, Z. (2012). Meiotic Prophase Requires Proteolysis of M Phase Regulators Mediated by the Meiosis-Specific APC/C(Ama1). *Cell, 151*(3), 603-618. doi: 10.1016/j.cell.2012.08.044S0092-8674(12)01180-4 [pii]

Page, S.L., & Hawley, R.S. (2004). The genetics and molecular biology of the synaptonemal complex. *Annu Rev Cell Dev Biol, 20*, 525-558. doi: 10.1146/annurev.cellbio.19.111301.155141

Paliulis, L.V., & Nicklas, R.B. (2000). The reduction of chromosome number in meiosis is determined by properties built into the chromosomes. *J Cell Biol, 150*(6), 1223-1232.

Pavletich, N.P. (1999). Mechanisms of cyclin-dependent kinase regulation: structures of Cdks, their cyclin activators, and Cip and INK4 inhibitors. *J Mol Biol, 287*(5), 821-828. doi: S0022-2836(99)92640-2 [pii]10.1006/jmbi.1999.2640

Peter, M., & Herskowitz, I. (1994). Direct inhibition of the yeast cyclin-dependent kinase Cdc28-Cln by Far1. *Science, 265*(5176), 1228-1231.

Petronczki, M., Matos, J., Mori, S., Gregan, J., Bogdanova, A., Schwickart, M. (2006). Monopolar attachment of sister kinetochores at meiosis I requires casein kinase 1. *Cell, 126*(6), 1049-1064. doi: 10.1016/j.cell.2006.07.029

Pinsky, B.A., Kung, C., Shokat, K.M., & Biggins, S. (2006). The Ipl1-Aurora protein kinase activates the spindle checkpoint by creating unattached kinetochores. *Nat Cell Biol, 8*(1), 78-83. doi: ncb1341 [pii]10.1038/ncb1341

Primig, M., Williams, R.M., Winzeler, E.A., Tevzadze, G.G., Conway, A.R., Hwang, S.Y. (2000). The core meiotic transcriptome in budding yeasts. *Nat Genet, 26*(4), 415-423. doi: 10.1038/82539

Rabitsch, K.P., Petronczki, M., Javerzat, J.P., Genier, S., Chwalla, B., Schleiffer, A. (2003). Kinetochore recruitment of two nucleolar proteins is required for homolog segregation in meiosis I. *Developmental cell, 4*(4), 535-548.

Rahal, R., & Amon, A. (2008). Mitotic CDKs control the metaphase-anaphase transition and trigger spindle elongation. *Genes Dev, 22*(11), 1534-1548. doi: 22/11/1534 [pii]10.1101/gad.1638308

Richardson, H., Lew, D.J., Henze, M., Sugimoto, K., & Reed, S.I. (1992). Cyclin-B homologs in Saccharomyces cerevisiae function in S phase and in G2. *Genes Dev, 6*(11), 2021-2034.

Riedel, C.G., Katis, V.L., Katou, Y., Mori, S., Itoh, T., Helmhart, W. (2006). Protein phosphatase 2A protects centromeric sister chromatid cohesion during meiosis I. *Nature, 441*(7089), 53-61. doi: 10.1038/nature04664

Roeder, G.S., & Bailis, J.M. (2000). The pachytene checkpoint. *Trends Genet, 16*(9), 395-403. doi: S0168-9525(00)02080-1 [pii]

Russell, P., Moreno, S., & Reed, S.I. (1989). Conservation of mitotic controls in fission and budding yeasts. *Cell, 57*(2), 295-303. doi: 0092-8674(89)90967-7 [pii]

Sakuno, T., Tada, K., & Watanabe, Y. (2009). Kinetochore geometry defined by cohesion within the centromere. *Nature, 458*(7240), 852-858. doi: nature07876 [pii]10.1038/nature07876

Schleiffer, A., Kaitna, S., Maurer-Stroh, S., Glotzer, M., Nasmyth, K., & Eisenhaber, F. (2003). Kleisins: a superfamily of bacterial and eukaryotic SMC protein partners. *Molecular cell, 11*(3), 571-575.

Schwab, M., Neutzner, M., Mocker, D., & Seufert, W. (2001). Yeast Hct1 recognizes the mitotic cyclin Clb2 and other substrates of the ubiquitin ligase APC. *EMBO J, 20*(18), 5165-5175. doi: 10.1093/emboj/20.18.5165

Schwacha, A., & Kleckner, N. (1997). Interhomolog bias during meiotic recombination: meiotic functions promote a highly differentiated interhomolog-only pathway. *Cell, 90*(6), 1123-1135. doi: S0092-8674(00)80378-5 [pii]

Schwob, E., Bohm, T., Mendenhall, M.D., & Nasmyth, K. (1994). The B-type cyclin kinase inhibitor p40SIC1 controls the G1 to S transition in S. cerevisiae. *Cell, 79*(2), 233-244. doi: 0092-8674(94)90193-7 [pii]

Schwob, E., & Nasmyth, K. (1993). CLB5 and CLB6, a new pair of B cyclins involved in DNA replication in Saccharomyces cerevisiae. *Genes Dev, 7*(7A), 1160-1175.

Shirayama, M., Toth, A., Galova, M., & Nasmyth, K. (1999). APC(Cdc20) promotes exit from mitosis by destroying the anaphase inhibitor Pds1 and cyclin Clb5. *Nature, 402*(6758), 203-207. doi: 10.1038/46080

Shonn, M.A., McCarroll, R., & Murray, A.W. (2002). Spo13 protects meiotic cohesin at centromeres in meiosis I. *Genes Dev, 16*(13), 1659-1671. doi: 10.1101/gad.975802

Shuster, E.O., & Byers, B. (1989). Pachytene arrest and other meiotic effects of the start mutations in Saccharomyces cerevisiae. *Genetics, 123*(1), 29-43.

Skowyra, D., Craig, K.L., Tyers, M., Elledge, S.J., & Harper, J.W. (1997). F-box proteins are receptors that recruit phosphorylated substrates to the SCF ubiquitin-ligase complex. *Cell, 91*(2), 209-219. doi: S0092-8674(00)80403-1 [pii]

Smith, A.V., & Roeder, G.S. (1997). The yeast Red1 protein localizes to the cores of meiotic chromosomes. *J Cell Biol, 136*(5), 957-967.

Smith, M.M. (2002). Centromeres and variant histones: what, where, when and why? *Curr Opin Cell Biol, 14*(3), 279-285. doi: S0955067402003319 [pii]

Sumara, I., Vorlaufer, E., Stukenberg, P.T., Kelm, O., Redemann, N., Nigg, E.A. (2002). The dissociation of cohesin from chromosomes in prophase is regulated by Polo-like kinase. *Mol Cell, 9*(3), 515-525. doi: S1097276502004732 [pii]

Surana, U., Robitsch, H., Price, C., Schuster, T., Fitch, I., Futcher, A.B. (1991). The role of CDC28 and cyclins during mitosis in the budding yeast S. cerevisiae. *Cell, 65*(1), 145-161. doi: 0092-8674(91)90416-V [pii]

Taieb, F.E., Gross, S.D., Lewellyn, A.L., & Maller, J.L. (2001). Activation of the anaphase-promoting complex and degradation of cyclin B is not required for progression from Meiosis I to II in Xenopus oocytes. *Curr Biol, 11*(7), 508-513. doi: S0960-9822(01)00145-2 [pii]

Tanaka, S., Umemori, T., Hirai, K., Muramatsu, S., Kamimura, Y., & Araki, H. (2007). CDK-dependent phosphorylation of Sld2 and Sld3 initiates DNA replication in budding yeast. *Nature, 445*(7125), 328-332. doi: nature05465 [pii]10.1038/nature05465

Tanaka, T.U., Rachidi, N., Janke, C., Pereira, G., Galova, M., Schiebel, E. (2002). Evidence that the Ipl1-Sli15 (Aurora kinase-INCENP) complex promotes chromosome bi-orientation by altering kinetochore-spindle pole connections. *Cell, 108*(3), 317-329. doi: S0092867402006335 [pii]

Tang, T.T., Bickel, S.E., Young, L.M., & Orr-Weaver, T.L. (1998). Maintenance of sister-chromatid cohesion at the centromere by the Drosophila MEI-S332 protein. *Genes Dev, 12*(24), 3843-3856.

Toth, A., Rabitsch, K.P., Galova, M., Schleiffer, A., Buonomo, S.B., & Nasmyth, K. (2000). Functional genomics identifies monopolin: a kinetochore protein required for segregation of homologs during meiosis i. *Cell, 103*(7), 1155-1168.

Tyers, M. (1996). The cyclin-dependent kinase inhibitor p40SIC1 imposes the requirement for Cln G1 cyclin function at Start. *Proc Natl Acad Sci U S A, 93*(15), 7772-7776.

Tyers, M., & Futcher, B. (1993). Far1 and Fus3 link the mating pheromone signal transduction pathway to three G1-phase Cdc28 kinase complexes. *Mol Cell Biol, 13*(9), 5659-5669.

Tytell, J.D., & Sorger, P.K. (2006). Analysis of kinesin motor function at budding yeast kinetochores. *J Cell Biol, 172*(6), 861-874. doi: jcb.200509101 [pii]10.1083/jcb.200509101

Ubersax, J.A., Woodbury, E.L., Quang, P.N., Paraz, M., Blethrow, J.D., Shah, K. (2003). Targets of the cyclin-dependent kinase Cdk1. *Nature, 425*(6960), 859-864. doi: 10.1038/nature02062nature02062 [pii]

Uhlmann, F., Lottspeich, F., & Nasmyth, K. (1999). Sister-chromatid separation at anaphase onset is promoted by cleavage of the cohesin subunit Scc1. *Nature, 400*(6739), 37-42. doi: 10.1038/21831

Uhlmann, F., Wernic, D., Poupart, M.A., Koonin, E.V., & Nasmyth, K. (2000). Cleavage of cohesin by the CD clan protease separin triggers anaphase in yeast. *Cell, 103*(3), 375-386.

van Hemert, M.J., Lamers, G.E., Klein, D.C., Oosterkamp, T.H., Steensma, H.Y., & van Heusden, G.P. (2002). The Saccharomyces cerevisiae Fin1 protein forms cell cycle-specific filaments between spindle pole bodies. *Proc Natl Acad Sci U S A, 99*(8), 5390-5393. doi: 10.1073/pnas.072556099072556099 [pii]

van Werven, F.J., & Amon, A. (2011). Regulation of entry into gametogenesis. *Philos Trans R Soc Lond B Biol Sci, 366*(1584), 3521-3531. doi: 10.1098/rstb.2011.0081366/1584/3521 [pii]

van Werven, F.J., Neuert, G., Hendrick, N., Lardenois, A., Buratowski, S., van Oudenaarden, A. (2012). Transcription of Two Long Noncoding RNAs Mediates Mating-Type Control of Gametogenesis in Budding Yeast. *Cell, 150*(6), 1170-1181. doi: 10.1016/j.cell.2012.06.049S0092-8674(12)00939-7 [pii]

Wagner, M.V., Smolka, M.B., de Bruin, R.A., Zhou, H., Wittenberg, C., & Dowdy, S.F. (2009). Whi5 regulation by site specific CDK-phosphorylation in Saccharomyces cerevisiae. *PLoS One, 4*(1), e4300. doi: 10.1371/journal.pone.0004300

Watanabe, Y., Yokobayashi, S., Yamamoto, M., & Nurse, P. (2001). Pre-meiotic S phase is linked to reductional chromosome segregation and recombination. *Nature, 409*(6818), 359-363. doi: 10.1038/35053103

Wei, R.R., Schnell, J.R., Larsen, N.A., Sorger, P.K., Chou, J.J., & Harrison, S.C. (2006). Structure of a central component of the yeast kinetochore: the Spc24p/Spc25p globular domain. *Structure, 14*(6), 1003-1009. doi: S0969-2126(06)00223-1 [pii]10.1016/j.str.2006.04.007

Weiss, E., & Winey, M. (1996). The Saccharomyces cerevisiae spindle pole body duplication gene MPS1 is part of a mitotic checkpoint. *J Cell Biol, 132*(1-2), 111-123.

Westermann, S., Drubin, D.G., & Barnes, G. (2007). Structures and functions of yeast kinetochore complexes. *Annu Rev Biochem, 76*, 563-591. doi: 10.1146/annurev.biochem.76.052705.160607

Westermann, S., Wang, H.W., Avila-Sakar, A., Drubin, D.G., Nogales, E., & Barnes, G. (2006). The Dam1 kinetochore ring complex moves processively on depolymerizing microtubule ends. *Nature, 440*(7083), 565-569. doi: nature04409 [pii]10.1038/nature04409

Widlund, P.O., Lyssand, J.S., Anderson, S., Niessen, S., Yates, J.R., 3rd, & Davis, T.N. (2006). Phosphorylation of the chromosomal passenger protein Bir1 is required for localization of Ndc10 to the spindle during anaphase and full spindle elongation. *Mol Biol Cell, 17*(3), 1065-1074. doi: E05-07-0640 [pii]10.1091/mbc.E05-07-0640

Winey, M., Mamay, C.L., O'Toole, E.T., Mastronarde, D.N., Giddings, T.H., Jr., McDonald, K.L. (1995). Three-dimensional ultrastructural analysis of the Saccharomyces cerevisiae mitotic spindle. *J Cell Biol, 129*(6), 1601-1615.

Winey, M., Morgan, G.P., Straight, P.D., Giddings, T.H., Jr., & Mastronarde, D.N. (2005). Three-dimensional ultrastructure of Saccharomyces cerevisiae meiotic spindles. *Mol Biol Cell, 16*(3), 1178-1188. doi: E04-09-0765 [pii]10.1091/mbc.E04-09-0765

Winey, M., & O'Toole, E.T. (2001). The spindle cycle in budding yeast. *Nat Cell Biol, 3*(1), E23-27. doi: 10.1038/35050663

Woodbury, E.L., & Morgan, D.O. (2007a). Cdk and APC activities limit the spindle-stabilizing function of Fin1 to anaphase. *Nat Cell Biol, 9*(1), 106-112. doi: ncb1523 [pii]10.1038/ncb1523

Woodbury, E.L., & Morgan, D.O. (2007b). The role of self-association in Fin1 function on the mitotic spindle. *J Biol Chem, 282*(44), 32138-32143. doi: M705344200 [pii]10.1074/jbc.M705344200

Xu, L., Ajimura, M., Padmore, R., Klein, C., & Kleckner, N. (1995). NDT80, a meiosis-specific gene required for exit from pachytene in Saccharomyces cerevisiae. *Molecular and cellular biology, 15*(12), 6572-6581.

Xu, Z., Cetin, B., Anger, M., Cho, U.S., Helmhart, W., Nasmyth, K. (2009). Structure and function of the PP2A-shugoshin interaction. *Mol Cell, 35*(4), 426-441. doi: S1097-2765(09)00472-9 [pii]10.1016/j.molcel.2009.06.031

Yokobayashi, S., & Watanabe, Y. (2005). The kinetochore protein Moa1 enables cohesion-mediated monopolar attachment at meiosis I. *Cell, 123*(5), 803-817. doi: S0092-8674(05)00966-9 [pii]10.1016/j.cell.2005.09.013

Yokobayashi, S., Yamamoto, M., & Watanabe, Y. (2003). Cohesins determine the attachment manner of kinetochores to spindle microtubules at meiosis I in fission yeast. *Mol Cell Biol, 23*(11), 3965-3973.

Yu, H.G., & Koshland, D. (2005). Chromosome morphogenesis: condensin-dependent cohesin removal during meiosis. *Cell, 123*(3), 397-407. doi: 10.1016/j.cell.2005.09.014

Zegerman, P., & Diffley, J.F. (2007). Phosphorylation of Sld2 and Sld3 by cyclin-dependent kinases promotes DNA replication in budding yeast. *Nature, 445*(7125), 281-285. doi: nature05432 [pii]10.1038/nature05432

Chapter 2:

Meiosis I Chromosome Segregation is Established through Regulation of Microtubule-Kinetochore Interactions

The experiments presented in this Chapter were completed together with Dr. Elçin Ünal with the following exceptions:

M. Miller – Figure 2A,C-D; 5A-B; 8F-H; 9A,E-F; 10A and 11D

E. Ünal – Figure 1A-C; 3B,F-H; 6G-I and 7H

Dr. Gloria A. Brar performed the ribosome footprinting – Figure 10B-D; 11B,C,D; 12B-G

Reprinted from *eLife*.

INTRODUCTION

Cells have evolved intricate mechanisms to execute proper partitioning of the genetic material during cell division. This task is especially complex in meiosis, the cell division used by sexually reproducing organisms to generate gametes. The goal of meiosis is to reduce the genome content by half such that proper ploidy is maintained upon fusion of gametes. To achieve this, a single round of DNA replication is followed by two consecutive rounds of nuclear division called meiosis I and meiosis II. During meiosis I homologous chromosomes segregate. Meiosis II resembles mitosis in that sister chromatids segregate from each other. The establishment of this specialized chromosome segregation pattern requires three changes that modulate how chromosomes interact with each other and with the microtubule cytoskeleton: (1) reciprocal recombination between homologous chromosomes, (2) the way linkages between sister chromatids, known as sister-chromatid cohesion, are removed from chromosomes and (3) the manner in which chromosomes attach to the meiotic spindle.

Homologous recombination is initiated by programmed double-strand breaks (DSBs), which are catalyzed by Spo11 following premeiotic DNA replication (Keeney, Giroux, & Kleckner, 1997). Subsequent repair of DSBs by crossover recombination generates physical linkages between homologous chromosomes. This, in turn, allows homologs to attach to the meiosis I spindle such that each homolog interacts with microtubules emanating from opposite spindle poles. As a result, homologous chromosomes biorient on the meiosis I spindle. The spindle assembly checkpoint prevents the onset of chromosome segregation until this process is completed. Once

each pair of homologs is bioriented, checkpoint signaling ceases and anaphase entry ensues. A ubiquitin ligase known as the anaphase promoting complex/cyclosome and its specificity factor Cdc20 (APC/C-Cdc20) targets Securin for degradation, relieving Separase inhibition (Ciosk et al., 1998; Cohen-Fix, Peters, Kirschner, & Koshland, 1996). Separase is a protease that cleaves the kleisin subunit of cohesin, the protein complex that mediates sister-chromatid cohesion (Schleiffer et al., 2003; Uhlmann, Lottspeich, & Nasmyth, 1999; Uhlmann, Wernic, Poupart, Koonin, & Nasmyth, 2000). In meiosis I, cleavage of cohesin at chromosome arms allows homologs to segregate (Buonomo et al., 2000). However, cohesin around the centromeres is protected from cleavage during meiosis I, which is essential for the accurate segregation of sister chromatids during meiosis II. Protection of centromeric cohesin is accomplished by preventing phosphorylation of Rec8, the meiosis-specific kleisin. This occurs, at least in part, by Sgo1 (MEI-S332)-dependent recruitment of the protein phosphatase PP2A to centromeric regions where it antagonizes Rec8 phosphorylation (Katis, Galova, Rabitsch, Gregan, & Nasmyth, 2004; Kerrebrock, Moore, Wu, & Orr-Weaver, 1995; Kitajima, Kawashima, & Watanabe, 2004; Kitajima et al., 2006; Riedel et al., 2006).

The third modification necessary to bring about the meiotic chromosome segregation pattern is the manner in which kinetochores attach to microtubules during meiosis I and meiosis II. In meiosis I, kinetochores of sister chromatid pairs (henceforth sister kinetochores) attach to microtubules emanating from the same spindle pole, a process called sister kinetochore coorientation. During meiosis II, as during mitosis, sister kinetochores attach to microtubules emanating from opposite spindle poles and

are thus bioriented (reviewed in Marston & Amon, 2004). In budding yeast, sister kinetochore coorientation is brought about by the monopolin complex, which consists of Mam1, Lrs4, Csm1 and the casein kinase 1, Hrr25 (Petronczki et al., 2006; Rabitsch et al., 2003; Toth et al., 2000). Lrs4 and Csm1 localize to the nucleolus during interphase. During exit from pachytene, a stage of prophase I, Lrs4 and Csm1 associate with Mam1 and Hrr25 at kinetochores, a process that requires the Polo kinase Cdc5 (Clyne et al., 2003; B. H. Lee & Amon, 2003; Matos et al., 2008). How the association of monopolin with kinetochores is coordinated with respect to kinetochore assembly and microtubule-kinetochore interactions during meiosis is not understood.

Cyclin-dependent kinases (CDKs) are the central regulators of the mitotic and meiotic divisions. In budding yeast, a single CDK associates with one of six B-type cyclins (Clb1-Clb6) (reviewed in Morgan, 1997). In meiosis, Clb5- and Clb6-CDKs drive DNA replication and recombination, whereas Clb1-, Clb3- and Clb4-CDKs promote the meiotic nuclear divisions (reviewed in Marston & Amon, 2004). Meiotic cyclin-CDK activity is regulated both at the transcriptional and translational level (Carlile & Amon, 2008; Grandin & Reed, 1993). Transcription of *CLB1*, *CLB3* and *CLB4* occurs only after exit from pachytene (Chu & Herskowitz, 1998); *CLB3* is also translationally repressed during meiosis I, thus restricting Clb3-CDK activity to meiosis II (Carlile & Amon, 2008). The major mitotic cyclin, *CLB2*, is not expressed during meiosis (Grandin & Reed, 1993).

Here we investigate the importance of cyclin-CDK regulation in establishing the meiotic chromosome segregation pattern. We show that expression of a subset of

cyclins during premeiotic S phase and early prophase I, defined as the prophase stages up to exit from pachytene, causes premature microtubule-kinetochore interactions. This, in turn, disrupts both sister kinetochore coorientation and protection of centromeric cohesin during meiosis I, revealing that the temporal control of microtubule-kinetochore interactions is essential for meiosis I chromosome morphogenesis. Furthermore, we define the mechanism by which premature microtubule-kinetochore interactions are prevented; through regulation of cyclin-CDK activity and of outer kinetochore assembly. Our results demonstrate that preventing premature microtubule-kinetochore interactions is essential for establishing a meiosis I-specific chromosome architecture and provide critical insights into how the mitotic chromosome segregation machinery is modulated to achieve a meiosis I-specific pattern of chromosome segregation.

RESULTS

Cyclin expression is sufficient to induce spindle formation and microtubule-kinetochore interactions.

We previously reported that *CLB3* expression prior to meiosis I induces a change in the pattern of chromosome segregation such that sister chromatids, instead of homologous chromosomes, segregate during the first nuclear division (Carlile & Amon, 2008). To determine how Clb-CDKs impact meiotic chromosome segregation and whether Clb-CDKs play redundant or specific roles in regulating this process, we examined the consequences of prematurely expressing *CLB1*, *CLB3*, *CLB4* or *CLB5*.

In our previous studies we expressed *CLB3* from the *GAL1-10* promoter driven by an estrogen inducible Gal4-ER fusion (Carlile & Amon, 2008). Expression from the *GAL1-10* promoter led to Clb3 accumulation in meiosis I to levels that are comparable to those seen in meiosis II in wild-type cells (Carlile & Amon, 2008). However, estrogen interferes with meiotic progression when added during early stages of sporulation (Figure 1A). To circumvent this problem we utilized the copper-inducible *CUP1* promoter to drive Clb3 expression. Expression from the *CUP1* promoter led to approximately five-fold higher levels of Clb3 protein compared to expression from the *GAL1-10* promoter (Figure 1B). To examine the consequences of the two *CLB3* constructs on chromosome segregation we used *GAL-CLB3* and *CUP-CLB3* strains in which one of the two homologs of chromosome III was marked by integrating a tandem array of tetO

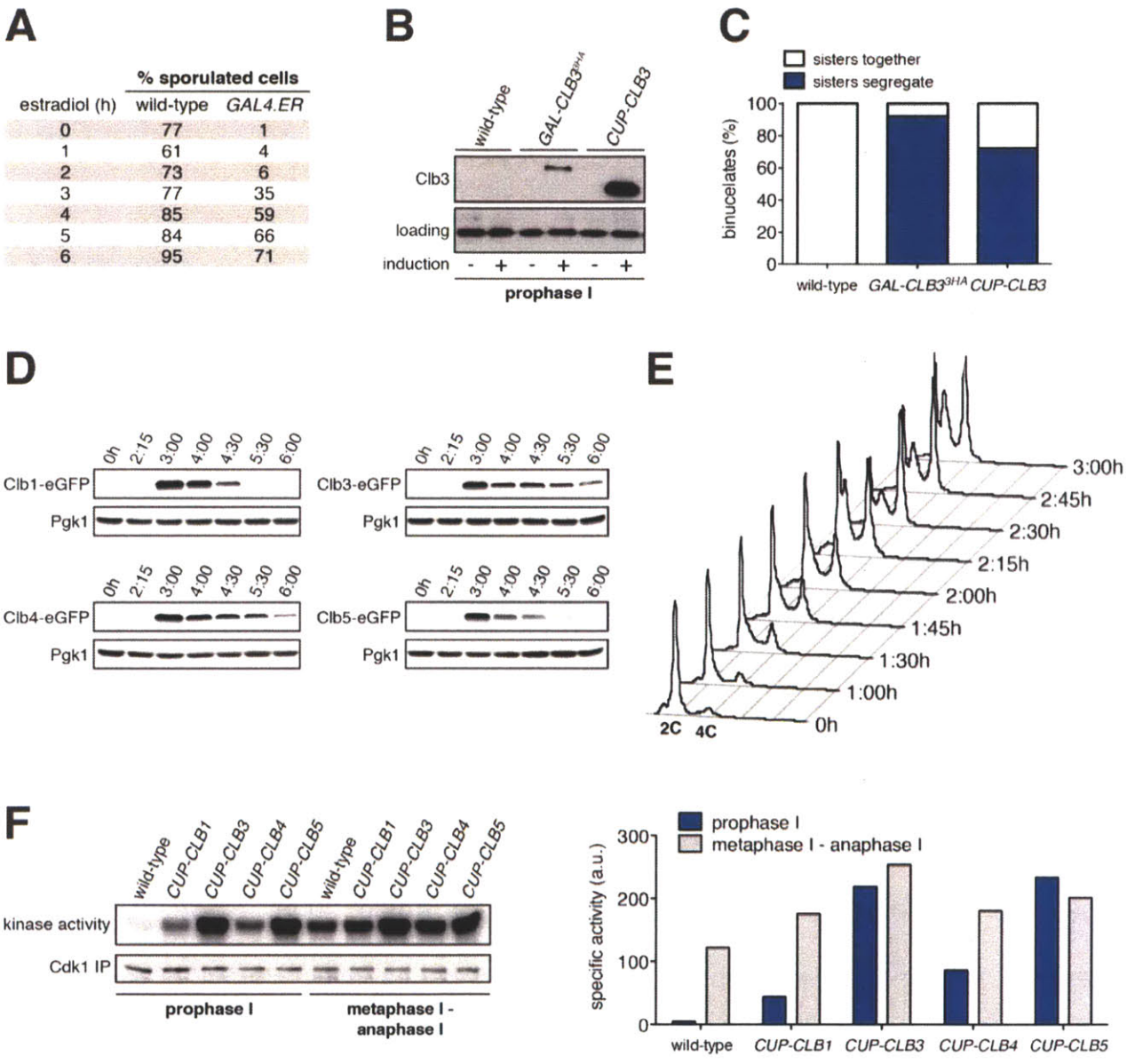

Figure 1. Characterization of premature cyclin expression and corresponding total CDK activity.

(A) Wild-type (A4962) and *GAL4-ER* (A19151) cells were induced to sporulate. At the indicated time points, an aliquot was removed and treated with estradiol (1µM). The percentage of cells that had sporulated after 24h was calculated as the sum of

dyads, triads and tetrads divided by the total number of cells (n>100 cells counted for each condition).

(B) Wild-type (A18686), *GAL-CLB3-3HA* (A23084) and *CUP-CLB3* (A23086) cells also carrying the *GAL4-ER* fusion were induced to sporulate. After 3h, *CLB3* was induced. Each culture was treated with estradiol (1μM) and $CuSO_4$ (50μM). Cells were harvested after 1h of estradiol and $CuSO_4$ treatment for protein extraction. Levels of Clb3 were examined by Western blot analysis. A cross-reacting band was used as a loading reference.

(C) Segregation of sister chromatids (equational division) using heterozygous GFP dots integrated at *LEU2* (~20kb from CENIII) was quantified in binucleate cells from wild-type (A18686), *GAL-CLB3-3HA* (A23084) and *CUP-CLB3* (A23086). Note that the samples were collected from the same experiment described in **(B)** at a time point when a fraction of the cells had completed meiosis I (6h 30 min and 7h after induction of sporulation) (n>100 for each sample). Using a chi-square test (df 1), the fraction of binucleates that display a reductional or equational division was compared between wild-type and *GAL-CLB3-3HA* $\chi^2 = 166.4$, $p < 0.0001$ and between wild-type and *CUP-CLB3* $\chi^2 = 108.7$, $p < 0.0001$.

(D) Wild-type or *CUP-CLB-eGFP* cells also carrying the *GAL4-ER* and *GAL-NDT80* fusions were induced to sporulate. After 2h 15min, cyclins were induced by addition of $CuSO_4$ (50μM). Cells were released from the *NDT80* block at 4h 30min post transfer to sporulation medium. Cyclin levels monitored by Western blot at the indicated time points in *CUP-CLB1-eGFP* (A28531), *CUP-CLB3-eGFP* (A28533), *CUP-CLB4-eGFP* (A28535) and *CUP-CLB5-eGFP* (A33199) cells. Pgk1 was used as a loading control.

(E) Wild-type (A22678) cells carrying the *GAL4-ER* and *GAL-NDT80* fusions were induced to sporulate and $CuSO_4$ (50μM) was added 2h 15min after transfer into sporulation medium. Samples were taken at indicated time points to determine DNA content by flow cytometry. By 2h 15min 43% of cells had a 4C DNA content.

(F) Left: Wild-type (A28663), *CUP-CLB1* (A28665), *CUP-CLB3* (A28667), *CUP-CLB4* (A28669) and *CUP-CLB5* (A28671) cells carrying the *GAL4-ER* and *GAL-NDT80*

fusions were induced to sporulate and $CuSO_4$ (50μM) was added 2h 30min after transfer into sporulation medium. *In vitro* kinase assays were performed with Cdc28-3V5 (Cdk1) immunoprecipitated from prophase I samples (collected 4h 30min after sporulation induction, at the time of *NDT80*-block release) and metaphase I-anaphase I samples (collected 1h 30min after release from the *NDT80*-block). Right: Specific activity was calculated by normalizing the amount of phosphorylated Histone H1 to the amount of immunoprecipitated Cdc28-3V5 using ImageQuant software (Molecular Dynamics).

sequences ~20kb from CENIII (heterozygous LEU2-GFP dots). These cells also expressed a tetR-GFP fusion, which allowed visualization of the tetO arrays (Michaelis, Ciosk, & Nasmyth, 1997). The analysis of GFP dot segregation during the first meiotic division revealed that despite the difference in Clb3 protein levels, the extent of sister chromatid segregation in meiosis I was similar between *GAL-CLB3* and *CUP-CLB3* cells (Figure 1C). This finding indicates that expression of Clb3 from either the *CUP1* or *GAL1-10* promoter efficiently induces sister chromatid segregation during meiosis I. Furthermore, the timing of when Clb3 is expressed, rather than the amount of Clb3 present, appears to be the primary determinant of this phenotype. Based on this observation and the finding that all four cyclins showed equal expression when produced from the *CUP1* promoter (Figure 1D) we utilized the *CUP1* promoter for most subsequent analyses.

Having established a system to effectively express various cyclins prior to meiosis I we next examined the consequences of their premature expression on meiosis I events. We first asked whether misexpression of various cyclins is sufficient to induce

spindle formation in cells arrested in pachytene of prophase I, due to lack of the transcription factor Ndt80 (Chu & Herskowitz, 1998; Xu, Ajimura, Padmore, Klein, & Kleckner, 1995). We induced cyclin expression from the *CUP1* promoter 135 minutes after the induction of sporulation when typically 40-65% of the cells have replicated their DNA (Figure 1E; Blitzblau, Chan, Hochwagen, & Bell, 2012) and examined spindle pole body (SPB, centrosome equivalent in budding yeast) separation and spindle morphology following induction. As expected, wild-type cells did not form spindles in the absence of *NDT80* function. Expression of *CLB5* from the *CUP1* promoter did not lead to SPB separation and spindle formation either, although expression of *CLB5* in the prophase I arrest led to a significant increase in total CDK activity (Figure 1F, Figure 2A, Figure 3A). In contrast, *CUP-CLB1*, *CUP-CLB3* and *CUP-CLB4* cells separated SPBs and formed bipolar spindles, shortly after copper addition (Figure 2A and Figure 3A). Similar results were observed in cells with intact *NDT80* (data not shown). We conclude that expression of *CLB1*, *CLB3* or *CLB4* is sufficient to promote bipolar spindle assembly in *NDT80*-depleted cells.

Next, we determined whether expression of *CLB1, CLB3* or *CLB4* in pachytene-arrested cells also affects the manner in which chromosomes attach to the meiotic spindle using live-cell imaging. To this end we used strains carrying heterozygous CENV-GFP dots and an Spc42-mCherry fusion (Spc42 is an SPB component) to monitor the behavior of the marked centromere with respect to the spindle axis. In wild-type and *CUP-CLB5* cells, sister kinetochores remained closely associated with each other and did not appear to be tightly associated with SPBs, consistent with the

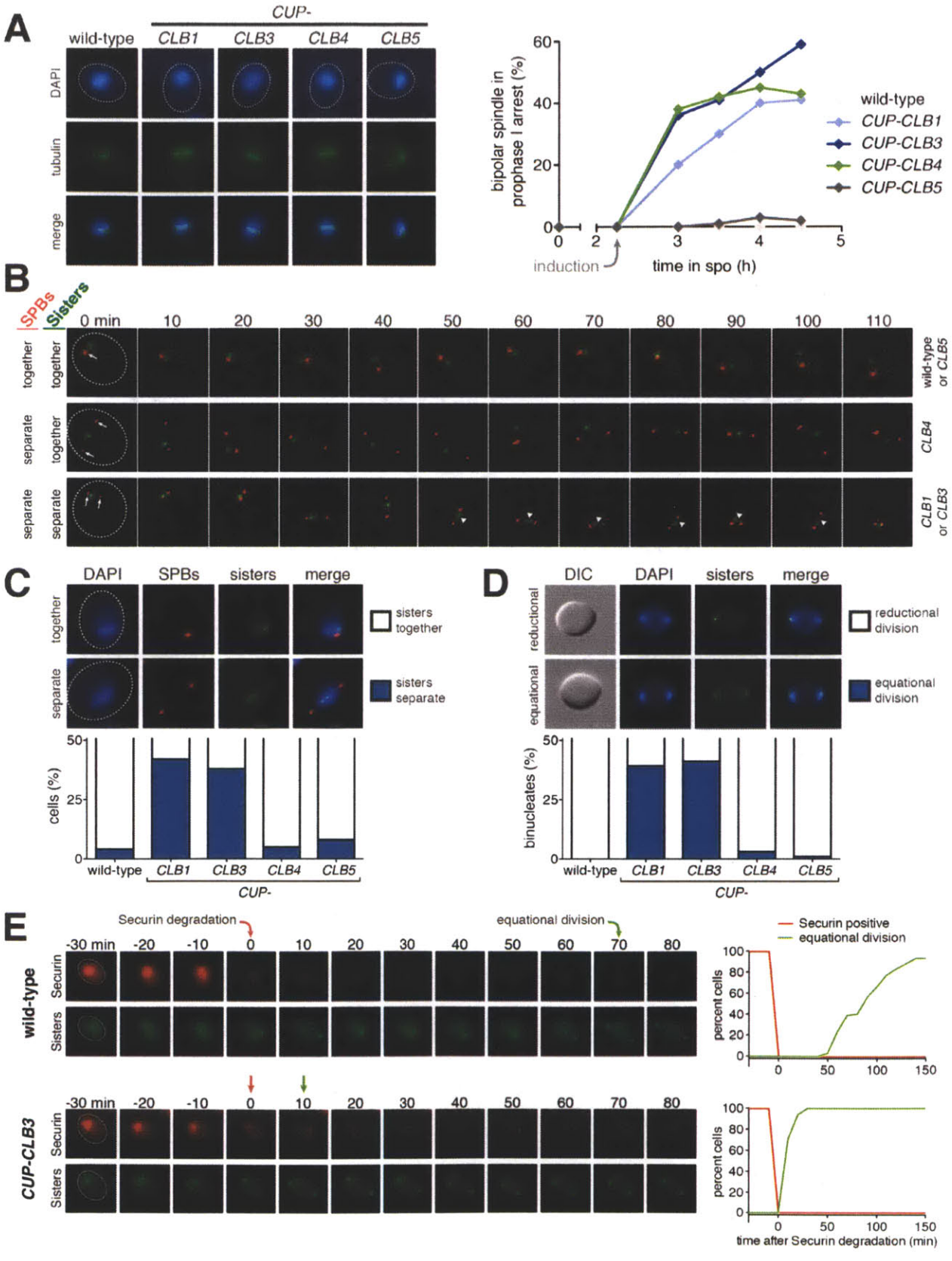
A
wild-type
CUP-
CLB1
CLB3
CLB4
CLB5
DAPI
tubulin
merge
bipolar spindle in prophase I arrest (%)
induction
time in spo (h)
wild-type
CUP-CLB1
CUP-CLB3
CUP-CLB4
CUP-CLB5
B
SPBs
Sisters
0 min
10
20
30
40
50
60
70
80
90
100
110
together
separate
wild-type or CLB5
CLB4
CLB1 or CLB3
C
DAPI
SPBs
sisters
merge
sisters together
sisters separate
cells (%)
D
DIC
reductional
equational
reductional division
equational division
binucleates (%)
E
Securin degradation
equational division
-30 min
-20
-10
wild-type
CUP-CLB3
Securin
Sisters
Securin positive
equational division
percent cells
time after Securin degradation (min)

Figure 2. Premature expression of *CLB1* or *CLB3* causes sister kinetochore biorientation during prophase I and sister chromatid segregation in meiosis I.

Wild-type or *CUP-CLB* cells were induced to sporulate. After 2h 15min, cyclins were induced by addition of $CuSO_4$. Cells were either arrested during prophase I or released from an *NDT80* block 4h 30min after induction of sporulation.

(A) Bipolar spindle formation determined in wild-type (A22678), *CUP-CLB1* (A27421), *CUP-CLB3* (A22702), *CUP-CLB4* (A27423) and *CUP-CLB5* (A27425) during prophase I (n=100 per time point). Images on left show spindle formation in *CUP-CLB* cells 4h after induction of sporulation; in this and all subsequent Figures microtubules are shown in green and DNA in blue. The dotted line depicts the cell membrane.

(B) Microtubule-kinetochore engagement monitored during prophase I, starting at 1h after $CuSO_4$ addition in wild-type (A30700), *CUP-CLB1* (A30702), *CUP-CLB3* (A30704), *CUP-CLB4* (A30707) and *CUP-CLB5* (A30708) by live cell microscopy. SPBs (marked by arrow) and heterozygous CENV-GFP dots are shown (arrowheads mark separated CENV dots). In this and all subsequent Figures SPBs are in red, GFP dots are in green.

(C) Top panel: representative images of wild-type (A30700) and *CUP-CLB3* (A30704). Bottom panel: Separation of heterozygous CENV-GFP dots in prophase I-arrested cells quantified in wild-type (A22678), *CUP-CLB1* (A27421), *CUP-CLB3* (A22702), *CUP-CLB4* (A27423) and *CUP-CLB5* (A27425) by live cell microscopy (over the duration of 8h, n>100) as described in the Materials and Methods. The fraction of nuclei that display sister kinetochores as separate or together for each *CUP-CLB* strain was compared to wild-type using a chi-square test (df 1): *CUP-CLB1*, $\chi^2 = 40.77$, $p < 0.0001$; *CUP-CLB3*, $\chi^2 = 34.84$, $p < 0.0001$; *CUP-CLB4*, $\chi^2 = 0.1163$, $p = 0.7330$; *CUP-CLB5*, $\chi^2 = 1.418$, $p = 0.2337$.

(D) Segregation of sister chromatids (equational division) using heterozygous CENV-GFP dots quantified in binucleates from wild-type (A22678), *CUP-CLB1* (A27421), *CUP-CLB3* (A22702), *CUP-CLB4* (A27423) and *CUP-CLB5* (A27425) (n=100).

The fraction of binucleates that display a reductional or equational division for each *CUP-CLB* strain was compared to wild-type using a chi-square test (df 1): *CUP-CLB1*, $\chi^2 = 45.13$, $p < 0.0001$; *CUP-CLB3*, $\chi^2 = 48.22$, $p < 0.0001$; *CUP-CLB4*, $\chi^2 = 1.020$, $p = 0.3124$; *CUP-CLB5*, $\chi^2 = 0$, $p = 1$.

(E) Wild-type (A31019) and *CUP-CLB3* (A31021) cells monitored for segregation of heterozygous CENV-GFP dots with respect to Pds1 (Securin, red) degradation by live cell microscopy (n>17). Time of Pds1 degradation set to t=0, percent cells were plotted as a Kaplan-Meier curve. Note that for A31021, the analysis of cells that segregate sister chromatids in the first nuclear division is shown. Pds1 accumulation during prophase II is not observed using the Pds1-tdTomato construct, likely due to delayed maturation of the fluorophore (Katis et al., 2010).

observation that these cells failed to form a spindle. In contrast, we observed dynamic separation of heterozygous CENV-GFP dots upon expression of *CLB1* or *CLB3*, with sister kinetochores frequently splitting and coming together (Figure 2B-C). This observation is reminiscent of the behavior of bioriented sister chromatids during metaphase of mitosis (Pearson, Maddox, Salmon, & Bloom, 2001).

Cells expressing *CLB4* did not show transient splitting of sister kinetochores in prophase I, indicating that chromosomes are either unable to attach to the spindle or that homologous chromosomes, instead of sister chromatids, are bioriented as occurs in wild-type cells during metaphase I. To distinguish between these possibilities, we examined the behavior of *CUP-CLB4* cells in which both homologs of chromosome V harbor CENV-GFP dots (henceforth homozygous CENV-GFP dots). Similar to wild-type, we observed that in *CUP-CLB4* cells the two CENV-GFP dots remained tightly

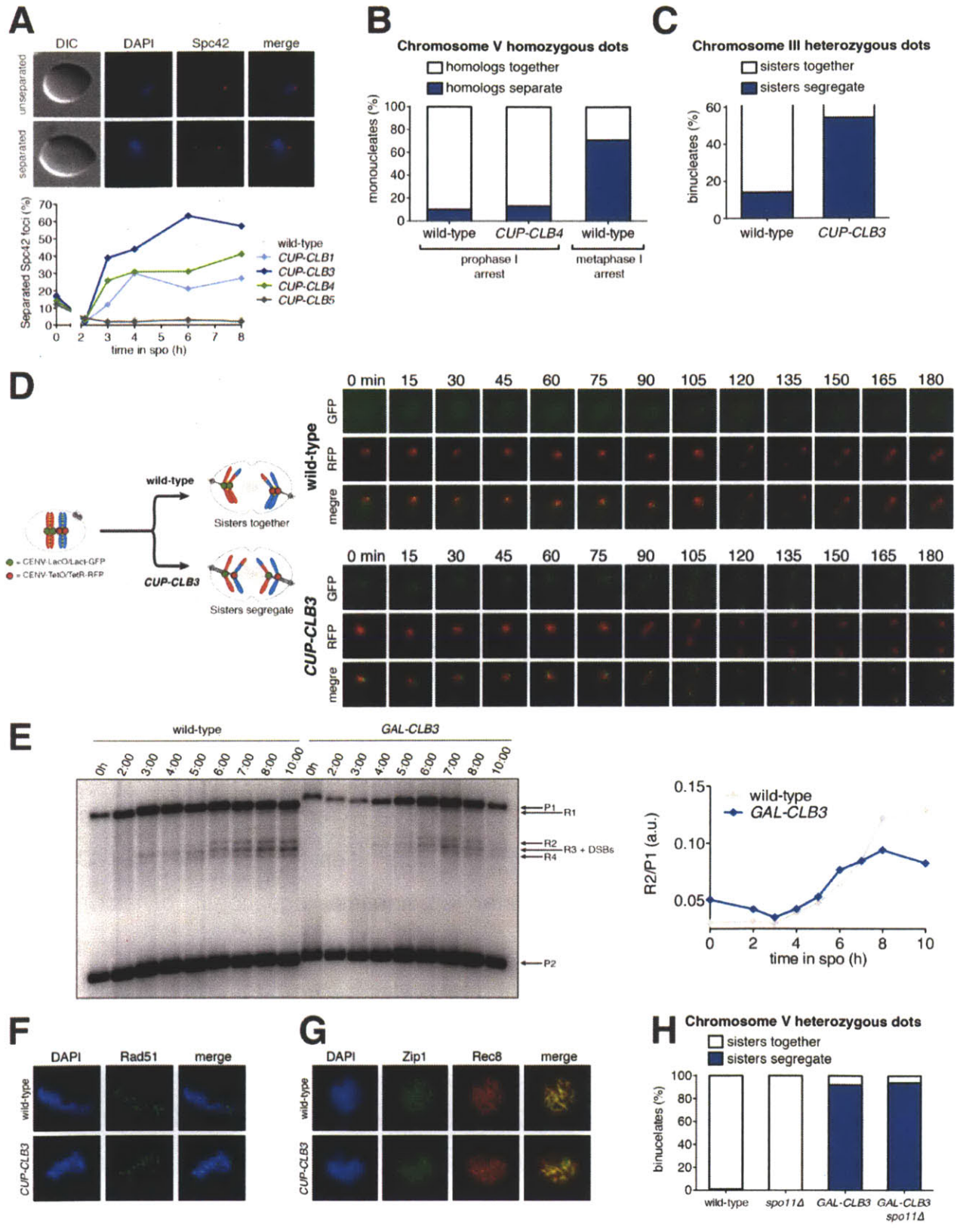
A
DIC
DAPI
Spc42
merge
unseparated
separated
Separated Spc42 foci (%)
time in spo (h)
wild-type
CUP-CLB1
CUP-CLB3
CUP-CLB4
CUP-CLB5
B
Chromosome V homozygous dots
homologs together
homologs separate
monucleates (%)
wild-type
CUP-CLB4
wild-type
prophase I arrest
metaphase I arrest
C
Chromosome III heterozygous dots
sisters together
sisters segregate
binucleates (%)
wild-type
CUP-CLB3
D
wild-type
CUP-CLB3
Sisters together
Sisters segregate
= CENV-LacO/LacI-GFP
= CENV-TetO/TetR-RFP
0 min 15 30 45 60 75 90 105 120 135 150 165 180
GFP
RFP
megre
E
wild-type
GAL-CLB3
0h 2:00 3:00 4:00 5:00 6:00 7:00 8:00 10:00
P1
R1
R2
R4
R3 + DSBs
P2
R2/P1 (a.u.)
time in spo (h)
F
DAPI
Rad51
merge
wild-type
CUP-CLB3
G
DAPI
Zip1
Rec8
merge
wild-type
CUP-CLB3
H
Chromosome V heterozygous dots
sisters together
sisters segregate
binucelates (%)
wild-type
spo11Δ
GAL-CLB3
GAL-CLB3 spo11Δ

Figure 3. Spindle pole body separation, homolog separation, sister chromatid segregation and recombination in *CUP-CLB* cells.

(A) Wild-type or *CUP-CLB* cells also carrying the *GAL4-ER* and *GAL-NDT80* fusions were induced to sporulate. After 2h 15min, cyclins were induced by addition of $CuSO_4$ (50μM). Cells were arrested during prophase I and the percentage of cells with separated Spc42 foci (red dots) was determined at indicated time points in wild-type (A29581), *CUP-CLB1* (A29582), *CUP-CLB3* (A29583), *CUP-CLB4* (A29584) and *CUP-CLB5* (A29585) (n>100 for each time point).

(B) Wild-type (A22688), *CUP-CLB4* (A32470) also carrying the *GAL4-ER* and *GAL-NDT80* fusions or *cdc20-mn* (A15163) cells all carrying homozygous CENV GFP dots were induced to sporulate. After 2h 15min, cyclins were induced by addition of $CuSO_4$ (50μM). Cells were arrested either during prophase I (A22688, A324470) or metaphase I (A15163). Separated GFP foci (homologs separate) were analyzed 6h (prophase I-arrest) or 8h 30min (metaphase I-arrest) after induction of sporulation (n>100 for each time point). Using a chi-square test (df 1), the fraction of mononucleates that display homologs as together or separate during a prophase I arrest was compared between wild-type and *CUP-CLB4* $\chi^2 = 0.4422$, $p = 0.5061$.

(C) Wild-type (A18185) and *CUP-CLB3* (A22682) cells also carrying the *GAL4-ER* and *GAL-NDT80* fusions were induced to sporulate. After 3h, *CLB3* was induced by addition of $CuSO_4$ (50μM). At 6h, cells were released from the *NDT80* block. Subsequently, segregation of sister chromatids (equational division) using heterozygous GFP dots integrated at *LEU2* (~20kb from CENIII) was quantified in binucleate cells. The appearance of segregated sister chromatids in wild-type is likely due to recombination between *LEU2* and *CEN3*. Using a chi-square test (df 1), the fraction of binucleates that display a reductional or equational division was compared between wild-type and *CUP-CLB3* $\chi^2 = 35.65$, $p < 0.0001$.

(D) Wild-type (A27476) and *CUP-CLB3* (A27480) cells carrying the *GAL4-ER* and *GAL-NDT80* fusions and CENV-LacO/LacI-GFP on one homolog of chromosome V (green) and CENV-tetO/tetR-RFP on the other homolog of chromosome V (red)

were induced to sporulate and $CuSO_4$ (50μM) was added at 2h 15min. At 4h 30min, cells were released from *NDT80* block and monitored by live cell microscopy starting 30min after estradiol addition, and monitored every 15min for 8h.

(E) Left panel: Wild-type (A21104) and *GAL-CLB3* (A21105) cells were induced to sporulate and estradiol (1μM) was added 3h after transfer into sporulation medium. Genomic DNA was prepared and digested with XhoI and MluI and hybridized with Probe A. See (Storlazzi, Xu, Cao, & Kleckner, 1995) for details. Right panel: Recombination products were quantified as R2/P1. Note: A21104 and A21105 contain auxotrophies and have reduced meiotic kinetics relative to prototrophic strains.

(F) Wild-type (A22864) and *CUP-CLB3* (A22866) cells were induced to sporulate and $CuSO_4$ (50μM) was added 3h after transfer into sporulation medium. Localization of the double-strand break repair protein Rad51 (green) was determined by nuclear spreads 4h after transfer to sporulation medium. DNA is shown in blue.

(G) Wild-type (A22836) and *CUP-CLB3* (A22838) cells were induced to sporulate and $CuSO_4$ (50μM) was added 3h after transfer into sporulation medium. Localization of the synaptonemal complex component Zip1 (green) and the cohesin subunit Rec8-13myc (red) was determined by nuclear spreads 5h after transfer to sporulation medium. DNA is shown in blue.

(H) Wild-type (A19396), *GAL-CLB3* (A19400), *spo11Δ* (A21193) and *spo11Δ GAL-CLB3* (A21194) cells were induced to sporulate and estradiol (1μM) was added 3h after transfer into sporulation medium. Subsequently, segregation of sister chromatids (equational division) was quantified using heterozygous CENV GFP dots in binucleate cells (n=100). Note that *CLB3*-induced meiosis I sister chromatid segregation is higher in *GAL-CLB3* cells than in *CUP-CLB3* cells. This is presumably due to the more homogenous expression of *CLB3* in cells where expression is driven from the *GAL1-10* promoter. Using a chi-square test (df 1), the fraction of binucleates that display a reductional or equational division was compared between *GAL-CLB3* and *GAL-CLB3 spo11Δ* $\chi^2 = 0.3072$, $p = 0.5794$.

associated in prophase I, indicating that the homologous chromosomes are paired and not attached to the prematurely formed spindle (Figure 3B). Together, these results indicate that *CUP-CLB1*, *CUP-CLB3* or *CUP-CLB4* expression promotes bipolar spindle formation in pachytene-arrested cells, but only *CLB1* and *CLB3* expression can promote stable microtubule-kinetochore attachments sufficient to generate tension.

To determine whether different amounts of total CDK activity were responsible for the phenotypic differences of prematurely expressing Clb1 or Clb3 compared to Clb4, we measured total CDK activity (Cdc28 in budding yeast) using Histone H1 a substrate. Cdc28-associated kinase activity was low during prophase I and increased more than 25-fold during metaphase I/anaphase I in wild-type cells (Figure 1F). Expression of all four cyclins led to a significant increase in total CDK activity in prophase I (Figure 1F), but importantly, the degree of increase did not correlate with the ability to induce sister chromatid splitting in the *NDT80* arrest. For example, Clb1 expression led to a similar increase in Cdc28-associated kinase activity as expression of Clb4, yet Clb1 induced sister chromatid splitting whereas Clb4 did not (Figure 1F, Figure 2B-C). We conclude that the ability to induce sister chromatid splitting does not correlate with total CDK activity produced by the various *CUP-CLB* fusions. Furthermore, SPB separation and spindle formation are not sufficient to induce microtubule-kinetochore interactions. Events that can be triggered by Clb1 and Clb3, but not Clb4 are also necessary to promote attachments sufficient to generate tension. Determining why *CLB4* expressing

cells fail to form productive microtubule-kinetochore interactions could provide important insights into substrate specificity of cyclin-CDK complexes.

Expression of *CLB3* or *CLB1* during premeiotic S-phase/prophase I causes sister chromatids to segregate during meiosis I.

To determine the consequences of premature cyclin expression on meiosis I chromosome segregation, we examined the segregation of heterozygous CENV-GFP dots in cells that were reversibly arrested in pachytene using the *NDT80* block-release system. In this system, expression of *NDT80* is controlled by the *GAL1-10* promoter, which is regulated by an estrogen-inducible Gal4-ER fusion (Benjamin, Zhang, Shokat, & Herskowitz, 2003; Carlile & Amon, 2008). Cells were induced to sporulate and after 135min, copper was added to induce cyclin expression. 4h 30min after sporulation induction, estrogen was added to allow cells to synchronously proceed through the meiotic divisions. In wild-type, *CUP-CLB4* and *CUP-CLB5* cells, sister chromatids cosegregated in the first division, resulting in binucleate cells with a GFP dot in one of the two nuclei. In contrast, 39% of *CUP-CLB1* and 41% of *CUP-CLB3* cells segregated sister chromatids in the first division, as judged by the presence of binucleate cells with a GFP dot in each nucleus (Figure 2D). We observed a similar result for chromosome III and cells in which one copy of chromosome V was marked with a GFP dot and the other copy with an RFP dot (Figure 3C-D).

To confirm that sister chromatids indeed split during meiosis I in cells expressing *CLB3* during prophase I, we examined when sister chromatid separation occurred with respect to Securin (Pds1 in budding yeast) degradation in *CUP-CLB3* cells. In wild-type cells harboring heterozygous CENV-GFP dots, Pds1 degradation was immediately followed by movement of the single GFP dot to one side of the cell, indicating that homologous chromosomes had segregated. Subsequently, these cells underwent meiosis II and sister chromatids segregated (median= 86min after Pds1 degradation; Figure 2E). In contrast, *CUP-CLB3* cells segregated sister chromatids immediately after Pds1 degradation (median= 7min after Pds1 degradation; Figure 2E). These results demonstrate that *CUP-CLB3* cells segregate sister chromatids during the first meiotic division. Thus, *CUP-CLB3* cells must be defective in two key aspects of meiosis I chromosome segregation: coorientation of sister kinetochores and maintenance of centromeric cohesion. We note that another essential aspect of meiosis I chromosome segregation, homologous recombination, was not affected by premature *CLB3* expression. We observed no major defects in DSB formation, synaptonemal complex assembly and generation of recombination products, nor did preventing homologous recombination affect the phenotypes caused by premature *CLB3* expression (Figure 3E-H).

Premature expression of *CLB3* interferes with monopolin localization.

The finding that *CUP-CLB1* or *CUP-CLB3* cells segregate sister chromatids during meiosis I indicates that sister kinetochore coorientation is defective. To investigate this further, we examined monopolin localization in cells that segregate sister chromatids in

meiosis I (*CUP-CLB3* cells) and cells that do not exhibit chromosome missegregation despite cyclin misexpression (*CUP-CLB4* cells). Colocalization of Lrs4 or Mam1 with the kinetochore component Ndc10 was dramatically reduced in *CUP-CLB3* but not *CUP-CLB4* cells (Figure 4A and Figure 5A-B). Hyperphosphorylation of Lrs4, which correlates with monopolin function (Clyne et al., 2003; B. H. Lee & Amon, 2003; Matos et al., 2008), was also significantly reduced in *CUP-CLB3*, but not in *CUP-CLB4* cells (Figure 4B and Figure 5C). These results indicate that premature expression of *CLB3* prevents monopolin association with kinetochores.

Centromeric cohesin is lost during meiosis I in *CUP-CLB3* cells.

Sister chromatids segregate during meiosis I in *CUP-CLB3* cells, indicating that centromeric cohesin either fails to associate with chromosomes or is lost prematurely. To test the first possibility, we examined chromosome association of the cohesin subunit Rec8 and the cohesion maintenance factor Pds5 with chromosomes. Chromatin immunoprecipitation (ChIP) and chromosome spreads revealed that association of both proteins with chromosomes in *CUP-CLB3* cells was indistinguishable from that of wild-type cells during prophase I or metaphase I (Figure 6A and Figure 7A-B). Thus, loading of cohesion factors onto chromosomes is not affected in *CUP-CLB3* cells.

To test the possibility that *CUP-CLB3* cells fail to maintain centromeric cohesion beyond anaphase I, we first determined the localization of the cohesin subunit Rec8 in cells that had progressed past metaphase I. Rec8 colocalized with the kinetochore component Ndc10 in binucleate wild-type and *CUP-CLB4* cells, demonstrating that

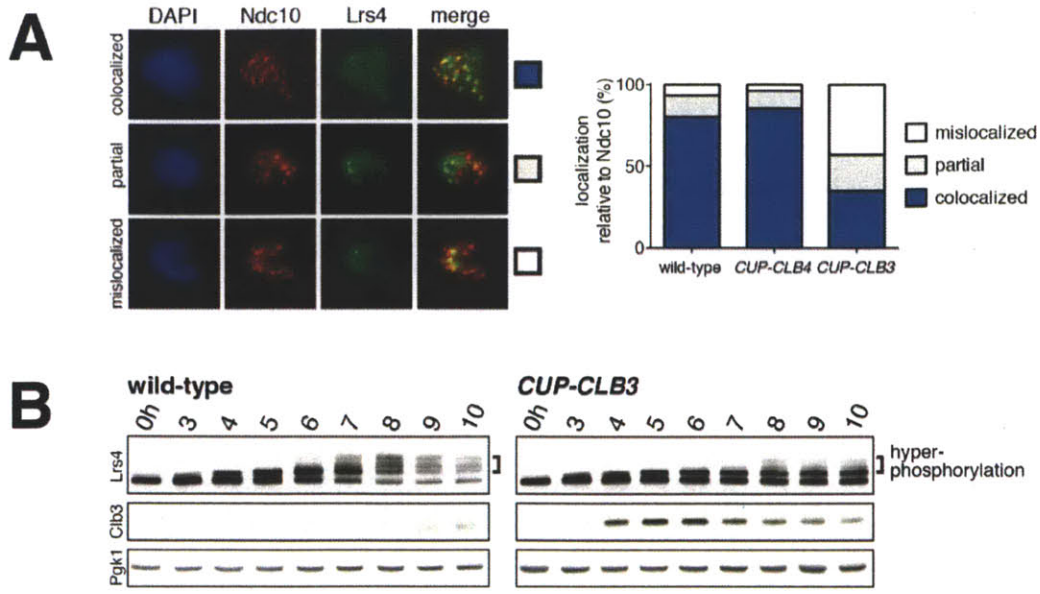

Figure 4. Premature *CLB3* expression disrupts monopolin function.

(A) Lrs4-13myc (green) localization relative to Ndc10-6HA (red) was determined in spread nuclei from wild-type (A9217), *CUP-CLB3* (A26278) and *CUP-CLB4* (A29643) harboring a Cdc20 depletion allele (*cdc20-mn*) were induced to undergo sporulation and arrested in metaphase I due to depletion of Cdc20. $CuSO_4$ was added at 3h after induction of sporulation (n>40). The fraction of spread nuclei that display colocalized, partial or mislocalized Lrs4 with respect to Ndc10 was compared to wild-type using a chi-square test (df 2): *CUP-CLB4*, $\chi^2 = 1.136$, $p = 0.5666$; *CUP-CLB3*, $\chi^2 = 45.84$, $p < 0.0001$.

(B) Western blots for Lrs4-13myc, Clb3 and Pgk1 from wild-type (A9217) and *CUP-CLB3* (A26278) cells. Cells were sporulated as described in **(A)**.

---

centromeric cohesin is protected from removal until the onset of anaphase II. In contrast, Rec8 was not detected around centromeres in a substantial fraction of binucleate *CUP-CLB3* cells (Figure 6B). Functional assays confirmed the defect in centromeric cohesion maintenance in *CUP-CLB3* cells. Although *mam1Δ* cells biorient

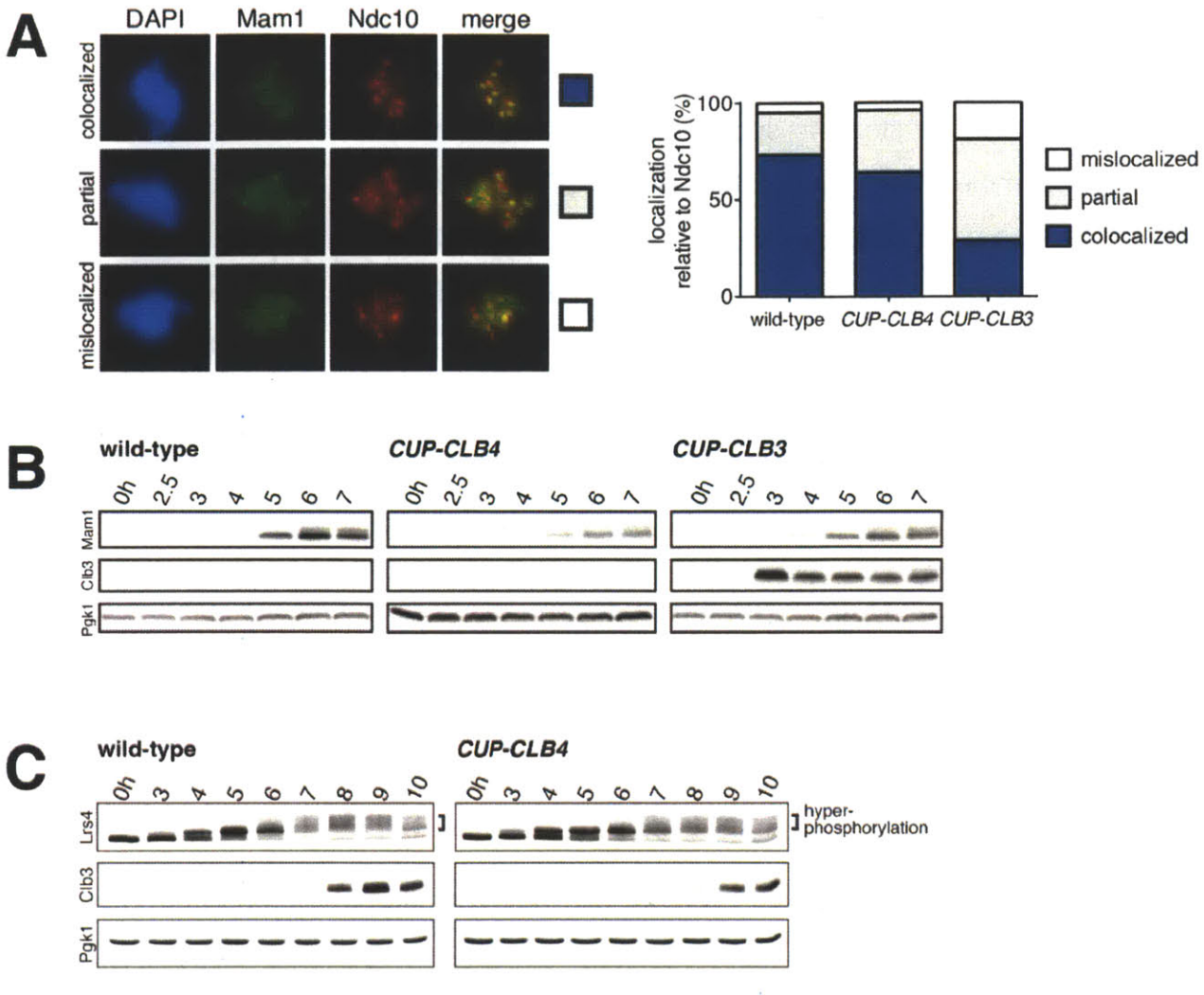

Figure 5. Monopolin association with kinetochores is disrupted in *CUP-CLB3* but not in *CUP-CLB4* cells.

(A) Wild-type (A7450), *CUP-CLB3* (A28673) and *CUP-CLB4* (A28674) cells carrying the *cdc20-mn* allele were induced to sporulate and $CuSO_4$ (50µM) was added 2h 30min after transfer into sporulation medium. Mam1-9myc (green) localization relative to Ndc10-6HA (red) was determined in spread nuclei from metaphase I-arrested cells (n>40). DNA is shown in blue. Using a chi-square test (df 2) the fraction of spread nuclei that display colocalized, partial or mislocalized Mam1 with respect to Ndc10 was compared to wild-type: *CUP-CLB4*, $\chi^2 = 2.554$, $p = 0.2788$; *CUP-CLB3*, $\chi^2 = 39.31$, $p < 0.0001$.

(B) Wild-type (A7450), *CUP-CLB3* (A28673) and *CUP-CLB4* (A28674) cells carrying the *cdc20-mn* allele were induced to sporulate and $CuSO_4$ (50μM) was added 2h 30min after transfer into sporulation medium. Mam1 protein levels were analyzed to determine whether premature Clb3 expression interferes with Mam1 expression. Pgk1 was used as a loading control.

(C) Wild-type (A26277) and *CUP-CLB4* (A29643) cells carrying the *cdc20-mn* allele were induced to sporulate and $CuSO_4$ (50μM) was added 2h 30min after transfer into sporulation medium. Levels of Lrs4, Clb3 and Pgk1 from cells arrested in metaphase I were examined by Western blot analysis.

---

sister chromatids during meiosis I, they delay nuclear division until meiosis II due to the presence of centromeric cohesin (Rabitsch et al., 2003; Toth et al., 2000). The delay in nuclear division of a *mam1Δ* was partially alleviated by the expression of *CUP-CLB3* (Figure 7C). This partial effect is likely due to not all *CUP-CLB3* cells losing centromeric cohesion prematurely in meiosis I (Figure 6B). We conclude that both centromeric and arm cohesin are lost from chromosomes at the onset of anaphase I in *CUP-CLB3* cells.

Next, we investigated the cause of premature centromeric cohesin removal in *CUP-CLB3* cells. Cleavage of cohesin by separase requires the phosphorylation of Rec8 at multiple residues (Brar et al., 2006; Katis et al., 2010). A recessive allele of *REC8* in which 29 *in vivo* phosphorylation sites were mutated to alanine (*rec8-29A*) (Brar et al., 2006) was not cleaved in *CUP-CLB3* cells, but wild-type Rec8 was (Figure 6C and Figure 7D). Furthermore, the *rec8-29A* allele caused a similar metaphase I delay in wild-type and *CUP-CLB3* cells when expressed as the sole source of *REC8* (Figure 6D and Figure 7E-F). We noticed that the Rec8 cleavage product was detected

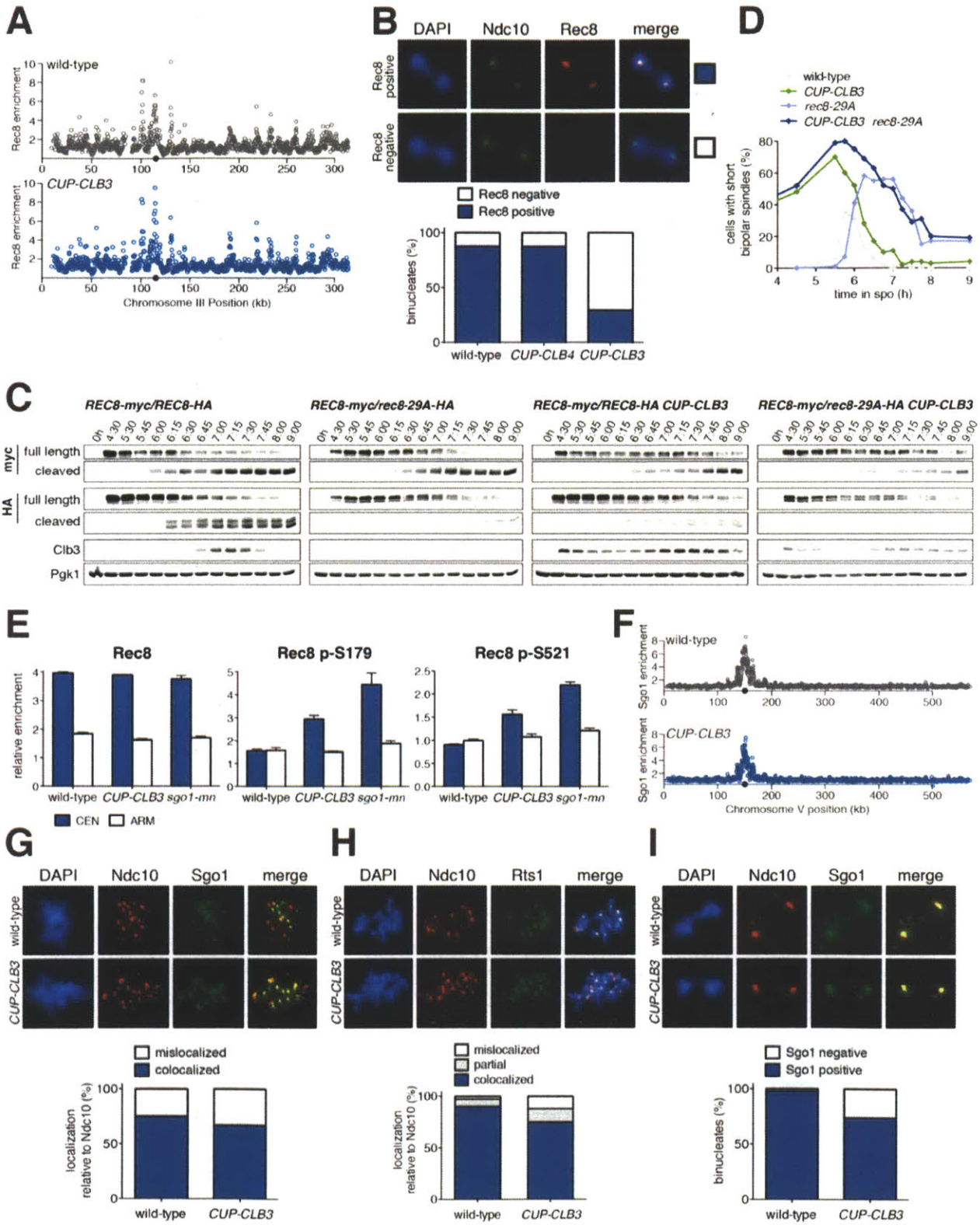
A
wild-type
CUP-CLB3
Rec8 enrichment
Chromosome III Position (kb)
B
DAPI
Ndc10
Rec8
merge
Rec8 positive
Rec8 negative
Rec8 negative
Rec8 positive
binucleates (%)
wild-type
CUP-CLB4
CUP-CLB3
D
wild-type
CUP-CLB3
rec8-29A
CUP-CLB3 rec8-29A
cells with short bipolar spindles (%)
time in spo (h)
C
REC8-myc/REC8-HA
REC8-myc/rec8-29A-HA
REC8-myc/REC8-HA CUP-CLB3
REC8-myc/rec8-29A-HA CUP-CLB3
myc
HA
full length
cleaved
Clb3
Pgk1
E
Rec8
Rec8 p-S179
Rec8 p-S521
relative enrichment
wild-type
CUP-CLB3
sgo1-mn
CEN
ARM
F
wild-type
CUP-CLB3
Sgo1 enrichment
Chromosome V position (kb)
G
DAPI
Ndc10
Sgo1
merge
wild-type
CUP-CLB3
mislocalized
colocalized
localization relative to Ndc10 (%)
H
DAPI
Ndc10
Rts1
merge
mislocalized
partial
colocalized
I
DAPI
Ndc10
Sgo1
merge
Sgo1 negative
Sgo1 positive
binucleates (%)

Figure 6. *CLB3* misexpression disrupts protection of centromeric cohesin.

Cyclin expression was induced after 2h 15min (C and D), 2h 30min (A, B, E, F and H) or 3h (G and I) of sporulation.

(A) Chromosomal association of Rec8-13myc was monitored by ChIP-chip in wild-type (A28716) and *CUP-CLB3* (A28718) during prophase I arrest. Centromere position is identified by a black circle.

(B) Centromeric Rec8 localization was monitored in spread nuclei from wild-type (A28684), *CUP-CLB3* (A28685) and *CUP-CLB4* (A28686) cells carrying *REC8-3HA* (red) and *NDC10-13myc* (green)(n>40). The fraction of spread nuclei that were Rec8 positive or negative was compared to wild-type using a chi-square test (df 1): *CUP-CLB4*, $\chi^2 = 0.001323$, $p = 0.9710$; *CUP-CLB3*, $\chi^2 = 32.79$, $p < 0.0001$.

(C) Rec8 cleavage monitored by Western blot after release from an *NDT80* block (4h 30min) in wild-type and *CUP-CLB3* carrying both a myc-tagged *REC8* allele as well as either HA-tagged *REC8* or *rec8-29A* allele (Left to right: A29957, A29959, A29961, A29963).

(D) Percentage of cells with short bipolar spindles was determined at indicated times in wild-type (A22804), *CUP-CLB3* (A29965), *rec8-29A* (A22803) and *CUP-CLB3 rec8-29A* (A29967) after release from an *NDT80* block (4h 30min) (n=100 per time point).

(E) ChIP analysis for total Rec8, p-S179 Rec8 or p-S521 Rec8 from metaphase I-arrested (*cdc20-mn*) wild-type (A28681), *CUP-CLB3* (A28682) and Sgo1-depleted (*sgo1-mn;* A29994) cells. Relative occupancy at a chromosome arm site (c194) or at a centromeric site (CEN5) was determined relative to a low binding region (c281). Error bars represent range (n=2).

(F) Chromosomal association of Sgo1-3V5 was monitored by ChIP-chip in wild-type (A29795) and *CUP-CLB3* (A29799) cells during prophase I-arrest. Centromere position is identified by a black circle.

(G, H) Localization of Sgo1-9myc (G, green) or Rts1-13myc (H, green) relative to Ndc10-6HA (red) determined by nuclear spreads in **(G)** wild-type (A22868) and

CUP-CLB3 (A22870) or **(H)** wild-type (A28329) and *CUP-CLB3* (A28330) during prophase I (n>40). For **(G)**, the fraction of spread nuclei that display colocalized or mislocalized Sgo1 relative to Ndc10 was compared between wild-type and *CUP-CLB3* using a chi-square test (df 1) $\chi^2 = 1.554$, $p = 0.2125$. For **(H)**, the fraction of spread nuclei that display colocalized, partial or mislocalized Rts1 relative to Ndc10 was compared between wild-type and *CUP-CLB3* using a chi-square test (df 2) $\chi^2 = 3.712$, $p = 0.1563$.

(I) Localization of Sgo1-9myc (green) in binucleates relative to Ndc10-6HA (red) determined by nuclear spreads from wild-type (A22868) and *CUP-CLB3* (A22870) (n>40). The fraction of spread nuclei that were Sgo1 positive or negative was compared between wild-type and *CUP-CLB3* using a chi-square test (df 1) $\chi^2 = 23.92$, $p < 0.0001$.

at lower levels in *CUP-CLB3* cells (Figure 6C and Figure 7E). The cause of this reduction is currently unclear, but could indicate that in *CUP-CLB3* cells, cohesin removal also relies on a separase-independent pathway, i.e. the prophase removal pathway (Yu & Koshland, 2005).

Our results demonstrate that Rec8 phosphorylation is required for cohesin removal in *CUP-CLB3* cells and suggest that the defect in centromeric cohesin protection may result from increased phosphorylation of centromeric Rec8. To test this possibility, we used phospho-specific antibodies against two *in vivo* phosphorylation sites of Rec8 (pS179 and pS521) (Brar et al., 2006; Katis et al., 2010); M. Attner personal communication, October 2011) and analyzed the relative enrichment of total Rec8 and phospho-Rec8 at CENV or at an arm cohesin binding site by ChIP in metaphase I-arrested cells. The two phospho-specific antibodies immunoprecipitated

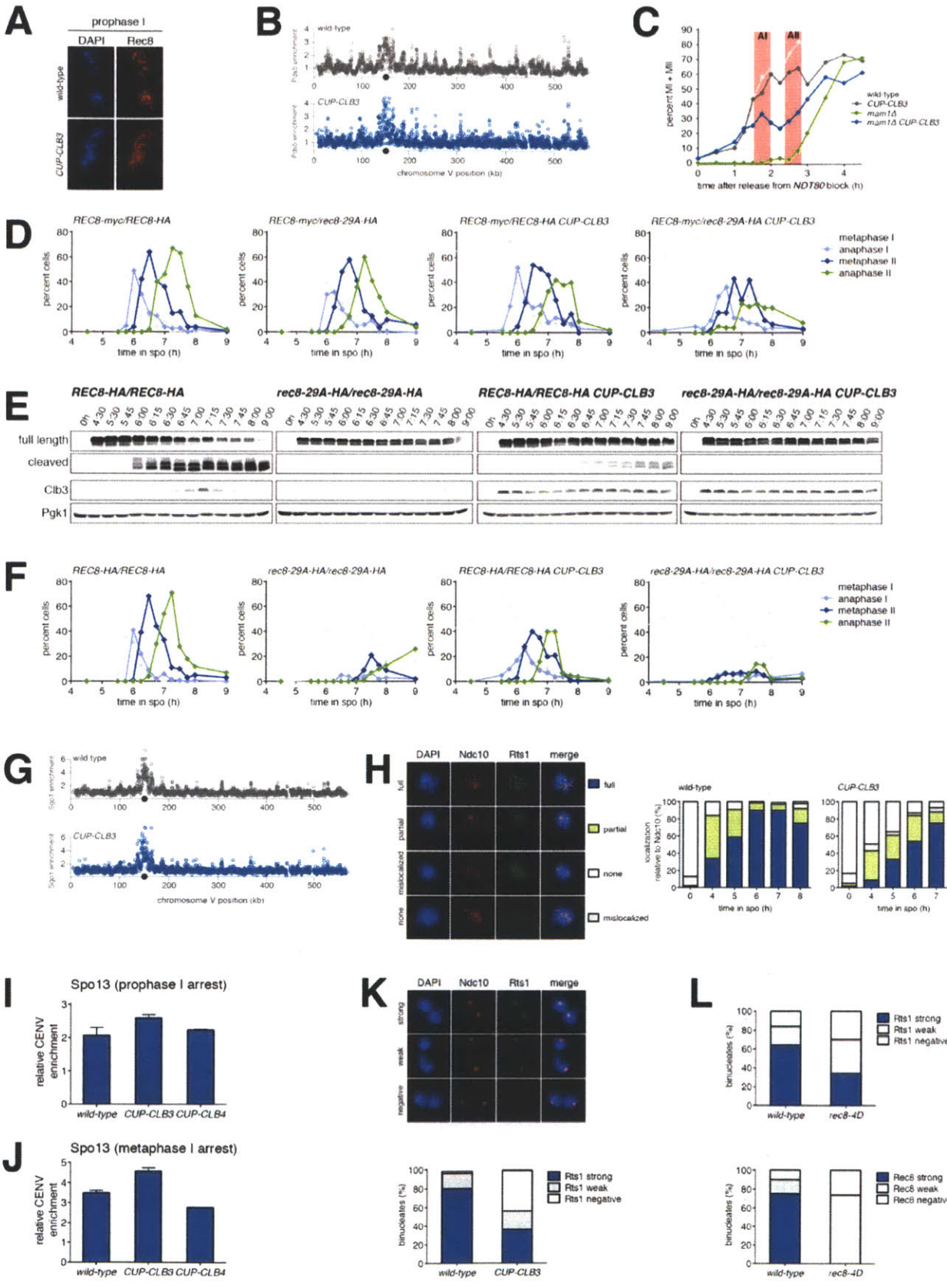
A
prophase I
DAPI
Rec8
wild-type
CUP-CLB3
B
wild-type
CUP-CLB3
chromosome V position (kb)
C
percent MI + MII
time after release from NDT80 block (h)
wild-type
CUP-CLB3
mam1Δ
mam1Δ CUP-CLB3
D
REC8-myc/REC8-HA
REC8-myc/rec8-29A-HA
REC8-myc/REC8-HA CUP-CLB3
REC8-myc/rec8-29A-HA CUP-CLB3
percent cells
time in spo (h)
metaphase I
anaphase I
metaphase II
anaphase II
E
REC8-HA/REC8-HA
rec8-29A-HA/rec8-29A-HA
REC8-HA/REC8-HA CUP-CLB3
rec8-29A-HA/rec8-29A-HA CUP-CLB3
full length
cleaved
Clb3
Pgk1
F
REC8-HA/REC8-HA
rec8-29A-HA/rec8-29A-HA
REC8-HA/REC8-HA CUP-CLB3
rec8-29A-HA/rec8-29A-HA CUP-CLB3
percent cells
time in spo (h)
metaphase I
anaphase I
metaphase II
anaphase II
G
wild type
CUP-CLB3
chromosome V position (kb)
H
DAPI
Ndc10
Rts1
merge
full
partial
none
mislocalized
wild-type
CUP-CLB3
localization relative to Ndc10 (%)
time in spo (h)
I
Spo13 (prophase I arrest)
relative CEN enrichment
wild-type
CUP-CLB3
CUP-CLB4
J
Spo13 (metaphase I arrest)
relative CEN enrichment
wild-type
CUP-CLB3
CUP-CLB4
K
DAPI
Ndc10
Rts1
merge
strong
weak
negative
binucleates (%)
Rts1 strong
Rts1 weak
Rts1 negative
wild-type
CUP-CLB3
L
binucleates (%)
Rts1 strong
Rts1 weak
Rts1 negative
wild-type
rec8-4D
Rec8 strong
Rec8 weak
Rec8 negative
wild-type
rec8-4D

Figure 7. Analysis of cohesin association and the cohesin protective machinery in *CUP-CLB3* cells.

(A) Wild-type (A26547) and *CUP-CLB3* (A26548) cells were induced to sporulate and $CuSO_4$ (50μM) was added 3h after transfer into sporulation medium. Rec8-3HA localization (red) was determined in spread nuclei from prophase I cells. DNA is shown in blue.

(B) Wild-type (A28681) and *CUP-CLB3* (A28682) cells carrying the *cdc20-mn* allele were induced to sporulate and $CuSO_4$ (50μM) was added 2h 30min after transfer into sporulation medium. Pds5 localization was determined by ChIP-chip from metaphase I-arrested cells. Black balls depict centromere positions.

(C) Wild-type (A22678), *CUP-CLB3* (A22702), *mam1Δ* (A31340) and *mam1Δ CUP-CLB3* (A31342) cells carrying the *GAL4-ER* and *GAL-NDT80* fusions were induced to sporulate and $CuSO_4$ (50μM) was added 2h 15min after transfer into sporulation medium. Cells were released from the *NDT80* block 4h 30min after transfer into sporulation medium. The percentage of cells that had undergone one or two meiotic divisions was determined at the indicated time points (n=100 per time point).

(D) *REC8-myc/REC8-HA* (A29957), *REC8-myc/rec8-29A-HA* (A29961), *REC8-myc/REC8-HA CUP-CLB3* (A29959) and *REC8-myc/rec8-29A-HA CUP-CLB3* (A29963) cells carrying the *GAL4-ER* and *GAL-NDT80* fusions were induced to sporulate and $CuSO_4$ (50μM) was added 2h 15min after transfer into sporulation medium. Cells were released from the *NDT80* block 4h 30min after transfer into sporulation medium. The percentage of cells in metaphase I (grey symbols), anaphase I (violet symbols), metaphase II (dark blue symbols) and anaphase II (green symbols) was determined at the indicated times (n=100 per time point). Note that these graphs represent meiotic progression of cells analyzed for Rec8 cleavage in Figure 3C.

(E) Wild-type (A22804), *CUP-CLB3* (A29965), *rec8-29A* (A22803) and *rec8-29A CUP-CLB3* (A29967) cells carrying the *GAL4-ER* and *GAL-NDT80* fusions were induced to sporulate and $CuSO_4$ (50μM) was added 2h 15min after transfer into sporulation

medium. Cells were released from the *NDT80* block 4h 30min after transfer into sporulation medium. Levels of full-length Rec8, cleaved Rec8, Clb3 and Pgk1 were monitored by Western blot.

(F) The percentage of cells in metaphase I (grey symbols), anaphase I (violet symbols), metaphase II (dark blue symbols) and anaphase II (green symbols) was also determined at the indicated times from the experiment described in **(E)** (n=100 per time point).

(G) Wild-type (A28712) and *CUP-CLB3* (A28713) cells carrying the *cdc20-mn* allele were induced to sporulate and $CuSO_4$ (50μM) was added 2h 30min after transfer into sporulation medium. Sgo1-3V5 localization was determined by ChIP-chip, 7h after transfer into sporulation medium when cells were arrested in metaphase I. Arm peaks for Sgo1 correspond to cohesin-associated regions. The basis for Sgo1 enrichment at these sites is currently unclear. Black balls depict centromere positions.

(H) Wild-type (A28331) and *CUP-CLB3* (A28332) cells carrying the *cdc20-mn* allele were induced to sporulate and $CuSO_4$ (50μM) was added 2h 30min after transfer into sporulation medium. Rts1-13myc (green) localization relative to Ndc10-6HA (red) was determined in spread nuclei from metaphase I-arrested cells (n>40).

(I) Wild-type (A30856), *CUP-CLB3* (A30858) and *CUP-CLB4* (A30860) cells carrying the *GAL4-ER* and *GAL-NDT80* fusions were induced to sporulate and $CuSO_4$ (50μM) was added 2h 15min after transfer into sporulation medium. Spo13-3V5 localization was determined by ChIP from prophase I-arrested cells. Relative occupancy at a centromeric site (CEN5) relative to a low binding region (HMR) was determined. Error bars represent the range (n=2).

(J) Wild-type (A30743), *CUP-CLB3* (A30745) and *CUP-CLB4* (A30747) cells carrying the *cdc20-mn* allele were induced to sporulate and $CuSO_4$ (50μM) was added 2h 30min after transfer into sporulation medium. Spo13-3V5 localization was determined by ChIP 7h after transfer into sporulation medium when cells were arrested in metaphase I. Relative occupancy at a centromeric site (CEN5) relative

to a low binding region (HMR) was determined. Error bars represent the range (n=2).

(K) Wild-type (A28329) and *CUP-CLB3* (A28330) cells were induced to sporulate and $CuSO_4$ (50μM) was added 2h 30min after transfer into sporulation medium. Rts1-13myc (green) localization relative to Ndc10-6HA (red) was determined in spread nuclei from binucleates (n>40). Using a chi-square test (df 2) the fraction of spread nuclei that display strong, weak or negative Rts1 with respect to Ndc10 was compared between wild-type and *CUP-CLB3* $\chi^2 = 54.49$, $p < 0.0001$.

(L) Wild-type (A29645) and *rec8-S136D S179D S197D T209D* (A29647) cells were induced to sporulate and Rec8-3HA/rec8-4D-3HA or Rts1-3V5 localization relative to Ndc10-13myc was determined in spread nuclei from binucleates (n>40). Characterization of *rec8-S136D S179D S197D T209D* has been described in (Katis et al., 2010). Note that strains carrying this allele fail to maintain centromeric cohesin beyond metaphase I (bottom panel). These binucleates also have weak Rts1 staining (top panel), suggesting that Rts1 maintenance at centromeric regions in anaphase I depends on cohesin. For top panel, using a chi-square test (df 2) the fraction of spread nuclei that display strong, weak or negative Rts1 with respect to Ndc10 was compared between wild-type and *CUP-CLB3* $\chi^2 = 18.02$, $p = 0.0001$. For bottom panel, using a chi-square test (df 2) the fraction of spread nuclei that display strong, weak or negative Rec8 with respect to Ndc10 was compared between wild-type and *CUP-CLB3* $\chi^2 = 121.2$, $p < 0.0001$.

---

similar amounts of Rec8 in wild-type and *CUP-CLB3* cells at the arm site (Figure 6E), which is consistent with arm cohesin being primed for Separase cleavage. However, the amount of phosphorylated Rec8 was increased at the centromere in *CUP-CLB3* cells compared to wild-type cells, albeit not to the same extent as in cells depleted for Sgo1 (*sgo1-mn*), in which meiosis I centromeric-cohesin protection is completely defective

(Figure 6E). We conclude that *CUP-CLB3* cells are compromised in preventing centromeric Rec8 phosphorylation during meiosis I.

Sgo1-PP2A localization is not affected in *CUP-CLB3* cells.

Sgo1-PP2A and the meiosis-specific protein Spo13 prevent centromeric Rec8 phosphorylation during meiosis I to protect this cohesin pool from cleavage. All three proteins localize to kinetochores during meiosis I, which is thought to be critical for their cohesin-protective function (Katis, Galova et al., 2004; Katis, Matos et al., 2004; Kitajima et al., 2004; Kitajima et al., 2006; B. H. Lee, Kiburz, & Amon, 2004; Riedel et al., 2006). Surprisingly, Sgo1, the PP2A regulatory subunit Rts1 and Spo13 localized normally in prophase I- and metaphase I-arrested *CUP-CLB3* cells (Figure 6F-H and Figure 7G-J). We noticed a moderate reduction of Sgo1 and Rts1 at centromeres in binucleate *CUP-CLB3* cells (Figure 6I and Figure 7K). However, this reduction during anaphase I is most likely a consequence rather than a cause of premature loss of centromeric cohesin. In cells expressing a phosphomimetic version of Rec8 (*rec8-4D*) that cannot be retained at centromeres beyond meiosis I, Rts1 localization is also reduced in anaphase I (Figure 7L). It is thus unlikely that the reduction of Sgo1 and Rts1 at centromeres during anaphase I contributes to the premature loss of centromeric cohesin. These findings, together with our observation that centromeric Rec8 phosphorylation is increased in *CUP-CLB3* cells, indicate that Sgo1-PP2A function, but not localization, is impaired in *CUP-CLB3* cells.

Modulating microtubule-kinetochore interactions affects monopolin-induced sister chromatid cosegregation during mitosis.

How does premature expression of *CLB3* interfere with establishment of the meiosis I chromosome segregation pattern? The comparison of the effects caused by *CLB3* and *CLB4* misexpression provided insight into this question. Both cyclins induce spindle formation in prophase I. However, chromosomes are able to attach to this spindle and experience pulling forces only in *CUP-CLB3* cells. Thus, the ability to form tension-generating attachments (i.e. *CUP-CLB1* or *CUP-CLB3* cells) correlates with defects in meiosis I chromosome morphogenesis and segregation. This correlation suggests that premature microtubule-kinetochore engagement during premeiotic S phase/early prophase I is the underlying cause of chromosome missegregation in *CUP-CLB3* cells and predicts that tension generating microtubule-kinetochore attachments should inhibit meiosis I chromosome morphogenesis. Conversely, preventing them should enable building a proper meiosis I chromosome architecture.

We tested the first prediction using a previously described method in which monopolin-dependent sister kinetochore coorientation is induced during mitosis (Monje-Casas, Prabhu, Lee, Boselli, & Amon, 2007). Overexpression of *MAM1* and *CDC5* upon a pheromone-induced G1 arrest is sufficient to induce cosegregation of sister chromatids in mitotic anaphase ((Monje-Casas et al., 2007), Figure 8A). However, when cells are allowed to form microtubule-kinetochore attachments prior to *CDC5* and *MAM1*

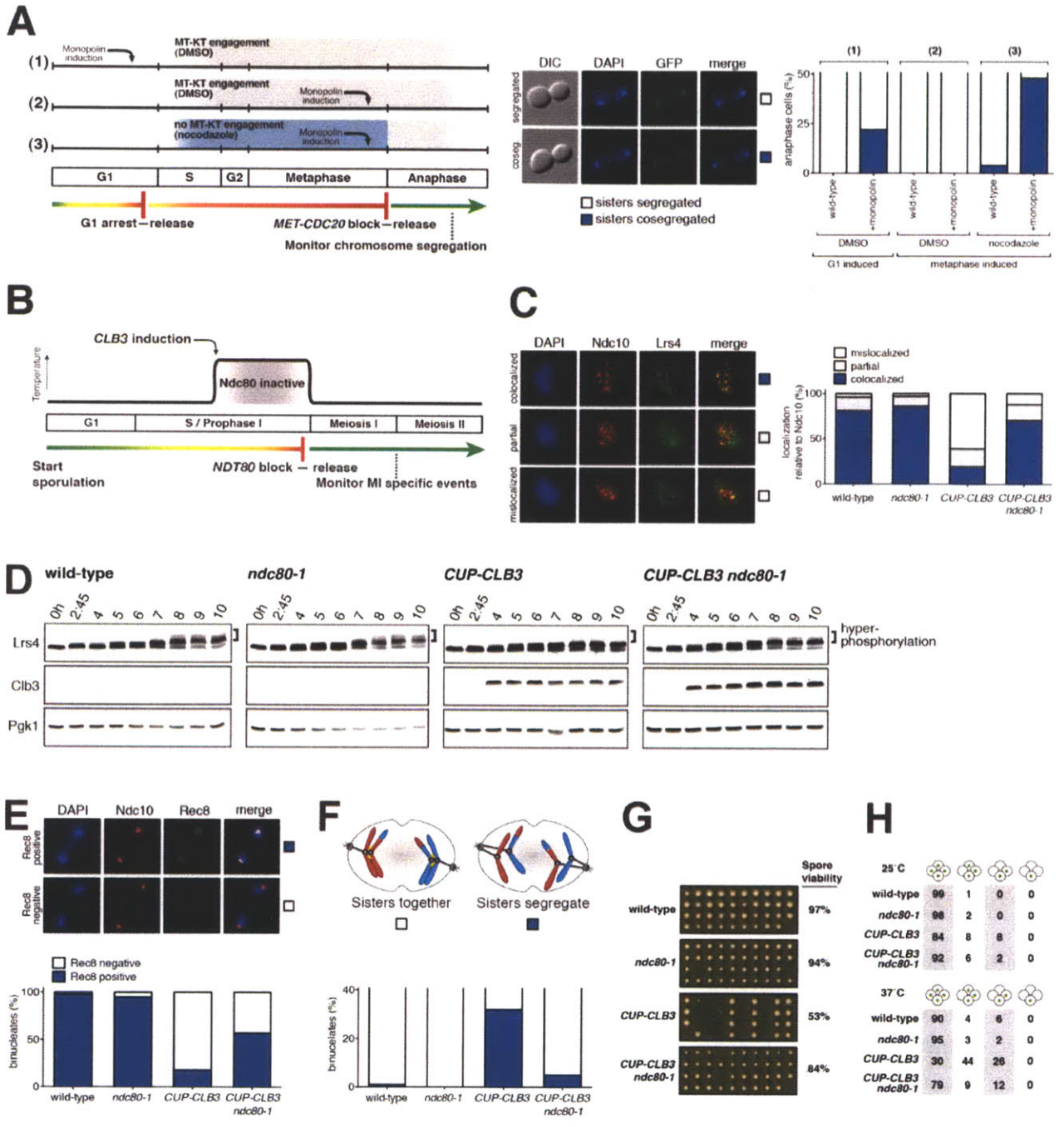

Figure 8. Transient disruption of microtubule-kinetochore interactions suppresses the chromosome segregation defects in *CUP-CLB3* cells.

(A) Wild-type (A10684) and *GAL-CDC5 GAL-MAM1* (A26546) cells, carrying a *MET-CDC20* allele and CENIV-GFP dots, were monitored for chromosome segregation in anaphase (see text and Materials and Methods for details). MT= microtubule,

KT= kinetochore, (n=100). The fraction of anaphase cells that segregate or cosegregate sister chromatids was compared between *GAL-CDC5 GAL-MAM1* condition (2) and *GAL-CDC5 GAL-MAM1* condition (3) using a chi-square test (df 1) $\chi^2 = 59.71$, $p < 0.0001$

(B) Schematic description of the experimental regime used for **(C)** through **(H)** See Materials and Methods for details.

(C) Localization of Lrs4-13myc (green) in mononucleates relative to Ndc10-6HA (red) determined by nuclear spreads (n>40) and **(D)** phosphorylation of Lrs4-13myc determined by gel mobility shift in wild-type (A29612), *ndc80-1* (A29614), *CUP-CLB3* (A29616) and *CUP-CLB3 ndc80-1* (A29618). For **(C)**, using a chi-square test (df 2) the fraction of spread nuclei that display colocalized, partial or mislocalized Lrs4 with respect to Ndc10 was compared between wild-type and *ndc80-1* $\chi^2 = 0.9668$, $p = 0.6167$ and between *CUP-CLB3* and *CUP-CLB3 ndc80-1* $\chi^2 = 56.34$, $p < 0.0001$.

(E) Localization of Rec8-13myc (green) in binucleates relative to Ndc10-6HA (red) determined by nuclear spreads in wild-type (A28716), *ndc80-1* (A28720), *CUP-CLB3* (A28718) and *CUP-CLB3 ndc80-1* (A28722) (n>40). Using a chi-square test (df 1) the fraction of spread nuclei that were Rec8 positive or negative was compared between wild-type and *ndc80-1* $\chi^2 = 1.185$, $p = 0.2764$ and between *CUP-CLB3* and *CUP-CLB3 ndc80-1* $\chi^2 = 23.96$, $p < 0.0001$.

(F) Segregation of sister chromatids using heterozygous CENV-GFP dots quantified in binucleates (n=100) and **(G)** spore viability from wild-type (A22678), *ndc80-1* (A28621), *CUP-CLB3* (A22702) and *CUP-CLB3 ndc80-1* (A28623) [n= 40 tetrads for wild-type and *ndc80-1*, n> 60 tetrads for *CUP-CLB3* and *CUP-CLB3 ndc80-1*] (nonpermissive temperature > 36°C). Using a chi-square test (df 1) the fraction of binucleates with a reductional or equational division was compared between *CUP-CLB3* and *CUP-CLB3 ndc80-1* $\chi^2 = 24.18$, $p < 0.0001$.

(H) Segregation of chromosome V using homozygous CENV-GFP dots quantified in tetranucleates from wild-type (A22688), *ndc80-1* (A28625), *CUP-CLB3* (A22708) and *CUP-CLB3 ndc80-1* (A28627). Top panel: Cells kept at 25°C for the duration

of the experiment. Bottom panel: Cells treated as in **(B)** but monitored after meiosis II (n=100).

expression, cosegregation of sister chromatids is prevented. We reversibly arrested cells in metaphase using a methionine repressible *CDC20* allele (*MET-CDC20*) and induced *MAM1* and *CDC5* expression after cells had arrested in metaphase and had formed microtubule-kinetochore interactions. Under these conditions, *MAM1* and *CDC5* expression did not induce sister chromatid cosegregation when cells were released into anaphase (Figure 8A). Importantly, disrupting microtubule-kinetochore interactions by depolymerizing microtubules with nocodazole during the metaphase arrest resulted in robust cosegregation of sister chromatids in anaphase (48% cosegregation, Figure 8A). These results show that microtubule-kinetochore interactions modulate the ability of monopolin to induce sister chromatid cosegregation.

Transient disruption of microtubule-kinetochore interactions restores meiosis I chromosome segregation in *CUP-CLB3* cells.

If the defects in sister kinetochore coorientation and centromeric cohesin maintenance of *CUP-CLB3* cells are caused by premature microtubule-kinetochore interactions, proper meiosis I chromosome morphogenesis should be restored by transiently disrupting microtubule-kinetochore interactions. To test this, we used a temperature sensitive allele of *NDC80* (*ndc80-1*), which encodes a component of the outer

kinetochore. *ndc80-1* cells grow and sporulate normally at 25°C, but fail to undergo any nuclear divisions at temperatures above 34°C (Figure 9A).

We first asked whether disrupting microtubule-kinetochore interactions suppresses the kinetochore localization defect of monopolin in *CUP-CLB3* cells. Using the *NDT80* block-release system, we induced cells to sporulate at 25°C. After 165min, we induced cyclin expression and concurrently transferred cells to 34°C to inactivate the *ndc80-1* allele. Cells were then incubated for an additional 135min to arrest them in the *NDT80*-depletion block. We then transferred cells to the permissive temperature and released them from the *NDT80* block into a metaphase I-arrest by depleting *CDC20* (*cdc20-mn*)(Figure 8B). Under these conditions, wild-type and *ndc80-1* cells arrested in metaphase I with the monopolin subunit Lrs4 localized to kinetochores, while *CUP-CLB3* cells showed a defect in Lrs4 localization (Figure 8C). Remarkably, *CUP-CLB3 ndc80-1* cells showed near wild-type levels of Lrs4 association with kinetochores (Figure 8C). Transient inactivation of *NDC80* also restored Lrs4 phosphorylation in *CUP-CLB3* cells (Figure 8D). Our results demonstrate that premature microtubule-kinetochore interactions prevent sister kinetochore coorientation by disrupting proper localization of the monopolin complex. The finding that transient disruption of microtubule-kinetochore interactions also suppresses the Lrs4 phosphorylation defect of *CUP-CLB3* cells, furthermore suggests that Lrs4 hyperphosphorylation occurs not at the time of nucleolar release, but once Lrs4 localizes to kinetochores.

We next asked whether transient inactivation of microtubule-kinetochore interactions also suppresses the premature loss of centromeric cohesin observed in

A

	T (°C)	Sporulation Efficiency (%) Unsporulated	Dyad	Tetrad
wild-type	25	21	21	58
	34	61	5	34
ndc80-1	25	13	25	62
	34	98	2	0

B

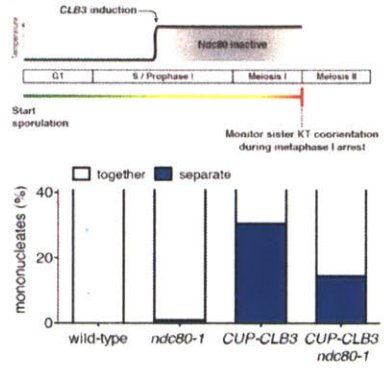

C

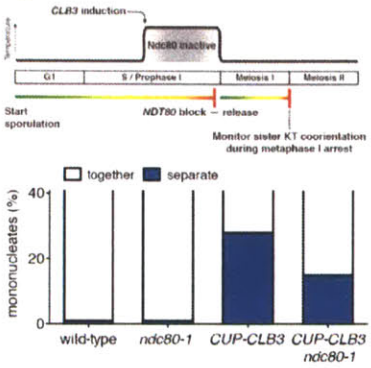

D

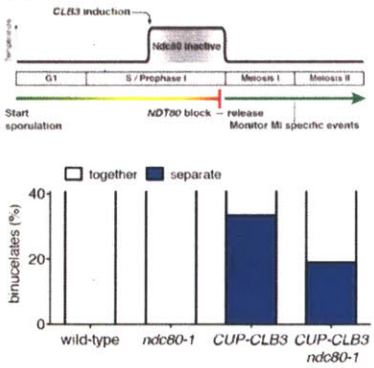

E

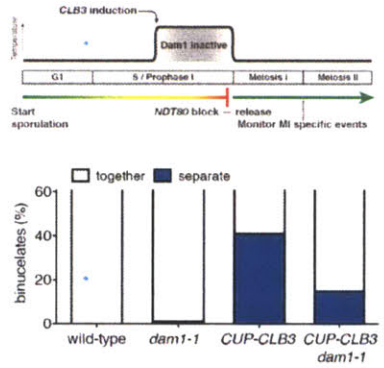

F

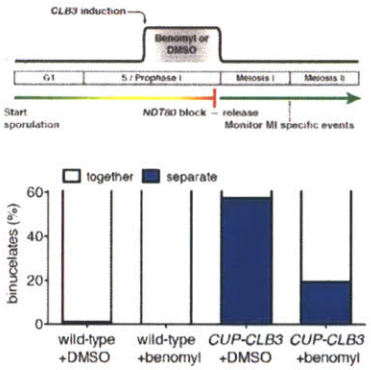

J

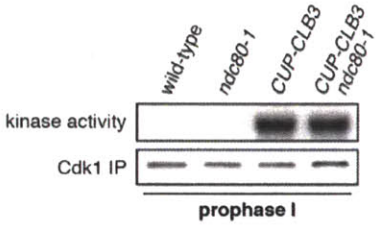

G

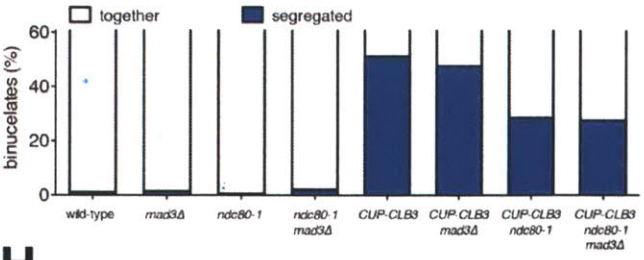

H

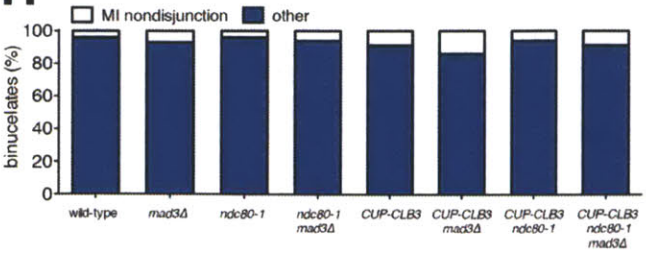

I

wild-type	**92**	**3**	**5**	**0**
ndc80-1	**97**	**0**	**3**	**0**
CUP-CLB3	**68**	**11**	**21**	**0**
CUP-CLB3 ndc80-1	**86**	**4**	**10**	**0**
mad3Δ	**92**	**2**	**6**	**0**
ndc80-1 mad3Δ	**84**	**5**	**11**	**0**
CUP-CLB3 mad3Δ	**46**	**17**	**37**	**0**
CUP-CLB3 ndc80-1 mad3Δ	**75**	**4**	**21**	**0**

Figure 9. Disrupting microtubule-kinetochore interactions during S phase/prophase I suppresses *CUP-CLB3*-induced meiosis I sister chromatid segregation in a spindle assembly checkpoint independent manner.

(A) Wild-type (A22678) and *ndc80-1* (A28221) cells were induced to sporulate at 25°C. 2h 30min after transfer into sporulation medium, cells were shifted to the indicated temperature and sporulation efficiency was determined after 24h.

(B) Wild-type (A7118), *CUP-CLB3* (A23074), *ndc80-1* (A29690) and *ndc80-1 CUP-CLB3* (A29692) cells also carrying the *cdc20-mn* allele, were induced to sporulate at 25°C. 2h 45min after transfer into sporulation medium, $CuSO_4$ (50µM) was added and concurrently, cultures were shifted to 34°C. The percentage of mononucleate cells with separated CENV-GFP dots was determined 7h 30min after transfer into sporulation medium when cells were arrested in metaphase I (n=100). The fraction of nuclei that display sister kinetochores as separate or together was compared between *CUP-CLB3* and *CUP-CLB3 ndc80-1* using a chi-square test (df 1) $\chi^2 = 7.228$, $p = 0.0072$.

(C) Wild-type (A20958), *CUP-CLB3* (A23076), *ndc80-1* (A29718) and *ndc80-1 CUP-CLB3* (A29720) cells also carrying the *GAL4-ER* and *GAL-NDT80* fusions and the *cdc20-mn* allele were induced to sporulate at 25°C. 2h 45min after transfer into sporulation medium $CuSO_4$ (50µM) was added and concurrently, cultures were shifted to 34°C. After 5 hours, when cells had arrested in the *NDT80* arrest, cells were released from the *NDT80* block and transferred to 25°C. The percentage of mononucleate cells with separated CENV-GFP dots was determined 7h 30min after transfer into sporulation medium when cells were arrested in metaphase I (n=100). The fraction of nuclei that display sister kinetochores as separate or together was compared between *CUP-CLB3* and *CUP-CLB3 ndc80-1* using a chi-square test (df 1) $\chi^2 = 5.007$, $p = 0.0252$.

(D) Wild-type (A22678), *ndc80-1* (A28621), *CUP-CLB3* (A22702) and *CUP-CLB3 ndc80-1* (A28623) cells also carrying the *GAL4-ER* and *GAL-NDT80* fusions were induced to sporulate at 25°C. 2h 45min after transfer into sporulation medium

$CuSO_4$ (50μM) was added and concurrently, cultures were shifted to 34°C. After 5hr, when cells had arrested in the *NDT80* block, cells were released and transferred to 25°C. The percentage of binucleate cells with segregated heterozygous CENV-GFP dots was determined 7h 30min after transfer into sporulation medium (n=100). Note that a greater suppression of meiosis I sister chromatid segregation was observed in *ndc80-1 CUP-CLB3* cells when cells were incubated at temperatures higher than 34°C (Figure 4F and data not shown). The fraction of binucleates that underwent reductional or equational division was compared between *CUP-CLB3* and *CUP-CLB3 ndc80-1* using a chi-square test (df 1) $\chi^2 = 5.776$, $p = 0.0162$.

(E) Wild-type (A22678), *dam1-1* (A28311), *CUP-CLB3* (A22702) and *CUP-CLB3 dam1-1* (A28341) cells also carrying the *GAL4-ER* and *GAL-NDT80* fusions were induced to sporulate at 25°C. 2h 45min after transfer into sporulation medium $CuSO_4$ (50μM) was added and concurrently, cultures were shifted to 34°C. After 5hr, when cells had arrested in the *NDT80* block, cells were released and transferred to 25°C. The percentage of binucleate cells with segregated heterozygous CENV-GFP dots was determined 7h 30min after transfer into sporulation medium (n=100). The fraction of binucleates that underwent reductional or equational division was compared between *CUP-CLB3* and *CUP-CLB3 dam1-1* using a chi-square test (df 1) $\chi^2 = 16.77$, $p < 0.0001$.

(F) Wild-type (A22678) and *CUP-CLB3* (A22702) cells also carrying the *GAL4-ER* and *GAL-NDT80* fusions were induced to sporulate at 30°C. 2h 15min after transfer into sporulation medium $CuSO_4$ (50μM) was added and concurrently, cells were treated with DMSO or benomyl (120 μg/ml). Cells were subsequently released from *NDT80* block 4h 30min after transfer into sporulation medium and benomyl was washed out concomitant with *NDT80*-block release. The percentage of binucleate cells with segregated heterozygous CENV-GFP dots was determined 6h after transfer into sporulation medium (n=100). See Materials and Methods for further details. The fraction of binucleates that underwent reductional or equational

division was compared between *CUP-CLB3* +DMSO and *CUP-CLB3* +benomyl using a chi-square test (df 1) $\chi^2 = 32.12$, $p < 0.0001$.

(G) Wild-type (A22678), *mad3Δ* (A30386), *ndc80-1* (A28621), *ndc80-1 mad3Δ* (A30390), *CUP-CLB3* (A22702), *CUP-CLB3 mad3Δ* (A30388), *CUP-CLB3 ndc80-1* (A28623) and *CUP-CLB3 ndc80-1 mad3Δ* (A30392) cells also carrying the *GAL4-ER* and *GAL-NDT80* fusions were induced to sporulate at 25°C. 2h 45min after transfer into sporulation medium $CuSO_4$ (50μM) was added and concurrently, cultures were shifted to 36°C. Cells were subsequently released from *NDT80* block at 5h and transferred to 25°C. Percent binucleates with segregated heterozygous CENV-GFP dots was determined (n=100). Using a chi-square test (df 1) the fraction of binucleates that underwent reductional or equational division was compared between *CUP-CLB3* and *CUP-CLB3 mad3Δ* $\chi^2 = 0.1800$, $p = 0.6714$ and between *CUP-CLB3 ndc80-1* and *CUP-CLB3 ndc80-1 mad3Δ* $\chi^2 = 0.02454$, $p = 0.8755$.

(H) Wild-type (A22688), *mad3Δ* (A30638), *ndc80-1* (A28625), *ndc80-1 mad3Δ* (A30642), *CUP-CLB3* (A22708), *CUP-CLB3 mad3Δ* (A30640), *CUP-CLB3 ndc80-1* (A28627) and *CUP-CLB3 ndc80-1 mad3Δ* (A30644) cells also carrying the *GAL4-ER* and *GAL-NDT80* fusions were induced to sporulate at 25°C. 2h 45min after transfer to sporulation medium $CuSO_4$ (50μM) was added and concurrently, cultures were shifted to 36°C. After 5hr, when cells had arrested in the *NDT80* block, cells were released and transferred to 25°C. The percentage of binucleate cells with segregated homozygous CENV-GFP dots was determined 7h 30min after transfer into sporulation medium. Binucleate cells with GFP signal in only one of the two nuclei were categorized as having experienced a meiosis I non-disjunction event (n=100). Using a chi-square test (df 1) the fraction of binucleates that displayed MI nondisjunction or other was compared between *CUP-CLB3* and *CUP-CLB3 mad3Δ* $\chi^2 = 1.228$, $p = 0.2678$ and between *CUP-CLB3 ndc80-1* and *CUP-CLB3 ndc80-1 mad3Δ* $\chi^2 = 0.6486$, $p = 0.4206$.

(I) Wild-type (A22688), *ndc80-1* (A28625), *CUP-CLB3* (A22708), *CUP-CLB3 ndc80-1* (A28627), *mad3Δ* (A30638), *ndc80-1 mad3Δ* (A30642), *CUP-CLB3 mad3Δ*

(A30640) and *CUP-CLB3 ndc80-1 mad3Δ* (A30644) cells also carrying the *GAL4-ER* and *GAL-NDT80* fusions were induced to sporulate at 25°C. 2h 45min after transfer to sporulation medium $CuSO_4$ (50μM) was added and concurrently, cultures were shifted to 36°C. After 5hr, when cells had arrested in the *NDT80* block, cells were released and transferred to 25°C. Segregation of homozygous CENV-GFP dots was determined in tetranucleates 12h after transfer into sporulation medium (n=100).

(J) Wild-type (A25508), *ndc80-1* (A33203), *CUP-CLB3* (A33201) and *CUP-CLB3 ndc80-1* (A33205) cells also carrying the *GAL4-ER* and *GAL-NDT80* fusions were induced to sporulate at 25°C. 2h 45min after transfer to sporulation medium $CuSO_4$ (50μM) was added and concurrently, cultures were shifted to 35°C. Samples were harvested 5h post transfer to sporulation medium, when cells were arrested in the *NDT80* block. *In vitro* kinase assays were performed with Cdc28-3V5 (Cdk1) immunoprecipitated from prophase I-arrested samples. Amounts of phosporylated Histone H1 and immunoprecipitated Cdc28-3V5 are shown.

CUP-CLB3 cells. We used a similar protocol to the one described above, except cells were not arrested in metaphase I following release from the *NDT80* block, but were allowed to proceed into anaphase I to examine Rec8 localization. Remarkably, disrupting microtubule-kinetochore interactions at the time of Clb3 expression caused a considerable increase in the percentage of *CUP-CLB3* cells that retained Rec8 around centromeres during anaphase I (Figure 8E).

Finally, restoring centromeric cohesin protection and sister kinetochore coorientation to *CUP-CLB3* cells by transient inactivation of *NDC80* restored homolog segregation during meiosis I (Figure 8F and Figure 9B-D). Similar results were obtained with a temperature sensitive allele of the gene encoding the outer kinetochore

component Dam1 (*dam1-1*) or by disrupting microtubule-kinetochore interactions by benomyl treatment (Figure 9E-F). We further observed a striking improvement in overall chromosome segregation and spore viability in *CUP-CLB3 ndc80-1* compared to *CUP-CLB3* cells (Figure 8G-H). The suppression of chromosome missegregation in *CUP-CLB3 ndc80-1* cells did not depend on the spindle assembly checkpoint, because deletion of *MAD3* had no discernable effect on the extent of *ndc80-1* mediated suppression (Figure 9G-I), nor was it due to the *ndc80-1* allele lowering Clb3-CDK activity (Figure 9J). In summary, our results demonstrate that the defects associated with *CUP-CLB3* cells are due to premature microtubule-kinetochore interactions. Our results further suggest that preventing microtubule-kinetochore interactions during premeiotic S phase and prophase I is necessary to establish a meiosis I-specific chromosome architecture.

The outer kinetochore is disassembled during premeiotic S phase and prophase I.

Our results demonstrate that preventing premature interactions of microtubules with kinetochores is essential for establishing a meiosis I chromosome architecture. This occurs, at least in part, by restricting Clb-CDK activity during premeiotic S phase and prophase I. Are additional mechanisms in place to prevent premature microtubule-kinetochore interactions? Insight into this question came from the variability in *CUP-CLB3*-associated phenotypes.

We initially noticed that the timing of *CLB3* induction had an impact on the extent of sister chromatid segregation in meiosis I, especially in experiments that employed the *NDT80* block-release system. To investigate this further, we expressed *CLB3* at different times after induction of sporulation. We observed that the extent of meiosis I sister chromatid segregation declined as *CLB3* was expressed later during the *NDT80* block (Figure 10A). One possibility is that *CLB3*-induced sister chromatid segregation depends on additional factors that become limiting. Kinetochore components are good candidates for such additional factors, because previous studies in fission yeast demonstrated that a subset of outer kinetochore components dissociates from the kinetochore during prophase I (Asakawa, Hayashi, Haraguchi, & Hiraoka, 2005).

Using a high-resolution ribosome profiling dataset (Brar et al., 2012), we examined the timing of synthesis of all kinetochore components during meiotic progression by cluster analysis. This analysis revealed two major expression classes, one included kinetochore components that peak in expression prior to or during prophase I (early class), and the other contained components that instead show peak expression during the meiotic divisions (late class). The early class was enriched for inner kinetochore components (16 of 23), while the late class included primarily outer kinetochore components (13 of 18) (Figure 10B, Figure 11 and Figure 12). The inner kinetochore binds to the centromere and generates a platform for the assembly of the outer kinetochore, which mediates microtubule attachments (Tanaka, 2010). The temporal difference in expression suggests that the inner kinetochore is assembled prior

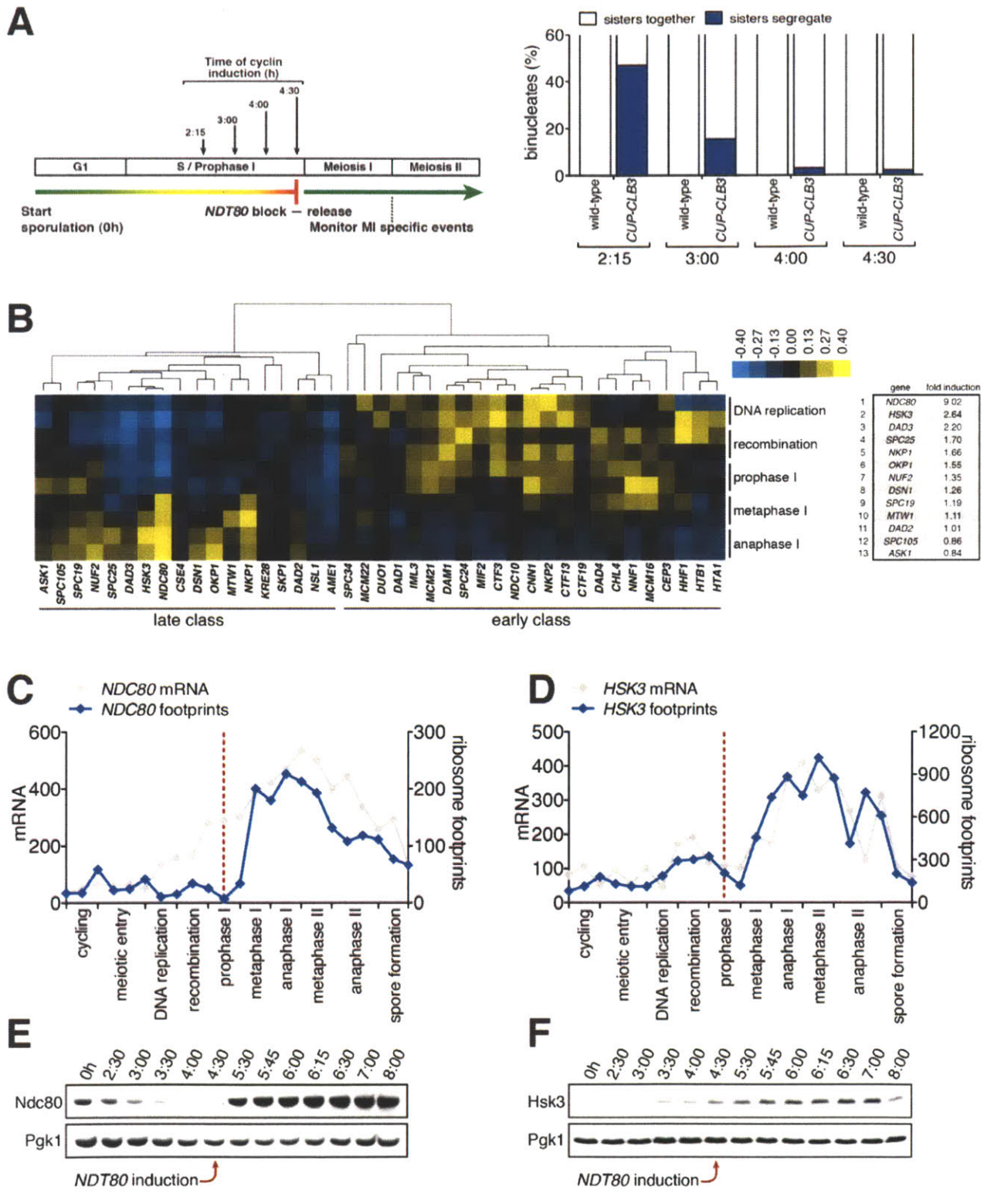
A
Time of cyclin induction (h)
2:15
3:00
4:00
4:30
G1
S / Prophase I
Meiosis I
Meiosis II
Start sporulation (0h)
NDT80 block — release
Monitor MI specific events
sisters together
sisters segregate
binucleates (%)
wild-type
CUP-CLB3
2:15
3:00
4:00
4:30
B
DNA replication
recombination
prophase I
metaphase I
anaphase I
late class
early class
gene
fold induction
C
NDC80 mRNA
NDC80 footprints
mRNA
ribosome footprints
cycling
meiotic entry
DNA replication
recombination
prophase I
metaphase I
anaphase I
metaphase II
anaphase II
spore formation
D
HSK3 mRNA
HSK3 footprints
E
Ndc80
Pgk1
NDT80 induction
F
Hsk3
Pgk1
NDT80 induction

Figure 10. Meiosis I sister chromatid segregation correlates with presence of outer kinetochore components.

(A) Schematic description of the experimental regime and segregation of sister chromatids using heterozygous CENV-GFP dots quantified in binucleates from wild-type (A22678) and *CUP-CLB3* (A29406) after cyclin induction at 2h 15min, 3h, 4h and 4h 30min post transfer to sporulation medium. Cells released from *NDT80*-block at 4h 30min (n=100). Using a chi-square test (df 1), the fraction of binucleates that display a reductional or equational division was compared between wild-type and *CUP-CLB3* for each induction timepoint: (2:15), $\chi^2 = 58.00$, $p < 0.0001$; (3:00), $\chi^2 = 14.46$, $p = 0.0001$; (4:00), $\chi^2 = 1.020$, $p = 0.3124$; (4:30), $\chi^2 = 0.3384$, $p = 0.5607$.

(B) Cluster analysis of kinetochore components from the indicated time points. Further details are in the Materials and Methods and in (Brar et al., 2012). Inner kinetochore=Cse4 nucleosomes, Cbf3, Ctf19 complexes and Mif2. Outer kinetochore=Spc105, Mis12, Ndc80 and DASH complexes. Fold induction is calculated by dividing the average expression from metaphase I-anaphase I by the average expression from DNA replication-prophase I.

(C) Ordered plot for mRNA-seq and ribosome footprinting data for *NDC80* and **(D)** *HSK3* at the indicated stages. Dotted line indicates time of release from *NDT80* block. Further details are in the Materials and Methods and in (Brar et al., 2012).

(E) Western blot for Ndc80-3V5 and Pgk1 from A30340 cells and **(F)** Hsk3-3V5 and Pgk1 from A31861 cells. Cells induced to sporulate and released from *NDT80*-block at 4h 30min.

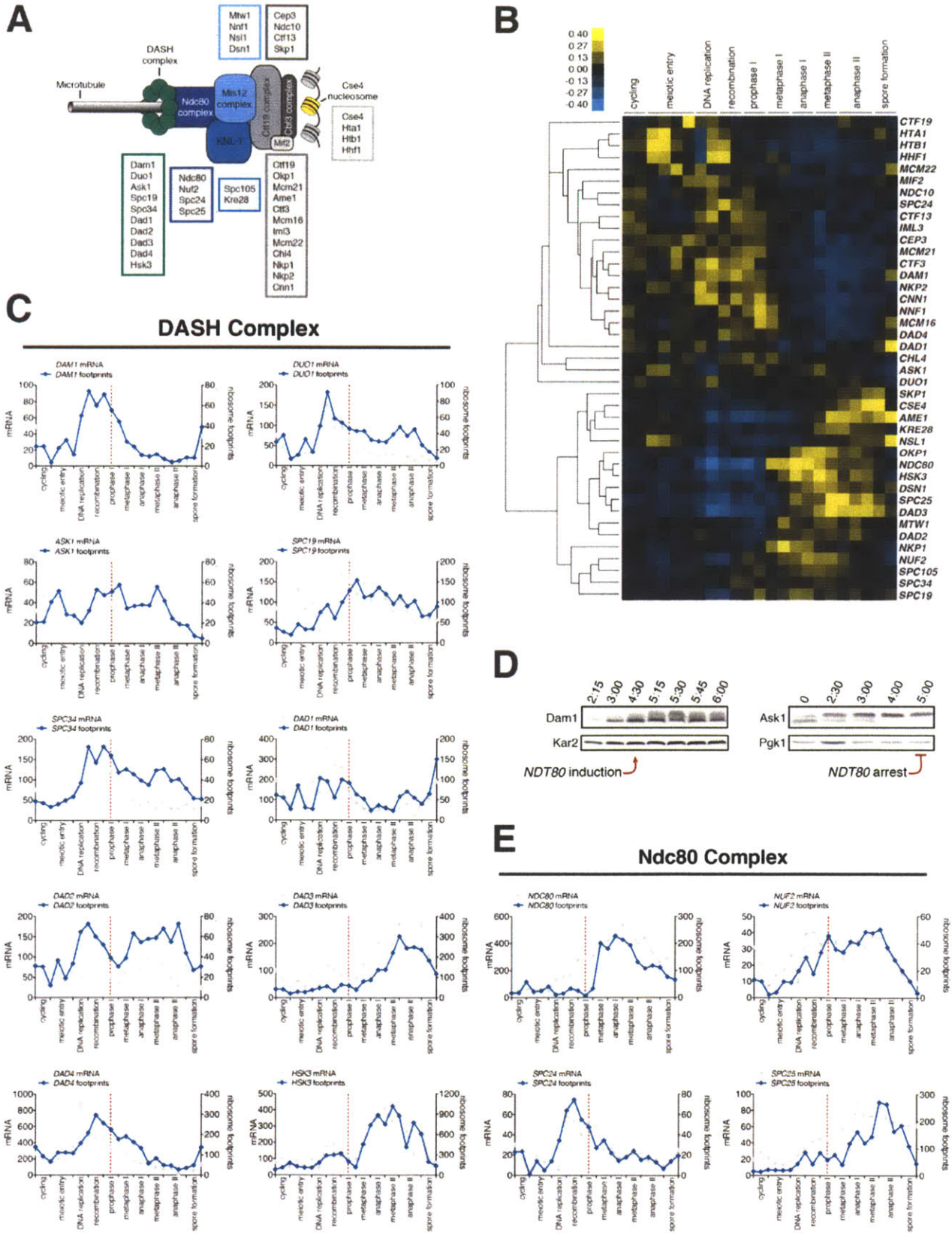
A
Mtw1
Nnf1
Nsl1
Dsn1
Cep3
Ndc10
Ctf13
Skp1
DASH complex
Microtubule
Ndc80 complex
Mis12 complex
KNL-1
Ctf19 complex
Chl3 complex
Mif2
Cse4 nucleosome
Cse4
Hta1
Htb1
Hhf1
Dam1
Duo1
Ask1
Spc19
Spc34
Dad1
Dad2
Dad3
Dad4
Hsk3
Ndc80
Nuf2
Spc24
Spc25
Spc105
Kre28
Ctf19
Okp1
Mcm21
Ame1
Ctf3
Mcm16
Iml3
Mcm22
Chl4
Nkp1
Nkp2
Cnn1
B
0.40
0.27
0.13
0.00
-0.13
-0.27
-0.40
cycling
meiotic entry
DNA replication
recombination
prophase I
metaphase I
anaphase I
metaphase II
anaphase II
spore formation
CTF19
HTA1
HTB1
HHF1
MCM22
MIF2
NDC10
SPC24
CTF13
IML3
CEP3
MCM21
CTF3
DAM1
NKP2
CNN1
NNF1
MCM16
DAD4
DAD1
CHL4
ASK1
DUO1
SKP1
CSE4
AME1
KRE28
NSL1
OKP1
NDC80
HSK3
DSN1
SPC25
DAD3
MTW1
DAD2
NKP1
NUF2
SPC105
SPC34
SPC19
C
DASH Complex
DAM1 mRNA
DAM1 footprints
DUO1 mRNA
DUO1 footprints
ASK1 mRNA
ASK1 footprints
SPC19 mRNA
SPC19 footprints
SPC34 mRNA
SPC34 footprints
DAD1 mRNA
DAD1 footprints
DAD2 mRNA
DAD2 footprints
DAD3 mRNA
DAD3 footprints
DAD4 mRNA
DAD4 footprints
HSK3 mRNA
HSK3 footprints
mRNA
ribosome footprints
D
2:15
3:00
4:30
5:15
5:30
5:45
6:00
Dam1
Kar2
NDT80 induction
0
2:30
3:00
4:00
5:00
Ask1
Pgk1
NDT80 arrest
E
Ndc80 Complex
NDC80 mRNA
NDC80 footprints
NUF2 mRNA
NUF2 footprints
SPC24 mRNA
SPC24 footprints
SPC25 mRNA
SPC25 footprints

Figure 11. Meiotic cluster analysis of kinetochore components and meiotic expression of the DASH and Ndc80 complexes.

(A) Schematic representation of the kinetochore-microtubule interface.

(B) Cluster analysis of kinetochore components from the indicated time points. Further details are in Materials and Methods and in (Brar et al., 2012).

(C) Ordered plot of mRNA-seq and ribosome footprinting data for the DASH complex components at indicated stages of sporulation. Dotted line indicates time of release from *NDT80* block See (Brar et al., 2012) for details.

(D) *DAM1-3V5* (A28898) cells carrying the *GAL4-ER* and *GAL-NDT80* fusion and *ASK1-13myc* (A29161) carrying *ndt80Δ* were induced to sporulate and were either released from (left panel) or arrested in (right panel) the *NDT80* block. Levels of Dam1-3V5, Ask1-13myc, Kar2 and Pgk1 were monitored by Western blot analysis. Pgk1 and Kar2 served as loading controls.

(E) Ordered plot of mRNA-seq and ribosome footprinting data for the Ndc80 complex at indicated stages. Dotted line indicates time of release from *NDT80* block See (Brar et al., 2012) for details.

to the meiotic divisions, while the outer kinetochore is constructed only as cells enter the meiotic divisions.

Among the outer kinetochore components that displayed peak synthesis during the divisions, *NDC80* and a subunit of the DASH complex, *HSK3,* displayed the most differential expression prior to meiosis I and during meiosis I, with a 9.02 and 2.64 fold induction, respectively (Figure 10B-D). This decline in Ndc80 expression is consistent with a previous study in fission yeast, showing that Ndc80 becomes undetectable during prophase I (Asakawa, Hayashi, Haraguchi, & Hiraoka, 2005). Analysis of Ndc80 protein

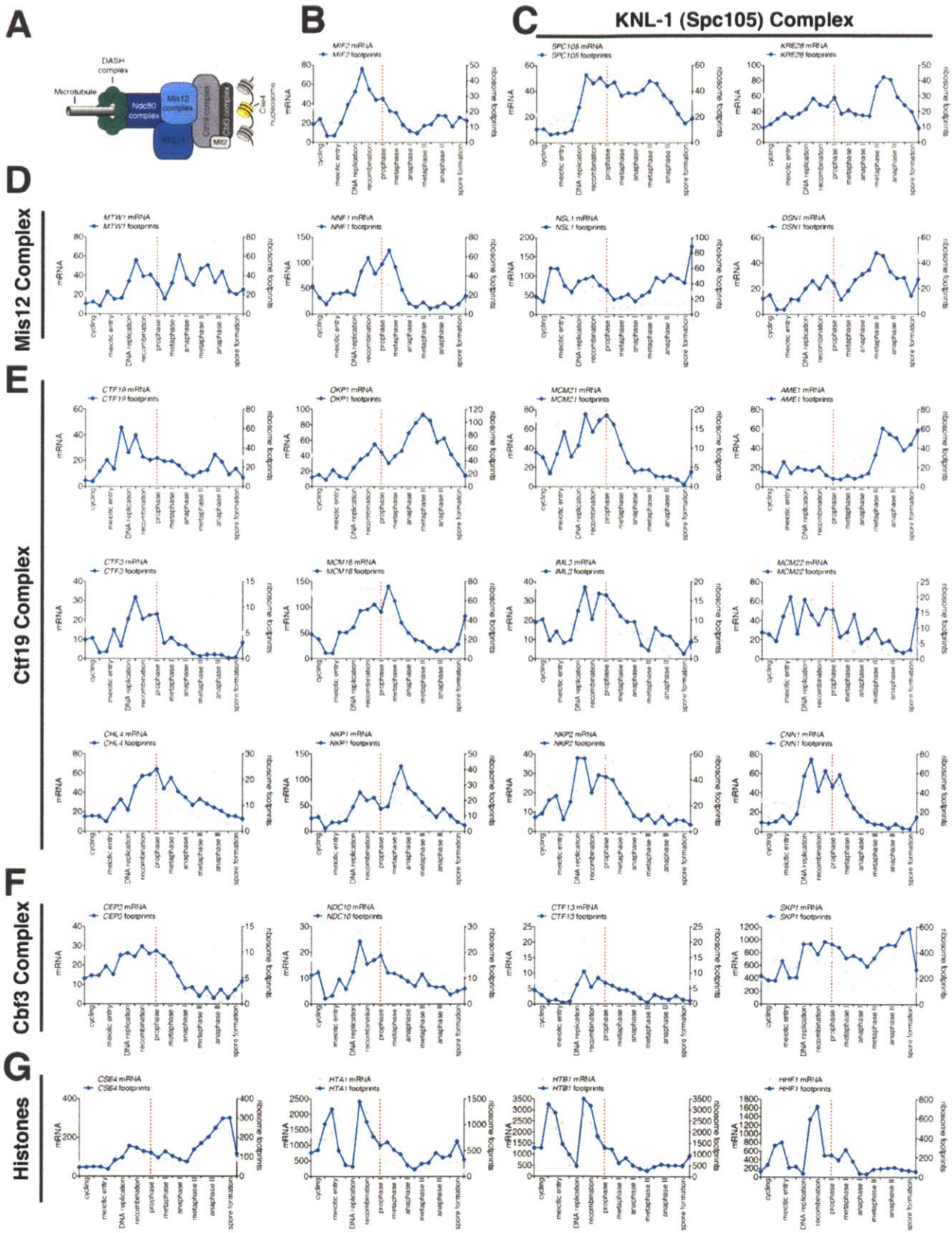
A
B
C
KNL-1 (Spc105) Complex
DASH complex
Microtubule
Ndc80 complex
Mis12 complex
Ctf19 complex
Cbf3 complex
Mif2
Cse4 nucleosome
D
Mis12 Complex
E
Ctf19 Complex
F
Cbf3 Complex
G
Histones
MIF2 mRNA
MIF2 footprints
SPC105 mRNA
SPC105 footprints
KRE28 mRNA
KRE28 footprints
MTW1 mRNA
MTW1 footprints
NNF1 mRNA
NNF1 footprints
NSL1 mRNA
NSL1 footprints
DSN1 mRNA
DSN1 footprints
CTF19 mRNA
CTF19 footprints
OKP1 mRNA
OKP1 footprints
MCM21 mRNA
MCM21 footprints
AME1 mRNA
AME1 footprints
CTF3 mRNA
CTF3 footprints
MCM16 mRNA
MCM16 footprints
IML3 mRNA
IML3 footprints
MCM22 mRNA
MCM22 footprints
CHL4 mRNA
CHL4 footprints
NKP1 mRNA
NKP1 footprints
NKP2 mRNA
NKP2 footprints
CNN1 mRNA
CNN1 footprints
CEP3 mRNA
CEP3 footprints
NDC10 mRNA
NDC10 footprints
CTF13 mRNA
CTF13 footprints
SKP1 mRNA
SKP1 footprints
CSE4 mRNA
CSE4 footprints
HTA1 mRNA
HTA1 footprints
HTB1 mRNA
HTB1 footprints
HHF1 mRNA
HHF1 footprints
mRNA
ribosome footprints
cycling
meiotic entry
DNA replication
recombination
prophase I
metaphase I
anaphase I
metaphase II
anaphase II
spore formation

Figure 12. Meiotic expression of Mif2, KNL-1, Mis12 complex, Ctf19 complex, Cbf3 complex subunits and histones.

(A) Schematic representation of the kinetochore-microtubule interface.

(B) Ordered plot of the mRNA-seq and ribosome footprinting data for Mif2 at the indicated stages. Dotted line indicates time of release from the *NDT80* block. See (Brar et al., 2012) for details.

(C) Ordered plot of the mRNA-seq and ribosome footprinting data for KNL-1 comples subunits (Spc105 complex) at the indicated stages. Dotted line indicates time of release from the *NDT80* block. See (Brar et al., 2012) for details.

(D) Ordered plot of the mRNA-seq and ribosome footprinting data for Mis12 complex subunits at the indicated stages. Dotted line indicates time of release from *NDT80* block. See (Brar et al., 2012) for details.

(E) Ordered plot for mRNA-seq and ribosome footprinting data for Ctf19 complex at indicated stages. Dotted line indicates time of release from the *NDT80* block. See (Brar et al., 2012) for details.

(F) Ordered plot of the mRNA-seq and ribosome footprinting data for Cbf3 complex subunits at the indicated stages. Dotted line indicates time of release from the *NDT80* block. See (Brar et al., 2012) for details.

(G) Ordered plot for mRNA-seq and ribosome footprinting data for the histones at indicated stages. Dotted line indicates time of release from *NDT80* block See (Brar et al., 2012) for details.

levels provided an explanation for why cells upregulate the synthesis of outer kinetochore components during entry into meiosis I. Ndc80 levels declined during premeiotic S phase and became undetectable during late prophase I (Figure 10E). Importantly, the ability of *CUP-CLB3* to induce sister-chromatid segregation during meiosis I tightly correlated with Ndc80 protein levels; as Ndc80 protein declines, so

does *CLB3*-induced meiosis I sister chromatid segregation (compare Figure 10A and 10E).

Hsk3 protein levels were also low until meiosis I entry (Figure 10F), but not all outer kinetochore components exhibited this decline in protein levels. For example, Ask1, a subunit of the DASH complex, was present throughout prophase I and levels of another DASH complex component, Dam1, increased during prophase I (Figure 11D). Our findings indicate that the assembly of the outer kinetochore is restricted prior to *NDT80* expression and pachytene exit due to low levels of a subset of outer kinetochore components.

Expression of *NDC80* and *HSK3* during premeiotic S phase/prophase I enhances *CLB3*-induced meiosis I sister chromatid segregation.

To determine whether reduced expression of the outer kinetochore components Ndc80 and Hsk3 contributes to preventing premature microtubule-kinetochore engagement, we examined the consequences of expressing the two genes from the *CUP1* promoter (Figure 13). We first assessed whether expression of the two proteins allows for the recruitment of the DASH complex to kinetochores, which occurs via delivery through microtubules and can thus be used as a means of assessing end-on attachment of kinetochores (Cheeseman, Enquist-Newman, Muller-Reichert, Drubin, & Barnes, 2001; Tanaka, 2010). Cells were induced to sporulate and after 4h, a time when Ndc80 levels are normally diminished, we induced the expression of *CLB3*, *NDC80* and/or *HSK3*. Whereas expression of either gene alone caused only a few cells to recruit Ask1 to

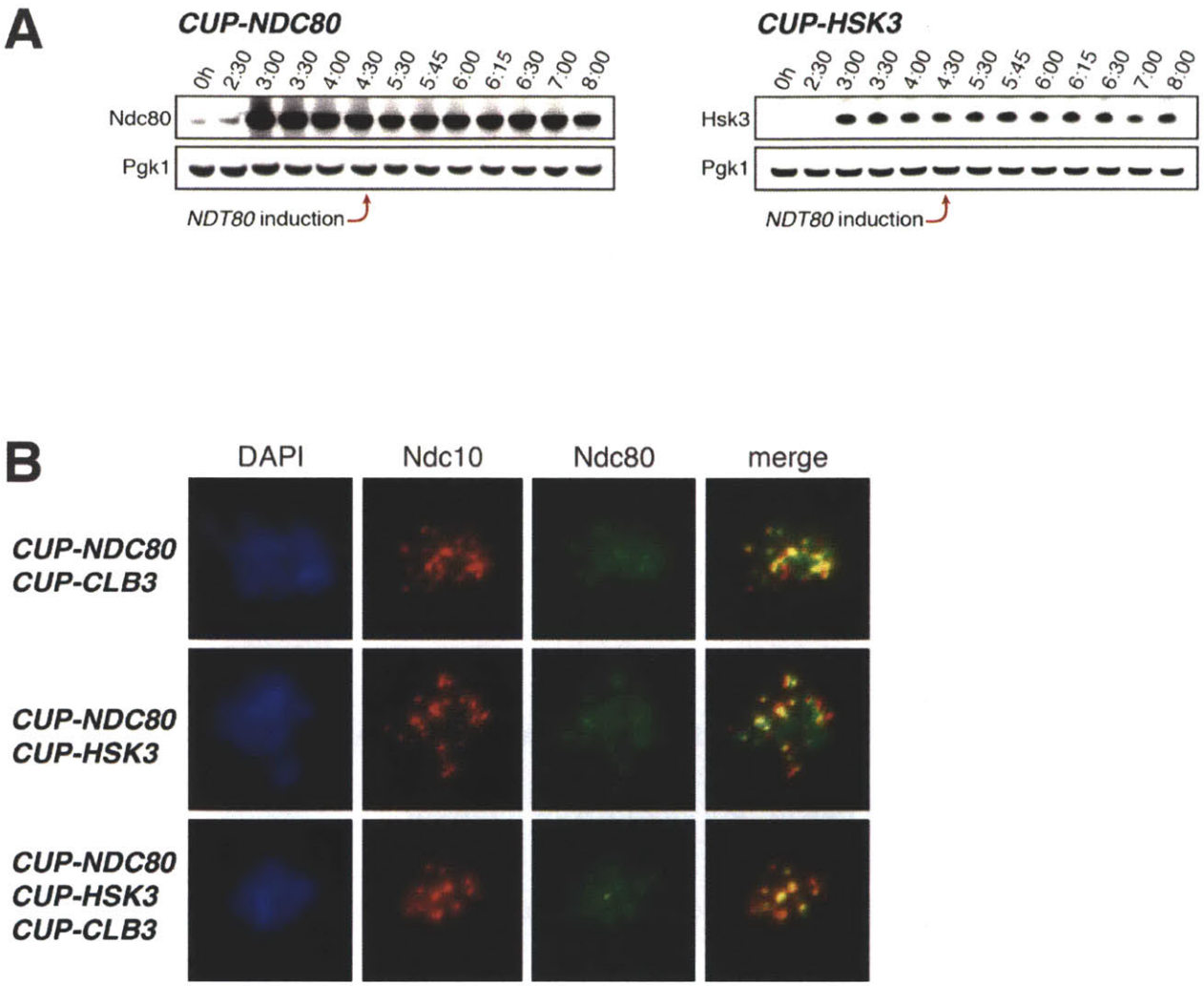

Figure 13. Characterization of *NDC80* and *HSK3* overexpression.

(A) *CUP-NDC80-3V5* (A30342) and *CUP-HSK3-3HA* (A32060) cells also carrying the *GAL4-ER* and *GAL-NDT80* fusions were induced to sporulate. After 2h 30min $CuSO_4$ (50µM) was added and cells were subsequently released from *NDT80* block 4h 30min after transfer into sporulation medium. The levels of Ndc80-3V5, Hsk3-3HA and Pgk1 were monitored by Western blot.

(B) *CUP-NDC80-3V5 CUP-CLB3* (A31949), *CUP-NDC80-3V5 CUP-HSK3* (A31951) and *CUP-NDC80-3V5 CUP-HSK3 CUP-CLB3* (A31953) cells were induced to sporulate. 4h after transfer into sporulation medium $CuSO_4$ (50µM) was added,

and localization of Ndc80-3V5 (green) relative to Ndc10-6HA (red) was determined by nuclear spreads 5h after transfer into sporulation medium.

---

kinetochores, cells simultaneously expressing *NDC80*, *HSK3* and *CLB3* during prophase I showed colocalization between Ask1 and the inner kinetochore component Ndc10, to an equal or greater extent than what was observed in metaphase I-arrested wild-type cells (Figure 14A-B). The difference in Ask1 localization was not due to a difference in *ASK1* expression (Figure 14C). In addition, induction of *CLB3* under the conditions mentioned above gave rise to bipolar spindles that appeared fragile with a weakened midzone. In contrast, consistent with stable microtubule-kinetochore interactions, coexpression of *CLB3, HSK3* and *NDC80* resulted in the formation of robust bipolar spindles (Figure 14D-E). Importantly, the expression of *NDC80* and/or *HSK3* during an *NDT80* block caused a considerable increase in meiosis I sister chromatid segregation in *CUP-CLB3* cells (Figure 14F). Furthermore, under conditions in which *CLB3* expression alone failed to induce meiosis I sister chromatid segregation, expression of *CLB3* together with *NDC80* and *HSK3* caused a substantial increase in meiosis I sister chromatid segregation (Figure 14G). This occurred even when cells were maintained in a prolonged *NDT80* block prior to expression of *CLB3*, *NDC80* and *HSK3* (Figure 15), ruling out the possibility that the expression of *NDT80* targets, such as *CDC5*, early during sporulation contributes to sister chromatid segregation during meiosis I. We conclude that limiting outer kinetochore assembly is an additional mechanism to prevent microtubule-kinetochore interactions during premeiotic S phase and prophase I.

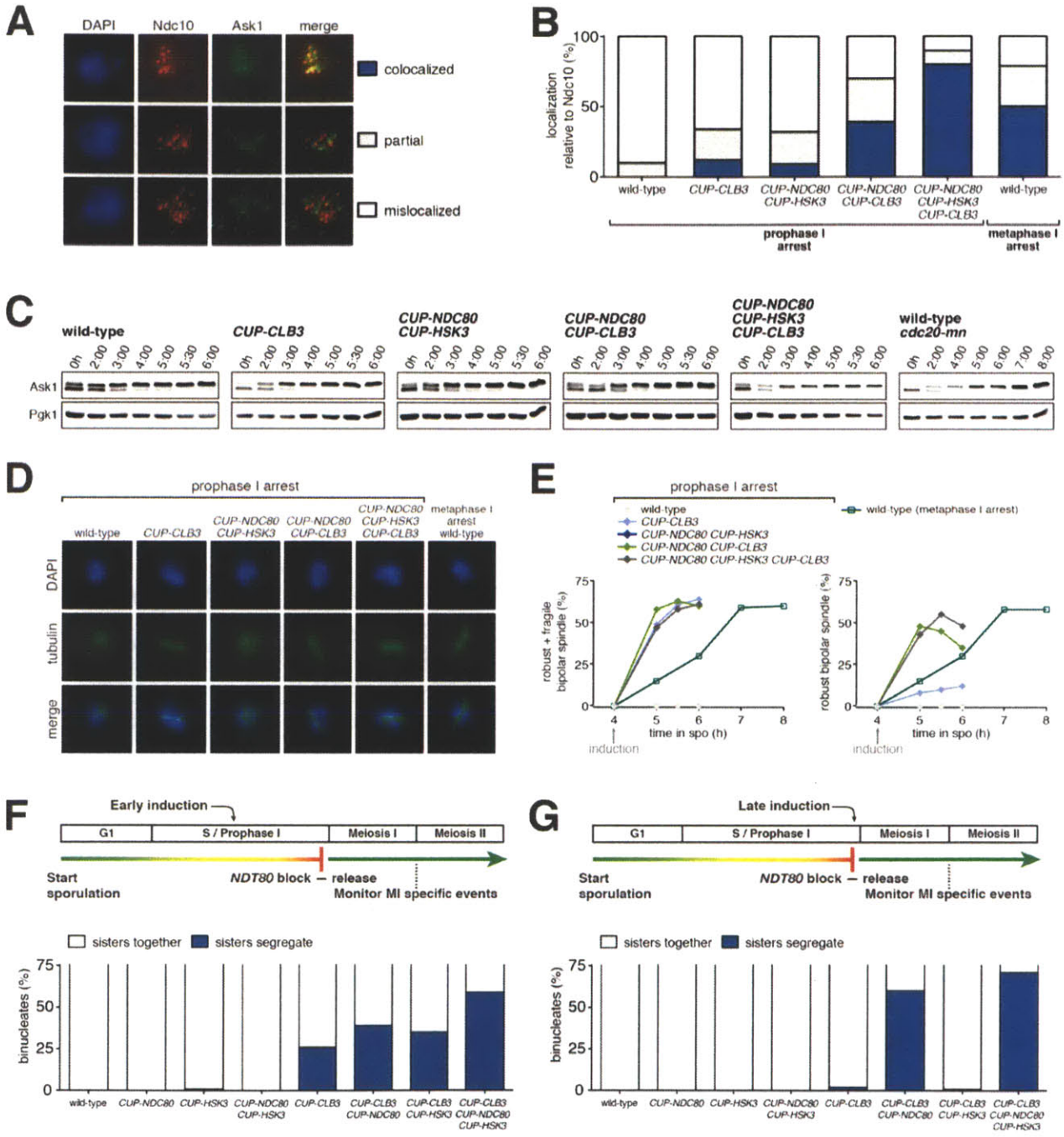

Figure 14. Expression of *NDC80* and *HSK3* in prophase I enhances Clb3-CDK-induced meiosis I sister chromatid segregation.

For **(A)-(E)**, wild-type (A31945), *CUP-CLB3* (A31947), *CUP-NDC80 CUP-HSK3* (A31951), *CUP-NDC80 CUP-CLB3* (A31949), *CUP-NDC80 CUP-HSK3 CUP-CLB3* (A31953) and *cdc20-mn* (A31955) cells were induced to sporulate and $CuSO_4$ was added at 4h after sporulation-induction.

(A) Representative images and **(B)** quantification of Ask1-13myc (green) in mononucleates relative to Ndc10-6HA (red) determined by nuclear spreads prepared after 1h of $CuSO_4$ induction (n>40 except for A31955 [n=28]). For **(B)**, using a chi-square test (df 2) the fraction of spread nuclei that display colocalized, partial or mislocalized Ask1 with respect to Ndc10 was compared between *CUP-CLB3* and *CUP-CLB3 CUP-NDC80 CUP-HSK3* $\chi^2 = 51.49$, $p < 0.0001$.

(C) Western blots of Ask1-13myc and Pgk1.

(D) Bipolar spindle morphology and **(E)** left panel, total (robust + fragile) bipolar spindle formation, and right panel, robust bipolar spindle formation determined at the indicated time points (see Materials and Methods for further description) (n=100 per time point). Note: *CUP-NDC80 CUP-HSK3* (dark blue) data points occluded by wild-type (grey) data points.

(F) and **(G)** Segregation of sister chromatids using heterozygous CENV-GFP dots quantified in binucleates from wild-type (A30340), *CUP-NDC80* (A30342), *CUP-HSK3* (A31849), *CUP-NDC80 CUP-HSK3* (A31855), *CUP-CLB3* (A31847), *CUP-CLB3 CUP-NDC80* (A31853), *CUP-CLB3 CUP-HSK3* (A31851) and *CUP-CLB3 CUP-NDC80 CUP-HSK3* (A31857) [Early induction= 2:15h, late induction= 4:30h after induction of sporulation; release from *NDT80*-block at 4:30h] (n=100). For **(F)**, using a chi-square test (df 1) the fraction of binucleates with a reductional or equational division was compared between *CUP-CLB3* and *CUP-CLB3 CUP-NDC80 CUP-HSK3* $\chi^2 = 22.28$, $p < 0.0001$. For **(G)**, using a chi-square test (df 1) the fraction of binucleates with a reductional or equational division was compared between *CUP-CLB3* and *CUP-CLB3 CUP-NDC80 CUP-HSK3* $\chi^2 = 102.7$, $p < 0.0001$.

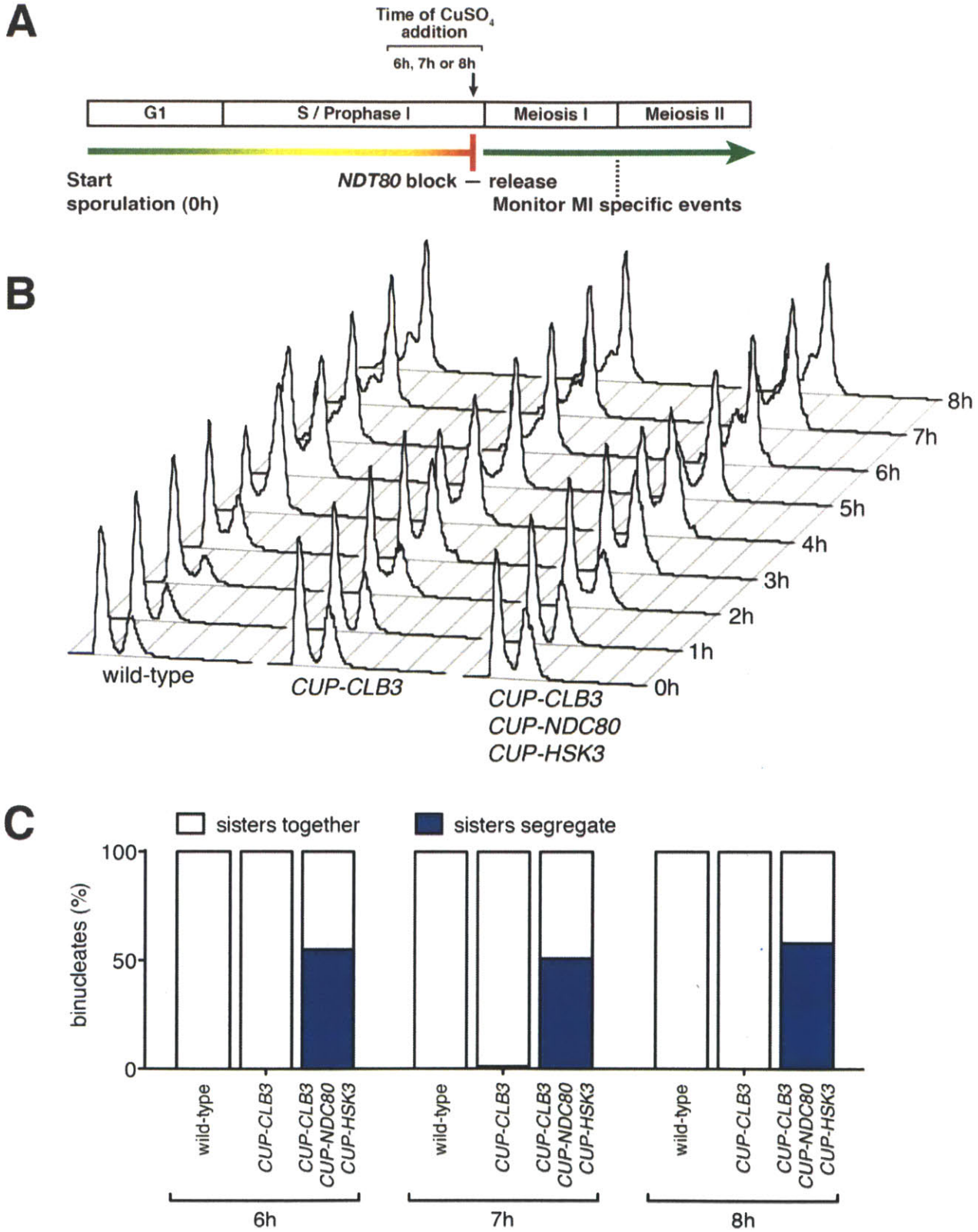
A
Time of CuSO4 addition
6h, 7h or 8h
G1
S / Prophase I
Meiosis I
Meiosis II
Start sporulation (0h)
NDT80 block — release
Monitor MI specific events
B
8h
7h
6h
5h
4h
3h
2h
1h
0h
wild-type
CUP-CLB3
CUP-CLB3
CUP-NDC80
CUP-HSK3
C
sisters together
sisters segregate
binucleates (%)
100
50
0
wild-type
CUP-CLB3
CUP-CLB3 CUP-NDC80 CUP-HSK3
6h
7h
8h

Figure 15. *CUP-CLB3 CUP-NDC80 CUP-HSK3* induced meiosis I sister chromatid segregation is independent of the length of the prophase I arrest.

(A) Schematic description of the experimental regime used in **(B)** and **(C)**.

(B, C) Wild-type (A22678), *CUP-CLB3* (A22702) and *CUP-CLB3 CUP-NDC80 CUP-HSK3* (A31857) cells also carrying the *GAL4-ER* and *GAL-NDT80* fusions were induced to sporulate. Cells were released from the *NDT80* block and concurrently *pCUP1*-dependent expression was induced at either 6h, 7h or 8h post transfer to sporulation medium (by addition of 1μM estradiol and 50 μM $CuSO_4$ respectively). Samples were taken at the indicated time points to determine DNA content **(B)** and the percentage of binucleate cells with segregated sister chromatids **(C)**. For **(C)**, using a chi-square test (df 1), the fraction of binucleates that display a reductional or equational division in *CUP-CLB3 CUP-NDC80 CUP-HSK3* cells was compared between 6h and 7h induction $\chi^2 = 0.3212$, $p = 0.5709$ and between 6h and 8h induction $\chi^2 = 0.1831$, $p = 0.6687$.

DISCUSSION

The specialized chromosome segregation pattern in meiosis likely evolved through modifications of the mitotic cell division program. We find that preventing microtubule-kinetochore interactions during premeiotic S phase and prophase I is essential for transforming mitosis into meiosis I. Meiosis I chromosome morphogenesis, including the assembly of cohesin protective structures around centromeres and sister kinetochore coorientation, occurs during prophase I. We propose that when microtubules interact with kinetochores prior to completion of this remodeling process, they establish a default attachment, biorientation, which is incompatible with establishing sister kinetochore coorientation and a cohesin protective domain around centromeres (Figure 16). Our findings reveal a novel regulatory event that is essential for accurate meiosis I chromosome segregation and demonstrate that temporal restriction of microtubule-kinetochore interactions is instrumental in transforming mitosis into meiosis.

The effects of premature microtubule-kinetochore engagement on meiosis I chromosome morphogenesis.

Transcriptional and translational controls restrict *CLB3* expression to meiosis II (Carlile and Amon, 2008). Eliminating both, by placing the gene under the control of the *GAL1-10* promoter or the *CUP1* promoter has dramatic effects on meiosis I chromosome segregation. *CLB3* expression from the *GAL1-10* promoter, which leads to Clb3 levels comparable to those seen for wild-type cells in meiosis II, causes a significant suppression of the meiosis I chromosome segregation pattern. This defect is not further enhanced by overexpression of the protein (by expression from the *CUP1* promoter),

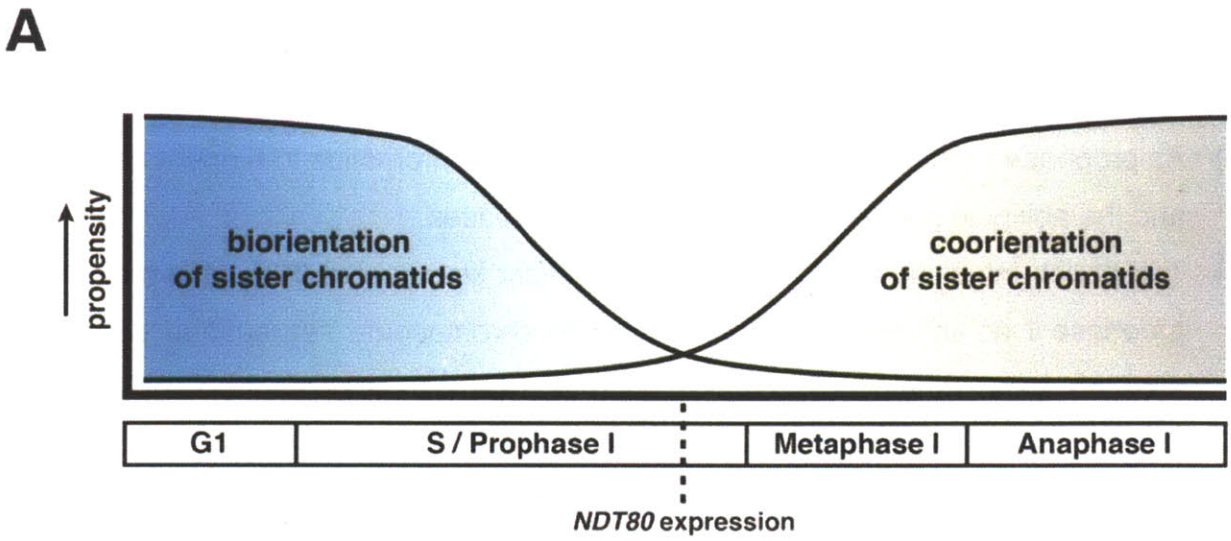
A
propensity
biorientation
of sister chromatids
coorientation
of sister chromatids
G1
S / Prophase I
Metaphase I
Anaphase I
NDT80 expression

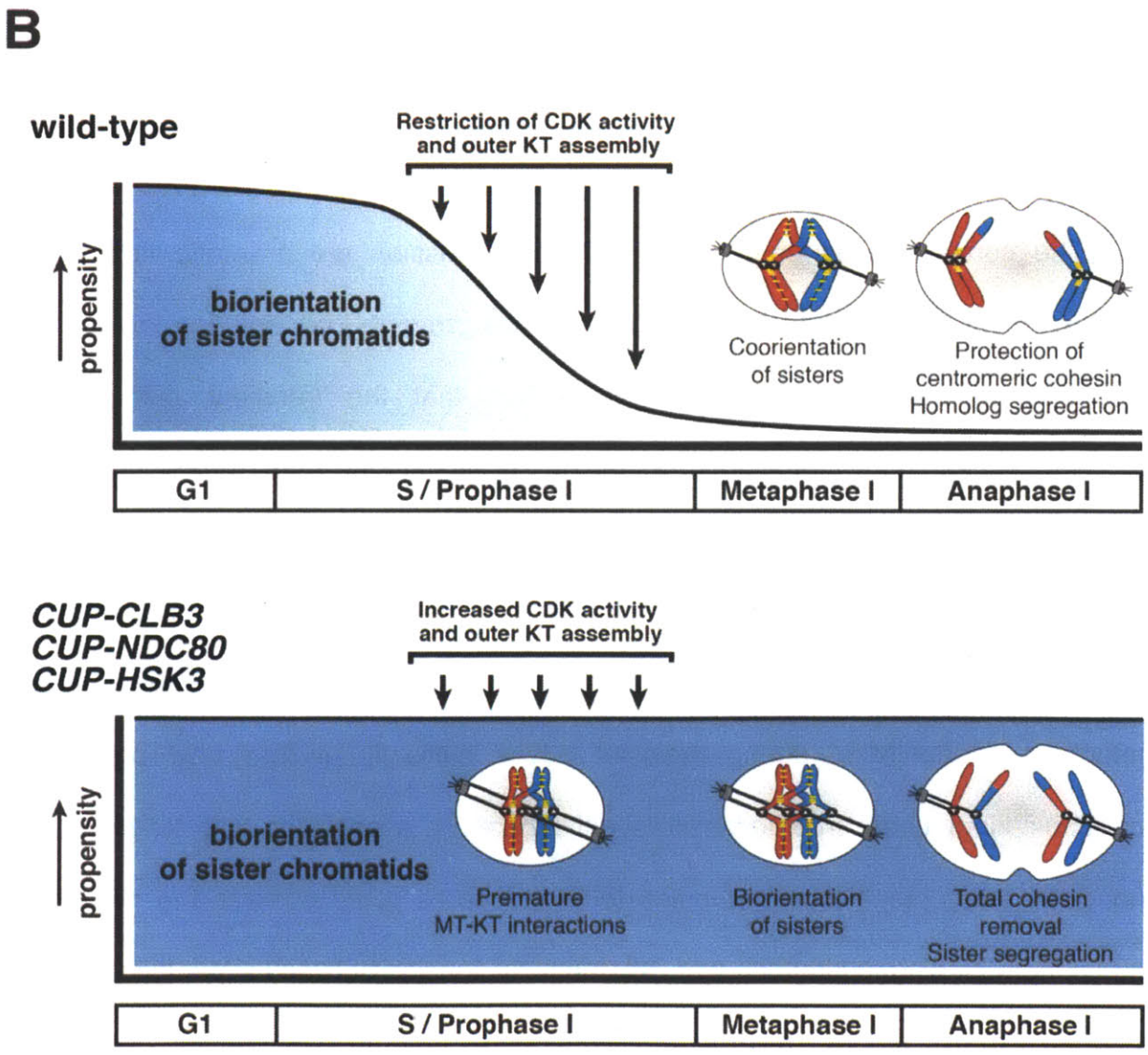
B
wild-type
Restriction of CDK activity
and outer KT assembly
propensity
biorientation
of sister chromatids
Coorientation
of sisters
Protection of
centromeric cohesin
Homolog segregation
G1
S / Prophase I
Metaphase I
Anaphase I
CUP-CLB3
CUP-NDC80
CUP-HSK3
Increased CDK activity
and outer KT assembly
propensity
biorientation
of sister chromatids
Premature
MT-KT interactions
Biorientation
of sisters
Total cohesin
removal
Sister segregation
G1
S / Prophase I
Metaphase I
Anaphase I

Figure 16. Model for temporal regulation of microtubule-kinetochore interactions during meiosis.

(A) As prophase I progresses, the propensity of sister chromatids to biorient decreases and the ability to coorient sister chromatids increases.

(B) Top panel: Inhibiting Clb-CDK activity and outer kinetochore (KT) assembly during prophase I establishes a meiosis I-specific chromosome segregation pattern by allowing sister kinetochore coorientation and protection of centromeric cohesin. Bottom panel: Disrupting the regulation of microtubule-kinetochore (MT-KT) interactions causes sister chromatid segregation in meiosis I.

which further indicates that this phenotype does not emanate from expressing exceedingly high levels of the cyclin, but is a consequence of premature expression.

The consequences of premature *CLB3* expression are dramatic. It leads to premature microtubule-kinetochore interactions and prevents coorientation factors from associating with kinetochores. The observation that the transient disruption of microtubule-kinetochore interactions, either by inactivating the outer kinetochore or by microtubule depolymerization, allowed coorientation factors to associate with kinetochores, despite *CLB3* misexpression, led us to conclude that it is premature microtubule-kinetochore interactions that interfere with the establishment of sister kinetochore coorientation during meiosis I. It is currently unclear how preexisting microtubule-kinetochore interactions prevent monopolin association with kinetochores. Precocious attachment of microtubules to kinetochores could occlude the monopolin complex from binding to kinetochores. Alternatively, tension between sister kinetochores generated from stable microtubule-kinetochore interactions could induce a

conformational change at the kinetochore and/or pericentric chromatin such that coorientation factors can no longer associate with the kinetochore.

In addition to preventing sister kinetochore coorientation, premature expression of *CLB3* interferes with protecting centromeric cohesin from removal during meiosis I. The same logic as outlined for coorientation factors applies to the conclusion that it is Clb3-CDK mediated premature microtubule-kinetochore interactions that lead to loss of centromeric cohesin protection in *CUP-CLB3* cells; disrupting microtubule-kinetochore interactions by various means restores stepwise loss of cohesin in *CUP-CLB3* cells. A simple interpretation of this result is that the centromeric-cohesin protective domain can be disrupted by tension between sister kinetochores at any meiotic stage prior to anaphase I. This does not appear to be the case. In cells lacking the coorientation factor *MAM1*, sister kinetochores come under tension in metaphase I, yet in these cells centromeric cohesin is not removed prematurely (Toth et al., 2000 and Figure 7C). Thus, the timing of microtubule-kinetochore interactions is of importance. It is tempting to speculate that the establishment of the centromeric-cohesin protective domain, which occurs during prophase I or perhaps even earlier, is sensitive to premature microtubule-kinetochore interactions and/or tension that promote biorientation of sister kinetochores. However, once this domain is established, its maintenance during meiosis I can no longer be disrupted by tension between sister kinetochores.

How premature microtubule-kinetochore interactions affect the centromeric cohesin protection machinery is not yet known. A defect in localization of the protective machinery to kinetochores does not appear to be the cause of this defect. Sgo1 and

PP2A localize normally to kinetochores in *CUP-CLB3* cells. Therefore, lack of cohesin protection upon premature microtubule-kinetochore engagement must either result from a defect in an unknown cohesin protection pathway or from a decrease in the activity of Sgo1 and/or PP2A. Premature association of kinetochores with microtubules could result in the untimely recruitment of a factor (e.g. Clb-CDKs themselves) to the pericentromere that inhibits the cohesin protective machinery. Alternatively, microtubule-kinetochore engagement could directly affect the activity of the protective machinery. Two mechanisms have been previously proposed whereby tension modulates the activity of the cohesin protective machinery. In mammalian cells, tension spatially separates centromeric cohesin from Sgo1-PP2A, perhaps leading to loss of protection (J. Lee et al., 2008). Tension has also been proposed to cause a deformation in PP2A, thus inhibiting its catalytic activity (Grinthal, Adamovic, Weiner, Karplus, & Kleckner, 2010). Irrespective of whether it is tension-dependent perturbation of Sgo1-PP2A and/or recruitment of inhibitory factors, it is clear that premature microtubule-kinetochore engagement is a *bona fide* modulator of the cohesin protective machinery.

Regulated kinetochore assembly contributes to preventing microtubule-kinetochore interactions.

Cyclin-CDKs regulate multiple aspects of microtubule-kinetochore dynamics. Cyclin-CDKs promote centrosome separation and bipolar spindle assembly (Fitch et al., 1992), kinetochore maturation (Holt et al., 2009) and chromosomal passenger complex

localization (Tsukahara, Tanno, & Watanabe, 2010). Given the importance of preventing premature microtubule-kinetochore engagement to meiosis I chromosome morphogenesis, it is not surprising that cyclin-CDK activity is regulated at multiple levels in budding yeast; transcription of *CLB1, CLB3* and *CLB4* is not activated until cells exit pachytene (Chu & Herskowitz, 1998) and *CLB3* translation is restricted to meiosis II (Carlile & Amon, 2008).

Cyclin-CDK activity is also tightly regulated in other eukaryotes. Metazoan oocytes arrest for an extended period of time in prophase I. Multiple mechanisms keep cyclin-CDK activity low to maintain this arrest (reviewed in Von Stetina & Orr-Weaver, 2011). Similar regulation is observed in *D. melanogaster* and *C. elegans*. Remarkably, inappropriate activation of *Cyclin A* or cyclin E during prophase I in fruit flies and worms, respectively, results in a mitosis-like division (Biedermann et al., 2009; Sugimura & Lilly, 2006). Thus, restricting cyclin-CDK activity during premeiotic S phase and prophase I also appears to be required to establish a meiosis I-specific chromosome architecture in higher eukaryotes.

Restriction of cyclin-CDK activity during premeiotic S phase and prophase I appears to be the major mechanism preventing premature microtubule-kinetochore interactions, but our data indicate that regulation of outer kinetochore assembly serves as an additional mechanism to prevent this from occurring. *CUP-CLB3* can only induce meiosis I sister chromatid segregation when expressed during premeiotic S phase/early prophase I, but fails to do so when expressed during late prophase I. This difference is likely due to the outer kinetochore being present only until early prophase I. When

Ndc80, Hsk3 and Clb3 are coexpressed during late prophase I, sister chromatid segregation occurs in meiosis I. This result demonstrates that the presence of Clb3-CDKs alone during late prophase I is not sufficient to cause meiosis I sister chromatid segregation but that outer kinetochore components must also be expressed. Whether outer kinetochore disassembly solely occurs to prevent microtubule kinetochore interactions remains to be determined. Outer kinetochore disassembly could also serve additional purposes during prophase I such as enabling telomere-mediated chromosome movements. Further study of the kinetochore assembly/disassembly cycle during meiosis will provide insights into the full impact of kinetochore regulation on meiotic chromosome segregation.

In budding yeast, two essential components of the outer kinetochore, Ndc80 and Hsk3, are downregulated during prophase I. In *S. pombe*, Ndc80 and its binding partner Nuf2 dissociate from kinetochores in prophase I (Asakawa et al., 2005) raising the interesting possibility that deconstruction of the outer kinetochore is a conserved feature of meiotic prophase I. This dissociation depends on the mating pheromone signaling pathway (Asakawa et al., 2005). Intriguingly, ectopic induction of meiosis without mating pheromone signaling (i.e. in *pat1* mutants), results in segregation of sister chromatids instead of homologous chromosomes in meiosis I (A. Yamamoto & Hiraoka, 2003; T. G. Yamamoto, Chikashige, Ozoe, Kawamukai, & Hiraoka, 2004). Perhaps this change in the pattern of chromosome segregation in *pat1* mutants arises from premature microtubule-kinetochore interactions due to a defect in outer kinetochore disassembly. Interestingly, in mouse oocytes, the Ndc80 complex is recruited to chromosomes only

after nuclear envelope breakdown (Sun, Zhang, Lee, Xu, & Kim, 2011), raising the possibility that outer kinetochore assembly is also prevented in meiotic prophase I in vertebrates.

Concluding remarks

Proper segregation of the genome during gametogenesis is critical for the proliferation of sexually reproducing species. Errors in chromosome segregation during meiosis result in aneuploidy, the leading cause of birth defects and miscarriages in humans (Hassold & Hunt, 2001). Thus, it is crucial to understand how accurate meiotic chromosome segregation is achieved. We discovered that the establishment of a meiosis-specific chromosome segregation pattern depends on the regulation of microtubule-kinetochore interactions. This is achieved by regulating cyclin-CDK activity as well as assembly of the outer kinetochore. There is evidence for similar regulatory events across different organisms (Asakawa et al., 2005; Biedermann et al., 2009; Sugimura & Lilly, 2006; Von Stetina & Orr-Weaver, 2011), suggesting that temporal restriction of microtubule-kinetochore interactions is an evolutionarily conserved event required to execute proper meiotic chromosome segregation.

MATERIAL AND METHODS

Strains and plasmids

Strains used in this study are described in Supplementary file 1 and are derivatives of SK1 (all meiosis experiments) or W303 (Figure 8A). *GAL-NDT80* and *GAL4.ER* constructs are described in (Benjamin et al., 2003). *CUP-CLB1, CUP-CLB3, CUP-CLB4, CUP-CLB5, SPC42-mCherry, SGO1-3V5, RTS1-13myc, RTS1-3V5, HSK3-3V5, NDC80-3V5, ASK1-13myc, CUP-NDC80-3V5, CUP-HSK3, mam1Δ, SPO13-3V5, mad3Δ, DAM1-3V5, CUP-HSK3-3HA* were constructed by PCR-based methods described in (Longtine et al., 1998). Primer sequences for strain constructions are available upon request. *ndc80-1* and *dam1-1* are described in (Jones, Bachant, Castillo, Giddings, & Winey, 1999; Wigge et al., 1998) and SK1 strains carrying these alleles were constructed via backcrossing (>9X). CENV-LacO was constructed by cloning a CENV homology region with XhoI restriction sites into the SalI cut plasmid pCM40 (gift from Doug Koshland) and integrated near *CDEIII* (<1kb) by BamHI digest. pHG40 carrying *CUP1* promoter was a gift from Hong-Guo Yu. 3V5 tagging plasmids were provided by Vincent Guacci.

Sporulation conditions

Strains were grown to saturation in YPD at room temperature, diluted in BYTA (1% yeast extract, 2% tryptone, 1% potassium acetate, 50mM potassium phthalate) to OD_{600} = 0.25, and grown overnight at 30°C (room temperature for *ndc80-1* and *dam1-1* experiments). Cells were resuspended in sporulation medium (0.3% potassium acetate

[pH 7], 0.02% raffinose) to OD_{600} = 1.85 and sporulated at 30°C unless otherwise indicated. *GAL-NDT80 GAL4.ER* strains were released from the *NDT80* block by the addition of 1 μM β-estradiol (5 mM stock in ethanol, Sigma E2758-1G) at 4hr 30min unless otherwise indicated. Note: strains released from *NDT80* block at 4hr 30min are prototrophic and have accelerated meiotic kinetics relative to strains containing auxotrophies. Strains with *CUP1* promoter driven alleles were induced by addition of $CuSO_4$ (50μM final concentration; 100mM stock made from anhydrous powder [FW=159.6 g/mol]; Mallinkrodt) at indicated times.

Transient inactivation of the *ndc80-1* or *dam1-1* alleles

Wild-type, *ndc80-1* or *dam1-1* cells carrying *GAL-NDT80 GAL4.ER* were induced to sporulate at room temperature (permissive temperature). After 2h 45min, cyclin expression was induced by addition of 50μM $CuSO_4$ and cells were concurrently shifted to the semi-permissive (34°C) or non-permissive (>35.5°C) temperature and allowed to arrest in pachytene. Cells were then transferred to the permissive temperature and released from the *NDT80* block by addition of 1μM β-estradiol into either a metaphase I arrest (by depleting Cdc20) or allowed to proceed through the meiotic divisions.

Benomyl treatment of meiotic cultures

Wild-type or *CUP-CLB3* cells carrying the *GAL-NDT80 GAL4.ER* constructs were induced to sporulate at 30°C. 2h 15min after transfer into sporulation medium, cells were filtered and transferred to medium containing $CuSO_4$ (50μM) and either 0.4% DMSO or benomyl (120 μg/ml). After an additional 2h 15min incubation, benomyl was

washed out by filtering and washing cells with 10 volumes of sterile dH_20 containing 0.4% DMSO. Cells were subsequently resuspended in sporulation medium containing 1μM β-estradiol to release from *NDT80* block. The efficacy of benomyl treatment was confirmed by spindle morphology. See (Hochwagen et al., 2005) for further technical details regarding benomyl resuspension in sporulation medium.

Mitotic induction of monopolin

MATa haploid cells carrying the *MET-CDC20* or *MET-CDC20 GAL-CDC5 GAL-MAM1* fusions and CENIV-GFP dots cultured in complete synthetic medium without methionine (CSM -MET) containing 2% raffinose were arrested in G1 with 5μg/ml α-factor. For Figure 8A condition (1), cells were treated with galactose (to induce Cdc5 and Mam1 production) for 1h prior to α-factor release. When arrest was complete, cells were released into rich medium (YEP) with 2% raffinose lacking pheromone and containing 2% galactose, 1% DMSO and 8mM methionine (to repress Cdc20 production). 8mM methionine was added every hour to maintain metaphase arrest. When metaphase arrest was complete, cells were released into CSM -MET medium, containing 2% dextrose, 1% DMSO and 5μg/ml α-factor. For condition (2), G1 arrested cells were released into YEP medium with 2% raffinose, lacking pheromone, containing 8mM methionine and 1% DMSO. 8mM methionine was added every hour to maintain the metaphase arrest. After 2h, cells were treated with 2% galactose for 1h and were subsequently released into CSM -MET medium, containing 2% dextrose, 1% DMSO and 5μg/ml α-factor. For condition (3), G1 arrested cells were released into YEP medium with 2% raffinose, lacking pheromone, containing 8mM methionine and

15μg/ml nocodazole in DMSO. 8mM methionine was added every hour to maintain the metaphase arrest. After 2h, cells were treated with 2% galactose for 1h and were subsequently released into CSM -MET medium, containing 2% dextrose, 1% DMSO and 5μg/ml α-factor. Samples were taken every 15min after release from metaphase arrest to determine GFP dot segregation in anaphase.

Indirect immunofluorescence

Indirect immunofluorescence was performed as described in (Kilmartin & Adams, 1984). Spindle morphologies were classified as follows: Metaphase I or Metaphase I-like spindles were defined as a short, bipolar spindle spanning a single DAPI mass. Anaphase I spindles were defined as an elongated spindle spanning two distinct DAPI masses. Metaphase II spindles were defined as two short, bipolar spindles, each spanning a DAPI mass. Anaphase II spindles were defined as two elongated spindles, each spanning two distinct DAPI masses (four DAPI masses total). For Figure 14D-E, robust bipolar spindle was classified as a short, thick, bipolar spindle with equal intensity tubulin staining across the entire length of the spindle. A fragile spindle was classified as a short bipolar spindle with lower intensity tubulin staining in the middle of the spindle axis.

Live cell imaging

Cells were induced to sporulate and $CuSO_4$ was added at the indicated times. After 30-60min post $CuSO_4$ induction, cells were layered on a Concanavalin A (2mg/ml; stock solution 20mg/ml diluted in 50mM $CaCl_2$, 50mM $MnSO_4$) coated cover slip and

assembled into an FCS2 fluidic chamber (Bioptechs Inc. Butler, PA). Sporulation medium was heated to 30°C, aerated using an aquarium air pump (Petco Animal Supplies, Inc. Cambridge, MA) and was perfused into the fluidic chamber using a peristaltic pump (Gilson) with a flow rate of 4-7ml/h. Alternatively, cells were induced to sporulate as above and transferred to a microfluidic chamber (CellASIC Corp. Hayward, CA). Cells were imaged using a Zeiss Axio Observer-Z1 with a 100X objective (NA=1.45), equipped with a Hamamatsu ORCA-ER digital camera. 11 Z-stacks (1 micron apart) were acquired and maximally projected. Metamorph software was used for image acquisition and processing. Images for Figure 2B was processed using Metamorph deconvolution software. For Figure 2C, a cell was scored as harboring a separated pair of sister kinetochores if the heterozygous CENV-GFP dot signal underwent transient splitting for at least two time points for the duration of the movie.

GFP-dot and Spc42-mCherry cell fixation conditions

An aliquot of cells was fixed with 3.7% formaldehyde in 100mM phosphate buffer (pH 6.4) for 10-15min. Cells were washed once with 100mM phosphate, 1.2M sorbitol buffer (pH 7.5) and permeabilized with 1% Triton X-100 stained with 0.05µg/ml 4', 6-diamidino-2-phenylindole (DAPI). Cells were imaged using a Zeiss Axioplan 2 microscope or a Zeiss Axio Observer-Z1 with a 100X objective (NA=1.45), equipped with a Hamamatsu ORCA-ER digital camera. Openlab or Metamorph software was used for image acquisition and processing.

Chromosome spreads

4 OD_{600} units of cells were harvested and spheroplasted with 0.1mg/ml zymolyase 100T (Seikagaku Corp, Japan) and 15mM DTT in solution 1 (2% potassium acetate, 0.8% sorbitol) for 10-13min at 37°C. Ice-cold solution 2 (100mM MES (pH6.4), 1mM EDTA, 0.5mM $MgCl_2$, 1M sorbitol) was added to stop spheroplasting and cells were centrifuged at 2500 rpm for 2-3min. The supernatant was discarded and the pellet was gently resuspended in 100-200µl of solution 2. 15µl of the resuspension was spread onto a glass slide. Subsequently, 30µl of fixative solution (4% paraformaldehyde, 3.4% sucrose), 60µl of 1% lipsol and 60µl of fixative solution were added on top of cell suspension and spread using a glass rod seven to ten times back and forth. The slides were dried for at least 2h at room temperature, rehydrated in PBS pH7.4, blocked with 0.2% gelatin, 0.5% BSA in PBS, and stained as described in the Antibody section. For quantifications of spread nuclei, images were acquired using a Zeiss Axioplan 2 microscope or a Zeiss Axio Observer-Z1 with a 100X objective (NA=1.45), equipped with a Hamamatsu ORCA-ER digital camera. Openlab or Metamorph software was used for image acquisition and processing. 40-100 spread nuclei were counted for each sample, except for strain A31955 in Figure 14B (n=28). Two proteins were identified as colocalized in spread nuclei when more than 90% of foci overlapped. They were defined as partially colocalized when the overlap between foci was approximately 50% and as mislocalized when the overlap was negligible.

In vitro kinase assay

In vitro kinase assays were performed as described in (Carlile & Amon, 2008) with the following modifications: 1mg of total protein was incubated with 40µl of 50% slurry anti-V5 agarose affinity gel (Sigma) for 2h at 4°C. One half of the immunoprecipitate was used for the *in vitro* kinase assay, while the other half was used for Western blotting to detect Cdc28-3V5.

Western blot analysis

For immunoblot analysis, ~10 OD_{600} units of cells were harvested and treated with 5% trichloroacetic acid for at least 10min at 4°C. The acid was washed away with acetone and the cell pellet was subsequently dried. The cell pellet was pulverized with glass beads in 100µL of lysis buffer (50mM Tris-HCl at pH 7.5, 1mM EDTA, 2.75mM DTT, complete protease inhibitor cocktail [Roche]) using a bead-beater (Biospec Products, Inc. Bartlesville, OK). 3X SDS Sample buffer was added and the cell homogenates were boiled. Standard procedures for sodium dodecyl sulfate-polyacrylamide gel electrophoresis (SDS-PAGE) and Western blotting were followed (Burnette, 1981; Laemmli, 1970; Towbin, Staehelin, & Gordon, 1979). A nitrocellulose membrane (VWR) was used to transfer proteins from polyacrylamide gels. Antibody dilutions are described in the Antibody section.

Flow cytometry

1ml aliquot of a meiotic culture was spun down and the pellet was re-suspended in 70% ethanol and fixed for at least 60 min. Ethanol was removed and the cell pellet was

washed with 50mM sodium citrate, pH 7 and sonicated for 6 seconds at 50% output. The sample was subsequently incubated with 0.25mg/ml Ribonuclease A (sigma) in 50mM sodium citrate overnight at 37°C, washed once with 50mM sodium citrate and re-suspended in 50mM sodium citrate with either 1μM Sytox Green (Molecular Probes) or 16 μg/ml propidium iodide (Sigma). Samples were analyzed using FACSCalibur (BD).

Chromatin Immunoprecipitation

400 OD_{600} units of cells were fixed for 15 min at room temperature in 1% formaldehyde. The formaldehyde was quenched by addition of 125 mM glycine. Samples were processed as previously described (Vader et al., 2011). Before immunoprecipitation, one twentieth of the sample was removed as the input sample. The antibodies used for immunoprecipitation are described in the Antibody section. For ChIP-chip, samples were processed and analyzed as described in (Vader et al., 2011). For qPCR analysis, DNA was amplified using SYBR Premix ExTaq Perfect Real Time Kit (Takara). PCR reactions were 40 cycles of 95°C, 20sec; 55°C, 30sec; 72°C, 30sec using a Roche LightCycler 480 II. The following primers were used (5'-3'):

CENV F: CTT GTT TAG TGC AAG CCA CTG TT

CENV R: CCG CAT TTC CTT GAT TTA CTG TC

c281 F: CAA CGA ACC GTG GGA ACG TTA TAG

c281 R: GAA ACT TTC CTG GTA CCT TCT GC

c194 F: GCT GAA AGC ATG CCA CTG TA

c194 R: GGT GTT CCT GCT TCG TTG TTA G

HMR F: ACG ATC CCC GTC CAA GTT ATG

HMR R: CTT CAA AGG AGT CTT AAT TTC CCT G

Recombination Southern

~20 OD_{600} units of cells were harvested and treated with sodium azide (0.1% final concentration). Cells were pelleted and snap frozen in liquid nitrogen. Genomic DNA was extracted as follows: Cells were washed once in TE and spheroplasted with 1/100 volume of beta-mercaptoethanol and 250 µg/ml zymolyase T100 in spheroplasting buffer (1M sorbitol, 42 mM K_2HPO_4, 8 mM KH_2PO_4,5 mM EDTA) for 30min at 37°C on a rotating rack. 100µl preheated (65°C) lysis buffer (1:1 mix of 1 M Tris pH8 and 0.5 M EDTA, 2.5 - 3% SDS) was added and mixed by inverting. 15µl proteinase K (18±4 mg/ml PCR grade solution, Roche) was added and incubated at 65°C for ~1.5 hours. Subsequently, 150µl 5M potassium acetate was added, mixed by inverting and transferred to 4°C for 10min. Samples were centrifuged at 4°C for 20min and 650µl of supernatant was transferred into a 2mL tube containing 750µl 100% ethanol, avoiding as much of the white fluff as possible. Samples were mixed by inverting and left at 4°C for 10min. Nucleic acid was precipitated at 15,000rpm for 10min, 4°C. Samples were subsequently resuspended in TE and treated with RNase A (50 µg/ml, Roche), for 15-20min at 37°C and kept at 4°C overnight. DNA was extracted with phenol/chloroform/isopropanol and was resuspended in 125µl TE. XhoI-MluI digested DNA fragments were separated on 0.6% agarose gel in 1× TBE and transferred onto Hybond-XL plus membranes (GE Healthcare) by alkaline transfer. Southern blotting was performed as previously described (Hunter & Kleckner, 2001).

Antibodies

Indirect immunofluorescence

Spindle morphology was determined using a rat anti-tubulin antibody (Oxford Biotechnology) used at a dilution of 1:100, and anti-rat FITC antibodies (Jackson) used at a dilution of 1:100-200.

Western blotting

Lrs4-13myc, Rec8-13myc, Ask1-13myc and Mam1-9myc were detected using a mouse anti-Myc antibody (Covance) at a 1:500 dilution. Rec8-3HA and Hsk3-3HA were detected using a mouse anti-HA antibody (HA.11, Covance) at a 1:1000 dilution. Hsk3-3V5, Ndc80-3V5 and Dam1-3V5 were detected using a mouse anti-V5 antibody (Invitrogen) at a 1:2000 dilution. Pgk1 was detected using a mouse anti-Pgk1 antibody (Molecular Probes) at a 1:10000 dilution. Clb3 was detected using a rabbit anti-Clb3 antibody (Sc7167, Santa Cruz) at a 1:500 dilution. Kar2 was detected using a rabbit anti-Kar2 antibody (kindly provided by Mark Rose) at a 1:200,000 dilution. The secondary antibodies used were a sheep anti-mouse antibody conjugated to horseradish peroxidase (HRP) (GE Biosciences) at a 1:5000 dilution or a goat anti-rabbit antibody conjugated to HRP (BioRad) at a 1:10000 dilution. Antibodies were detected using the SuperSignal West Pico Chemiluminescent Substrate (Thermo Scientific).

Chromatin immunoprecipitation

Rec8-3HA was immunoprecipitated using 2-5µg of rat anti-HA antibody (3F10, Roche) in combination with 50µl of 50% slurry Protein G beads (Roche). Rec8-13myc was immunoprecipitated using 2-5µg of mouse anti-myc antibody (9E11) in combination with 50µl of 50% slurry Protein G beads (Roche). Sgo1-3V5 and Spo13-3V5 were immunoprecipitated with 40-50µl of 50% slurry anti-V5 agarose affinity gel (Sigma). Pds5 was immunoprecipitated using 1.3µl of rabbit anti-Pds5 antibody (kindly provided by Vincent Guacci) in combination with 50µl of 50% slurry Protein A beads (Roche). Phosphorylated Rec8 was immunoprecipitated using 2µg of rabbit anti-phospho-S179 Rec8 or rabbit anti-phospho-S521 Rec8 in combination with 50µl of 50% slurry Protein A beads (Roche).

Chromosome spreads

Lrs4-13myc, Ndc10-13myc, Sgo1-9myc, Rts1-13myc, Rec8-13myc, Ask1-13myc, and Mam1-9myc were detected using a preabsorbed rabbit anti-Myc antibody (Gramsch) at a 1:400 dilution. Ndc10-6HA and Rec8-3HA were detected using either a preabsorbed mouse anti-HA antibody (HA.11, Covance) or a rat anti-HA antibody (3F10, Roche) at a 1:400 dilution. Ndc80-3V5 was detected using a mouse anti-V5 antibody (Invitrogen) at a 1:400 dilution. Zip1 was detected using the y-300 rabbit antibody (Santa Cruz Biotechnology) at a 1:400 dilution. Rad51 was detected using the y-180 rabbit IgG (Santa Cruz Biotechnology) at a 1:400 dilution. Secondary antibodies used were preabsorbed anti-rabbit FITC antibody (Jackson ImmunoResearch), preabsorbed anti-

rat CY3 antibody (Jackson ImmunoResearch) or preabsorbed anti-mouse CY3 antibody (Jackson ImmunoResearch) at a 1:400-1:800 dilution.

Cluster analysis and ordered plots for mRNA-seq and ribosome footprinting data

Cluster analysis of the ribosome footprinting data for the kinetochore components listed in Figure 11A was performed using Cluster 3.0. Genes were clustered by hierarchical average based on Spearman correlation using mean centered arrays. Clustering data (Figure 10B and Figure 11B) were visualized using Java Treeview. Note that ribosome footprints are normalized such that the sum of expression across the time course is equivalent for each gene. For plots in Figure 10C, 10D, Figure 11 and Figure 12, mRNA-seq and ribosome footprinting data were plotted for indicated genes based on the dataset from (Brar et al., 2012). The meiotic stages plotted on the x-axis are in the following order: vegetative (gb15 exponential and A14201 exponential), meiotic entry (1, A, B and D), DNA replication (E and F), recombination (G and I), prophase I (3 and 4), metaphase I (5 and 6), anaphase I (7 and 8), metaphase II (9 and 10), anaphase II (11, 12 and 13) and spore formation (15 and 18). The detailed explanation of the above letter and number codes can be found in (Brar et al., 2012).

Statistical analysis

Chi-square (χ^2) tests were performed using GraphPad Prism 6.0 software with two-tailed P values and 95% confidence intervals. Corresponding degrees of freedom (df), χ^2 and P values are shown in the figure legends.

Accession codes

Primary accessions

Gene Expression Omnibus

GSE41339

STRAINS USED

Table 1. Strains used in this chapter.

strain	*Relevant Genotype*
W303	*MATa, ade2-1, leu2-3, ura3, trp1-1, his3-11,15, can1-100, GAL, psi+*
A10684	*MATa MET-CDC20::URA3 promURA3::tetR::GFP::LEU2, cenIV::tetOx448::URA3*
A26546	*MATa promURA3::tetR::GFP::LEU2, CenIV::tetOx448::URA3 mam1::GAL-3HA-MAM1::KanMX6 GAL-3MYC-CDC5::URA3 MET-CDC20::URA3*
SK1 (A4962)	*MATa/MATalpha ho::LYS2/ho::LYS2 lys2/lys2 ura3/ura3 leu2::hisG/leu2::hisG his3::hisG/his3::hisG trp1::hisG/trp1::hisG*
A7118	*MATa/alpha cdc20::pCLB2-CDC20::KanMX6/cdc20::pCLB2-CDC20::KanMX6 leu2::pURA3-TetR-GFP::LEU2 CENV::tetOx224::HIS3*
A7450	*MATa/alpha cdc20::pCLB2-CDC20::KanMX6/cdc20::pCLB2-CDC20::KanMX6 NDC10-6HA::HIS3MX6/NDC10-6HA::HIS3MX6 MAM1-9MYC::TRP1/MAM1-9MYC::TRP1*
A9217	*MATa/alpha cdc20::pCLB2-CDC20::KanMX6/cdc20::pCLB2-CDC20::KanMX6 NDC10-6HA::HIS3MX6/NDC10-6HA::HIS3MX6 LRS4-13MYC::KanMX6/LRS4-13MYC::KanMX6*
A15163	*MATa/alpha cdc20::pCLB2-CDC20::KanMX6/cdc20::pCLB2-CDC20::KanMX6 leu2::pURA3-TetR-GFP::LEU2/leu2::pURA3-TetR-GFP::LEU2 CENV::TetOx224::HIS3/CENV::TetOx224::HIS3*
A18185	*MATa/alpha ura3::pGPD1-GAL4(848).ER::URA3/ura3::pGPD1-GAL4(848).ER::URA3 GAL-NDT80::TRP1/GAL-NDT80::TRP1 CLB3-3HA::KANR/CLB3-3HA::KANR leu2::tetR-GFP::LEU2, TetO-HIS3*
A18686	*MATa/alpha ura3::pGPD1-GAL4(848).ER::URA3/ura3::pGPD1-GAL4(848).ER::URA3 CLB3-3HA:KANR/CLB3-3HA::KANR leu2::tetR-GFP::LEU2, TetO-HIS3*
A19151	*MATa/alpha ura3::pGPD1-GAL4(848).ER::URA3/ura3::pGPD1-GAL4(848).ER::URA3*
A19396	*MATa/alpha ura3::pGPD1-GAL4(848).ER::URA3 leu2::pURA3-TetR-GFP::LEU2 CENV::TetOx224::HIS3*
A19400	*MATa/alpha ura3::pGPD1-GAL4(848).ER::URA3 pGAL-CLB3-3HA::KANR::HIS3/pGAL-CLB3-3HA::KANR::HIS3 leu2::pURA3-TetR-GFP::LEU2, CENV::TetOx224::HIS3*

A20958	*MATa/alpha ura3::pGPD1-GAL4(848).ER::URA3 GAL-NDT80::TRP1/GAL-NDT80::TRP1 cdc20::pCLB2-CDC20::KanMX/cdc20::pCLB2-CDC20::KanMX leu2::pURA3-TetR-GFP::LEU2 CENV::tetOx224::HIS3*
A21104	*MATa/alpha TRP1/TRP1 ura3::pGPD1-GAL4(848).ER::URA3/ura3::pGPD1-GAL4(848).ER::URA3 his4X::LEU2-(Bam)-URA3, arg4-Nsp his4B::LEU2, arg4-Bgl II*
A21105	*MATa/alpha TRP1/ trp1::hisG ura3::pGPD1-GAL4(848).ER::URA3/ura3::pGPD1-GAL4(848).ER::URA3 pGAL-CLB3-3HA::KANR::HIS3/pGAL-CLB3-3HA::KANR::HIS3 his4X::LEU2-(Bam)-URA3, arg4-Nsp his4B::LEU2, arg4-Bgl II*
A21193	*MATa/alpha ura3::pGPD1-GAL4(848).ER::URA3 spo11::URA3/spo11::URA3 leu2::pURA3-TetR-GFP::LEU2, CENV::TetOx224::HIS3*
A21194	*MATa/alpha ura3::pGPD1-GAL4(848).ER::URA3 spo11::URA3/spo11::URA3 pGAL-CLB3-3HA::KANR::HIS3/pGAL-CLB3-3HA::KANR::HIS3 leu2::pURA3-TetR-GFP::LEU2, CENV::TetOx224::HIS3*
A22678	*MATa/alpha ura3::pGPD1-GAL4(848).ER::URA3/ura3::pGPD1-GAL4(848).ER::URA3 GAL-NDT80::TRP1/GAL-NDT80::TRP1 CENV::TetOx224::HIS3, leu2::pURA3-TetR-GFP::LEU2*
A22682	*MATa/alpha ura3::pGPD1-GAL4(848).ER::URA3/ura3::pGPD1-GAL4(848).ER::URA3 GAL-NDT80::TRP1/GAL-NDT80::TRP1 leu2::tetR-GFP::LEU2, TetO-HIS3 pCup1-CLB3::KANMX*
A22688	*MATa/alpha ura3::pGPD1-GAL4(848).ER::URA3/ura3::pGPD1-GAL4(848).ER::URA3 GAL-NDT80::TRP1/GAL-NDT80::TRP1 CENV::TetOx224::HIS3/CENV::TetOx224::HIS3 leu2::pURA3-TetR-GFP::LEU2/leu2::pURA3-TetR-GFP::LEU2*
A22702	*MATa/alpha ura3::pGPD1-GAL4(848).ER::URA3/ura3::pGPD1-GAL4(848).ER::URA3 GAL-NDT80::TRP1/GAL-NDT80::TRP1 leu2::pURA3-TetR-GFP::LEU2, CENV::TetOx224::HIS3 pCup1-CLB3::KANMX*
A22708	*MATa/alpha ura3::pGPD1-GAL4(848).ER::URA3/ura3::pGPD1-GAL4(848).ER::URA3 GAL-NDT80::TRP1/GAL-NDT80::TRP1 leu2::pURA3-TetR-GFP::LEU2/leu2::pURA3-TetR-GFP::LEU2 , CENV::TetOx224::HIS3/CENV::TetOx224::HIS3 pCup1-CLB3::KANMX*

A22803	*MATa/alpha ura3::pGPD1-GAL4(848).ER::URA3/ura3::pGPD1-GAL4(848).ER::URA3 GAL-NDT80::TRP1/GAL-NDT80::TRP1 ubr1::HIS3/ubr1::HIS3 rec8::KanMX4::Rec8S197AS386AS387AS136AT173AS199AS245AT249A-S521AS522AS314AS410AS179AS215AS465AS466AS285AS494AS421AY14AS552AT18AT19AS292AS425AS404AS125AT126AS224A-3HA/ rec8::KanMX4::Rec8S197AS386AS387AS136AT173AS199AS245AT249A-S521AS522AS314AS410AS179AS215AS465AS466AS285AS494AS421AY14AS552AT18AT19AS292AS425AS404AS125AT126AS224A-3HA*
A22804	*MATa/alpha ura3::pGPD1-GAL4(848).ER::URA3/ura3::pGPD1-GAL4(848).ER::URA3 GAL-NDT80::TRP1/GAL-NDT80::TRP1 ubr1::HIS3/ubr1::HIS3 rec8::KanMX4::Rec8-3HA/rec8::KanMX4::Rec8-3HA*
A22836	*MATa/alpha NDC10-6HA::HIS3MX6 REC8-13MYC-KanMX6*
A22838	*MATa/alpha NDC10-6HA::HIS3MX6 REC8-13MYC-KanMX6 pCup1-CLB3::KANMX*
A22864	*MATa/alpha NDC10-6HA::HIS3MX6 MAM1-9MYC::TRP1*
A22866	*MATa/alpha NDC10-6HA::HIS3MX6 MAM1-9MYC::TRP1 pCup1-CLB3::KANMX*
A22868	*MATa/alpha SGO1-9MYC:TRP1 NDC10-6HA::HIS3MX6*
A22870	*MATa/alpha SGO1-9MYC:TRP1 NDC10-6HA::HIS3MX6 pCup1-CLB3::KANMX*
A23074	*MATa/alpha cdc20::pCLB2-CDC20::KanMX6/cdc20::pCLB2-CDC20::KanMX6 pCup1-CLB3::KANMX leu2::pURA3-TetR-GFP::LEU2, CENV::TetOx224::HIS3*
A23076	*MATa/alpha ura3::pGPD1-GAL4(848).ER::URA3/ura3::pGPD1-GAL4(848).ER::URA3 GAL-NDT80::TRP1/GAL-NDT80::TRP1 cdc20::pCLB2-CDC20::KanMX/cdc20::pCLB2-CDC20::KanMX pCup1-CLB3::KANMX CENV::TetOx224::HIS3, leu2::pURA3-TetR-GFP::LEU2*
A23084	*MATa/alpha ura3::pGPD1-GAL4(848).ER::URA3/ura3::pGPD1-GAL4(848).ER::URA3 PGAL-CLB3-3HA:KANMX::HIS3 leu2::tetR-GFP::LEU2, TetO-HIS3*
A23086	*MATa/alpha ura3::pGPD1-GAL4(848).ER::URA3 PCUP-CLB3-KANMX leu2::tetR-GFP::LEU2, TetO-HIS3*
A25508	*MATa/alpha ura3::pGPD1-GAL4(848).ER::URA3/ura3::pGPD1-GAL4(848).ER::URA3 GAL-NDT80::TRP1/GAL-NDT80::TRP1 CDC28-3V5::KanMX*

A26277	*MATa/alpha cdc20::pCLB2-CDC20::KanMX6/cdc20::pCLB2-CDC20::KanMX6 LRS4-13MYC::KanMX6/LRS4-13MYC::KanMX6 NDC10-6HA::HIS3MX6*
A26278	*MATa/alpha cdc20::pCLB2-CDC20::KanMX6/cdc20::pCLB2-CDC20::KanMX6 LRS4-13MYC::KanMX6/LRS4-13MYC::KanMX6 NDC10-6HA::HIS3MX6 pCup1-CLB3::KANMX*
A26547	*MATa/alpha cdc20::pCLB2-CDC20::KanMX6/cdc20::pCLB2-CDC20::KanMX6 REC8-3HA::URA3/REC8-3HA::URA3 PDS1-18MYC::LEU2*
A26548	*MATa/alpha cdc20::pCLB2-CDC20::KanMX6/cdc20::pCLB2-CDC20::KanMX6 REC8-3HA::URA3/REC8-3HA::URA3 PDS1-18MYC::LEU2 clb3::pCup1-CLB3:KANMX*
A27421	*MATa/alpha ura3::pGPD1-GAL4(848).ER::URA3/ura3::pGPD1-GAL4(848).ER::URA3 GAL-NDT80::TRP1/GAL-NDT80::TRP1 CENV::TetOx224::HIS3, leu2::pURA3-TetR-GFP::LEU2 KanMX:pCUP1-Clb1*
A27423	*MATa/alpha ura3::pGPD1-GAL4(848).ER::URA3/ura3::pGPD1-GAL4(848).ER::URA3 GAL-NDT80::TRP1/GAL-NDT80::TRP1 CENV::TetOx224::HIS3, leu2::pURA3-TetR-GFP::LEU2 pCup1-CLB4::KANMX*
A27425	*MATa/alpha ura3::pGPD1-GAL4(848).ER::URA3/ura3::pGPD1-GAL4(848).ER::URA3 GAL-NDT80::TRP1/GAL-NDT80::TRP1 CENV::TetOx224::HIS3, leu2::pURA3-TetR-GFP::LEU2 pCup1-CLB5::KANMX*
A27476	*MATa/alpha ura3::pGPD1-GAL4(848).ER::URA3 GAL-NDT80::TRP1/GAL-NDT80::TRP1 ura3::pCyc1-GFP-LacI::URA3 leu2::URA3p-tetR-tdTomato::LEU2 CENV::tetOx224::HIS3/CENV::LacO::CNAT*
A27480	*MATa/alpha ura3::pGPD1-GAL4(848).ER::URA3 GAL-NDT80::TRP1/GAL-NDT80::TRP1 ura3::pCyc1-GFP-LacI::URA3 leu2::URA3p-tetR-tdTomato::LEU2 CENV::tetOx224::HIS3/CENV::LacO::CNAT pCup1-CLB3::KANMX*
A28221	*MATa/alpha ura3::pGPD1-GAL4(848).ER::URA3/ura3::pGPD1-GAL4(848).ER::URA3 GAL-NDT80::TRP1/GAL-NDT80::TRP1 leu2::pURA3-TetR-GFP::LEU2 CENV::TetOx224::HIS3 ndc80-1/ndc80-1 (4X backcrossed)*
A28311	*MATa/alpha ura3::pGPD1-GAL4(848).ER::URA3/ura3::pGPD1-GAL4(848).ER::URA3 GAL-NDT80::TRP1/GAL-NDT80::TRP1 leu2::pURA3-TetR-GFP::LEU2 CENV::TetOx224::HIS3 dam1-1/dam1-1*
A28329	*MATa/alpha his3::hisG/HIS3 NDC10-6HA::HIS3MX6 Rts1-13Myc:HIS3MX/Rts1-13Myc:HIS3MX*

A28330	*MATa/alpha his3::hisG/HIS3 NDC10-6HA::HIS3MX6 Rts1-13Myc:HIS3MX/Rts1-13Myc:HIS3MX pCup1-CLB3::KANMX*
A28331	*MATa/alpha cdc20::pCLB2-CDC20::KanMX6/cdc20::pCLB2-CDC20::KanMX6 NDC10-6HA::HIS3MX6 Rts1-13Myc:HIS3MX/Rts1-13Myc:HIS3MX*
A28332	*MATa/alpha cdc20::pCLB2-CDC20::KanMX6/cdc20::pCLB2-CDC20::KanMX6 NDC10-6HA::HIS3MX6 Rts1-13Myc:HIS3MX/Rts1-13Myc:HIS3MX pCup1-CLB3::KANMX*
A28341	*MATa/alpha ura3::pGPD1-GAL4(848).ER::URA3/ura3::pGPD1-GAL4(848).ER::URA3 GAL-NDT80::TRP1/GAL-NDT80::TRP1 leu2::pURA3-TetR-GFP::LEU2 CENV::TetOx224::HIS3 dam1-1/dam1-1 pCup1-CLB3::KANMX*
A28531	*MATa/alpha ura3::pGPD1-GAL4(848).ER::URA3/ura3::pGPD1-GAL4(848).ER::URA3 GAL-NDT80::TRP1/GAL-NDT80::TRP1 leu2::URA3p-tetR-tdTomato::LEU2 CENV::tetOx224::HIS3 KanMX:pCUP1-Clb1-eGFP:HIS3MX*
A28533	*MATa/alpha ura3::pGPD1-GAL4(848).ER::URA3/ura3::pGPD1-GAL4(848).ER::URA3 GAL-NDT80::TRP1/GAL-NDT80::TRP1 leu2::URA3p-tetR-tdTomato::LEU2 CENV::tetOx224::HIS3 KanMX:pCUP1-Clb3-eGFP:HIS3MX*
A28535	*MATa/alpha ura3::pGPD1-GAL4(848).ER::URA3/ura3::pGPD1-GAL4(848).ER::URA3 GAL-NDT80::TRP1/GAL-NDT80::TRP1 leu2::URA3p-tetR-tdTomato::LEU2 CENV::tetOx224::HIS3 KanMX:pCUP1-Clb4-eGFP:HIS3MX*
A28621	*MATa/alpha ura3::pGPD1-GAL4(848).ER::URA3/ura3::pGPD1-GAL4(848).ER::URA3 GAL-NDT80::TRP1/GAL-NDT80::TRP1 leu2::pURA3-TetR-GFP::LEU2 CENV::TetOx224::HIS3 ndc80-1/ndc80-1*
A28623	*MATa/alpha ura3::pGPD1-GAL4(848).ER::URA3/ura3::pGPD1-GAL4(848).ER::URA3 GAL-NDT80::TRP1/GAL-NDT80::TRP1 leu2::pURA3-TetR-GFP::LEU2 CENV::TetOx224::HIS3 ndc80-1/ndc80-1 pCup1-CLB3::KANMX*
A28625	*MATa/alpha ura3::pGPD1-GAL4(848).ER::URA3/ura3::pGPD1-GAL4(848).ER::URA3 GAL-NDT80::TRP1/GAL-NDT80::TRP1 leu2::pURA3-TetR-GFP::LEU2/leu2::pURA3-TetR-GFP::LEU2 CENV::TetOx224::HIS3/CENV::TetOx224::HIS3 ndc80-1/ndc80-1*
A28627	*MATa/alpha ura3::pGPD1-GAL4(848).ER::URA3/ura3::pGPD1-GAL4(848).ER::URA3 GAL-NDT80::TRP1/GAL-NDT80::TRP1 leu2::pURA3-TetR-GFP::LEU2/leu2::pURA3-TetR-GFP::LEU2 CENV::TetOx224::HIS3/CENV::TetOx224::HIS3 ndc80-1/ndc80-1 pCup1-CLB3::KANMX*

A28663	*MATa/alpha ura3::pGPD1-GAL4(848).ER::URA3/ura3::pGPD1-GAL4(848).ER::URA3 GAL-NDT80::TRP1/GAL-NDT80::TRP1 Cdc28-3V5::KanMX leu2::pURA3-TetR-GFP::LEU2,CENV::TetOx224::HIS3*
A28665	*MATa/alpha ura3::pGPD1-GAL4(848).ER::URA3/ura3::pGPD1-GAL4(848).ER::URA3 GAL-NDT80::TRP1/GAL-NDT80::TRP1 Cdc28-3V5::KanMX leu2::pURA3-TetR-GFP::LEU2,CENV::TetOx224::HIS3 KanMX:pCUP1-Clb1*
A28667	*MATa/alpha ura3::pGPD1-GAL4(848).ER::URA3/ura3::pGPD1-GAL4(848).ER::URA3 GAL-NDT80::TRP1/GAL-NDT80::TRP1 Cdc28-3V5::KanMX leu2::pURA3-TetR-GFP::LEU2,CENV::TetOx224::HIS3 KanMX:pCUP1-Clb3*
A28669	*MATa/alpha ura3::pGPD1-GAL4(848).ER::URA3/ura3::pGPD1-GAL4(848).ER::URA3 GAL-NDT80::TRP1/GAL-NDT80::TRP1 Cdc28-3V5::KanMX leu2::pURA3-TetR-GFP::LEU2,CENV::TetOx224::HIS3 KanMX:pCUP1-Clb4*
A28671	*MATa/alpha ura3::pGPD1-GAL4(848).ER::URA3/ura3::pGPD1-GAL4(848).ER::URA3 GAL-NDT80::TRP1/GAL-NDT80::TRP1 Cdc28-3V5::KanMX leu2::pURA3-TetR-GFP::LEU2,CENV::TetOx224::HIS3 KanMX:pCUP1-Clb5*
A28673	*MATa/alpha cdc20::pCLB2-CDC20::KanMX6/cdc20::pCLB2-CDC20::KanMX6 NDC10-6HA::HIS3MX6/NDC10-6HA::HIS3MX6 MAM1-9MYC::TRP1/MAM1-9MYC::TRP1 pCup1-CLB3::KANMX*
A28674	*MATa/alpha cdc20::pCLB2-CDC20::KanMX6/cdc20::pCLB2-CDC20::KanMX6 NDC10-6HA::HIS3MX6/NDC10-6HA::HIS3MX6 MAM1-9MYC::TRP1/MAM1-9MYC::TRP1 pCup1-CLB4::KANMX*
A28681	*MATa/alpha cdc20::pCLB2-CDC20::KanMX6/cdc20::pCLB2-CDC20::KanMX6 NDC10-13MYC::KanMX6/NDC10-13MYC::KanMX6 REC8-3HA::URA3/REC8-3HA::URA3*
A28682	*MATa/alpha cdc20::pCLB2-CDC20::KanMX6/cdc20::pCLB2-CDC20::KanMX6 NDC10-13MYC::KanMX6/NDC10-13MYC::KanMX6 REC8-3HA::URA3/REC8-3HA::URA3 pCup1-CLB3::KANMX*
A28684	*MATa/alpha NDC10-13MYC::KanMX6/NDC10-13MYC::KanMX6 REC8-3HA::URA3/REC8-3HA::URA3*
A28685	*MATa/alpha NDC10-13MYC::KanMX6/NDC10-13MYC::KanMX6 REC8-3HA::URA3/REC8-3HA::URA3 pCup1-CLB3::KANMX*
A28686	*MATa/alpha NDC10-13MYC::KanMX6/NDC10-13MYC::KanMX6 REC8-3HA::URA3/REC8-3HA::URA3 pCup1-CLB4::KANMX*
A28712	*MATa/alpha cdc20::pCLB2-CDC20::KanMX6/cdc20::pCLB2-CDC20::KanMX6 Sgo1-3V5:KanMX/Sgo1-3V5:KanMX*

A28713	*MATa/alpha cdc20::pCLB2-CDC20::KanMX6/cdc20::pCLB2-CDC20::KanMX6 Sgo1-3V5:KanMX/Sgo1-3V5:KanMX pCup1-CLB3::KANMX*
A28716	*MATa/alpha ura3::pGPD1-GAL4(848).ER::URA3/ura3::pGPD1-GAL4(848).ER::URA3 GAL-NDT80::TRP1/GAL-NDT80::TRP1 NDC10-6HA::HIS3MX6/NDC10-6HA::HIS3MX6 REC8-13MYC-KanMX6/REC8-13MYC-KanMX6*
A28718	*MATa/alpha ura3::pGPD1-GAL4(848).ER::URA3/ura3::pGPD1-GAL4(848).ER::URA3 GAL-NDT80::TRP1/GAL-NDT80::TRP1 NDC10-6HA::HIS3MX6/NDC10-6HA::HIS3MX6 REC8-13MYC-KanMX6/REC8-13MYC-KanMX6 pCup1-CLB3::KANMX*
A28720	*MATa/alpha ura3::pGPD1-GAL4(848).ER::URA3/ura3::pGPD1-GAL4(848).ER::URA3 GAL-NDT80::TRP1/GAL-NDT80::TRP1 NDC10-6HA::HIS3MX6/NDC10-6HA::HIS3MX6 REC8-13MYC-KanMX6/REC8-13MYC-KanMX6 ndc80-1/ndc80-1*
A28722	*MATa/alpha ura3::pGPD1-GAL4(848).ER::URA3/ura3::pGPD1-GAL4(848).ER::URA3 GAL-NDT80::TRP1/GAL-NDT80::TRP1 NDC10-6HA::HIS3MX6/NDC10-6HA::HIS3MX6 REC8-13MYC-KanMX6/REC8-13MYC-KanMX6 ndc80-1/ndc80-1 pCup1-CLB3::KANMX*
A28898	*MATa/alpha ura3::pGPD1-GAL4(848).ER::URA3/ura3::pGPD1-GAL4(848).ER::URA3 GAL-NDT80::TRP1/GAL-NDT80::TRP1 Dam1-3V5:His3MX*
A29161	*MATa/alpha trp1::hisG(?)/trp1::hisG(?) his3::hisG/his3::hisG(?) ndt80::LEU2/ndt80::LEU2 Ask1-13myc:KanMX/Ask1-13myc:KanMX NDC10-6HA::HIS3MX6/NDC10-6HA::HIS3MX6*
A29406	*MATa/alpha ura3::pGPD1-GAL4(848).ER::URA3/ura3::pGPD1-GAL4(848).ER::URA3 GAL-NDT80::TRP1/GAL-NDT80::TRP1 leu2::pURA3-TetR-GFP::LEU2, CENV::TetOx224::HIS3 pCup1-CLB3::KANMX/ pCup1-CLB3::KANMX*
A29581	*MATa/alpha ura3::pGPD1-GAL4(848).ER::URA3/ura3::pGPD1-GAL4(848).ER::URA3 GAL-NDT80::TRP1/GAL-NDT80::TRP1 SPC42-mCherry::NAT*
A29582	*MATa/alpha ura3::pGPD1-GAL4(848).ER::URA3/ura3::pGPD1-GAL4(848).ER::URA3 GAL-NDT80::TRP1/GAL-NDT80::TRP1 SPC42-mCherry::NAT KanMX:pCUP1-Clb1*
A29583	*MATa/alpha ura3::pGPD1-GAL4(848).ER::URA3/ura3::pGPD1-GAL4(848).ER::URA3 GAL-NDT80::TRP1/GAL-NDT80::TRP1 SPC42-mCherry::NAT pCup1-CLB3::KANMX*
A29584	*MATa/alpha ura3::pGPD1-GAL4(848).ER::URA3/ura3::pGPD1-GAL4(848).ER::URA3 GAL-NDT80::TRP1/GAL-NDT80::TRP1 SPC42-mCherry::NAT pCup1-CLB4::KANMX*

A29585	*MATa/alpha ura3::pGPD1-GAL4(848).ER::URA3/ura3::pGPD1-GAL4(848).ER::URA3 GAL-NDT80::TRP1/GAL-NDT80::TRP1 SPC42-mCherry::NAT pCup1-CLB5::KANMX*
A29612	*MATa/alpha ura3::pGPD1-GAL4(848).ER::URA3/ura3::pGPD1-GAL4(848).ER::URA3 GAL-NDT80::TRP1/GAL-NDT80::TRP1 cdc20::pCLB2-CDC20::KanMX6/cdc20::pCLB2-CDC20::KanMX6 LRS4-13MYC::KanMX6/LRS4-13MYC::KanMX6 NDC10-6HA::HIS3MX6*
A29614	*MATa/alpha ura3::pGPD1-GAL4(848).ER::URA3/ura3::pGPD1-GAL4(848).ER::URA3 GAL-NDT80::TRP1/GAL-NDT80::TRP1 cdc20::pCLB2-CDC20::KanMX6/cdc20::pCLB2-CDC20::KanMX6 LRS4-13MYC::KanMX6/LRS4-13MYC::KanMX6 NDC10-6HA::HIS3MX6 ndc80-1/ndc80-1*
A29616	*MATa/alpha ura3::pGPD1-GAL4(848).ER::URA3/ura3::pGPD1-GAL4(848).ER::URA3 GAL-NDT80::TRP1/GAL-NDT80::TRP1 cdc20::pCLB2-CDC20::KanMX6/cdc20::pCLB2-CDC20::KanMX6 LRS4-13MYC::KanMX6/LRS4-13MYC::KanMX6 NDC10-6HA::HIS3MX6 pCup1-CLB3::KANMX*
A29618	*MATa/alpha ura3::pGPD1-GAL4(848).ER::URA3/ura3::pGPD1-GAL4(848).ER::URA3 GAL-NDT80::TRP1/GAL-NDT80::TRP1 cdc20::pCLB2-CDC20::KanMX6/cdc20::pCLB2-CDC20::KanMX6 LRS4-13MYC::KanMX6/LRS4-13MYC::KanMX6 NDC10-6HA::HIS3MX6 ndc80-1/ndc80-1 pCup1-CLB3::KANMX*
A29643	*MATa/alpha cdc20::pCLB2-CDC20::KanMX6/cdc20::pCLB2-CDC20::KanMX6 LRS4-13MYC::KanMX6/LRS4-13MYC::KanMX6 NDC10-6HA::HIS3MX6 pCup1-CLB4::KANMX*
A29645	*MATa/alpha Rts1-3V5:KanMX/Rts1-3V5:KanMX NDC10 -13MYC::KANMX6/NDC10 -13MYC::KANMX6 REC8-3HA::URA3/REC8-3HA::URA3*
A29647	*MATa/alpha Rts1-3V5:KanMX/Rts1-3V5:KanMX NDC10 -13MYC::KANMX6/NDC10 -13MYC::KANMX6 leu2::REC8-S136DS179DS197DT209D-3HA:LEU2/leu2::REC8-S136DS179DS197DT209D-3HA:LEU2 rec8Δ::KanMX4/rec8Δ::KanMX4*
A29690	*MATa/alpha cdc20::pCLB2-CDC20::KanMX6/cdc20::pCLB2-CDC20::KanMX6 ndc80-1/ndc80-1 leu2::pURA3-TetR-GFP::LEU2, CENV::TetOx224::HIS3*
A29692	*MATa/alpha cdc20::pCLB2-CDC20::KanMX6/cdc20::pCLB2-CDC20::KanMX6 ndc80-1/ndc80-1 leu2::pURA3-TetR-GFP::LEU2, CENV::TetOx224::HIS3 pCup1-CLB3::KanMX*

A29718	*MATa/alpha ura3::pGPD1-GAL4(848).ER::URA3/ura3::pGPD1-GAL4(848).ER::URA3 GAL-NDT80::TRP1/GAL-NDT80::TRP1 cdc20::pCLB2-CDC20::KanMX6/cdc20::pCLB2-CDC20::KanMX6 ndc80-1/ndc80-1 CENV::TetOx224::HIS3, leu2::pURA3-TetR-GFP::LEU2*
A29720	*MATa/alpha ura3::pGPD1-GAL4(848).ER::URA3/ura3::pGPD1-GAL4(848).ER::URA3 GAL-NDT80::TRP1/GAL-NDT80::TRP1 cdc20::pCLB2-CDC20::KanMX6/cdc20::pCLB2-CDC20::KanMX6 ndc80-1/ndc80-1 CENV::TetOx224::HIS3, leu2::pURA3-TetR-GFP::LEU2 pCup1-CLB3::KanMX*
A29795	*MATa/alpha ura3::pGPD1-GAL4(848).ER::URA3/ura3::pGPD1-GAL4(848).ER::URA3 GAL-NDT80::TRP1/GAL-NDT80::TRP1 Sgo1-3V5:KanMX/Sgo1-3V5:KanMX NDC10-6HA::HIS3MX6*
A29799	*MATa/alpha ura3::pGPD1-GAL4(848).ER::URA3/ura3::pGPD1-GAL4(848).ER::URA3 GAL-NDT80::TRP1/GAL-NDT80::TRP1 Sgo1-3V5:KanMX/Sgo1-3V5:KanMX NDC10-6HA::HIS3MX6 pCup1-CLB3::KANMX*
A29957	*MATa/alpha ura3::pGPD1-GAL4(848).ER::URA3/ura3::pGPD1-GAL4(848).ER::URA3 GAL-NDT80::TRP1/GAL-NDT80::TRP1 ubr1::HIS3/ubr1::HIS3 REC8-13MYC-KanMX6/ rec8::KanMX4::Rec8-3HA*
A29959	*MATa/alpha ura3::pGPD1-GAL4(848).ER::URA3/ura3::pGPD1-GAL4(848).ER::URA3 GAL-NDT80::TRP1/GAL-NDT80::TRP1 ubr1::HIS3/ubr1::HIS3 REC8-13MYC-KanMX6/ rec8::KanMX4::Rec8-3HA pCup1-CLB3::KANMX*
A29961	*MATa/alpha ura3::pGPD1-GAL4(848).ER::URA3/ura3::pGPD1-GAL4(848).ER::URA3 GAL-NDT80::TRP1/GAL-NDT80::TRP1 ubr1::HIS3/ubr1::HIS3 REC8-13MYC-KanMX6/ rec8::KanMX4::Rec8S197AS386AS387AS136AT173AS199AS245AT249A-S521AS522AS314AS410AS179AS215AS465AS466AS285AS494AS421AY14AS552AT18AT19AS292AS425AS404AS125AT126AS224A-3HA*
A29963	*MATa/alpha ura3::pGPD1-GAL4(848).ER::URA3/ura3::pGPD1-GAL4(848).ER::URA3 GAL-NDT80::TRP1/GAL-NDT80::TRP1 ubr1::HIS3/ubr1::HIS3 REC8-13MYC-KanMX6/ rec8::KanMX4::Rec8S197AS386AS387AS136AT173AS199AS245AT249A-S521AS522AS314AS410AS179AS215AS465AS466AS285AS494AS421AY14AS552AT18AT19AS292AS425AS404AS125AT126AS224A-3HA pCup1-CLB3::KANMX*

A29965	*MATa/alpha ura3::pGPD1-GAL4(848).ER::URA3/ura3::pGPD1-GAL4(848).ER::URA3 GAL-NDT80::TRP1/GAL-NDT80::TRP1 ubr1::HIS3/ubr1::HIS3 rec8::KanMX4::Rec8-3HA/rec8::KanMX4::Rec8-3HA pCup1-CLB3::KANMX*
A29967	*MATa/alpha ura3::pGPD1-GAL4(848).ER::URA3/ura3::pGPD1-GAL4(848).ER::URA3 GAL-NDT80::TRP1/GAL-NDT80::TRP1 ubr1::HIS3/ubr1::HIS3 rec8::KanMX4::Rec8S197AS386AS387AS136AT173AS199AS245AT249A-S521AS522AS314AS410AS179AS215AS465AS466AS285AS494AS421AY14AS552AT18AT19AS292AS425AS404AS125AT126AS224A-3HA/rec8::KanMX4::Rec8S197AS386AS387AS136AT173AS199AS245AT249AS521AS522AS314AS410AS179AS215AS465AS466AS285AS494AS421AY14AS552AT18AT19AS292AS425AS404AS125AT126AS224A-3HA pCup1-CLB3::KANMX*
A29994	*MATa/ MATalpha HIS (?)/HIS (?)TRP (?)/TRP (?) sgo1::KanMX6::PCLB2-3HA-SGO1/sgo1::KanMX6::PCLB2-3HA-SGO1 cdc20::pCLB2-CDC20::KanMX6/cdc20::pCLB2-CDC20::KanMX6 REC8-3HA::URA3/REC8-3HA::URA3*
A30340	*MATa/alpha ura3::pGPD1-GAL4(848).ER::URA3/ura3::pGPD1-GAL4(848).ER::URA3 GAL-NDT80::TRP1/GAL-NDT80::TRP1 CENV::TetOx224::HIS3, leu2::pURA3-TetR-GFP::LEU2 Ndc80-3V5:KanMX*
A30342	*MATa/alpha ura3::pGPD1-GAL4(848).ER::URA3/ura3::pGPD1-GAL4(848).ER::URA3 GAL-NDT80::TRP1/GAL-NDT80::TRP1 CENV::TetOx224::HIS3, leu2::pURA3-TetR-GFP::LEU2 KanMX:pCup1-Ndc80-3V5:CNAT*
A30386	*MATa/alpha ura3::pGPD1-GAL4(848).ER::URA3/ura3::pGPD1-GAL4(848).ER::URA3 GAL-NDT80::TRP1/GAL-NDT80::TRP1 mad3Δ::CNAT/mad3Δ::CNAT leu2::pURA3-TetR-GFP::LEU2, CENV::TetOx224::HIS3*
A30388	*MATa/alpha ura3::pGPD1-GAL4(848).ER::URA3/ura3::pGPD1-GAL4(848).ER::URA3 GAL-NDT80::TRP1/GAL-NDT80::TRP1 mad3Δ::CNAT/mad3Δ::CNAT leu2::pURA3-TetR-GFP::LEU2, CENV::TetOx224::HIS3 pCup1-CLB3::KANMX*
A30390	*MATa/alpha ura3::pGPD1-GAL4(848).ER::URA3/ura3::pGPD1-GAL4(848).ER::URA3 GAL-NDT80::TRP1/GAL-NDT80::TRP1 mad3Δ::CNAT/mad3Δ::CNAT leu2::pURA3-TetR-GFP::LEU2, CENV::TetOx224::HIS3 ndc80-1/ndc80-1*
A30392	*MATa/alpha ura3::pGPD1-GAL4(848).ER::URA3/ura3::pGPD1-GAL4(848).ER::URA3 GAL-NDT80::TRP1/GAL-NDT80::TRP1 mad3Δ::CNAT/mad3Δ::CNAT leu2::pURA3-TetR-GFP::LEU2, CENV::TetOx224::HIS3 ndc80-1/ndc80-1 pCup1-CLB3::KANMX*

A30638	*MATa/alpha ura3::pGPD1-GAL4(848).ER::URA3/ura3::pGPD1-GAL4(848).ER::URA3 GAL-NDT80::TRP1/GAL-NDT80::TRP1 mad3Δ::CNAT/mad3Δ::CNAT leu2::pURA3-TetR-GFP::LEU2, CENV::TetOx224::HIS3/leu2::pURA3-TetR-GFP::LEU2, CENV::TetOx224::HIS3*
A30640	*MATa/alpha ura3::pGPD1-GAL4(848).ER::URA3/ura3::pGPD1-GAL4(848).ER::URA3 GAL-NDT80::TRP1/GAL-NDT80::TRP1 mad3Δ::CNAT/mad3Δ::CNAT leu2::pURA3-TetR-GFP::LEU2, CENV::TetOx224::HIS3/leu2::pURA3-TetR-GFP::LEU2, CENV::TetOx224::HIS3 pCup1-CLB3::KANMX*
A30642	*MATa/alpha ura3::pGPD1-GAL4(848).ER::URA3/ura3::pGPD1-GAL4(848).ER::URA3 GAL-NDT80::TRP1/GAL-NDT80::TRP1 leu2::pURA3-TetR-GFP::LEU2/leu2::pURA3-TetR-GFP::LEU2 CENV::TetOx224::HIS3/CENV::TetOx224::HIS3 mad3Δ::CNAT/mad3Δ::CNAT ndc80-1/ndc80-1*
A30644	*MATa/alpha ura3::pGPD1-GAL4(848).ER::URA3/ura3::pGPD1-GAL4(848).ER::URA3 GAL-NDT80::TRP1/GAL-NDT80::TRP1 leu2::pURA3-TetR-GFP::LEU2/leu2::pURA3-TetR-GFP::LEU2 CENV::TetOx224::HIS3/CENV::TetOx224::HIS3 mad3Δ::CNAT/mad3Δ::CNAT ndc80-1/ndc80-1 pCup1-CLB3::KANMX*
A30700	*MATa/alpha ura3::pGPD1-GAL4(848).ER::URA3/ura3::pGPD1-GAL4(848).ER::URA3 GAL-NDT80::TRP1/GAL-NDT80::TRP1 CENV::TetOx224::HIS3, leu2::pURA3-TetR-GFP::LEU2 SPC42-mCherry::NAT*
A30702	*MATa/alpha ura3::pGPD1-GAL4(848).ER::URA3/ura3::pGPD1-GAL4(848).ER::URA3 GAL-NDT80::TRP1/GAL-NDT80::TRP1 CENV::TetOx224::HIS3, leu2::pURA3-TetR-GFP::LEU2 SPC42-mCherry::NAT KanMX:pCUP1-Clb1*
A30704	*MATa/alpha ura3::pGPD1-GAL4(848).ER::URA3/ura3::pGPD1-GAL4(848).ER::URA3 GAL-NDT80::TRP1/GAL-NDT80::TRP1 CENV::TetOx224::HIS3, leu2::pURA3-TetR-GFP::LEU2 SPC42-mCherry::NAT pCup1-CLB3::KANMX*
A30707	*MATa/alpha ura3::pGPD1-GAL4(848).ER::URA3/ura3::pGPD1-GAL4(848).ER::URA3 GAL-NDT80::TRP1/GAL-NDT80::TRP1 CENV::TetOx224::HIS3, leu2::pURA3-TetR-GFP::LEU2 SPC42-mCherry::NAT pCup1-CLB4::KANMX*
A30708	*MATa/alpha ura3::pGPD1-GAL4(848).ER::URA3/ura3::pGPD1-GAL4(848).ER::URA3 GAL-NDT80::TRP1/GAL-NDT80::TRP1 CENV::TetOx224::HIS3, leu2::pURA3-TetR-GFP::LEU2 SPC42-mCherry::NAT pCup1-CLB5::KANMX*
A30743	*MATa/MATalpha Spo13-3V5:HisMX/Spo13-3V5:HisMX cdc20::pCLB2-CDC20::KanMX6/cdc20::pCLB2-CDC20::KanMX6*

A30745	*MATa/MATalpha Spo13-3V5:HisMX/Spo13-3V5:HisMX cdc20::pCLB2-CDC20::KanMX6/cdc20::pCLB2-CDC20::KanMX6 pCup1-CLB3::KANMX*
A30747	*MATa/MATalpha Spo13-3V5:HisMX/Spo13-3V5:HisMX cdc20::pCLB2-CDC20::KanMX6/cdc20::pCLB2-CDC20::KanMX6 pCup1-CLB4::KANMX*
A30856	*MATa/alpha ura3::pGPD1-GAL4(848).ER::URA3/ura3::pGPD1-GAL4(848).ER::URA3 GAL-NDT80::TRP1/GAL-NDT80::TRP1 Spo13-3V5:HisMX/Spo13-3V5:HisMX*
A30858	*MATa/alpha ura3::pGPD1-GAL4(848).ER::URA3/ura3::pGPD1-GAL4(848).ER::URA3 GAL-NDT80::TRP1/GAL-NDT80::TRP1 Spo13-3V5:HisMX/Spo13-3V5:HisMX pCup1-CLB3::KANMX*
A30860	*MATa/alpha ura3::pGPD1-GAL4(848).ER::URA3/ura3::pGPD1-GAL4(848).ER::URA3 GAL-NDT80::TRP1/GAL-NDT80::TRP1 Spo13-3V5:HisMX/Spo13-3V5:HisMX pCup1-CLB4::KANMX*
A31019	*MATa/alpha ura3::pGPD1-GAL4(848).ER::URA3 GAL-NDT80::TRP1/GAL-NDT80::TRP1 leu2::pURA3-TetR-GFP::LEU2, CENV::TetOx224::HIS3 PDS1-tdTomato-KITRP1/PDS1-tdTomato-KITRP1*
A31021	*MATa/alpha ura3::pGPD1-GAL4(848).ER::URA3 GAL-NDT80::TRP1/GAL-NDT80::TRP1 leu2::pURA3-TetR-GFP::LEU2, CENV::TetOx224::HIS3 PDS1-tdTomato-KITRP1/PDS1-tdTomato-KITRP1 pCup1-CLB3::KANMX*
A31340	*MATa/alpha ura3::pGPD1-GAL4(848).ER::URA3/ura3::pGPD1-GAL4(848).ER::URA3 GAL-NDT80::TRP1/GAL-NDT80::TRP1 mam1Δ::NAT/mam1Δ::NAT CENV::TetOx224::HIS3, leu2::pURA3-TetR-GFP::LEU2*
A31342	*MATa/alpha ura3::pGPD1-GAL4(848).ER::URA3/ura3::pGPD1-GAL4(848).ER::URA3 GAL-NDT80::TRP1/GAL-NDT80::TRP1 mam1Δ::NAT/mam1Δ::NAT CENV::TetOx224::HIS3, leu2::pURA3-TetR-GFP::LEU2 pCup1-CLB3::KANMX*
A31847	*MATa/alpha ura3::pGPD1-GAL4(848).ER::URA3/ura3::pGPD1-GAL4(848).ER::URA3 GAL-NDT80::TRP1/GAL-NDT80::TRP1 CENV::TetOx224::HIS3, leu2::pURA3-TetR-GFP::LEU2 Ndc80-3V5:KanMX pCup1-CLB3::KANMX*
A31849	*MATa/alpha ura3::pGPD1-GAL4(848).ER::URA3/ura3::pGPD1-GAL4(848).ER::URA3 GAL-NDT80::TRP1/GAL-NDT80::TRP1 CENV::TetOx224::HIS3, leu2::pURA3-TetR-GFP::LEU2 Ndc80-3V5:KanMX KanMX:pCUP1-Hsk3-3HA*
A31851	*MATa/alpha ura3::pGPD1-GAL4(848).ER::URA3/ura3::pGPD1-GAL4(848).ER::URA3 GAL-NDT80::TRP1/GAL-NDT80::TRP1 CENV::TetOx224::HIS3, leu2::pURA3-TetR-GFP::LEU2 Ndc80-3V5:KanMX KanMX:pCUP1-Hsk3-3HA KanMX:pCUP1-Hsk3-3HA*

A31853	*MATa/alpha ura3::pGPD1-GAL4(848).ER::URA3/ura3::pGPD1-GAL4(848).ER::URA3 GAL-NDT80::TRP1/GAL-NDT80::TRP1 CENV::TetOx224::HIS3, leu2::pURA3-TetR-GFP::LEU2 KanMX:pCup1-Ndc80-3V5:CNAT pCup1-CLB3::KANMX*
A31855	*MATa/alpha ura3::pGPD1-GAL4(848).ER::URA3/ura3::pGPD1-GAL4(848).ER::URA3 GAL-NDT80::TRP1/GAL-NDT80::TRP1 CENV::TetOx224::HIS3, leu2::pURA3-TetR-GFP::LEU2 KanMX:pCup1-Ndc80-3V5:CNAT KanMX:pCUP1-Hsk3-3HA*
A31857	*MATa/alpha ura3::pGPD1-GAL4(848).ER::URA3/ura3::pGPD1-GAL4(848).ER::URA3 GAL-NDT80::TRP1/GAL-NDT80::TRP1 CENV::TetOx224::HIS3, leu2::pURA3-TetR-GFP::LEU2 KanMX:pCup1-Ndc80-3V5:CNAT pCup1-CLB3::KANMX KanMX:pCUP1-Hsk3-3HA*
A31861	*MATa/alpha ura3::pGPD1-GAL4(848).ER::URA3/ura3::pGPD1-GAL4(848).ER::URA3 GAL-NDT80::TRP1/GAL-NDT80::TRP1 Hsk3-3V5:HisMX*
A31945	*MATa/ MATalpha trp1::hisG(?) GAL-NDT80::TRP1/ndt80::LEU2 Ask1-13myc:KanMX NDC10-6HA::HIS3MX6*
A31947	*MATa/ MATalpha trp1::hisG(?) GAL-NDT80::TRP1/ndt80::LEU2 Ask1-13myc:KanMX NDC10-6HA::HIS3MX6 pCup1-CLB3::KANMX*
A31949	*MATa/ MATalpha trp1::hisG(?) GAL-NDT80::TRP1/ndt80::LEU2 Ask1-13myc:KanMX NDC10-6HA::HIS3MX6 KanMX:pCup1-Ndc80-3V5:CNAT pCup1-CLB3::KANMX*
A31951	*MATa/ MATalpha trp1::hisG(?) GAL-NDT80::TRP1/ndt80::LEU2 Ask1-13myc:KanMX NDC10-6HA::HIS3MX6 KanMX:pCUP1-Hsk3 KanMX:pCup1-Ndc80-3V5:CNAT*
A31953	*MATa/ MATalpha trp1::hisG(?) GAL-NDT80::TRP1/ndt80::LEU2 Ask1-13myc:KanMX NDC10-6HA::HIS3MX6 KanMX:pCUP1-Hsk3 KanMX:pCup1-Ndc80-3V5:CNAT pCup1-CLB3::KANMX*
A31955	*MATa/ MATalpha TRP1/trp1::hisG cdc20::pCLB2-CDC20::KanMX6/cdc20::pCLB2-CDC20::KanMX6 NDC10-6HA::HIS3MX6 Ask1-13myc:KanMX*
A32060	*MATa/alpha ura3::pGPD1-GAL4(848).ER::URA3/ura3::pGPD1-GAL4(848).ER::URA3 GAL-NDT80::TRP1/GAL-NDT80::TRP1 KanMX:pCUP1-Hsk3-3HA:HisMX*
A32470	*MATa/alpha ura3::pGPD1-GAL4(848).ER::URA3/ura3::pGPD1-GAL4(848).ER::URA3 GAL-NDT80::TRP1/GAL-NDT80::TRP1 leu2::pURA3-TetR-GFP::LEU2/leu2::pURA3-TetR-GFP::LEU2 , CENV::TetOx224::HIS3/CENV::TetOx224::HIS3 pCup1-CLB4::KANMX*

A33199	*MATa/alpha ura3::pGPD1-GAL4(848).ER::URA3/ura3::pGPD1-GAL4(848).ER::URA3 GAL-NDT80::TRP1/GAL-NDT80::TRP1 leu2::URA3p-tetR-tdTomato::LEU2 CENV::tetOx224::HIS3 KanMX:pCUP1-Clb5-eGFP:HIS3MX*
A33201	*MATa/alpha ura3::pGPD1-GAL4(848).ER::URA3/ura3::pGPD1-GAL4(848).ER::URA3 GAL-NDT80::TRP1/GAL-NDT80::TRP1 CDC28-3V5::KanMX pCup1-CLB3::KANMX*
A33203	*MATa/alpha ura3::pGPD1-GAL4(848).ER::URA3/ura3::pGPD1-GAL4(848).ER::URA3 GAL-NDT80::TRP1/GAL-NDT80::TRP1 ndc80-1/ndc80-1 CDC28-3V5::KanMX*
A33205	*MATa/alpha ura3::pGPD1-GAL4(848).ER::URA3/ura3::pGPD1-GAL4(848).ER::URA3 GAL-NDT80::TRP1/GAL-NDT80::TRP1 ndc80-1/ndc80-1 CDC28-3V5::KanMX pCup1-CLB3::KANMX*

ACKNOWLEDGEMENTS

We are grateful to Hong Guo Yu, Vincent Guacci, and Wolfgang Zachariae for reagents, Hannah Blitzblau, Gerben Vader, Jingxun Chen, Kristin Kuhn, Kristin Knouse, Ann Thompson, André and Charles Felts for technical assistance, Steve Bell, Leon Chan, Dean Dawson, Doug Koshland, Andrew Murray, Terry Orr-Weaver and members of the Amon lab for their critical reading of this manuscript.

REFERENCES

Asakawa, H., Hayashi, A., Haraguchi, T., & Hiraoka, Y. (2005). Dissociation of the Nuf2-Ndc80 complex releases centromeres from the spindle-pole body during meiotic prophase in fission yeast. *Molecular biology of the cell, 16*(5), 2325-2338. doi: 10.1091/mbc.E04-11-0996

Benjamin, K.R., Zhang, C., Shokat, K.M., & Herskowitz, I. (2003). Control of landmark events in meiosis by the CDK Cdc28 and the meiosis-specific kinase Ime2. *Genes & development, 17*(12), 1524-1539. doi: 10.1101/gad.1101503

Biedermann, B., Wright, J., Senften, M., Kalchhauser, I., Sarathy, G., Lee, M.H. (2009). Translational repression of cyclin E prevents precocious mitosis and embryonic gene activation during C. elegans meiosis. *Developmental cell, 17*(3), 355-364. doi: 10.1016/j.devcel.2009.08.003

Blitzblau, H., Chan, C., Hochwagen, A., & Bell, S. (2012). Separation of DNA replication from the assembly of break-competent meiotic chromosomes. *Plos Genetics, e1002643.*

Brar, G.A., Kiburz, B.M., Zhang, Y., Kim, J.E., White, F., & Amon, A. (2006). Rec8 phosphorylation and recombination promote the step-wise loss of cohesins in meiosis. *Nature, 441*(7092), 532-536. doi: 10.1038/nature04794

Brar, G.A., Yassour, M., Friedman, N., Regev, A., Ingolia, N.T., & Weissman, J.S. (2012). High-resolution view of the yeast meiotic program revealed by ribosome profiling. *Science, 335*(6068), 552-557. doi: 10.1126/science.1215110

Buonomo, S.B., Clyne, R.K., Fuchs, J., Loidl, J., Uhlmann, F., & Nasmyth, K. (2000). Disjunction of homologous chromosomes in meiosis I depends on proteolytic cleavage of the meiotic cohesin Rec8 by separin. *Cell, 103*(3), 387-398.

Burnette, W.N. (1981). "Western blotting": electrophoretic transfer of proteins from sodium dodecyl sulfate--polyacrylamide gels to unmodified nitrocellulose and radiographic detection with antibody and radioiodinated protein A. *Analytical biochemistry, 112*(2), 195-203.

Carlile, T.M., & Amon, A. (2008). Meiosis I is established through division-specific translational control of a cyclin. *Cell, 133*(2), 280-291. doi: S0092-8674(08)00283-3 [pii] 10.1016/j.cell.2008.02.032

Cheeseman, I.M., Enquist-Newman, M., Muller-Reichert, T., Drubin, D.G., & Barnes, G. (2001). Mitotic spindle integrity and kinetochore function linked by the Duo1p/Dam1p complex. *The Journal of cell biology, 152*(1), 197-212.

Chu, S., & Herskowitz, I. (1998). Gametogenesis in yeast is regulated by a transcriptional cascade dependent on Ndt80. *Molecular cell, 1*(5), 685-696.

Ciosk, R., Zachariae, W., Michaelis, C., Shevchenko, A., Mann, M., & Nasmyth, K. (1998). An ESP1/PDS1 complex regulates loss of sister chromatid cohesion at the metaphase to anaphase transition in yeast. *Cell, 93*(6), 1067-1076.

Clyne, R.K., Katis, V.L., Jessop, L., Benjamin, K.R., Herskowitz, I., Lichten, M. (2003). Polo-like kinase Cdc5 promotes chiasmata formation and cosegregation of sister centromeres at meiosis I. *Nature cell biology, 5*(5), 480-485. doi: 10.1038/ncb977

Cohen-Fix, O., Peters, J.M., Kirschner, M.W., & Koshland, D. (1996). Anaphase initiation in Saccharomyces cerevisiae is controlled by the APC-dependent degradation of the anaphase inhibitor Pds1p. *Genes & development, 10*(24), 3081-3093.

Fitch, I., Dahmann, C., Surana, U., Amon, A., Nasmyth, K., Goetsch, L. (1992). Characterization of four B-type cyclin genes of the budding yeast Saccharomyces cerevisiae. *Molecular biology of the cell, 3*(7), 805-818.

Grandin, N., & Reed, S.I. (1993). Differential function and expression of Saccharomyces cerevisiae B-type cyclins in mitosis and meiosis. *Molecular and cellular biology, 13*(4), 2113-2125.

Grinthal, A., Adamovic, I., Weiner, B., Karplus, M., & Kleckner, N. (2010). PR65, the HEAT-repeat scaffold of phosphatase PP2A, is an elastic connector that links force and catalysis. *Proc Natl Acad Sci U S A, 107*(6), 2467-2472. doi: 0914073107 [pii] 10.1073/pnas.0914073107

Hassold, T., & Hunt, P. (2001). To err (meiotically) is human: the genesis of human aneuploidy. *Nature reviews. Genetics, 2*(4), 280-291. doi: 10.1038/35066065

Hochwagen, A., Wrobel, G., Cartron, M., Demougin, P., Niederhauser-Wiederkehr, C., Boselli, M.G. (2005). Novel response to microtubule perturbation in meiosis. *Molecular and cellular biology, 25*(11), 4767-4781. doi: 10.1128/MCB.25.11.4767-4781.2005

Holt, L.J., Tuch, B.B., Villen, J., Johnson, A.D., Gygi, S.P., & Morgan, D.O. (2009). Global analysis of Cdk1 substrate phosphorylation sites provides insights into evolution. *Science, 325*(5948), 1682-1686. doi: 10.1126/science.1172867

Hunter, N., & Kleckner, N. (2001). The single-end invasion: an asymmetric intermediate at the double-strand break to double-holliday junction transition of meiotic recombination. *Cell, 106*(1), 59-70.

Jones, M.H., Bachant, J.B., Castillo, A.R., Giddings, T.H., Jr., & Winey, M. (1999). Yeast Dam1p is required to maintain spindle integrity during mitosis and interacts with the Mps1p kinase. *Molecular biology of the cell, 10*(7), 2377-2391.

Katis, V.L., Galova, M., Rabitsch, K.P., Gregan, J., & Nasmyth, K. (2004). Maintenance of cohesin at centromeres after meiosis I in budding yeast requires a kinetochore-associated protein related to MEI-S332. *Current biology : CB, 14*(7), 560-572. doi: 10.1016/j.cub.2004.03.001

Katis, V.L., Lipp, J.J., Imre, R., Bogdanova, A., Okaz, E., Habermann, B. (2010). Rec8 phosphorylation by casein kinase 1 and Cdc7-Dbf4 kinase regulates cohesin cleavage by separase during meiosis. *Developmental cell, 18*(3), 397-409. doi: 10.1016/j.devcel.2010.01.014

Katis, V.L., Matos, J., Mori, S., Shirahige, K., Zachariae, W., & Nasmyth, K. (2004). Spo13 facilitates monopolin recruitment to kinetochores and regulates maintenance of centromeric cohesion during yeast meiosis. *Current biology : CB, 14*(24), 2183-2196. doi: 10.1016/j.cub.2004.12.020

Keeney, S., Giroux, C.N., & Kleckner, N. (1997). Meiosis-specific DNA double-strand breaks are catalyzed by Spo11, a member of a widely conserved protein family. *Cell, 88*(3), 375-384. doi: S0092-8674(00)81876-0 [pii]

Kerrebrock, A.W., Moore, D.P., Wu, J.S., & Orr-Weaver, T.L. (1995). Mei-S332, a Drosophila protein required for sister-chromatid cohesion, can localize to meiotic centromere regions. *Cell, 83*(2), 247-256.

Kilmartin, J.V., & Adams, A.E. (1984). Structural rearrangements of tubulin and actin during the cell cycle of the yeast Saccharomyces. *The Journal of cell biology, 98*(3), 922-933.

Kitajima, T.S., Kawashima, S.A., & Watanabe, Y. (2004). The conserved kinetochore protein shugoshin protects centromeric cohesion during meiosis. *Nature, 427*(6974), 510-517. doi: 10.1038/nature02312

Kitajima, T.S., Sakuno, T., Ishiguro, K., Iemura, S., Natsume, T., Kawashima, S.A. (2006). Shugoshin collaborates with protein phosphatase 2A to protect cohesin. *Nature, 441*(7089), 46-52. doi: 10.1038/nature04663

Laemmli, U.K. (1970). Cleavage of structural proteins during the assembly of the head of bacteriophage T4. *Nature, 227*(5259), 680-685.

Lee, B.H., & Amon, A. (2003). Role of Polo-like kinase CDC5 in programming meiosis I chromosome segregation. *Science, 300*(5618), 482-486. doi: 10.1126/science.1081846

Lee, B.H., Kiburz, B.M., & Amon, A. (2004). Spo13 maintains centromeric cohesion and kinetochore coorientation during meiosis I. *Current biology : CB, 14*(24), 2168-2182. doi: 10.1016/j.cub.2004.12.033

Lee, J., Kitajima, T.S., Tanno, Y., Yoshida, K., Morita, T., Miyano, T. (2008). Unified mode of centromeric protection by shugoshin in mammalian oocytes and somatic cells. *Nat Cell Biol, 10*(1), 42-52. doi: ncb1667 [pii] 10.1038/ncb1667

Longtine, M.S., McKenzie, A., 3rd, Demarini, D.J., Shah, N.G., Wach, A., Brachat, A. (1998). Additional modules for versatile and economical PCR-based gene deletion and modification in Saccharomyces cerevisiae. *Yeast, 14*(10), 953-961. doi: 10.1002/(SICI)1097-0061(199807)14:10<953::AID-YEA293>3.0.CO;2-U

Marston, A.L., & Amon, A. (2004). Meiosis: cell-cycle controls shuffle and deal. *Nature reviews. Molecular cell biology, 5*(12), 983-997. doi: 10.1038/nrm1526

Matos, J., Lipp, J.J., Bogdanova, A., Guillot, S., Okaz, E., Junqueira, M. (2008). Dbf4-dependent CDC7 kinase links DNA replication to the segregation of homologous chromosomes in meiosis I. *Cell, 135*(4), 662-678. doi: 10.1016/j.cell.2008.10.026

Michaelis, C., Ciosk, R., & Nasmyth, K. (1997). Cohesins: chromosomal proteins that prevent premature separation of sister chromatids. *Cell, 91*(1), 35-45.

Monje-Casas, F., Prabhu, V.R., Lee, B.H., Boselli, M., & Amon, A. (2007). Kinetochore orientation during meiosis is controlled by Aurora B and the monopolin complex. *Cell, 128*(3), 477-490. doi: 10.1016/j.cell.2006.12.040

Morgan, D.O. (1997). Cyclin-dependent kinases: engines, clocks, and microprocessors. *Annual review of cell and developmental biology, 13*, 261-291. doi: 10.1146/annurev.cellbio.13.1.261

Pearson, C.G., Maddox, P.S., Salmon, E.D., & Bloom, K. (2001). Budding yeast chromosome structure and dynamics during mitosis. *The Journal of cell biology, 152*(6), 1255-1266.

Petronczki, M., Matos, J., Mori, S., Gregan, J., Bogdanova, A., Schwickart, M. (2006). Monopolar attachment of sister kinetochores at meiosis I requires casein kinase 1. *Cell, 126*(6), 1049-1064. doi: 10.1016/j.cell.2006.07.029

Rabitsch, K.P., Petronczki, M., Javerzat, J.P., Genier, S., Chwalla, B., Schleiffer, A. (2003). Kinetochore recruitment of two nucleolar proteins is required for homolog segregation in meiosis I. *Developmental cell, 4*(4), 535-548.

Riedel, C.G., Katis, V.L., Katou, Y., Mori, S., Itoh, T., Helmhart, W. (2006). Protein phosphatase 2A protects centromeric sister chromatid cohesion during meiosis I. *Nature, 441*(7089), 53-61. doi: 10.1038/nature04664

Schleiffer, A., Kaitna, S., Maurer-Stroh, S., Glotzer, M., Nasmyth, K., & Eisenhaber, F. (2003). Kleisins: a superfamily of bacterial and eukaryotic SMC protein partners. *Molecular cell, 11*(3), 571-575.

Sugimura, I., & Lilly, M.A. (2006). Bruno inhibits the expression of mitotic cyclins during the prophase I meiotic arrest of Drosophila oocytes. *Developmental cell, 10*(1), 127-135. doi: 10.1016/j.devcel.2005.10.018

Sun, S.C., Zhang, D.X., Lee, S.E., Xu, Y.N., & Kim, N.H. (2011). Ndc80 regulates meiotic spindle organization, chromosome alignment, and cell cycle progression in mouse oocytes. *Microscopy and microanalysis : the official journal of Microscopy Society of America, Microbeam Analysis Society, Microscopical Society of Canada, 17*(3), 431-439. doi: 10.1017/S1431927611000274

Tanaka, T.U. (2010). Kinetochore-microtubule interactions: steps towards bi-orientation. *The EMBO journal, 29*(24), 4070-4082. doi: 10.1038/emboj.2010.294

Toth, A., Rabitsch, K.P., Galova, M., Schleiffer, A., Buonomo, S.B., & Nasmyth, K. (2000). Functional genomics identifies monopolin: a kinetochore protein required for segregation of homologs during meiosis i. *Cell, 103*(7), 1155-1168.

Towbin, H., Staehelin, T., & Gordon, J. (1979). Electrophoretic transfer of proteins from polyacrylamide gels to nitrocellulose sheets: procedure and some applications. *Proceedings of the National Academy of Sciences of the United States of America, 76*(9), 4350-4354.

Tsukahara, T., Tanno, Y., & Watanabe, Y. (2010). Phosphorylation of the CPC by Cdk1 promotes chromosome bi-orientation. *Nature, 467*(7316), 719-723. doi: 10.1038/nature09390

Uhlmann, F., Lottspeich, F., & Nasmyth, K. (1999). Sister-chromatid separation at anaphase onset is promoted by cleavage of the cohesin subunit Scc1. *Nature, 400*(6739), 37-42. doi: 10.1038/21831

Uhlmann, F., Wernic, D., Poupart, M.A., Koonin, E.V., & Nasmyth, K. (2000). Cleavage of cohesin by the CD clan protease separin triggers anaphase in yeast. *Cell, 103*(3), 375-386.

Vader, G., Blitzblau, H.G., Tame, M.A., Falk, J.E., Curtin, L., & Hochwagen, A. (2011). Protection of repetitive DNA borders from self-induced meiotic instability. *Nature, 477*(7362), 115-119. doi: 10.1038/nature10331

Von Stetina, J.R., & Orr-Weaver, T.L. (2011). Developmental control of oocyte maturation and egg activation in metazoan models. *Cold Spring Harbor perspectives in biology, 3*(10), a005553. doi: 10.1101/cshperspect.a005553

Wigge, P.A., Jensen, O.N., Holmes, S., Soues, S., Mann, M., & Kilmartin, J.V. (1998). Analysis of the Saccharomyces spindle pole by matrix-assisted laser desorption/ionization (MALDI) mass spectrometry. *The Journal of cell biology, 141*(4), 967-977.

Xu, L., Ajimura, M., Padmore, R., Klein, C., & Kleckner, N. (1995). NDT80, a meiosis-specific gene required for exit from pachytene in Saccharomyces cerevisiae. *Molecular and cellular biology, 15*(12), 6572-6581.

Yamamoto, A., & Hiraoka, Y. (2003). Monopolar spindle attachment of sister chromatids is ensured by two distinct mechanisms at the first meiotic division in fission yeast. *The EMBO journal, 22*(9), 2284-2296. doi: 10.1093/emboj/cdg222

Yamamoto, T.G., Chikashige, Y., Ozoe, F., Kawamukai, M., & Hiraoka, Y. (2004). Activation of the pheromone-responsive MAP kinase drives haploid cells to undergo ectopic meiosis with normal telomere clustering and sister chromatid segregation in fission yeast. *Journal of cell science, 117*(Pt 17), 3875-3886. doi: 10.1242/jcs.01248

Yu, H.G., & Koshland, D. (2005). Chromosome morphogenesis: condensin-dependent cohesin removal during meiosis. *Cell, 123*(3), 397-407. doi: 10.1016/j.cell.2005.09.014

Chapter 3:

Mechanisms of Clb1-CDK Regulation during Meiosis

INTRODUCTION

Meiosis is a unique type of cell division in which a single round of DNA replication is followed by two rounds of nuclear division (termed meiosis I and meiosis II). In the first meiotic division, homologous chromosomes segregate to opposite poles while during the second meiotic division, sister chromatids segregate, thus generating haploid gametes (review in Lee & Amon, 2001; Marston & Amon, 2004). As in mitosis, cyclin-dependent kinases (CDKs) promote progression through meiosis (Dahmann & Futcher, 1995; Grandin & Reed, 1993). CDKs are serine/threonine kinases that, when associated with a regulatory subunit (cyclin), promote key meiotic events such as DNA replication, recombination and the meiotic divisions. Budding yeast contains three G1 cyclins (Cln1-3) and six B-type cyclins (Clb1-6), which associate with a single CDK, Cdc28 (Bloom & Cross, 2007; Fitch et al., 1992). In the meiotic program, the G1 cyclins are not expressed, but rather a different kinase, Ime2, performs the functions of G1 cyclin-CDKs (Holt, Hutti, Cantley, & Morgan, 2007; Schindler & Winter, 2006). Ime2 promotes activation of S-phase CDK complexes (Clb5- & Clb6-CDKs) (Dirick, Goetsch, Ammerer, & Byers, 1998; Stuart & Wittenberg, 1998), by triggering the destruction of the Clb-CDK inhibitor, Sic1, as well as by inactivating a ubiquitin ligase, the anaphase promoting complex or cyclosome (APC/C), thus allowing accumulation of Clb cyclins (Benjamin, Zhang, Shokat, & Herskowitz, 2003; Marston & Amon, 2004; Peters, 2006). The ensuing rise in S-phase CDK activity drives meiotic DNA replication and the initiation of

recombination, which is required for homolog segregation at meiosis I, because it links homologous chromosomes through structures known as chiasmata (Henderson, Kee, Maleki, Santini, & Keeney, 2006).

The initiation of recombination results in severe DNA damage in the form of double strand breaks. It is therefore essential that the initiation of the meiotic divisions does not occur until all of the damage has been repaired through proper recombination (Marston & Amon, 2004). The recombination checkpoint is at least one mechanism that ensures this is the case. In the presence of recombination intermediates, the recombination checkpoint prevents entry into meiosis I by preventing (Clb1-4)-CDK activation in at least two ways. First, the activated checkpoint results in continuous activity of the tyrosine kinase, Swe1, which inhibits CDK activity by phosphorylating Cdc28 on Thr18 and Tyr19. Second, when activated, the checkpoint prevents expression of the meiotic transcription factor *NDT80*. This transcription factor is responsible for the expression of the cyclins Clb1, Clb3 and Clb4 along with a large set of meiotic genes (Marston & Amon, 2004; Roeder & Bailis, 2000; Shuster & Byers, 1989). The recombination checkpoint therefore arrests cells in a G2-like stage until all DNA damage has been repaired.

Once recombination has been completed and all DNA damage has been repaired, Clb1, Clb3 and Clb4-associated CDKs drive progression through the meiotic divisions (Dahmann & Futcher, 1995; Grandin & Reed, 1993). In the frog (*Xenopus laevis*), meiotic CDKs are only partially inactivated between meiosis I

and meiosis II. The residual CDK activity prevents DNA replication between the two meiotic divisions (Furuno et al., 1994; Iwabuchi, Ohsumi, Yamamoto, Sawada, & Kishimoto, 2000). Entry into meiosis II is triggered by a subsequent rise in meiotic CDK activity, followed by exit from meiosis II, which is brought about by complete inactivation of meiotic CDKs.

Examination of mitotic control of Clb-CDK activity has demonstrated multiple levels of regulation. During the mitotic divisions, transcriptional control, in addition to cell cycle-regulated ubiquitin-dependent protein degradation, is responsible for restricting Clb-CDK activity to the required cell cycle stage (Bloom & Cross, 2007; Mendenhall & Hodge, 1998). Previous work from our lab revealed that meiotic regulation of Clb-CDK activity shows a wide diversity of mechanisms and that proper regulation of specific Clb-CDK activities to certain stages of meiosis is essential for proper meiotic chromosome segregation (Carlile & Amon, 2008; Chapter 2).

Of the mechanisms observed, the regulation of Clb1-CDK and Clb3-CDK activity were most striking. Clb1-CDK activity was observed to be restricted to meiosis I while Clb3-CDK activity was shown to be restricted to meiosis II. The restriction of Clb3-CDK activity to MII was found to occur via 5' UTR mediated meiosis I-specific translational inhibition of the *CLB3* mRNA. Clb1-CDK activity appeared to be regulated at the posttranslational level. Clb1 protein levels were observed to rise during meiosis I and maintained until exit from meiosis II, however, Clb1-CDK activity was decreased during meiosis II (Carlile & Amon,

2008). The experiments presented in this chapter are aimed at elucidating the posttranslational mechanism(s) that inhibit Clb1-CDK activity during exit from meiosis I and during meiosis II.

First, we determined cyclin-dependent kinase activity of all cyclin-CDKs as cells proceed through the divisions of a synchronous meiosis. Next, we examined the nature of the observed MI-specific posttranslational modification of Clb1 and its role in Clb1-CDK regulation. Then, we attempted to determine the regions of Clb1 that are required for the observed downregulation of activity. To identify factors involved in the meiotic regulation of Clb1-CDK, we next investigated the interaction of Cdc28 and Clb1. Then, we identified factors that co-purify with this complex during both meiosis and mitosis and determined the role these factors play in Clb1-CDK regulation, and finally, examined the regulation of Clb1-CDK during meiosis compared to that of the mitotic cell cycle. We find that the in vitro kinase activity of Clb1-CDK is significantly higher from meiotic protein extracts compared to mitotic. We were not able to determine the mechanism by which Clb1-CDK is downregulated during meiosis II, however, putative binding partners of Clb1 were identified during mitosis, meiosis I and meiosis II. Further work will be required to determine whether these are substrates of Clb1-CDK.

RESULTS

Total CDK activity peaks during metaphase I of meiosis.

To understand how the various cyclin-CDKs contribute to promoting the meiotic divisions, we first wished to examine the in vitro CDK activity of all cyclin-CDKs during a synchronous meiosis. To this end, cells carrying a Cdc28 allele tagged with a 3x V5 epitope (Cdc28-3V5) were induced to undergo a synchronous *GAL-NDT80 GAL4-ER* block-release meiosis. Total CDK activity was monitored by in vitro kinase assays with immunoprecipitated Cdc28-3V5 (Figure 1). The levels of Cdc28-3V5 remained relatively constant as cells proceeded through meiosis. CDK activity increased as cells arrested in pachytene (6h after sporulation induction) and peaked as cells entered metaphase I (7.5h), likely due to expression of Clb1 and Clb4, as the presence of Clb3 is restricted until meiosis II (Carlile & Amon, 2008). Interestingly, total CDK activity dropped as cells exited meiosis I and a second peak of total CDK activity was not observed in meiosis II. Somewhat surprisingly, the levels of total CDK activity in meiosis II were similar to the levels present in pachytene-arrested cells (when only Clb5 and Clb6 are present). It will be interesting to determine whether the regulation of Clb1-CDK activity plays a role in the observed drop in total CDK activity as cells exit from meiosis I. Experiments to determine how the various cyclins promote the overall CDK activity pattern will be quite useful in determining how the activities of the various cyclin-CDKs are combined to promote the specialized meiotic cell division.

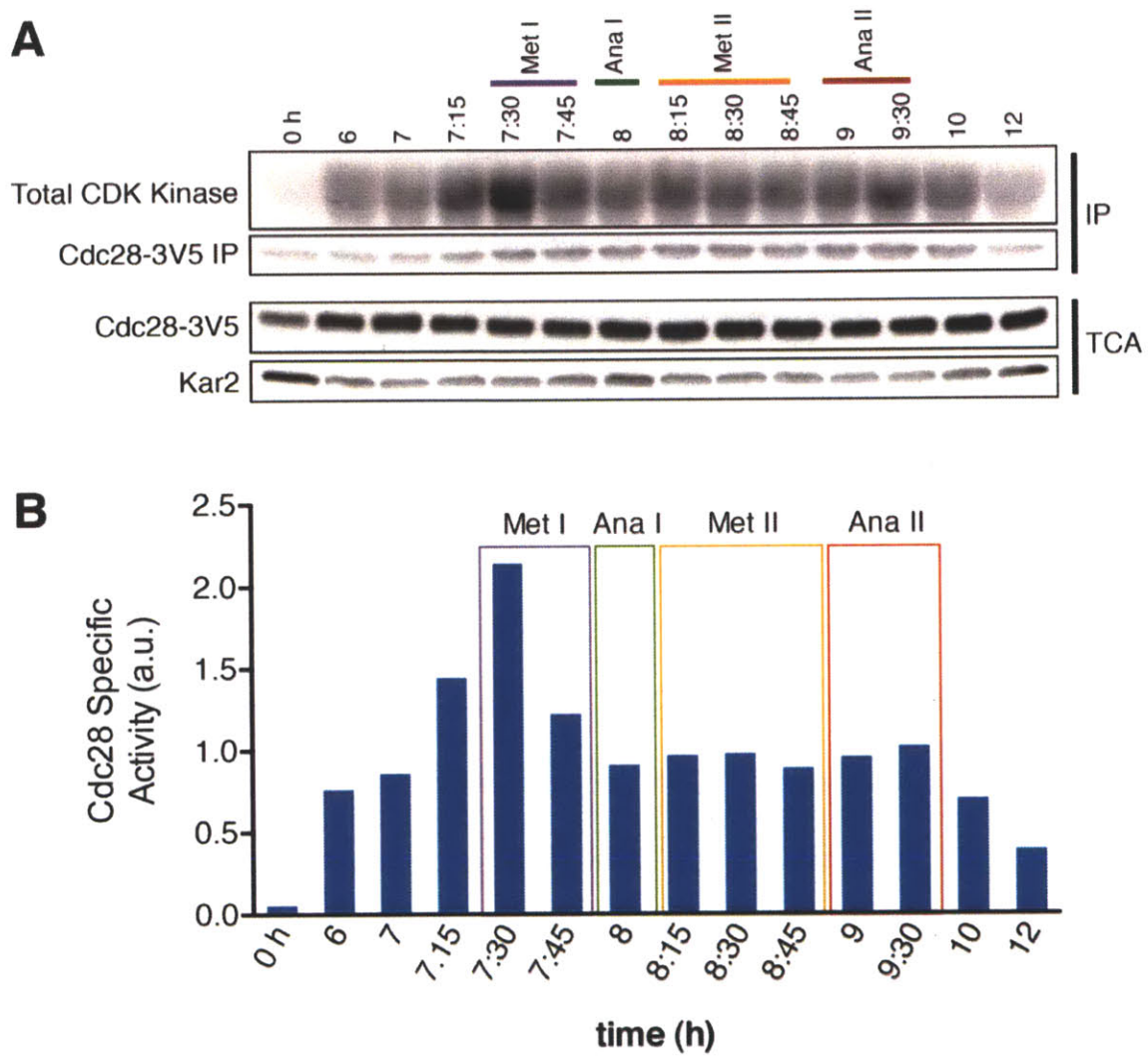

Figure 1. Total CDK activity during meiosis.

(A) Cells carrying the *GAL4-ER*, *GAL-NDT80* and *CDC28-3V5* fusions (A25508) were induced to sporulate. Cells were released from the *NDT80* block at 6h post transfer to sporulation medium. Cdc28 levels and associated kinase activity were determined at the indicated time points (see Materials and Methods for details). Kar2 was used as a loading control.

(B) Specific activity was calculated by normalizing the amount of phosphorylated Histone H1 to the amount of immunoprecipitated Cdc28-3V5 using ImageQuant software (Molecular Dynamics) for samples described in **(A)**. Samples corresponding to meiotic stage are indicated.

Clb1-CDK activity is downregulated during meiosis II.

Our lab previously reported that Clb1-CDK activity is downregulated during meiosis II despite Clb1 and Cdc28 protein levels remaining high (Carlile & Amon, 2008). To further define when Clb1-CDK activity becomes downregulated during meiosis, we tagged Clb1 with a 3x V5 epitope and determined protein levels as well as associated *in vitro* kinase activity during a synchronous meiosis, using the previously described *GAL-NDT80* block-release system (Carlile & Amon, 2008). In this system, expression of *NDT80* is controlled by the *GAL1-10* promoter, which is regulated by an estrogen-inducible Gal4-ER fusion (henceforth *GAL4.ER*) (Benjamin et al., 2003; Carlile & Amon, 2008). We induced *GAL-NDT80 GAL4.ER* cells to sporulate and subsequently arrest in pachytene of prophase I due to lack of *NDT80* expression. 6h after sporulation induction, estrogen was added to induce *NDT80* expression and to allow cells to synchronously proceed through the meiotic divisions.

We observed that Clb1 protein levels increased as cells entered the first meiotic division and remained high throughout the remainder of the time course, consistent with Clb1-associated kinase activity promoting the meiotic divisions (Figure 2A; Carlile & Amon, 2008). Consistent with previous observations, Clb1-CDK kinase activity increased and correlated quite well with Clb1 protein levels during meiosis I. Interestingly, Clb1-CDK activity diminished as cells entered meiosis II, however, Clb1 proteins levels remained high (Figure 2B). We also observed a mobility shift by Western blot, which was most prominent in samples

taken during meiosis I and thus correlated with active Clb1-CDK (Figure 2A; Carlile & Amon, 2008). The remainder of this chapter describes experiments aimed at elucidating the mechanisms by which Clb1-CDK activity is regulated during meiosis.

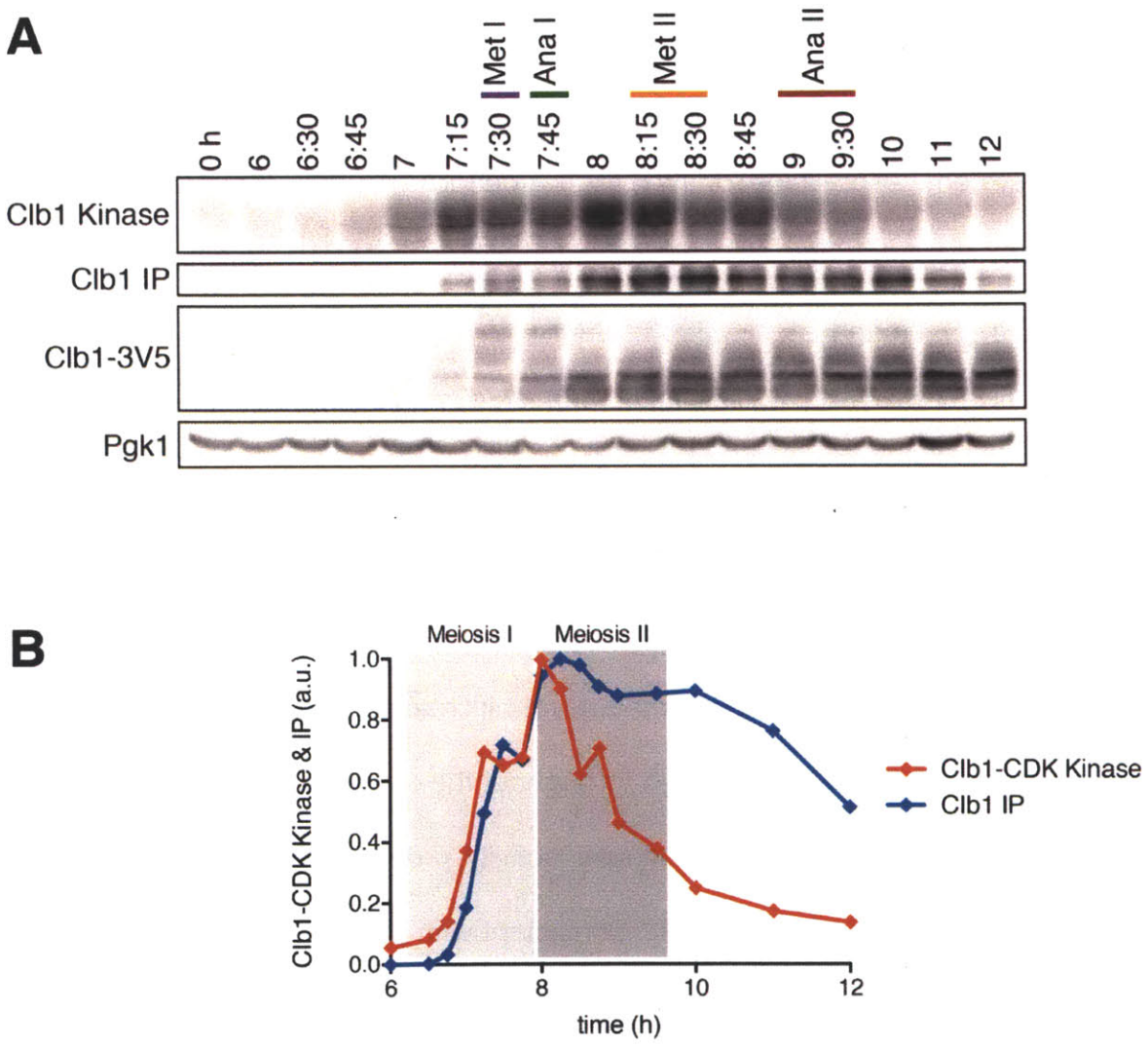

Figure 2. Clb1-CDK activity is down regulated in meiosis II.

(A) Cells carrying the *GAL4-ER*, *GAL-NDT80* and *CLB1-3V5* fusions (A22762) were induced to sporulate. Cells were released from the *NDT80* block at 6h post transfer to sporulation medium. Clb1 levels and associated kinase

activity were determined at the indicated time points (see Materials and Methods for details). Pgk1 was used as a loading control.

(B) Clb1-CDK activity was determined by quantifying the amount of phosphorylated Histone H1 using ImageQuant software (Molecular Dynamics). The amount of immunoprecipitated Clb1-3V5 from the kinase reaction was determined similarly.

Clb1 phosphorylation is meiosis I-specific.

As previously observed, Clb1 shows a mobility shift during meiosis I that correlates with Clb1-CDK activity (Figure 2A; Carlile & Amon, 2008). To determine whether Clb1 is posttranslationally modified during meiosis I and whether this modification plays a role in the regulation of Clb1-CDK activity, we sought to determine the nature of this mobility shift. To examine whether the observed mobility shift was due to phosphorylation, meiosis I samples were taken from cultures with a *CLB1-9myc* allele synchronously proceeding through the meiotic divisions after release from an *NDT80* block. Denaturing immunoprecipitation followed by phosphatase treatment showed that the majority, if not all, of the observed mobility shift of Clb1 results from phosphorylation of the protein. Samples treated with phosphatase after immunoprecipitation, but not mock treated samples, showed a reduced mobility shift (Figure 3A).

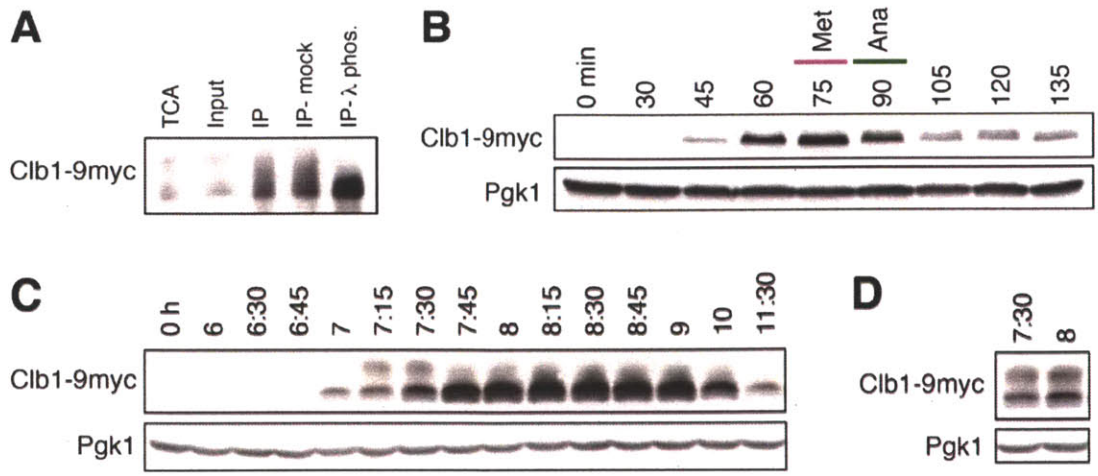

Figure 3. Meiosis I specific phosphorylation of Clb1.

(A) Cells carrying the *GAL4-ER*, *GAL-NDT80* and *CLB1-9myc* fusions (A15591) were induced to sporulate. Cells were released from the *NDT80* block at 6h post transfer to sporulation medium. 1h 30 min after release from *NDT80* block, cells were harvested for denaturing immunoprecipitation (IP) and phosphatase treatment. See Materials and Methods for more details. Clb1-9myc analyzed by Western blot after the following treatments (from left to right): cells treated with TCA; input (1:50) of immunoprecipitation; post-immunoprecipitation; post-immunoprecipitation including mock phosphatase treatment; post-immunoprecipitation including phosphatase treatment.

(B) *MATa* haploid cells carrying *GAL4-ER*, *GAL-NDT80* and *CLB1-9myc* fusions (A15514) were arrested in G1 with 5µg/ml α-factor. When arrest was complete, cells were released into rich medium (YEP) with 2% dextrose lacking pheromone and samples were taken at indicated time points to analyze Clb1-9myc levels and mobility shift by Western blot. Pgk1 was used as a loading control.

(C) Cells carrying the *GAL4-ER*, *GAL-NDT80* and *CLB1-9myc* fusions (A15591) were induced to sporulate. Cells were released from the *NDT80* block at 6h post transfer to sporulation medium. Samples were taken at indicated time

points to analyze Clb1-9myc levels and mobility shift by Western blot. Pgk1 was used as a loading control.

(D) Cells (A21817) carrying the *CLB1-9myc* fusion and also harboring a Cdc20 depletion allele (*cdc20-mn*) were induced to sporulate and arrested in metaphase I due to depletion of Cdc20. Samples were taken at indicated time points (spanning peak metaphase I arrest) to analyze Clb1-9myc levels and mobility shift by Western blot. Pgk1 was used as a loading control.

We next wished to examine whether Clb1 phosphorylation also occurs during mitosis. To this end, we examined the migration of Clb1-9myc on SDS-PAGE from cells synchronously proceeding through the mitotic cell cycle. *MATa* haploid cells were arrested in G1 by treatment with mating pheromone and subsequently released to synchronously proceed through the cell cycle. Interestingly, Clb1-9myc from cells growing vegitatively did not appear to be phosphorylated (Figure 3B). In contrast, meiotic cultures carrying the *CLB1-9myc* allele showed meiosis I-specific phosphorylation of Clb1 either in cultures synchronously proceeding through the meiotic divisions (Figure 3C) or arrested in metaphase I by depletion of the APC/C specificity factor Cdc20 (*cdc20-mn*) (Figure 3D). We conclude that Clb1 is phosphorylated during meiosis I and that this modification is meiosis-specific.

Phosphorylation of Clb1 depends on CDK activity.

Since meiosis I-specific phosphorylation of Clb1 correlates with Clb1-CDK activity, we next wished to examine whether modification of Clb1 was dependent on CDK activity. Wild-type cells or cells carrying an analog sensitive *cdc28-as1* allele, which can be specifically inhibited by addition of the ATP analog 1-NM-PP1, were induced to sporulate and subsequently arrested in metaphase I by depletion of Cdc20 (Figure 4A). After cells had arrested in metaphase I, cells were treated with 5 μM 1-NM-PP1 to specifically inhibit CDK activity in cells harboring the *cdc28-as1* allele. We observed that Clb1-9myc was rapidly dephosphorylated when CDK activity was inhibited (*cdc28-as1*) and maintained phosphorylated when CDK activity remained uninhibited (*CDC28*) (Figure 4B). These findings raise the possibility that Clb1 phosphorylation in meiosis I results from autophosphorylation of Clb1-CDK either in *cis* or in *trans*. To address this question, we mutated the only minimal CDK consensus site (SP or TP) of Clb1 to the non-phosphorylatable residue alanine (S302A). We observed no difference in the mobility shift of Clb1(S302A)-9myc relative to a wild-type allele either in cultures synchronously proceeding through the meiotic divisions (Figure 4C) or arrested in metaphase I by depletion of the APC/C specificity factor Cdc20 (*cdc20-mn*) (Figure 4D). Our observations are consistent with the notion that Clb1 phosphorylation in meiosis I is dependent on CDK activity, but that the phosphorylation of Clb1 does not occur on the sole minimal CDK consensus site.

These observations raise the possibility that CDK activity is required for activity of another kinase to phosphorylate Clb1 during meiosis I.

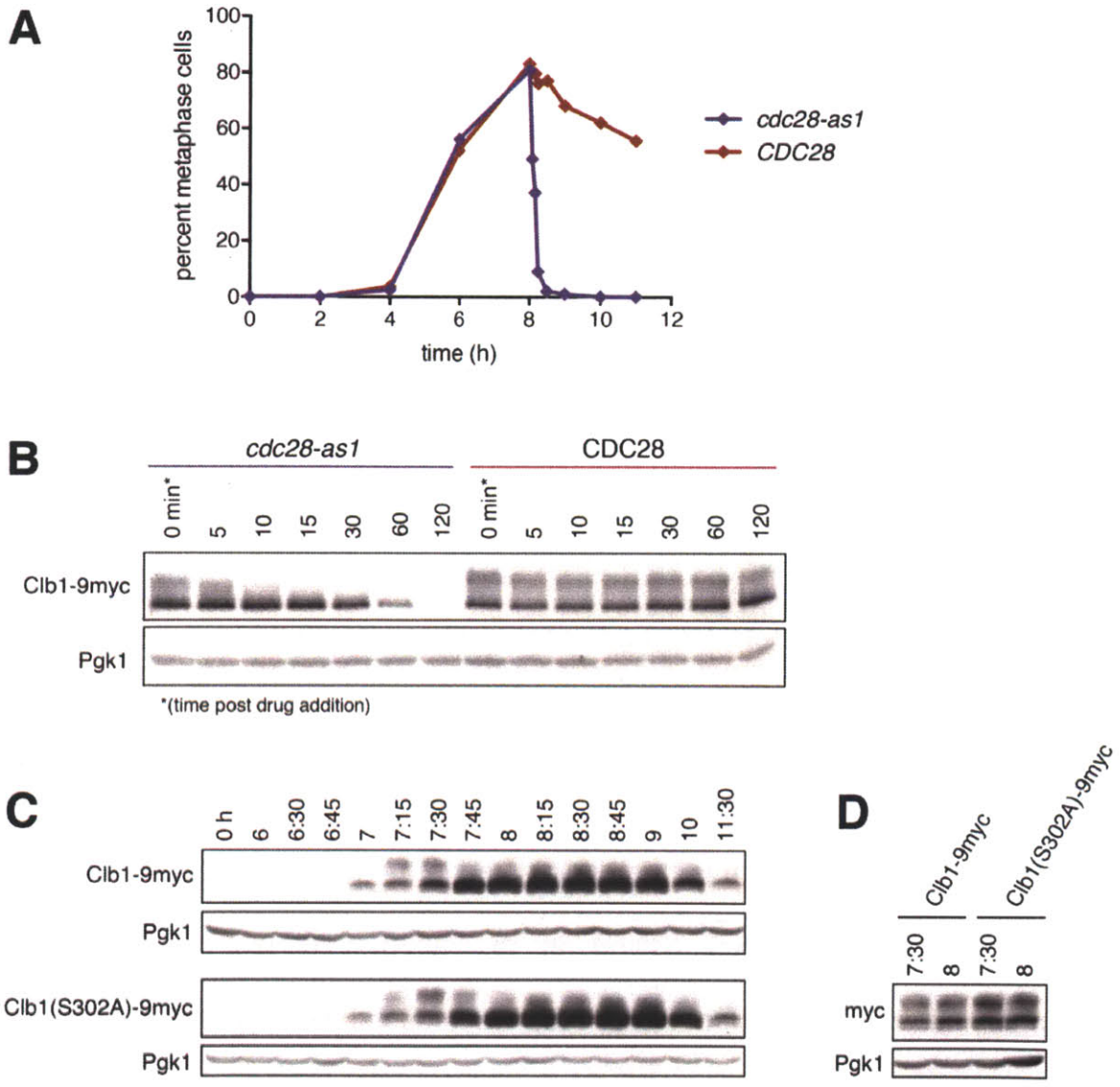

Figure 4. Meiosis I specific phosphorylation of Clb1 is CDK dependent.
Wild-type (A21817) or *cdc28-as1* (A21711) cells carrying the *CLB1-9myc* fusion and also harboring a Cdc20 depletion allele (*cdc20-mn*) were induced to sporulate and arrested in metaphase I due to depletion of Cdc20. 8h after induction of sporulation when the majority of cells had arrested in metaphase I, cells were treated with 5 μM 1-NM-PP1. Samples were taken at indicated time

points to monitor **(A)** percentage of cells with short bipolar spindles (metaphase I) and **(B)** to analyze Clb1-9myc levels and mobility shift by Western blot. Pgk1 was used as a loading control.

(C) Cells carrying the *GAL4-ER*, *GAL-NDT80* and either a wild-type *CLB1-9myc* fusion (A15591) or a *CLB1(S302A)-9myc* fusion (A22458) were induced to sporulate. Cells were released from the *NDT80* block at 6h post transfer to sporulation medium. Samples were taken at indicated time points to analyze Clb1-9myc levels and mobility shift by Western blot. Pgk1 was used as a loading control.

(D) Cells carrying either the *CLB1-9myc* fusion (A21817) or *CLB1(S302A)-9myc* fusion (A22457) and also harboring a Cdc20 depletion allele (*cdc20-mn*) were induced to sporulate and arrested in metaphase I due to depletion of Cdc20. Samples were taken at indicated time points to analyze Clb1-9myc levels and mobility shift by Western blot. Pgk1 was used as a loading control.

Clb1 phosphorylation depends on Cdc5 activity but phosphorylation does not affect Clb1-CDK activity.

Another kinase that has been implicated in the phosphorylation of Clb1 is the polo-like kinase, Cdc5 (Clyne et al., 2003). To test whether Clb1 phosphorylation is dependent on Cdc5, we induced wild-type cells or cells depleted of Cdc5 (*cdc5-mn*) to sporulate and subsequently arrest in metaphase I by depletion of Cdc20. Strikingly, Clb1-9myc from *cdc5-mn* cells did not appear to be phosphorylated as a mobility shift was not observed (Figure 5A). To examine the affect of Clb1 modification on Clb1-CDK activity, wild-type or *cdc5-mn* cells carrying a *CLB1-3V5* allele were induced to sporulate and arrest in

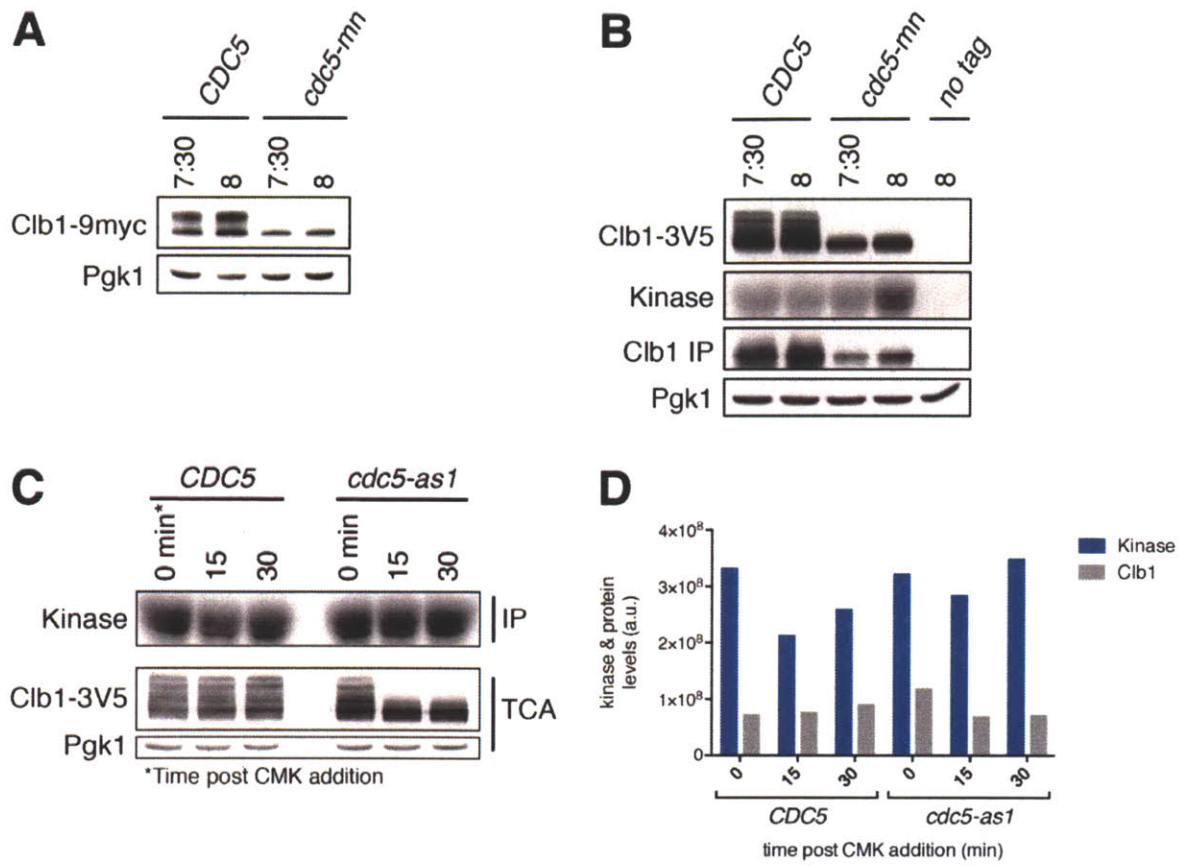

Figure 5. Meiosis I specific phosphorylation of Clb1 is Cdc5 dependent but does not affect Clb1-CDK activity.

(A) Wild-type (A21817) or *cdc5-mn* (A23785) cells carrying the *CLB1-9myc* fusion and also harboring a Cdc20 depletion allele (*cdc20-mn*) were induced to sporulate and arrested in metaphase I due to depletion of Cdc20. Samples were taken at indicated time points to analyze Clb1-9myc levels and mobility shift by Western blot. Pgk1 was used as a loading control.

(B) Wild-type (A24207) or *cdc5-mn* (A24208) cells carrying the *CLB1-3V5* fusion or a non-tagged allele of *CLB1* (A6138) and also harboring a Cdc20 depletion allele (*cdc20-mn*) were induced to sporulate and arrested in metaphase I due to depletion of Cdc20. Samples were taken at indicated time points to analyze Clb1-3V5 levels and mobility shift by Western blot and associated kinase activity via *in vitro* kinase assays. Pgk1 was used as a loading control.

(C) Wild-type (A24207) or *cdc5-as1* (A26176) cells carrying the *CLB1-3V5* fusion and also harboring a Cdc20 depletion allele (*cdc20-mn*) were induced to sporulate and arrested in metaphase I due to depletion of Cdc20. 8h after induction of sporulation when the majority of cells had arrested in metaphase I, cells were treated with 5 μM CMK. Samples were taken at indicated time points to analyze Clb1-3V5 levels and mobility shift by Western blot and associated kinase activity via *in vitro* kinase assays. Pgk1 was used as a loading control.

(D) Clb1-CDK activity was determined by quantifying the amount of phosphorylated Histone H1 using ImageQuant software (Molecular Dynamics). The amount of Clb1-3V5 from TCA extracts was determined similarly.

---

metaphase I (*cdc20-mn*). Similar to previous results, metaphase I cells depleted for Cdc5 showed a dramatic reduction in phosphorylation of Clb1-3V5, however, the associated Clb1-CDK kinase activity was similar if not higher in *cdc5-mn* cells (Figure 5B). The relatively lower amount of Clb1 protein in *cdc5-mn* cells is consistent with Cdc5 promoting the levels and transcriptional activity of the transcription factor Ndt80 (Acosta, Ontoso, & San-Segundo, 2011). Since *cdc5-mn* cells have reduced levels of Clb1, we wanted to transiently inactivate Cdc5 in cells arrested in metaphase I to examine the affect of Clb1 phosphorylation on associated kinase activity. To this end, we induced wild-type cells or cells carrying an analog sensitive *cdc5-as1* allele to sporulate and arrest in metaphase I (*cdc20-mn*). Once arrested in metaphase I, cells were treated with 5 μM CMK

(*cdc5-as1* inhibitor; pyrrolopyrimidine containing a chloromethylketone electrophile at the C-2 position) to inhibit Cdc5 activity. We observed inhibition of *cdc5-as1* led to a rapid decrease in the phosphorylated form of Clb1 (Figure 5C), however, in vitro Clb1-CDK kinase activity was not affected (Figure 5C-D). We conclude that Clb1 phosphorylation is dependent on Cdc5 activity but that this modification does not affect in vitro Clb1-CDK activity and most likely does not play a role in the downregulation that is observed in meiosis II. Further investigation into the role of Clb1 phosphorylation during meiosis I will be an area of interesting work.

The closely related cyclin, Clb2, is regulated differently than Clb1 in meiosis.

At a sequence level, the closest related cyclin to Clb1 is the paralog Clb2 (54% homology). Clb2 expression is downregulated during meiosis (Grandin & Reed, 1993), however, Clb2 can be exogenously expressed from the *GAL1-10* promoter without affecting meiotic progression (Carlile & Amon, 2008). To examine whether Clb2 is regulated similarly to Clb1 during meiosis, we examined expression levels and associated kinase activity from a strain harboring both *CLB1-3V5* and *GAL-CLB2* during a synchronous *GAL-NDT80* block-release meiosis. In this strain, Clb2 is expressed concurrent with release from the *NDT80* block and thus Clb2 protein accumulates with relatively similar kinetics as Clb1. We observed that the associated CDK activity increased for both Clb1 and Clb2 during meiosis I and that the kinase activity correlated with cyclin levels present.

Interestingly, while Clb1-CDK activity was restricted to meiosis I, Clb2-CDK activity remained elevated during meiosis II (Figure 6A-B). Thus, the activity of Clb1-CDK is regulated differentially compared to the closely related Clb2-CDK when expressed during meiosis. These results suggest that the activity of Clb1-CDK is downregulated during meiosis II and that this regulation is specific to Clb1-CDK. Comparing the closely related cyclins provides a useful tool to examine the sequence determinants of Clb1 that mediate this regulation.

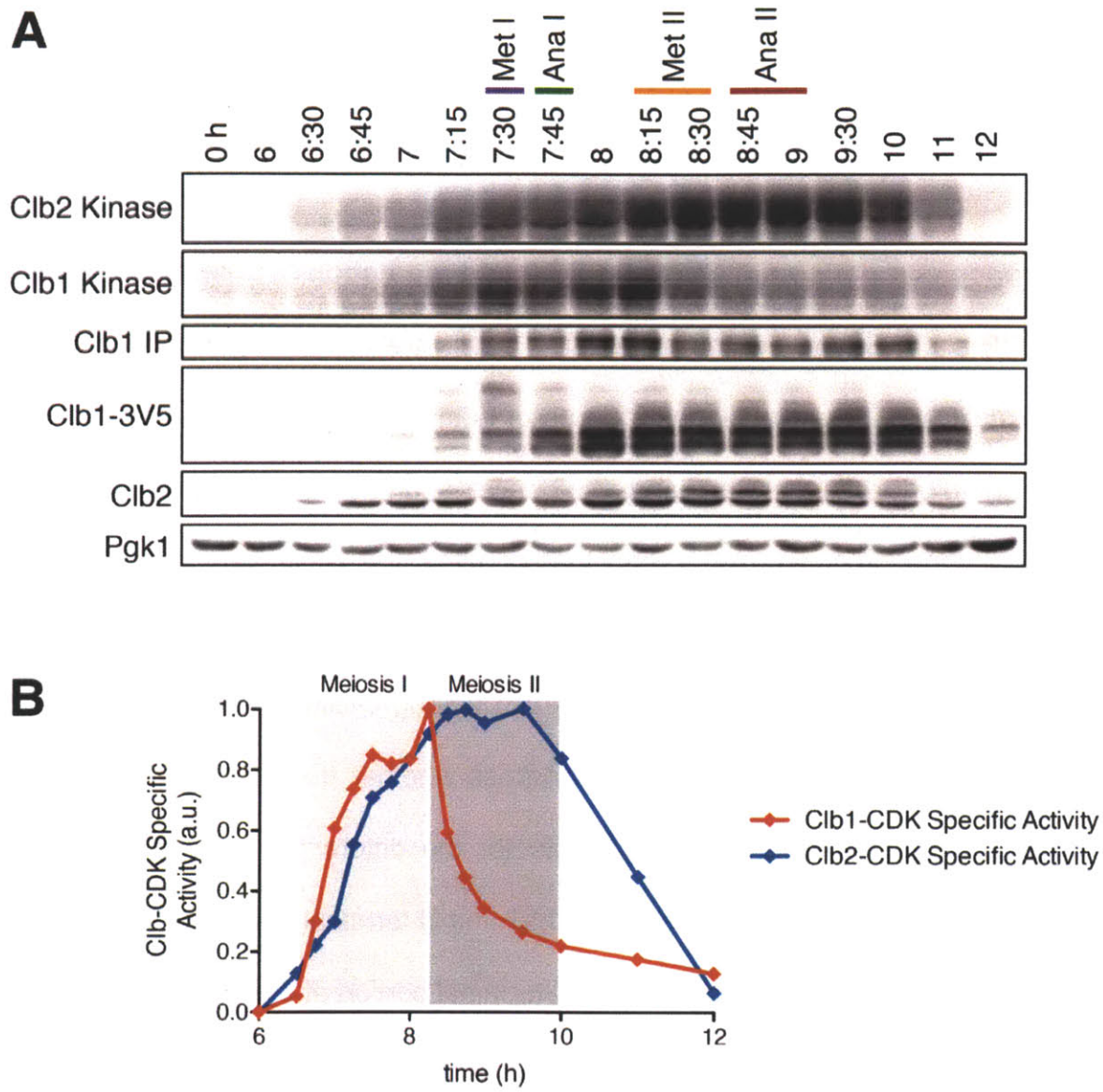

Figure 6. Meiotic regulation of Clb1 compared to paralog Clb2.

(A) Cells carrying the *GAL4-ER*, *GAL-NDT80*, *CLB1-3V5* and *GAL-CLB2* fusions (A22992) were induced to sporulate. Cells were released from the *NDT80* block at 6h post transfer to sporulation medium. Clb1 and Clb2 levels and associated kinase activity were determined at the indicated time points (see Materials and Methods for details). Pgk1 was used as a loading control.

(B) Clb1 and Clb2-CDK kinase activity was quantified as the amount of phosphorylated Histone H1 determined using ImageQuant software

(Molecular Dynamics). The amount of immunoprecipitated Clb1-3V5 from the kinase reaction or amount of Clb2 was determined similarly.

Sequence comparison of Clb1 and Clb2 and regulation of chimeric cyclins.

The six B-type cyclins in budding yeast are found in paralogous pairs. Clb1 and Clb2 share the highest degree of homology of any of these pairs with 54% homology overall. Clb1 and Clb2 have a divergent amino-terminus, but share a conserved carboxy-portion that contains the cyclin box domain (76% homology over the cyclin box containing carboxy-portion of the proteins) (Figure 7A). The cyclin box is a conserved domain among cyclins that consists of two compact 5-α helical subdomains. To address whether the divergent N-terminal portions of the proteins are responsible for the differential meiotic regulation observed, we made fusion proteins in which the N-terminal portion of each cyclin was fused to the cyclin box containing C-terminal portion of the respective protein (Figure 7B).

The respective chimeric fusion cyclins, Clb2(1-179)-Clb1(156-471) and Clb1(1-155)-Clb2(180-491) (henceforth Clb2-Clb1 and Clb1-Clb2 respectively), were examined for expression levels, mobility shift and associated kinase activity during a synchronous *GAL-NDT80* block-release meiosis. To address whether the divergent N-terminal 155 residues of Clb1 are necessary for the observed downregulation of Clb1-CDK activity during meiosis II, we first examined the

A

```
Clb1p          1 msrsllvensrtinsneekgvnesqyilqkrnvprtilgnvtnnanilqeismnrkigmk
Clb2p          1 msnpi-------entensqntsssrfl---rnvqrlalnnvtntt--fqksnannp-alt

Clb1p         61 nf-sklnnffplkddvsraddftssfndsrqgvkqevlnnken---ipeygyseqekqqc
Clb2p         48 nfkstlns---vkkegsripqftresvsrstaaqeekrtlkengiqlpknnllddkenqd

Clb1p        117 snddsfhtnstalscnrliysenksistqmewqkkimre--------------------
Clb2p        105 pssqqfga-ltsikegraelpanislqesssakeiiqhdplkgvgsstevvhnsvenekl

Clb1p        156 ----------------dskkkrpistlveqddqkkfklhelttteeevleeyewddldeed
Clb2p        164 hparsqlqvrnteset dsgkkrpistiveqelpkkfk----vcdengkeeyewedldaed

Clb1p        200 cddplmvseevndifdylhhleiitlpnkanlykhknikqnrdilvnwiikihnkfgllp
Clb2p        220 vndpfmvseyvndifeylhqlevitlpkkedlyqhrnihqnrdilvnwlvkihnkfgllp

Clb1p        260 etlylainimdrflceevvqlnrlqlvgtsclfiaskyeeiyspsikhfayetdgacsve
Clb2p        280 etlylainimdrflgkelvqldklqlvgtsclfiaskyeevyspsikhfasetdgacted

Clb1p        320 dikegerfilekldfqisfanpmnflrriskaddydiqsrtlakflmeisivdfkfigil
Clb2p        340 eikegekfilktlkfnlnypnpmnflrriskaddydiqsrtlakflleislvdfrfigil

Clb1p        380 pslcasaamflsrkmlgkgtwdgnlihysggytkaklypvcqllmdylvgstihdeflkk
Clb2p        400 pslcaaaamfmsrkmlgkgkwdgnlihysggytkeelapvchmimdylvspivhdefhrk

Clb1p        440 yqsrrflkasiisiewalkvrkngydimtlhe
Clb2p        460 yqsrrfmkasiisvqwalkvrkngydimtlhe
```

B

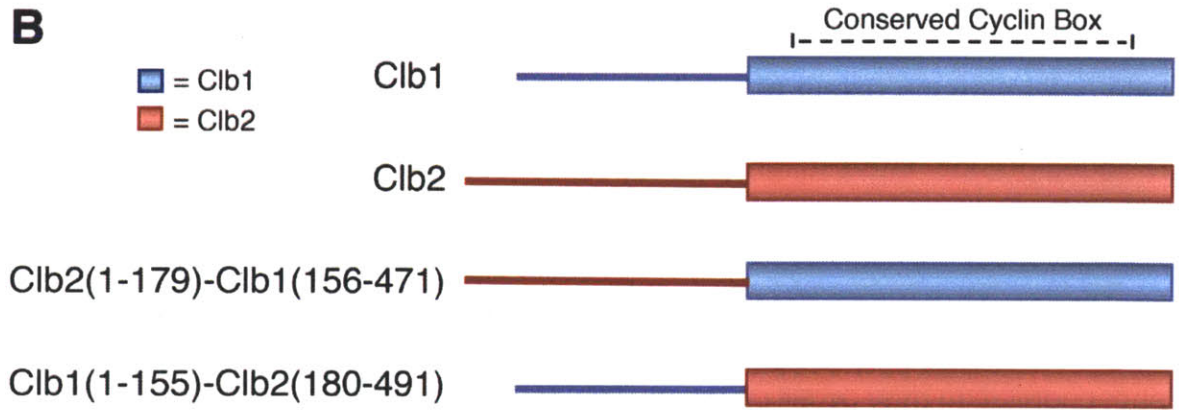

Figure 7. Sequence homology and predicted structure of Clb1 and design of chimeric cyclins.

(A) Alignment of protein sequence of Clb1 and mitosis-specific paralog Clb2. Alignment was performed using Clone Manager 6.0 and the FastScan - Max Qual method. Homology blocks are highlighted in green.

(B) Schematic for construction of chimeric cyclins. The non-conserved amino-terminal portion of each cyclin (Clb1 = residues 1-155; Clb2 = 1-179) fused

to conserved, cyclin box containing, carboxy-terminal portion of each cyclin (Clb1 = residues 156-471; Clb2 = 180-491).

---

activity of the Clb2-Clb1 fusion cyclin during meiosis. We observed that, as with Clb1, associated kinase activity of Clb2-Clb1 correlated with cyclin levels during meiosis I (Figure 8A & 8C). A second peak of kinase activity was present in meiosis II, suggesting that the N-terminal 155 residues of Clb1 may play some role in the downregulation of Clb1-CDK during meiosis II. However, the overall kinase activity did not correlate with Clb2-Clb1 protein levels during meiosis II, indicating that additional *cis* acting regions play a role in regulation of kinase activity. A more rigorous investigation of the regulation of this chimeric cyclin will help determine the extent of regulation that is determined by the N-terminal 155 residues of Clb1. Interestingly, the meiosis I-specific mobility shift (see Figures 2-5) was dramatically reduced if not absent in the Clb2-Clb1 fusion, suggesting that the N-terminus of Clb1 is required for phosphorylation and that this phosphorylation may occur on the N-terminal 155 residues.

To determine whether the N-terminus of Clb1 is sufficient to promote downregulation of cyclin-CDK activity in meiosis II, we next examined the activity of the Clb1-Clb2 fusion cyclin. We observed that the associated kinase activity of Clb1-Clb2 roughly correlated with cyclin levels during both meiosis I and meiosis II (Figure 8B & 8D). These results imply that the N-terminal 155 residues of Clb1 are not sufficient to promote downregulation of cyclin-CDK activity during

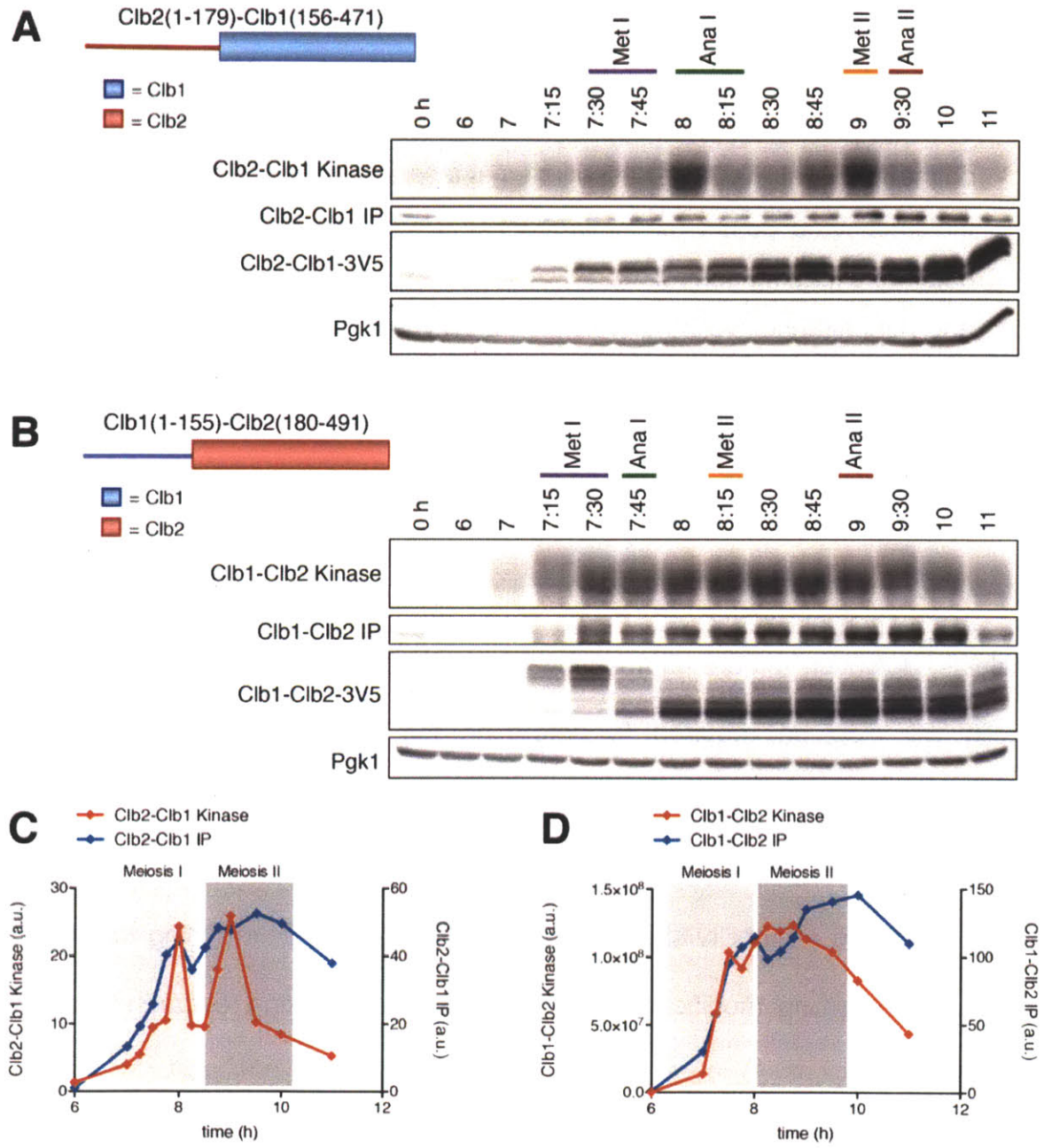

Figure 8. Meiotic regulation of chimeric cyclins.

(A) Cells carrying the *GAL4-ER*, *GAL-NDT80* and *CLB2(1-179)-CLB1(156-471)-3V5* fusions (A23924) were induced to sporulate. Cells were released from the *NDT80* block at 6h post transfer to sporulation medium. Clb2-Clb1 chimeric cyclin levels and associated kinase activity were determined at the indicated time points (see Materials and Methods for details). Pgk1 was used as a loading control.

(B) Cells carrying the *GAL4-ER*, *GAL-NDT80* and *CLB1(1-155)-CLB2(180-491)-3V5* fusions (A24320) were induced to sporulate. Cells were released from the *NDT80* block at 6h post transfer to sporulation medium. Clb1-Clb2 chimeric cyclin levels and associated kinase activity were determined at the indicated time points (see Materials and Methods for details). Pgk1 was used as a loading control.

(C) and **(D)** chimeric cyclin-CDK kinase activity was quantified as the amount of phosphorylated Histone H1 determined using ImageQuant software (Molecular Dynamics). The amount of immunoprecipitated cyclin from the kinase reaction was determined similarly.

---

meiosis. However, a more rigorous investigation of the regulation of this chimeric cyclin will also be required to determine the extent of regulation that is determined by the N-terminal 155 residues of Clb1. Consistent with the notion that Clb1 is phosphorylated on the N-terminal 155 residues, the Clb1-Clb2 fusion cyclin displayed a mobility shift in meiosis I (Figure 8B). Determining the role of this posttranslational modification will be an area of interesting research for future studies.

An interesting observation was the relative in vitro kinase activity associated with the various chimeric cyclins. The Clb1-Clb2 fusion displayed ~23-fold higher in vitro kinase activity relative to the Clb2-Clb1 chimeric cyclin. These findings are consistent with the observed difference in Clb1-3V5 associated kinase activity with that of Clb2 when expressed from the *GAL1-10* promoter during meiosis. Clb2-CDK displayed ~110-fold higher in vitro kinase

activity relative to Clb1-CDK (Figure 6), albeit not a perfect comparison as different antibodies were used to determine the in vitro kinase activity and cyclin expression was from different promoters. Further studies will help elucidate whether the Clb2 cyclin box can more effectively promote the in vitro kinase activity of CDK and, if so, the mechanism by which this occurs.

Downregulation of Clb1-CDK activity is not due to disrupted Clb1-Cdc28 interaction.

One way cyclin-CDK activity can be downregulated is by preventing the association of the cyclin with the CDK subunit. To examine whether the downregulation of Clb1-CDK activity during meiosis II is due to dissociation of the cyclin and CDK, we examined the expression levels, associated kinase activity and interaction of Clb1 and Cdc28 during a synchronous *GAL-NDT80* block-release meiosis. To this end, Clb1-3V5 was immunoprecipitated from meiotic extracts and the associated in vitro kinase activity as well as co-immunoprecipitating levels of Cdc28-3HA were determined. Consistent with previous results, Clb1-CDK activity correlated well with immunoprecipitated Clb1 levels during meiosis I, but the specific activity was reduced during meiosis II (Figure 9). Interestingly, the levels of co-immunoprecipitating Cdc28-3HA did not correlate with the observed kinase activity. In fact, the maximum levels of co-immunoprecipitated Cdc28-3HA were detected at timepoints in meiosis II when Clb1-CDK activity was downregulated. These results show that the downreguation of Clb1-CDK activity in meiosis II does not result from decreased

association of Clb1 with Cdc28 and suggest that additional mechanisms prevent the activity of the bound Clb1-CDK complex.

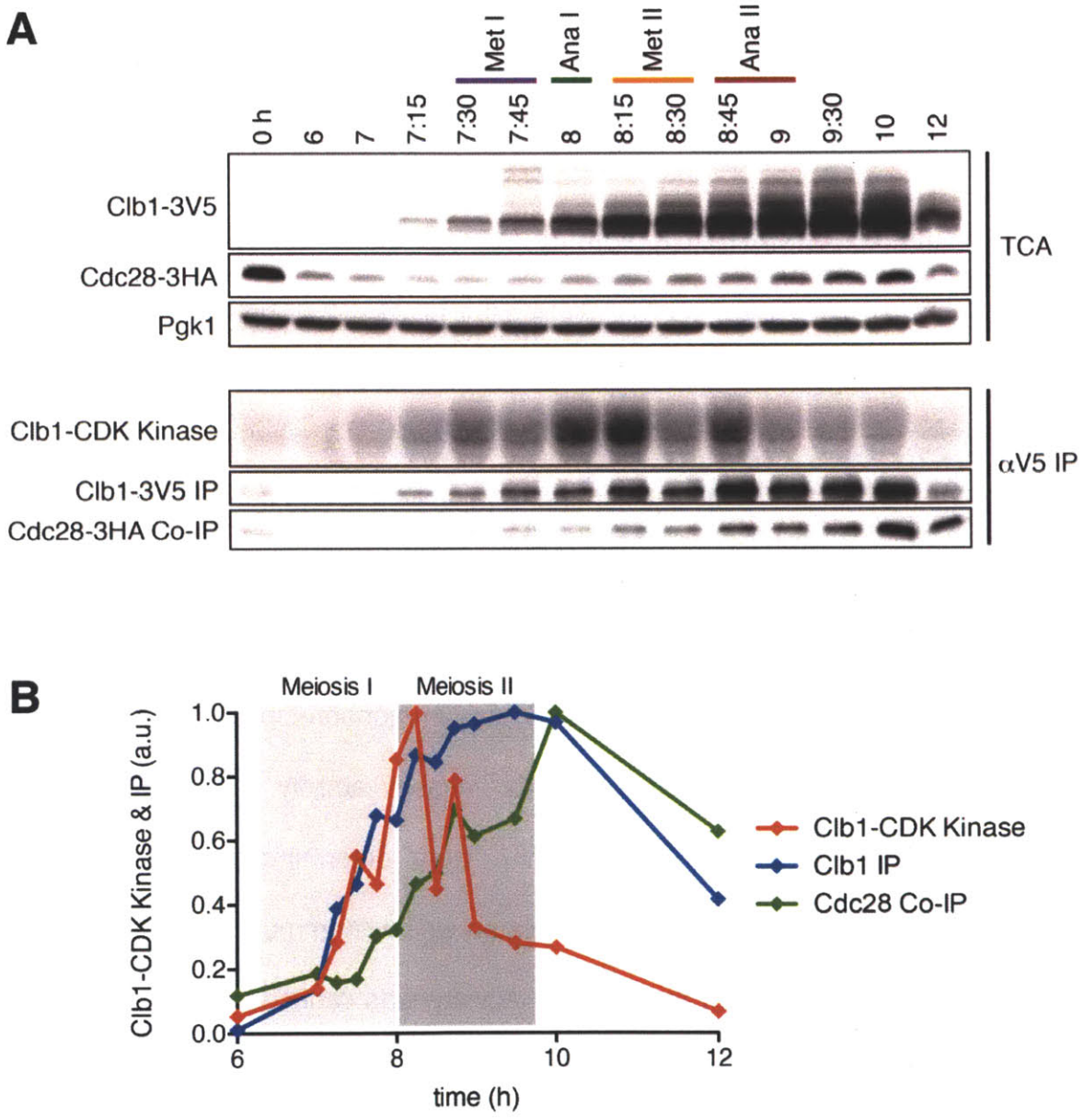

Figure 9. Downregulation of Clb1-CDK activity in MII not due to preventing Clb1-Cdc28 interaction.

(A) Cells carrying the *GAL4-ER*, *GAL-NDT80*, *CLB1-3V5* and *CDC28-3HA* fusions (A24900) were induced to sporulate. Cells were released from the

NDT80 block at 6h post transfer to sporulation medium. Clb1 levels, associated kinase activity and co-immunoprecipitated amounts of Cdc28 were determined at the indicated time points (see Materials and Methods for details). Pgk1 was used as a loading control.

(B) Clb1-CDK activity was determined by quantifying the amount of phosphorylated Histone H1 using ImageQuant software (Molecular Dynamics). The amount of immunoprecipitated Clb1-3V5 and co-immunoprecipitated Cdc28-3HA from the kinase reaction was determined similarly.

Role of the known CDK inhibitor Sic1 and Swe1 in Clb1-CDK regulation.

Several CDK inhibitors are known in budding yeast, and there is some evidence that some of these inhibitors can differentially affect the activity of various cyclin-CDK complexes (Keaton et al., 2007). One CDK inhibitor that does not show specificity with respect to the cyclin subunit that is in complex with CDK is Sic1. We wished to examine whether Sic1 played a role in the downregulation of Clb1-CDK during meiosis II. To this end, we constructed strains that have a deletion of *SIC1* or a meiotic depletion of Sic1 (*sic1-mn*). These strains, however, do not enter the meiotic divisions under our standard sporulation conditions (data not shown), preventing loss-of-function analysis. As a next step, we examined the levels of Sic1-9myc during a synchronous *GAL-NDT80* block-release meiosis. We observed that Sic1-9myc levels were high prior to premeiotic S-phase, decreased at timepoints correlating to premeiotic S-phase and remained

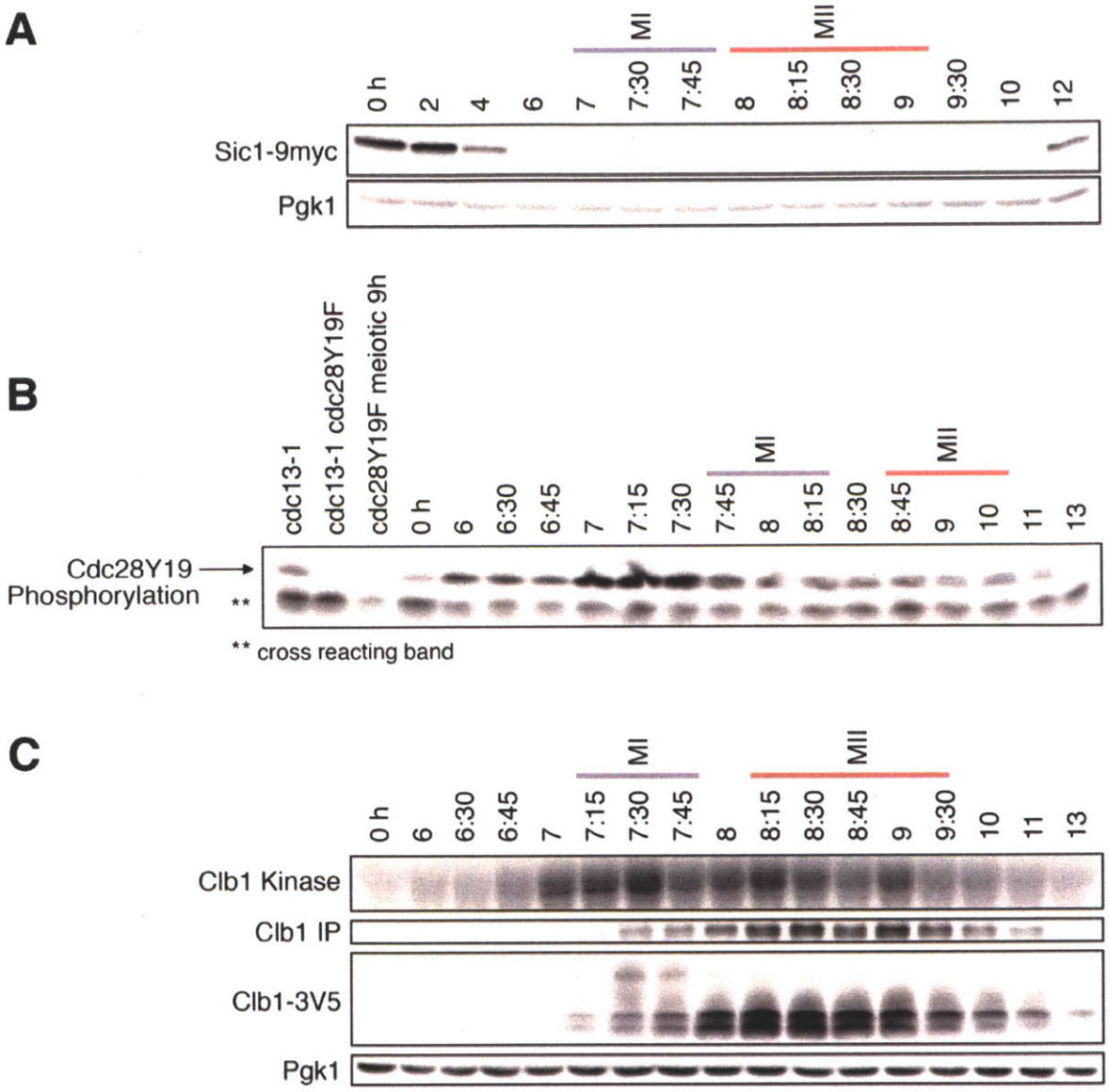

Figure 10. Known CDK inhibitor Sic1 as well as Swe1 do not play a role in downregulation of Clb1-CDK activity in MII.

(A) Cells carrying the *GAL4-ER*, *GAL-NDT80 SIC1-9myc* fusions (A24759) were induced to sporulate. Cells were released from the *NDT80* block at 6h post transfer to sporulation medium. Sic1 levels were determined at the indicated time points by Western blot. Pgk1 was used as a loading control.

(B) Cells carrying the *GAL4-ER* and *GAL-NDT80* fusions alone (A15591) or in combination with a *cdc28Y19F* allele (A16480) were induced to sporulate.

Cells were released from the *NDT80* block at 6h post transfer to sporulation medium. Phosphorylation of Cdc28Y19 was determined at the indicated time points by Western blot. A cross-reacting band was used as a loading control. Cells containing the *cdc13-1* allele alone (A343) or in combination with a *cdc28Y19F* allele (A386) were shifted to the non-permissive temperature (37°C) for 3h and samples were taken for Western blot and used as positive and negative controls for the phospho-Cdc28 antibody.

(C) Cells carrying the *GAL4-ER*, *GAL-NDT80* and *CLB1-3V5* fusions and a deletion of *SWE1* (A23235) were induced to sporulate. Cells were released from the *NDT80* block at 6h post transfer to sporulation medium. Clb1 levels and associated kinase activity were determined at the indicated time points (see Materials and Methods for details). Pgk1 was used as a loading control.

---

low during both meiosis I and meiosis II (Figure 10A). Thus, it is unlikely that Sic1 plays a major role in the downregulation of Clb1-CDK specifically during meiosis II, although further experiments will be required to rule this possibility out.

Another factor that regulates CDK activity is the tyrosine kinase, called Swe1 in budding yeast. Swe1 directly phosphorylates Cdc28 on T18 and Y19 to downregulate CDK activity and there is evidence that Swe1 differentially phosphorylates and inhibits certain cyclin-CDK complexes (Keaton et al., 2007). We first wished to examine overall Cdc28Y19 phosphorylation during a synchronous *GAL-NDT80* block-release meiosis. Using a phospho-specific antibody that recognizes Cdc28-phosphoY19, we observed that levels of Cdc28Y19 phosphorylation were low as cells were induced to sporulate,

increased as cells arrested in pachytene, peaked at timepoints after *NDT80* induction but prior to the meiotic divisions and then decreased during both meiotic divisions (Figure 10B).

We did not observe an increase in Cdc28Y19 phosphorylation during meiosis II as might be expected if this modification played a role in specifically downregulating Clb1-CDK activity. However, these analyses included the total Cdc28 pool and were not limited to the fraction that was specifically bound to Clb1. Accordingly, we wished to examine the direct role of Swe1 on Clb1-CDK activity. We determined Clb1-CDK activity from a strain carrying a deletion of *SWE1* during a synchronous *GAL-NDT80* block-release meiosis. We observed that Clb1-CDK activity remained downregulated during meiosis II in cells deleted for *SWE1* (Figure 10C), suggesting that Cdc28Y19 phosphorylation of Clb1-CDK complexes is likely not the mechanism by which meiosis II downregulation occurs. We conclude from these data that the known CDK inhibitors, Sic1 and Swe1, likely do not play a role in Clb1-CDK downregulation during meiosis II and that additional factors must be present that specifically inhibit these cyclin-CDK complexes.

Expression of *CLB1* from the *GAL1-10* promoter does not alter meiotic regulation.

We next wished to ask whether expression of *CLB1* from the *GAL1-10* promoter altered the observed regulation of Clb1-CDK activity. Meiotic expression of genes from the *GAL1-10* promoter using the *GAL4.ER* system

results in accumulation of protein 20-30 min after induction. The level of protein accumulation, however, is not greatly overexpressed (for example, levels of Clb3 accumulation in *GAL-CLB3* cells do not exceed the levels normally seen during meiosis II – see Chapter 2 and Carlile & Amon, 2008). Thus, *GAL-CLB1-3V5* cells proceeding through a synchronous *GAL-NDT80* block-release meiosis are expected to accumulate similar levels of Clb1, but protein will appear ~30min earlier compared to *CLB1-3V5* cells.

We determined Clb1-CDK activity during a synchronous *GAL-NDT80* block-release meiosis from a *GAL-CLB1-3V5* containing strain. As expected, Clb1-3V5 levels were abundant 1h after *GAL-CLB1* and *GAL-NDT80* induction (estradiol addition) and a robust meiosis I-specific Clb1 phosphorylation was detected by decreased gel mobility (Figure 11A). Interestingly, a very strong Clb1-CDK kinase activity was observed 1-1.25h after *GAL* induction (Figure 11A-B). Despite the very high Clb1-CDK activity found during early meiosis I, the specific Clb1-CDK activity rapidly dropped as cells proceeded through meiosis. These results show that expression of *CLB1* at the time of *NDT80* induction does not disrupt the observed downregulation of Clb1-CDK activity during meiosis II. These results also suggest that there is a window during early meiosis I when Clb1-CDK has very high in vitro kinase activity, which decreases as cells proceed through meiosis. Experiments to investigate what factors determine this window of high Clb1-CDK activity and additionally, when this window exists during

meiosis, will be useful to uncovering the mechanism by which Clb1-CDK is downregulated during meiosis II.

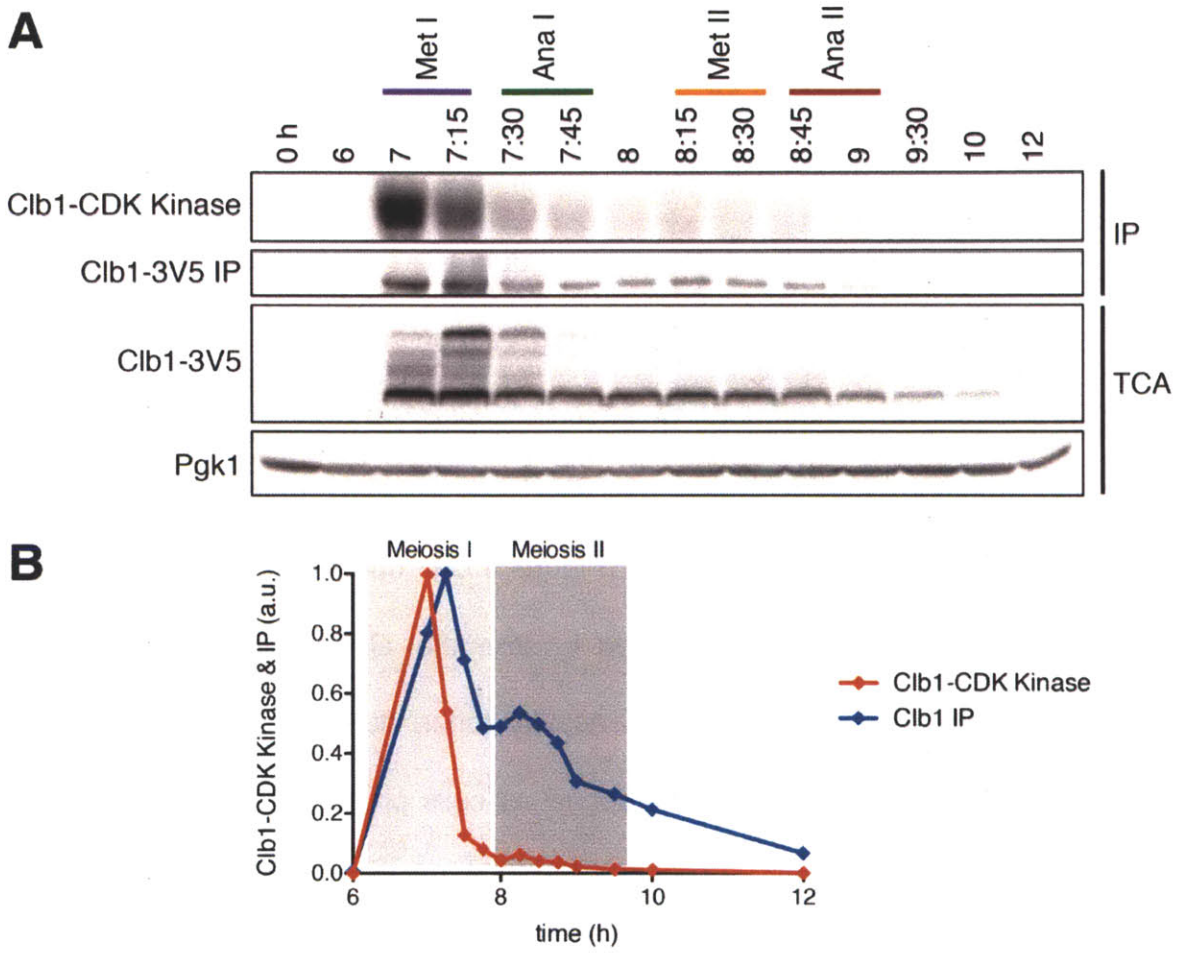

Figure 11. Expression of Clb1 from GAL promoter still results in downregulation of Clb1-CDK activity in meiosis II.

(A) Cells carrying the *GAL4-ER*, *GAL-NDT80* and *GAL-CLB1-3V5* fusions (A23650) were induced to sporulate. Cells were released from the *NDT80* block and Clb1 expression induced at 6h post transfer to sporulation medium by addition of 1 μM estradiol. Clb1 levels and associated kinase

activity were determined at the indicated time points (see Materials and Methods for details). Pgk1 was used as a loading control.

(B) Clb1-CDK activity was determined by quantifying the amount of phosphorylated Histone H1 using ImageQuant software (Molecular Dynamics). The amount of immunoprecipitated Clb1-3V5 from the kinase reaction was determined similarly.

Regulation of Clb1-CDK activity in meiosis compared to mitosis.

One interesting observation that came from our work with the *GAL-CLB1* system, was the relatively high amount of Clb1-CDK observed during early timepoints in meiosis I compared to that observed in meiosis II or mitosis. To investigate this observation further we compared in vitro Clb1-CDK activity from *GAL-CLB1-3V5* cells synchronously proceeding though both meiosis and mitosis. Cells carrying a *GAL-CLB1-3V5* allele were either induced to undergo a synchronous *GAL-NDT80* block-release meiosis or haploid *MATa GAL-CLB1-3V5* cells were arrested in G1 by treatment with mating pheromone and subsequently released to synchronously undergo mitosis. In vitro Clb1-CDK activity was determined at timepoints throughout meiosis and during mitosis. Consistent with previous results, Clb1-CDK activity peaked during early meiosis I and the specific activity was rapidly downregulated during meiosis II. Strikingly, the peak specific activity observed during meiosis I (6:45h after sporulation induction) was more than 150-fold higher than the peak specific activity observed during mitosis (Figure 12). These results are consistent with results obtained

from cells arrested in meiotic metaphase I (*cdc20-mn*) compared to cells arrested in mitotic metaphase (nocodazole treatment) (data not shown). These observations suggest that Clb1-CDK is specifically activated in meiosis I or that Clb1-CDK is specifically inhibited during mitosis and meiosis II. Work to understand the mechanism by which Clb1-CDK is regulated during both meiosis and mitosis will be a very interesting area for further research and may provide insight into the differential regulation of Clb1-CDK observed between meiosis I and meiosis II.

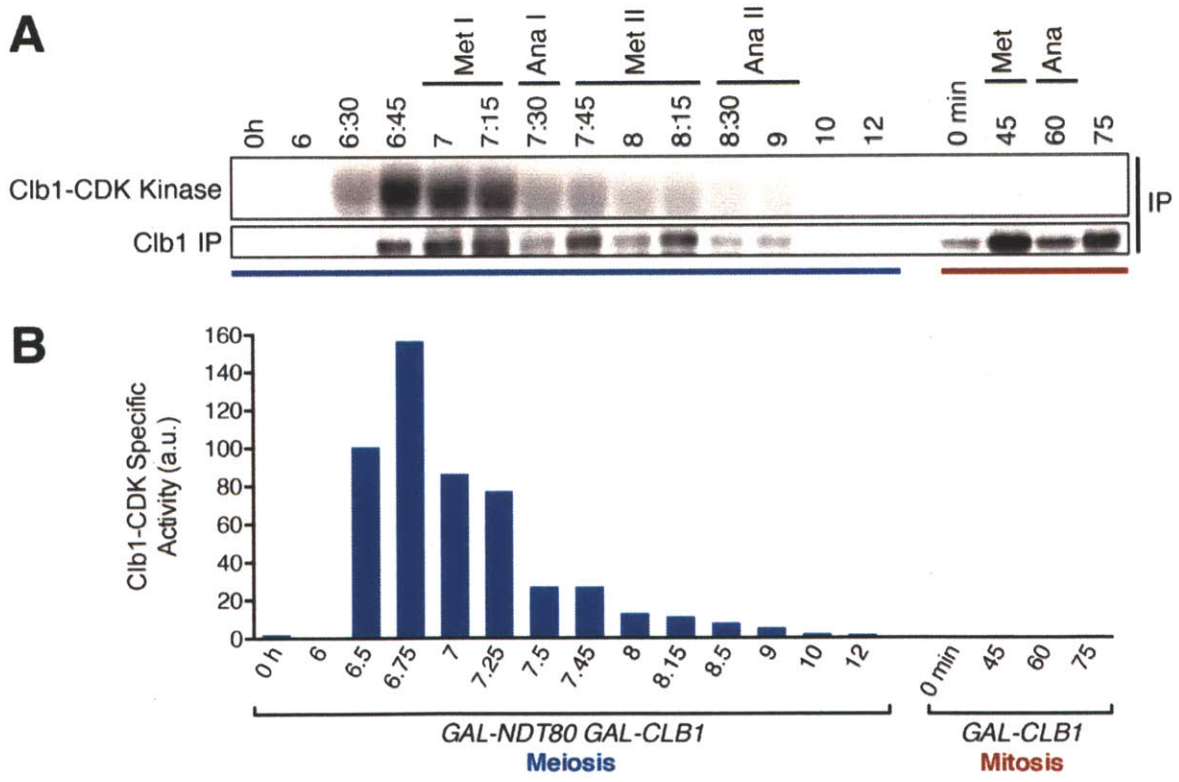

Figure 12. Regulation of Clb1-CDK in meiosis compared to mitosis.

(A) Left: Cells carrying the *GAL4-ER*, *GAL-NDT80* and *GAL-CLB1-3V5* fusions (A23650) were induced to sporulate. Cells were released from the *NDT80*

block and Clb1 expression induced at 6h post transfer to sporulation medium by addition of 1 μM estradiol (Meiosis = Blue).

Right: *MATa* haploid cells carrying *GAL4-ER* and *GAL-CLB1-3V5* fusions (A25645) were grown in rich medium (YEP) containing 2% raffinose and arrested in G1 with 5μg/ml α-factor. 45 min prior to release, 1 μM estradiol was added to culture. When arrest was complete, cells were released into rich medium (YEP) containing 2% raffinose, 1 μM estradiol and lacking pheromone (Mitosis = Red).

Samples were taken at indicated time points to examine Clb1 levels and associated kinase activity (see Materials and Methods for details).

(B) Clb1-CDK activity was determined by quantifying the amount of phosphorylated Histone H1 using ImageQuant software (Molecular Dynamics) for samples described in **(A)**. The amount of immunoprecipitated Clb1-3V5 from the kinase reaction was determined similarly.

Mitotic Clb1-CDK activity is not activated by ectopic *NDT80* expression.

One possible explanation for the observed difference in Clb1-CDK activity between meiosis I and mitosis is that a meiosis I-specific activator is present during meiosis I but not during mitosis or meiosis II. If such an activator exists, its expression may be dependent on the meiosis specific transcription factor Ndt80. We next investigated whether ectopic expression of Ndt80 during mitosis would modulate the in vitro kinase activity of Clb1-CDK. Ectopic expression of Ndt80 was previously shown to be at least partially functional when ectopically expressed during mitosis (Unal, Kinde, & Amon, 2011). To address the effect of Ndt80 expression on mitotic Clb1-CDK activity, *MATa GAL4.ER* cells carrying the

GAL-CLB1-3V5 allele alone or in combination with *GAL-NDT80* were arrested in mitotic metaphase by treatment with nocodazole (Figure 13A). Cells were then induced to express Clb1-3V5 alone or together with Ndt80 by addition of estradiol to the medium and Clb1-CDK activity was subsequently monitored. We observed that co-expression of Ndt80 with Clb1-3V5 led to slightly higher in vitro Clb1-CDK kinase activities than Clb1-3V5 alone (Figure 13B-C), however, the level of activity was still much less than that is observed in early meiosis I. If Clb1-CDK activity is regulated by a meiosis I-specific activator, these results suggest that additional factors, that are not dependent on Ndt80, must be present to modulate Clb1-CDK activity. Alternatively, it is possible that Ndt80 is not fully functional when ectopically expressed during mitosis. Determining the mechanism by which Clb1-CDK activity is regulated during mitosis will help uncover how Clb1-CDK is regulated during meiosis and may elucidate novel mechanisms of cyclin-CDK regulation.

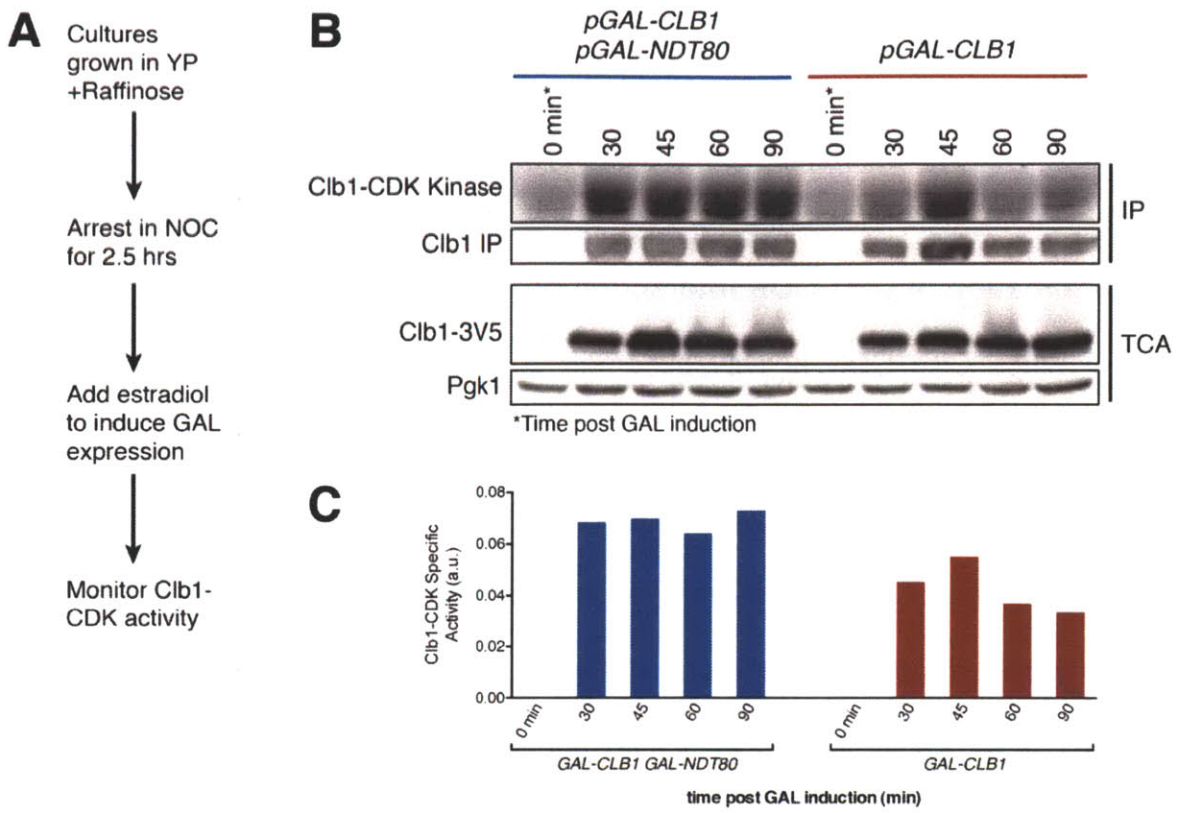

Figure 13. Expression of meiosis-specific transcription factor *NDT80* does not greatly affect mitotic Clb1-CDK activity.

(A) Schematic describing experimental design used for **(B)** and **(C)**.

(B) *MATa* haploid cells carrying *GAL4-ER* and *GAL-CLB1-3V5* fusions alone (A25645) or in combination with *GAL-NDT80* (A23469) were grown in rich medium (YEP) containing 2% raffinose and arrested in metaphase by treating with the microtubule depolymerizing drug nocodazole (15µg/ml). 2.5h after nocodazole treatment, when arrest was complete, cells were treated with 1 µM estradiol to induce *CLB1-3V5* and/or *NDT80* expression. Samples were taken at indicated time points to examine Clb1 levels and associated kinase activity (see Materials and Methods for details). Pgk1 was used as a loading control.

(C) Specific activity was calculated by normalizing the amount of phosphorylated Histone H1 to the amount of immunoprecipitated Clb1-3V5

using ImageQuant software (Molecular Dynamics) for samples described in **(B)**.

Determination of Clb1-CDK interacting proteins during meiosis.

Since Clb1-CDK activity becomes downregulated during meiosis II and this occurs by a mechanism that does not disrupt the interaction between Clb1 and Cdc28 (Figure 9), we reasoned that a likely mechanism for the downregulation of kinase activity was a factor that binds and inactivates Clb1-CDK specifically during meiosis II (Figure 14). To determine what proteins interact with Clb1-CDK specifically during meiosis II, we performed co-immunoprecipitation followed by protein identification by mass spectrometry from cells in either meiosis I, meiosis II or during exponential mitotic growth. Briefly, cells carrying either a *CLB1-TEV-ProA* allele or a non-tagged *CLB1* allele were induced to undergo a synchronous *GAL-NDT80* block-release meiosis. Samples were harvested for analysis when the majority of cells were either in meiosis I (1.5h after *NDT80* release) or in meiosis II (3h after *NDT80* release). In parallel, and as an additional control, samples were harvested from haploid *CLB1-TEV-ProA* cultures during exponential mitotic growth.

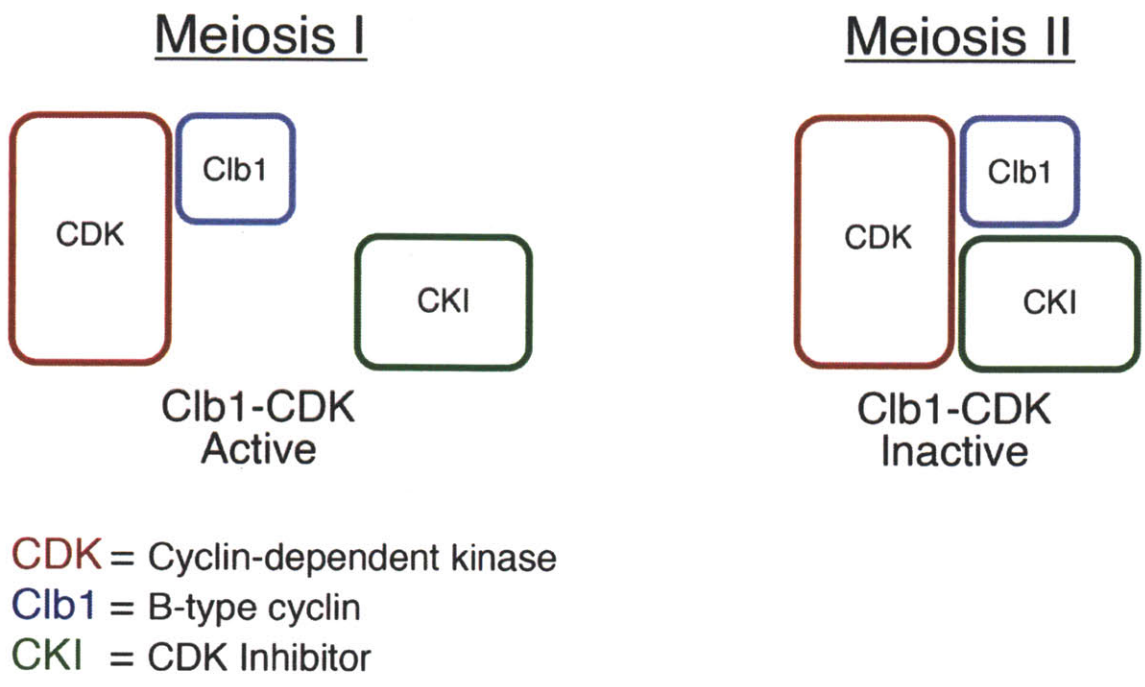

Figure 14. Model for trans-acting regulator of Clb1-CDK during meiosis
Downregulation of Clb1-CDK during meiosis II may involve a trans-acting factor binding the Clb1-CDK complex and downregulating its activity without disrupting Clb1-Cdc28 interaction.

Among the proteins identified that interact with Clb1 during both meiosis I and meiosis II as well as during mitotic growth were proteins that were expected to interact with Clb1 (and CDK) including Cdc28, Cks1 and Sic1 (Table 1). These results confirmed the methodology and gave us confidence that the proteins identified were *bona fide* Clb1 interacting proteins. The proteins that showed the highest enrichment of Clb1 binding in meiosis II relative to the meiosis I and mitosis samples were a significant number of polarisome components (Spa2, Kel1, Bni1, Yfr016c, Pea2, Kel2 and Bud6), proteins involved in APC/C regulation

(Cdh1 and Acm1), cytoskeleton organization (Bbc1 and She4) as well as the 14-3-3 minor isoform, Bmh2 (Table 1). A combined list of proteins that showed interaction with Clb1 during either meiosis I or meiosis II is shown in Table 2. To determine whether the factors listed above play a role in Clb1-CDK downregulation during meiosis, we chose to examine Clb1-CDK activity in the context of loss-of-function mutants for the above listed factors.

		Number of Peptides Identified				
Gene	**Molecular Weight**	**Cycling Cells**	**no tag**	**MI**	**MII**	**Function**
CDC28	34 kDa	**20**	0	**59**	**99**	Known interactors
CLB1	55 kDa	**22**	0	**32**	**47**	
CKS1	18 kDa	**7**	0	**15**	**32**	
SIC1	32 kDa	8	0	3	6	
SPA2	163 kDa	13	0	36	**99**	Polarisome/polarized growth
KEL1	131 kDa	0	0	23	**32**	
BNI1	220 kDa	0	0	4	19	
YFR016c	138 kDa	0	0	0	24	
PEA2	48 kDa	3	0	7	**13**	
KEL2	100 kDa	0	0	5	5	
BUD6	89 kDa	-	1	5	9	
CDH1	63 kDa	0	0	0	**42**	APC/C
ACM1	24 kDa	0	0	0	8	
BBC1	128 kDa	0	0	3	22	Cytoskeleton organization
SHE4	90 kDa	0	0	6	15	
BMH2	31 kDa	0	0	**13**	**24**	14-3-3 protein, minor isoform

Table 1. Proteins that interact with Clb1 during meiosis II determined by immunoprecipitation followed by mass spectrometry

Cells carrying the *GAL4-ER*, *GAL-NDT80* fusions alone (A14201) or in combination with a *CLB1-TEV-ProA* fusion (A23893) were induced to sporulate. Cells were released from the *NDT80* block at 6h post transfer to sporulation medium. Samples were taken for co-immunoprecipitation followed by mass spectrometry at both 7h 30min post sporulation induction (MI; A23893) and 9h

(MII; A14201, A23893). Haploid cells carrying a *CLB1-TEV-ProA* fusion (A23790) were grown in YEP + 2% dextrose. Samples were taken from exponential cultures for co-immunoprecipitation followed by mass spectrometry. See Materials and Methods for more details. Note: numbers shown in bold represent >20% coverage of protein from identified peptides by mass spectrometry. Additionally, these analyses are not quatitative.

Number of Peptides Identified

	Protein	Molecular Weight	Set #1 no tag	Set #1 MI (7:30h)	Set #1 MII (9 h)	Set #2 Cycling	Set #2 no tag	Set #2 MI (7:30h)	Set #2 MII (9 h)
1	Cdc28	34 kDa	0	22	26	20	0	59	99
2	Clb1	55 kDa	0	26	24	22	0	32	47
3	Cks1	18 kDa	0	6	5	7	0	15	32
4	Sic1	32 kDa	0	7	5	8	0	3	6
5	Bni1	220 kDa	0	39	59	0	0	4	19
6	Kel1	131 kDa	0	34	28	0	0	23	32
7	Lte1	163 kDa	0	23	26	0	0	8	16
8	Pea2	48 kDa	0	19	19	3	0	7	13
9	Cdh1	63 kDa	0	3	19	0	0	0	42
10	Bud15 or Ede	151 kDa	0	4	11	-	-	-	-
11	Yis3 or Aim21	75 kDa	0	3	10	0	0	3	5
12	Acm1	24 kDa	0	1	6	0	0	0	8
13	Spa2	163 kDa	1	46	58	13	0	36	99
14	Sec7	205 kDa	1	8	25	0	0	0	5
15	Apc1	196 kDa	2	8	21	0	0	0	3
16	Bud6	89 kDa	1	5	9	-	-	-	-
17	Bbc1	128 kDa	3	8	24	0	0	3	22
18	YFR016C	138 kDa	9	23	35	0	0	0	24
19	Cin8	113 kDa	6	9	20	0	0	0	3
20	Sla2	109 kDa	10	12	22	0	0	0	12
21	Bmh2	31 kDa	8	13	17	0	0	13	24
22	Sps22	52 kDa	15	5	12	0	0	0	8
23	She4	90 kDa	6	22	24	0	0	6	15
24	Kel2	100 kDa	0	15	12	0	0	5	5
25	Sum1	118 kDa	0	13	10	-	-	-	-
26	Cdc39	240 kDa	7	24	24	-	-	-	-
27	Atg1	102 kDa	4	13	10	0	0	4	3
28	Atg11	135 kDa	3	9	6	0	0	3	2
29	Cdc23	73 kDa	2	4	9	-	-	-	-
30	Ent2	72 kDa	5	9	13	0	0	0	8
31	Cdc16	95 kDa	5	5	13	0	0	0	2
32	Apc2	100 kDa	0	0	3	-	-	-	-
33	Ato3	30 kDa	0	0	3	-	-	-	-
34	YKL065C	23 kDa	0	0	1	-	-	-	-
35	Tom1	374 kDa	0	3	6	-	-	-	-
36	Tpm2	19 kDa	0	2	6	0	0	0	3
37	Akl1	124 kDa	0	0	5	-	-	-	-
38	Arc40	42 kDa	0	0	3	-	-	-	-
39	YHR159W	56 kDa	0	0	5	-	-	-	-
40	Hsp42	43 kDa	4	4	7	0	0	5	12
41	Myo5	137 kDa	10	7	16	0	0	0	5
42	Stu2	101 kDa	5	4	8	0	0	4	8
43	Ecm11	34 kDa	7	8	11	0	0	4	7
44	Gas4	54 kDa	8	3	7	0	0	0	3
45	Bud5	75 kDa	0	0	4	-	-	-	-
46	Spo19	25 kDa	2	0	2	0	0	0	4

Number of Peptides Identified Continued

	Protein	Molecular Weight	Set #1 no tag	Set #1 MI (7:30h)	Set #1 MII (9 h)	Set #2 Cycling	Set #2 no tag	Set #2 MI (7:30h)	Set #2 MII (9 h)
47	Red1	96 kDa	0	12	0	0	0	2	0
48	YMR124W	106 kDa	0	8	5	0	0	2	0
49	Zip2	83 kDa	0	13	0	-	-	-	-
50	Sec2	85 kDa	0	6	2	-	-	-	-
51	Ssp31	164 kDa	0	5	1	-	-	-	-
52	Mum2	41 kDa	0	6	2	-	-	-	-
53	Sli15	79 kDa	0	4	2	-	-	-	-
54	Pac11	60 kDa	0	4	2	-	-	-	-
55	Hop1	69 kDa	0	12	0	0	0	4	0
56	Drr1	281 kDa	0	5	2	-	-	-	-
57	Bud14	79 kDa	0	4	2	-	-	-	-
58	Mtc2	102 kDa	0	6	2	-	-	-	-
59	Gal4	99 kDa	0	6	2	-	-	-	-
60	Smc1	141 kDa	0	6	1	-	-	-	-
61	Cis1	22 kDa	0	3	1	-	-	-	-
62	Ddc1	70 kDa	0	5	0	-	-	-	-
63	Spo22	112 kDa	4	43	17	0	0	115	4
64	Kip1	126 kDa	2	13	7	-	-	-	-
65	Atg9	115 kDa	4	10	7	0	0	3	0
66	YHL024W	80 kDa	5	9	6	0	0	13	3
67	Cct8	62 kDa	3	5	1	0	0	3	2
68	Spo16	23 kDa	0	4	0	0	0	3	0
69	Cap2	32 kDa	0	6	8	0	0	0	6
70	Caf120	118 kDa	0	6	6	-	-	-	-
71	Brr2	246 kDa	0	5	4	-	-	-	-
72	Ndc80	80 kDa	0	3	3	-	-	-	-
73	She3	47 kDa	0	5	5	-	-	-	-
74	Ipl1	43 kDa	0	2	1	-	-	-	-
75	Myo4	169 kDa	2	7	9	0	0	2	0
76	Sec21	105 kDa	2	6	8	0	0	0	2
77	Bim1	38 kDa	2	6	4	0	0	2	0
78	Arp2	44 kDa	2	4	5	0	0	0	3
79	Dyn1	471 kDa	25	52	60	0	0	4	0
80	Cdc48	92 kDa	5	12	10	0	0	0	2
81	Cap1	31 kDa	3	6	5	0	0	2	5
82	Chc1	187 kDa	19	22	37	0	0	7	38
83	Bch1	82 kDa	2	3	1	0	0	2	0
84	Aim13	19 kDa	2	2	3	0	0	0	2
85	Ecm33	44 kDa	3	3	4	4	0	0	5
86	Sso1	23 kDa	3	2	4	0	0	0	2
87	Kar3	84 kDa	8	9	8	0	0	4	7
88	YBL104C	118 kDa	9	10	10	0	0	3	0
89	Sec4	24 kDa	6	6	5	0	0	2	3
90	Cdc10	37 kDa	5	3	5	3	0	0	3
91	Sec27	99 kDa	3	3	3	0	0	2	0
92	Fcj1	61 kDa	18	14	16	0	0	3	4
93	Cwp1	24 kDa	9	6	8	0	0	0	5
94	Ytm1	51 kDa	4	3	0	0	0	3	2
95	Cda1	35 kDa	4	0	3	0	0	0	2
96	Sec5	112 kDa	0	1	3	-	-	-	-

Table 2. Proteins that interact with Clb1 during meiosis determined by immunoprecipitation followed by mass spectrometry

Combined list of proteins that showed interaction with Clb1 during MI or MII by immunoprecipitation followed by mass spectrometry. Protein identification of 50% of eluate (Set #1) was determined by the lab of Karl Mechtler, IMP, Austria. Protein identification of other 50% of eluate (Set #2) was determined by the Koch Institute proteomics facility. Proteins in which peptides were identified in either the MI or MII sample (A23893) but not in the non-tagged sample (A14201) in either Set #1 or Set #2 are highlighted in green. Note: these analyses are not quatitative.

Role of putative Clb1 binding partners in meiotic Clb1-CDK regulation.

The polarisome is a protein complex that plays a role in cell polarity by directing the localized assembly of actin filaments at polarization sites (Park & Bi, 2007). The polarisome does not have a defined role during meiosis, however, as most polarisome and related components were specifically identified to interact with Clb1 during meiosis II we chose to further investigate the role of the polarisome as well as other Clb1 binding partners in the regulation of meiotic Clb1-CDK activity.

We determined Clb1-CDK activity during a synchronous *GAL-NDT80* block-release meiosis from strains carrying a deletion of *YFR016c, SPA2, ACM1, CDH1* or *SWE1* (Figure 15). In all cases, kinase activity correlated relatively well with the amount of Clb1 immunoprecipitated during meiosis I. However, the Clb1-CDK specific activity also decreased during meiosis II for each of these strains.

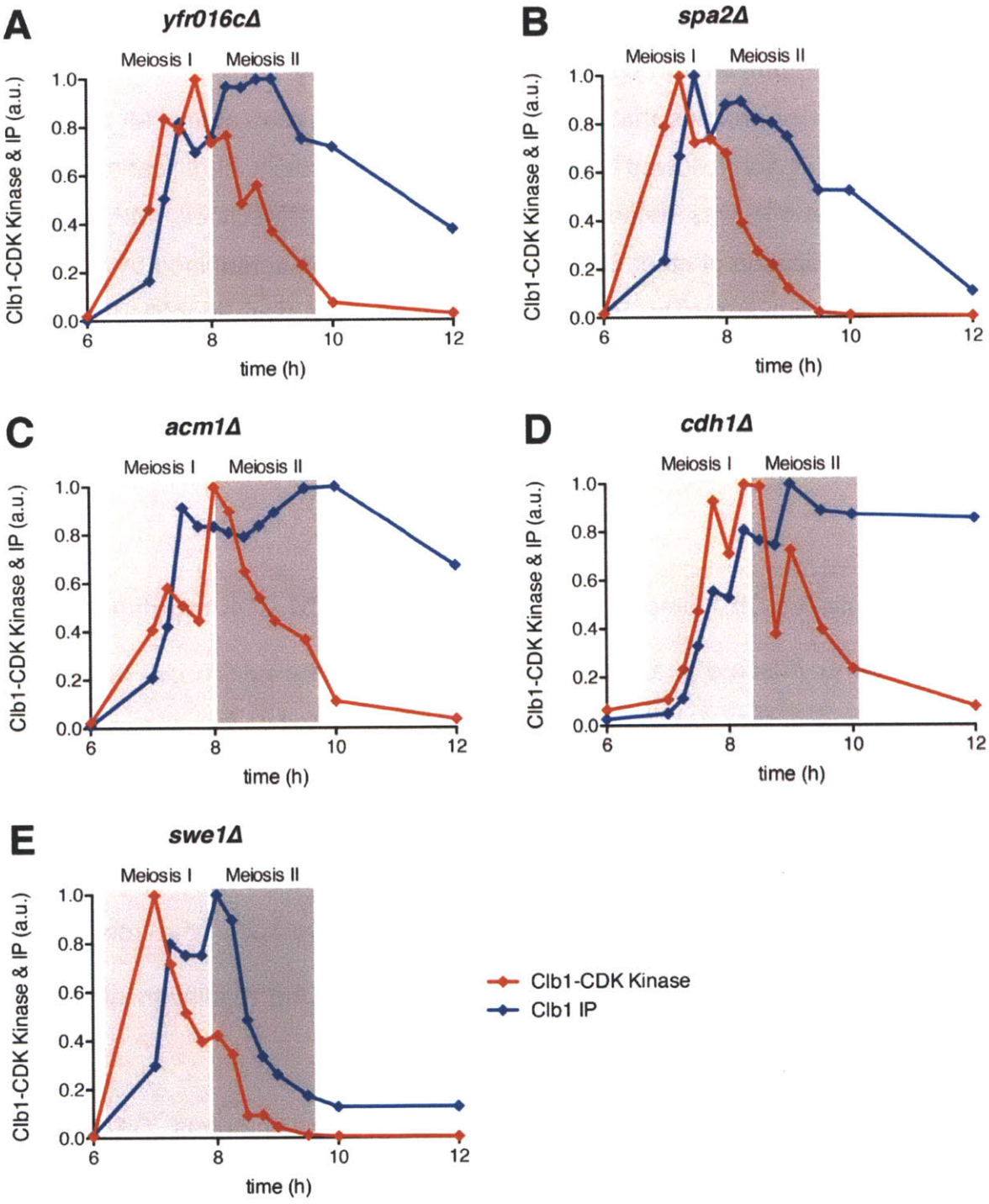

Figure 15. Deletion of candidate Clb1-CDK trans regulators and affect on Clb1-CDK activity during meiosis.

Cells carrying the *GAL4-ER*, *GAL-NDT80* and *CLB1-3V5* fusions and a deletion of either *YFR016C* [**(A)**; A25402], *SPA2* [**(B)**; A25404], *ACM1* [**(C)**; A25408],

CDH1 [**(D)**; A25470] or *SWE1* [**(E)**; A23235] were induced to sporulate. Cells were released from the *NDT80* block at 6h post transfer to sporulation medium. Clb1 levels and associated kinase activity were determined at the indicated time points (see Materials and Methods for details). Clb1-CDK activity was determined by quantifying the amount of phosphorylated Histone H1 using ImageQuant software (Molecular Dynamics). The amount of immunoprecipitated Clb1-3V5 from the kinase reaction was determined similarly.

These results suggest that these factors are not solely responsible for the observed downregulation of Clb1-CDK during meiosis II.

To address the role of additional putative meiosis II-specific Clb1 binding partners identified by co-immunoprecipitation mass spectrometry (Table 1 & 2), we chose to use the *GAL-CLB1* system (Figure 11). This system provides a more robust method to investigate the downregulation of Clb1-CDK activity, since there is a greater differential in activity in meiosis I relative to meiosis II compared to conditions in which Clb1 is expressed from the endogenous Clb1 promoter. Cells carrying a *GAL-CLB1-3V5* allele alone or in combination with a deletion of *SWE1*, *SPA2*, *BBC1*, *KEL2*, *PEA2*, *BUD6* or *KEL1* were induced to undergo a synchronous *GAL-NDT80* block-release meiosis. In vitro Clb1-CDK kinase activity was determined at two timepoints corresponding to meiosis I (6:45 and 7h after induction of sporulation) and at two timepoints corresponding to meiosis II (8:15 and 8:30h). For all strains, we observed robust Clb1-CDK activity for the meiosis I timepoints and a downregulation of activity for the meiosis II timepoints

(Figure 16). Although levels of immunoprecipitated Clb1 varied between strains, in each case, the specific activity of Clb1-CDK was reduced in the meiosis II timepoints. These results suggest that these factors are not solely responsible for the observed downregulation of Clb1-CDK during meiosis II.

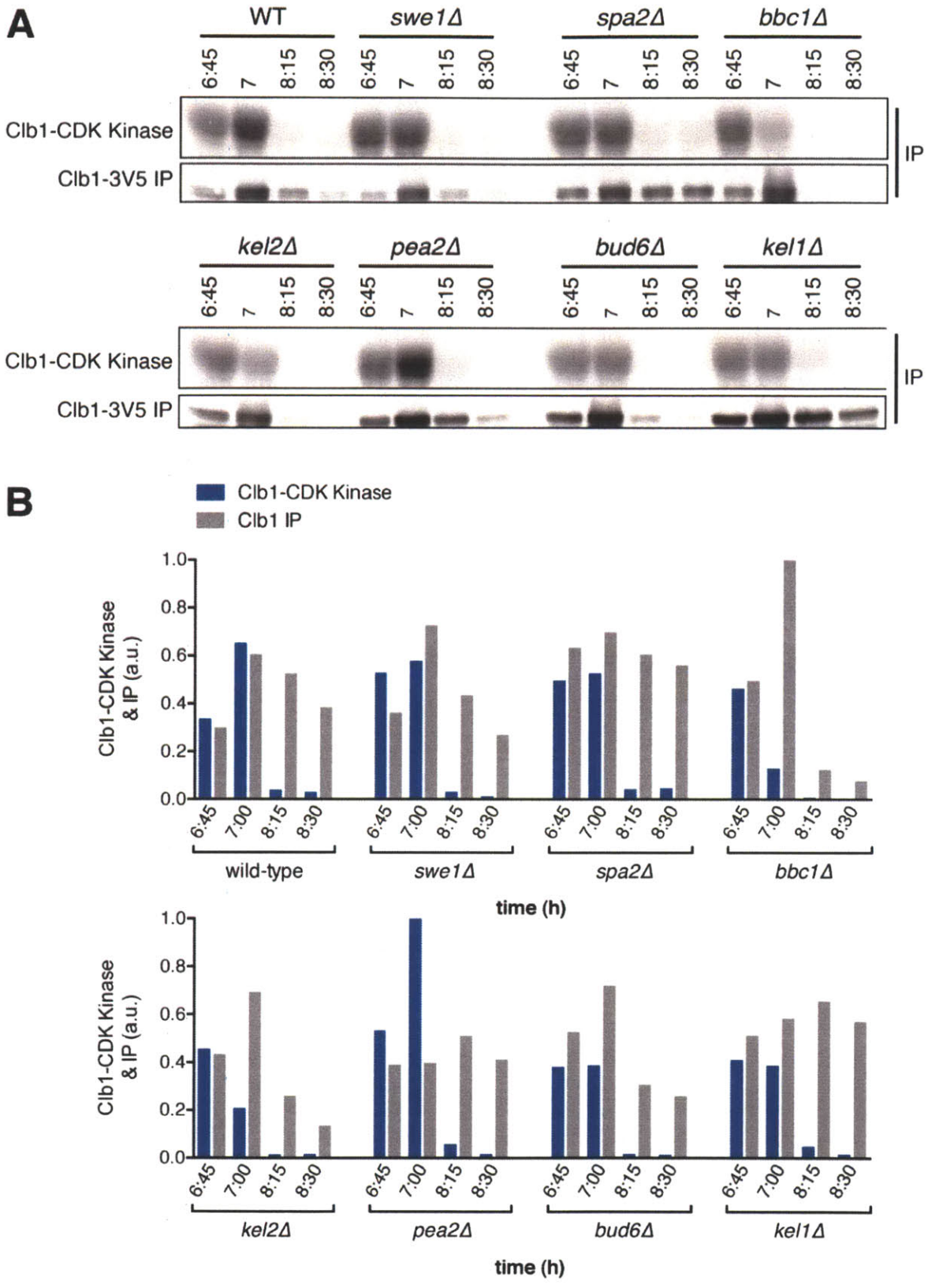
A
WT
swe1Δ
spa2Δ
bbc1Δ
6:45
7
8:15
8:30
Clb1-CDK Kinase
Clb1-3V5 IP
IP
kel2Δ
pea2Δ
bud6Δ
kel1Δ
B
Clb1-CDK Kinase
Clb1 IP
Clb1-CDK Kinase & IP (a.u.)
1.0
0.8
0.6
0.4
0.2
0.0
6:45
7:00
8:15
8:30
wild-type
swe1Δ
spa2Δ
bbc1Δ
time (h)
kel2Δ
pea2Δ
bud6Δ
kel1Δ

Figure 16. Deletion of candidate Clb1-CDK trans regulators and affect on Clb1-CDK activity during meiosis.

(A) Cells carrying the *GAL4-ER*, *GAL-NDT80* and *GAL-CLB1-3V5* fusions (A23650) or a deletion of *SWE1* (A26075), *SPA2* (A26076), *BBC1* (A26077), *KEL2* (A26079), *PEA2* (A26080), *BUD6* (A26081) or *KEL1* (A26118) were induced to sporulate. Cells were released from the *NDT80* block and Clb1 expression induced at 6h post transfer to sporulation medium by addition of 1 μM estradiol. Clb1 levels and associated kinase activity were determined at the indicated time points (see Materials and Methods for details). MI samples = 6:45 and 7h; MII samples = 8:15 and 8:30h.

(B) Clb1-CDK activity was determined by quantifying the amount of phosphorylated Histone H1 using ImageQuant software (Molecular Dynamics) from samples in **(A)**. The amount of immunoprecipitated Clb1-3V5 from the kinase reaction was determined similarly.

DISCUSSION

Cyclin-CDKs are the major drivers of both the mitotic and meiotic cell divisions. In order to establish the proper timing of events during cell division, cells have evolved intricate mechanisms to regulate cyclin-CDK activity. In budding yeast, the majority of cyclin-CDK regulation occurs at either the transcriptional level, with expression of the various cyclins being tightly regulated to cell cycle progression (Mendenhall & Hodge, 1998), or at the posttranslational level, with various CDK inhibitors regulating the activity of cyclin-CDKs to yield switch-like cell cycle transitions (Bloom & Cross, 2007; Peters, 2006). Here, we have described our work to uncover the mechanism by which the activity of Clb1-CDK is regulated during meiosis. We have found that Clb1-CDK has a high specific activity during early meiosis I relative to meiosis II and, surprisingly, a high specific activity relative to mitosis. Further work to understand the mechanism by which Clb1-CDK activity is regulated during mitosis and meiosis may yield insight into how the cell cycle machinery is modulated to bring about the specialized meiotic cell division and may elucidate novel mechanisms of cyclin-CDK regulation.

Sequence determinants of Clb1 required for meiotic regulation

In order to determine the mechanistic basis of Clb1-CDK regulation during meiosis, we first investigated the sequence determinants that were responsible for the observed downregulation during meiosis II. One possible mechanism of

regulating Clb1-CDK activity would be through posttranslational modification of Clb1. Clb1 shows a mobility shift that correlates with active kinase activity during meiosis I. We hypothesized that this modification may play a role in the relative upregulation of Clb1-CDK activity during meiosis I and thus, investigated the nature of this modification. We found that Clb1 is phosphorylated during meiosis I, and that this modification is largely reduced, if not absent, during meiosis II and mitosis (Figure 2). We also found that this modification depends on both CDK and Cdc5 activity (Figure 3 & 4). Additionally, it appears that the phosphorylation of Clb1 occurs on the N-terminal 155 residues of Clb1, as this region is both necessary and sufficient for the observed gel mobility shift (Figure 7). However, we also found that, under conditions in which this phosphorylation is absent (e.g. Cdc5 inactivation; Figure 4C-D), the in vitro activity of Clb1-CDK is unaffected relative to the control. These results suggest that this modification does not play a role in the regulation of in vitro Clb1-CDK activity. At present, it is not clear what physiological role the meiosis I-specific phosphorylation of Clb1 plays. This modification may affect the subcellular localization of Clb1, which has previously been shown to exit the nucleus at the meiosis I-meiosis II transition (Marston, Lee, & Amon, 2003). However, preliminary results suggest that Clb1 becomes nuclear localized in meiosis II (data not shown), suggesting that the nuclear localization of Clb1 is independent of its phosphorylation status. Alternatively, this modification may play a role in fine-tuning the in vivo activity and/or specificity of Clb1-CDK. An inherent drawback of studying the activity of Clb-CDKs in vitro is

that such regulation may not be observed due to a limitation of the assay including the likely non-physiological substrate used.

Whether other posttranslational modifications exist on Clb1 (or CDK) that affect the activity of this complex is another area that could be investigated. While alternative posttranslational modifications were not detected in our mass spectrometry studies, the nature of the protein purification (native immunoprecipitation) combined with the relatively low coverage of the proteins in these analyses (<50% coverage), may have precluded the detection of such moieties.

Another area that will require further clarification is the role of and interplay between CDK and Cdc5 activity in the phosphorylation of Clb1. Since the observed phosphorylation of Clb1 is not altered when the sole minimal CDK phosphorylation site on Clb1 is mutated to alanine (S302A) (Figure 3), CDK is not likely to phosphorylate Clb1 directly. It is possible that CDK phosphorylates a different subunit of the complex (e.g. Cdc28 or Cks1) to prime Cdc5 activity, which then phosphorylates Clb1. Future studies will be required to fully elucidate the relationship between CDK and Cdc5 in promoting this posttranslational modification.

Additionally, the observation that Clb1 is modified specifically in meiosis I in a Cdc5-dependent manner raises the possibility that this modification is a readout for Cdc5 activity in meiosis and that Cdc5 activity is restricted to meiosis

I. An interesting possibility and an area that was briefly investigated and is described in Appendix A.

Regulation of chimeric fusion cyclins

To further investigate the *cis* acting elements that are responsible for the observed downregulation of Clb1-CDK during meiosis II we attempted to map the regions of Clb1 that are necessary for this regulation. To this end, we took advantage of the fact that Clb1 and the closely related cyclin, Clb2, are differentially regulated in meiosis (Figure 5). We generated fusion cyclins in which the divergent N-terminal portion of Clb1 was fused to the conserved C-terminal portion of Clb2 as well as the converse in which the N-terminal portion of Clb2 was fused to the conserved C-terminal portion of Clb1 (Figure 6). Using the Clb2-Clb1 fusion, we observed a peak of associated kinase activity in both meiosis I and meiosis II (Figure 7), suggesting that the N-terminus of Clb1 may play some role in the downregulation of activity during meiosis II. However, the associated kinase activity did not correlate well with levels of purified cyclin suggesting that, in addition to the N-terminal 155 residues, other sequence determinants of Clb1 are required for regulation of specific kinase activity. In addition, the N-terminal 155 residues of Clb1 did not appear sufficient to promote downregulation of associated kinase activity (Clb1-Clb2 fusion). Further and more robust characterization of these fusion alleles will be required to determine

the exact role of the divergent N-terminus of Clb1 in the regulation of associated CDK activity.

One surprising observation from these studies was that cyclins containing the Clb2 cyclin box domain (both the Clb1-Clb2 fusion and Clb2 itself) have ~23-110 fold higher in vitro kinase activity than the Clb1 cyclin box domain-containing cyclins (Clb2-Clb1 and Clb1), respectively. It is not clear whether the drastic difference observed in associated kinase activity between Clb1 and Clb2 is an artifact of the in vitro assay used or whether this represents a physiologically relevant difference. Regardless, determining the basis for this difference may provide further insight into the mechanism of cyclin activation of cyclin-dependent kinases and the role of individual cyclins in promoting substrate specificity for the various cyclin-CDKs.

Examination of additional factors that regulate Clb1-CDK activity

To further examine the mechanistic basis of Clb1-CDK regulation during meiosis, we next chose to identify factors responsible for the observed downregulation during meiosis II. One possible mechanism of regulating Clb1-CDK activity would be through disrupting the interaction of Clb1 with Cdc28 during meiosis II. We found that this was, in fact, not the case (Figure 8). There was no correlation between the in vitro kinase activity observed and the amount of co-purifying Cdc28 (specifically in meiosis II) suggesting that Clb1 and Cdc28 are bound in meiosis II, but that the activity of this complex is inhibited. We also

examined the role of the known CDK inhibitor, Sic1, as well as Swe1, and found that these factors likely do not play a role in Clb1-CDK downregulation during meiosis II. Thus, we hypothesized that additional factors must be present that specifically inhibit these cyclin-CDK complexes.

With the aim of identifying factors that specifically inhibit Clb1-CDK during meiosis II, we chose to examine the proteins that co-purify with Clb1 during meiosis. The proteins that showed the highest enrichment of Clb1 binding in meiosis II relative to the meiosis I and mitosis were a large number of polarisome components (Spa2, Kel1, Bni1, Yfr016c, Pea2, Kel2 and Bud6) and proteins involved in APC/C regulation (Cdh1 and Acm1). We found that deletion of *YFR016c*, *SPA2*, *KEL2*, *PEA2*, *BUD6*, *KEL1*, *ACM1*, *CDH1* and *BBC1* had little to no affect on Clb1-CDK activity, suggesting that these factors are not solely responsible for downregulating Clb1-CDK activity during meiosis II.

The polarisome is a protein complex that plays a role in bud site selection and cell polarity by directing the localized assembly of actin filaments at polarization sites (Park & Bi, 2007). To date, there are no known roles of polarisome during meiosis, however, as most polarisome and related components were specifically identified to interact with Clb1 during meiosis II, it is possible that a previously unidentified function exists. Whether Clb1-CDK plays a role in this putative function will also need to be determined. It is also possible that the expression of the polarisome components during meiosis II, serves a function after meiosis is complete and the cells germinate and return to mitotic

growth. Again, determining whether Clb1-CDK plays some role in these functions will also need to be examined further.

Another category of proteins that we identified to co-purify with Clb1 during meiosis II were the APC/C regulators Cdh1 and Acm1. While it does not appear that these interactions serve to downregulate Clb1-CDK activity during meiosis II (Figure 13), it is possible that these interactions reflect physiological interactions either at the meiosis I-meiosis II transition or at exit from meiosis II. In order to ensure that meiosis I is followed by meiosis II, cells must exit meiosis I without completely inactivating CDKs (Peters, 2006). In fission yeast, the small protein Mes1 functions as an inhibitor of APC/C^{Cdc20} and prevents the complete degradation of cyclins during exit from meiosis I (Izawa, Goto, Yamashita, Yamano, & Yamamoto, 2005). Mes1 appears to inhibit APC/C activity by competing with cyclins for Cdc20 binding (Kimata et al., 2008). While there is no clear Mes1 homolog in budding yeast, Acm1 was identified as a Cdh1 binding partner and APC^{Cdh1} inhibitor in mitosis (Hall et al., 2008). It is not clear that APC^{Cdh1} is active during the meiosis I-meiosis II transition (Marston et al., 2003); an idea supported by the fact that Clb1 protein (a known substrate of APC^{Cdh1}) levels do not appear to decrease at this stage. Additionally, deletion of *CDH1* or *ACM1* does not affect Clb1 protein levels or meiotic progression (Figure 13). Whether Clb1-CDK phosphorylates these proteins to additionally regulate the APC/C or whether these interactions promote the degradation of Clb1 at the meiosis I-meiosis II transition (or after meiosis II) will require further work.

There are a number of explanations for why we did not identify regulators of Clb1-CDK activity using this method. First, it is possible that there are redundant mechanisms by which Clb1-CDK is downregulated. In our analysis, only single loss-of-function mutants were examined. Second, a meiosis II-specific inhibitor may be bound only transiently or the interaction between this factor and Clb1-CDK may not be stable enough to withstand the purification method used. Third, it is possible that the inhibitor is less amenable to identification by mass spectrometry and thus was missed or filtered out in our analyses. Fourth, it is possible that this method is more suitable for detecting Clb1-CDK phosphorylation targets. However, we did identify Sic1 as a co-purifying protein with Clb1-CDK. Thus, it is not likely that only Clb1-CDK targets were identified. It will be interesting to examine whether any of the co-purifying proteins are indeed phosphorylated by Clb1-CDK. Of the proteins identified, Spa2, Kel1, Kel2, Bud6, Cdh1 and Acm1 have been previously implicated as a CDK targets (Ostapenko, Burton, Wang, & Solomon, 2008; Ubersax et al., 2003).

Regulation of Clb1-CDK during meiosis compared to mitosis.

One of the most striking observations from the studies described in this chapter was the fact that the in vitro Clb1-CDK specific activity during early meiosis I was greater than 150-fold higher relative to the peak activity observed in mitosis (Figure 16). This could result from the presence of a meiosis II and mitosis specific inhibitor of Clb1-CDK activity or from the presence of a meiosis I

specific activator of Clb1-CDK activity that is not present during meiosis II and mitosis. We ectopically expressed the meiosis-specific transcription factor *NDT80* during mitosis with the idea that this may promote the expression of a hypothetical meiosis I-specific activator of Clb1-CDK activity. However, we did not observe a significant increase in Clb1-CDK activity under these conditions (Figure 17). It is possible that this hypothetical Clb1-CDK activator is not dependent on *NDT80* for expression or that Ndt80 is not fully functional when ectopically expressed, resulting in a subset of Ndt80 targets being absent. It is also possible that the expression of a hypothetical activator of Clb1-CDK is dependent on the function of a different transcription factor. Alternatively, the observed difference in Clb1-CDK activity may result from the activity of a meiosis II and mitosis specific inhibitor. If this is the case, a screen of the yeast deletion collection for suppressors of the lethality caused by expressing a non-degradable version of Clb1 (Clb1-dbΔ) during vegetative growth may result in the identification of such a factor. Determining whether Clb1-CDK is regulated by an activator of activity in meiosis I or an inhibitor in meiosis II and mitosis will be an important future research goal. A potentially simple way to distinguish between these possibilities will be to perform a rough biochemical experiment where extracts of meiosis I cells are mixed with Clb1 purified from mitotic extracts as well as the converse, mitotic extracts mixed with Clb1 purified from meiosis I extracts, to examine whether Clb1-CDK activity is modulated. Finally, it should be examined whether the CDK regulatory subunit and adaptor protein, Cks1, plays a

role in the differential regulation of Clb1-CDK activity during meiosis. This factor was not examined in our analyses. Regardless, determining how Clb1-CDK activity is regulated during mitosis and meiosis may yield new insight into how the cell cycle machinery is modulated to bring about the specialized meiotic cell division and will potentially elucidate novel mechanisms of cyclin-CDK regulation.

ACKNOWLEDGEMENTS

We are grateful to the lab of Karl Mechtler (Research Institute of Molecular Pathology (IMP, Austria) for protein identification using mass spectrometry, to Ioannis Papayannopoulos (Koch Institute Proteomic Facility) for help designing co-purification strategy and for protein identification using mass spectrometry and to Thomas Takara (Bell Lab – MIT) for help designing co-purification strategy and cell lysis optimization (freezer mill).

MATERIAL AND METHODS

Strains and plasmids

Strains used in this chapter are described in Table 1 and are derivatives of SK1 (all meiosis experiments) or W303. *GAL-NDT80* and *GAL4.ER* constructs are described in (Benjamin et al., 2003). Strains were constructed by PCR-based methods described in (Longtine et al., 1998). 3V5 tagging plasmids were provided by Vincent Guacci. Clb1(S302A)-9myc, Clb2(1-179)-Clb1(156-471)-3V5 and Clb1(1-155)-Clb2(180-491)-3V5 were contructed at the *CLB1* locus using the *K. lactis URA3* pop-in/pop-out system where *K. lactis URA3* was inserted at the desired site within the *CLB1* ORF and was subsequently popped-out using either annealed primers containing the S302A mutation or the desired homology to *CLB2*.

Sporulation conditions

Strains were grown to saturation in YPD at room temperature, diluted in BYTA (1% yeast extract, 2% tryptone, 1% potassium acetate, 50mM potassium phthalate) to OD_{600} = 0.25, and grown overnight at 30°C. Cells were resuspended in sporulation medium (0.3% potassium acetate [pH 7], 0.02% raffinose) to OD_{600} = 1.85 and sporulated at 30°C unless otherwise indicated. *GAL-NDT80 GAL4.ER* strains were released from the *NDT80* block by the

addition of 1 μM β-estradiol (5 mM stock in ethanol, Sigma E2758-1G) at 6hr unless otherwise indicated.

Indirect immunofluorescence

Indirect immunofluorescence was performed as described in (Kilmartin & Adams, 1984). Spindle morphologies were classified as follows: Metaphase I or Metaphase I-like spindles were defined as a short, bipolar spindle spanning a single DAPI mass. Anaphase I spindles were defined as an elongated spindle spanning two distinct DAPI masses. Metaphase II spindles were defined as two short, bipolar spindles, each spanning a DAPI mass. Anaphase II spindles were defined as two elongated spindles, each spanning two distinct DAPI masses (four DAPI masses total).

***In vitro* kinase assay**

In vitro kinase assays were performed as described in (Carlile & Amon, 2008) with the following modifications: 0.5-1mg of total protein was incubated with 40μl of 50% slurry anti-V5 agarose affinity gel (Sigma) for 2h at 4°C. Amount of immunoprecipitated protein from kinase reaction was determined by Western blot for either Clb1-3V5 and/or Cdc28-3V5.

Western blot analysis

For immunoblot analysis, ~10 OD_{600} units of cells were harvested and treated with 5% trichloroacetic acid for at least 10min at 4°C. The acid was washed away with acetone and the cell pellet was subsequently dried. The cell pellet was pulverized with glass beads in 100µL of lysis buffer (50mM Tris-Cl at pH 7.5, 1mM EDTA, 2.75mM DTT, complete protease inhibitor cocktail [Roche]) using a bead-beater (Biospec Products, Inc. Bartlesville, OK). 3X SDS Sample buffer was added and the cell homogenates were boiled. Standard procedures for sodium dodecyl sulfate-polyacrylamide gel electrophoresis (SDS-PAGE) and Western blotting were followed (Burnette, 1981; Laemmli, 1970; Towbin, Staehelin, & Gordon, 1979). A nitrocellulose membrane (VWR) was used to transfer proteins from polyacrylamide gels. Antibody dilutions are described in the Antibody section.

Antibodies

Indirect immunofluorescence

Spindle morphology was determined using a rat anti-tubulin antibody (Oxford Biotechnology) used at a dilution of 1:100, and anti-rat FITC antibodies (Jackson) used at a dilution of 1:100-200.

Western blotting

Clb1-9myc and Sic1-9myc were detected using a mouse anti-Myc antibody (Covance) at a 1:500 dilution. Clb1-3V5 and Cdc28-3V5 were detected using a

mouse anti-V5 antibody (Invitrogen) at a 1:2000 dilution. Pgk1 was detected using a mouse anti-Pgk1 antibody (Molecular Probes) at a 1:10000 dilution. Kar2 was detected using a rabbit anti-Kar2 antibody (kindly provided by Mark Rose) at a 1:200,000 dilution. Rabbit anti-Clb2 was used at a concentration of 1:2000 (kindly provided by Fred Cross). Cdc28-phosphoY19 was detected using a rabbit anti-phospho-cdc2 (Tyr15) antibody [Cdc2 is the mouse orthologue of Cdc28] (Cell Signaling Technology) at a 1:1000 dilution using TBST for all antibody dilutions and washes. The secondary antibodies used were a sheep anti-mouse antibody conjugated to horseradish peroxidase (HRP) (GE Biosciences) at a 1:5000 dilution or a donkey anti-rabbit antibody conjugated to HRP (GE Biosciences) at a 1:5000 dilution. Antibodies were detected using the SuperSignal West Pico Chemiluminescent Substrate (Thermo Scientific).

Immunoprecipitation

Clb1-3V5 was immunoprecipitated with 40µl of 50% slurry anti-V5 agarose affinity gel (Sigma). Clb2 was immunoprecipitated with 1µl of rabbit anti-Clb2. Immunoprecipitation of Clb1-9myc and Clb1-TEV-ProA are described in Denaturing Immunoprecipitation and Native Immunoprecipitation – Mass Spectrometry sections respectively.

Denaturing Immunoprecipitation and phosphatase treatment

40 OD_{600} units of Clb1-9myc cells harvested and treated with 5% TCA, washed with acetone and dried. Pellet resuspended in 180µl breakage buffer (50mM Tris-

HCl pH7.5, 1mM EDTA, 1X protease inhibitor (Roche), 15 mM pNPP, 60mM beta-glyercol phosphate, 50 mM DTT, 0.1mM Na-orthovanadate) and ~100µl glass beads. After lysis using bead mill, SDS added to 1% final concentration and sample boiled 5min. Then, 9 volumes NP40 buffer + 2 mg/ml BSA added and mixed by vortexing. Spin down twice at 13K for 10 min at 4°C with transfer of supernatant to new tubes after each spin. Primary antibody added to extracts (1:50 mouse anti-myc 9E10). Incubated at 4°C for 2 hours with rotation. Protein G sepharose (40µl) added and incubated at 4°C with rotation for 2 hours. Washed with 1 ml in the following order: 2x NP40 buffer, 1x NP40 buffer + 1% BME, 2x NP40 buffer + 1% BME + 2M Urea, 2x 10mM Tris-HCl pH7.5. For phosphatase treatment: residual liquid removed and beads resuspend in: 34µl of 50mM Tris pH 7.5, 4µl of NEB buffer 3, 2µl Alkaline Phosphatase (or mock treatment = 50% glyercol). Incubated at 37°C for 30min (flick tubes to mix every 10 minutes). After incubation, 3x SDS sample buffer added to 1x, samples boiled and run on SDS-PAGE gel.

Co-Immunoprecipitation followed by Mass Spectrometry

Modified from protocol in (Archambault et al., 2004). Cell harvested by centrifugation (4 L of OD 1.9) and washed 2x with cold cell wash buffer (20 mM K-HEPES [pH 7.4], 1.2% PVP-40 (Sigma), 0.2 mg/mL PMSF, 4 µg/ml pepstatin A) and 1x with cold cell extraction buffer (25 mM Na-HEPES [pH 7.4], 150 mM Na-acetate, 10% glycerol, 0.1% Tween-20, 1 mM DTT, 4 µg/ml Pepstatin A, 0.2

mg/ml PMSF). Cell pellet weighed and resuspended in ¼ volume cell extraction buffer (plus 20 µg/ml DNaseI and 5x protease inhibitor cocktail (Roche) e.g. 2.5 ml for 10 g pellet). Pellet resuspended with 5 ml pipette and "dipping dots" made by pipetting ~50-100µl drops of cell slurry into liquid nitrogen using P1000 and cut P1000 tip (small plastic beaker submergeed in liquid nitrogen containing dewer to catch dots). Dots stored in 50ml falcon tube at -80°C. Cells lysed using freezer mill. Cell powder thawed for 1 hr on ice in centrifugation tube. Lysate clarified at 24,000 rpm for 1hr at 4°C. Supernatant removed using P1000 leaving upper lipid layer and lower hard and "soft" pellet. Protein concentration determined using Bradford assay (~50mg/ml). Immunoprecipitation performed in 15 ml conical tube for 3.5h with 200µl streptavidin-dynabeads prebound to biotinylated rabbit IgG [Dynabeads M-280 Streptavadin (Invitrogen), Rabbit anti-goat IgG Biotinylated (Bethyl)]. Wash 5x with extraction buffer (with protease inhibitors) then 3x with TEV cleavage buffer (10 mM Tris-HCl pH 8.0, 150 mM NaCl, 0.1% Tween20, 0.5 mM EDTA, 1 mM DTT). TEV elution in 100µl of TEV cleavage buffer with 1µl AcTEV protease (Invitrogen) for 2 hr at 22°C in thermomixer. Eluate split into 2x 50µl and snap frozen in liquid nitrogen. Frozen eluate then lyophilized in speedvac for 25 min with both heat (50°C) and vacuum. Lyophilized eluate resuspended in 15 µl 1x LDS buffer (Invitrogen), boiled for 5 min and run on NuPAGE Novex 4-12% Bis-Tris Gel (Invitrogen). Gel was silver stained and the entire lane of the gel was cut into ~10 pieces based on molecular weight. The proteins that co-purified were then identified by mass spectrometry.

STRAINS USED

Table 1. Strains used in this chapter.

strain	Relevant Genotype
W303	*MATa, ade2-1, leu2-3, ura3, trp1-1, his3-11,15, can1-100, GAL, psi+*
A343	*MATa, cdc13-1, leu2-3, ura3, trp1-1, his3?, omns, (K2034), cdc13, 3 times backcrossed to K699/700*
A386	*MATa,CDC28-F19::TRP1 at the CDC28 locus, thus ura3, cdc13-1*
SK1 (haploid)	*MATa ho::LYS2 lys2 ura3 leu2::hisG his3::hisG trp1::hisG*
A15514	*MATa GAL-NDT80::TRP1 ura3::pGPD1-GAL4(848).ER::URA3 CLB1-9Myc::TRP1*
A23469	*MATa GAL-NDT80::TRP1 ura3::pGPD1-GAL4(848).ER::URA3 His3MX6:pGAL-Clb1-3V5:KanMX*
A23790	*MATa Clb1-TEV-ProA:KanMX6*
A25645	*MATa ura3::pGPD1-GAL4(848).ER::URA3 His3MX6:pGAL-Clb1-3V5:KanMX*
SK1 (diploid)	*MATa/MATalpha ho::LYS2/ho::LYS2 lys2/lys2 ura3/ura3 leu2::hisG/leu2::hisG his3::hisG/his3::hisG trp1::hisG/trp1::hisG*
A6138	*MATa/alpha cdc20::pCLB2-CDC20::KanMX6/cdc20::pCLB2-CDC20::KanMX6*

A14201	*MATa/alpha GAL-NDT80::TRP1/GAL-NDT80::TRP1 ura3::pGPD1-GAL4(848).ER::URA3/ura3::pGPD1-GAL4(848).ER::URA3*
A15591	*MATa/alpha GAL-NDT80::TRP1/GAL-NDT80::TRP1 ura3::pGPD1-GAL4(848).ER::URA3/ura3::pGPD1-GAL4(848).ER::URA3 CLB1-9Myc::TRP1*
A16480	*MATa/alpha GAL-NDT80::TRP1/GAL-NDT80::TRP1 ura3::pGPD1-GAL4(848).ER::URA3/ura3::pGPD1-GAL4(848).ER::URA3 CDC28A18F19::URA3/CDC28A18F19::URA3 CLB1-9Myc::TRP1*
A21711	*MATa/alpha cdc20::pCLB2-CDC20::KanMX6/cdc20::pCLB2-CDC20::KanMX6 cdc28-as1 (F88G)/cdc28-as1 (F88G) CLB1-9Myc::TRP1*
A21817	*MATa/alpha cdc20::pCLB2-CDC20::KanMX6/cdc20::pCLB2-CDC20::KanMX6 CLB1-9Myc::TRP1*
A22457	*MATa/alpha cdc20::pCLB2-CDC20::KanMX6/cdc20::pCLB2-CDC20::KanMX6 Clb1(S302A)-9Myc:TRP1*
A22458	*MATa/alpha GAL-NDT80::TRP1/GAL-NDT80::TRP1 ura3::pGPD1-GAL4(848).ER::URA3/ura3::pGPD1-GAL4(848).ER::URA3 Clb1(S302A)-9Myc:TRP1*
A22672	*MATa/alpha GAL-NDT80::TRP1/GAL-NDT80::TRP1 ura3::pGPD1-GAL4(848).ER::URA3/ura3::pGPD1-GAL4(848).ER::URA3 Clb1-3V5:KanMX/Clb1-3V5:KanMX*
A22992	*MATa/alpha GAL-NDT80::TRP1/GAL-NDT80::TRP1 ura3::pGPD1-GAL4(848).ER::URA3/ura3::pGPD1-GAL4(848).ER::URA3 CLB2::GAL-CLB2::TRP1 (2 copies) Clb1-3V5:KanMX*
A23235	*MATa/alpha GAL-NDT80::TRP1/GAL-NDT80::TRP1 ura3::pGPD1-GAL4(848).ER::URA3/ura3::pGPD1-GAL4(848).ER::URA3 Clb1-3V5:KanMX/Clb1-3V5:KanMX swe1D::KanMX6/swe1D::KanMX6*
A23650	*MATa/alpha GAL-NDT80::TRP1/GAL-NDT80::TRP1 ura3::pGPD1-GAL4(848).ER::URA3/ura3::pGPD1-GAL4(848).ER::URA3 His3MX6:pGAL-Clb1-3V5:KanMX/His3MX6:pGAL-Clb1-3V5:KanMX*

A23785	*MATa/alpha cdc20::pCLB2-CDC20::KanMX6/cdc20::pCLB2-CDC20::KanMX6 cdc5::pCLB2-CDC5::KanMX6/cdc5::pCLB2-CDC5::KanMX6 CLB1-9Myc::TRP1*
A23893	*MATa/alpha GAL-NDT80::TRP1/GAL-NDT80::TRP1 ura3::pGPD1-GAL4(848).ER::URA3/ura3::pGPD1-GAL4(848).ER::URA3 Clb1-TEV-ProA:KanMX6/Clb1-TEV-ProA:KanMX6*
A23924	*MATa/alpha GAL-NDT80::TRP1/GAL-NDT80::TRP1 ura3::pGPD1-GAL4(848).ER::URA3/ura3::pGPD1-GAL4(848).ER::URA3 Clb2(1-179)-Clb1(156-471)-3V5:KanMX/Clb2(1-179)-Clb1(156-471)-3V5:KanMX*
A24207	*MATa/alpha cdc20::pCLB2-CDC20::KanMX6/cdc20::pCLB2-CDC20::KanMX6 Clb1-3V5:KanMX/Clb1-3V5:KanMX*
A24208	*MATa/alpha cdc20::pCLB2-CDC20::KanMX6/cdc20::pCLB2-CDC20::KanMX6 cdc5::pCLB2-CDC5::KanMX6/cdc5::pCLB2-CDC5::KanMX6 Clb1-3V5:KanMX/Clb1-3V5:KanMX*
A24320	*MATa/alpha GAL-NDT80::TRP1/GAL-NDT80::TRP1 ura3::pGPD1-GAL4(848).ER::URA3/ura3::pGPD1-GAL4(848).ER::URA3 Clb1(1-155)-Clb2(180-491)-3V5:KanMX/Clb1(1-155)-Clb2(180-491)-3V5:KanMX*
A24759	*MATa/alpha GAL-NDT80::TRP1/GAL-NDT80::TRP1 ura3::pGPD1-GAL4(848).ER::URA3/ura3::pGPD1-GAL4(848).ER::URA3 SIC1-9Myc:TRP1*
A24900	*MATa/alpha GAL-NDT80::TRP1/GAL-NDT80::TRP1 ura3::pGPD1-GAL4(848).ER::URA3/ura3::pGPD1-GAL4(848).ER::URA3 CDC28-3HA::KanMX6 Clb1-3V5:KanMX*
A25402	*MATa/alpha GAL-NDT80::TRP1/GAL-NDT80::TRP1 ura3::pGPD1-GAL4(848).ER::URA3/ura3::pGPD1-GAL4(848).ER::URA3 Clb1-3V5:KanMX/Clb1-3V5:KanMX yfr016cD::HisMX6/yfr016cD::HisMX6*
A25404	*MATa/alpha GAL-NDT80::TRP1/GAL-NDT80::TRP1 ura3::pGPD1-GAL4(848).ER::URA3/ura3::pGPD1-GAL4(848).ER::URA3 Clb1-3V5:KanMX/Clb1-3V5:KanMX spa2D::HisMX6/spa2D::HisMX6*
A25408	*MATa/alpha GAL-NDT80::TRP1/GAL-NDT80::TRP1 ura3::pGPD1-GAL4(848).ER::URA3/ura3::pGPD1-GAL4(848).ER::URA3 Clb1-3V5:KanMX/Clb1-3V5:KanMX acm1D::KanMX6/acm1D::KanMX6*

A25470	*MATa/alpha GAL-NDT80::TRP1/GAL-NDT80::TRP1 ura3::pGPD1-GAL4(848).ER::URA3/ura3::pGPD1-GAL4(848).ER::URA3 Clb1-3V5:KanMX/Clb1-3V5:KanMX cdh1::KanMX6/cdh1::KanMX6*
A25508	*MATa/alpha GAL-NDT80::TRP1/GAL-NDT80::TRP1 ura3::pGPD1-GAL4(848).ER::URA3/ura3::pGPD1-GAL4(848).ER::URA3 Cdc28-3V5::KanMX*
A26075	*MATa/alpha GAL-NDT80::TRP1/GAL-NDT80::TRP1 ura3::pGPD1-GAL4(848).ER::URA3/ura3::pGPD1-GAL4(848).ER::URA3 His3MX6:pGAL-Clb1-3V5:KanMX/His3MX6:pGAL-Clb1-3V5:KanMX swe1D::KanMX6/swe1D::KanMX6*
A26076	*MATa/alpha GAL-NDT80::TRP1/GAL-NDT80::TRP1 ura3::pGPD1-GAL4(848).ER::URA3/ura3::pGPD1-GAL4(848).ER::URA3 His3MX6:pGAL-Clb1-3V5:KanMX/His3MX6:pGAL-Clb1-3V5:KanMX spa2D::HisMX6/spa2D::HisMX6*
A26077	*MATa/alpha GAL-NDT80::TRP1/GAL-NDT80::TRP1 ura3::pGPD1-GAL4(848).ER::URA3/ura3::pGPD1-GAL4(848).ER::URA3 His3MX6:pGAL-Clb1-3V5:KanMX/His3MX6:pGAL-Clb1-3V5:KanMX bbc1::KanMX/bbc1::KanMX*
A26079	*MATa/alpha GAL-NDT80::TRP1/GAL-NDT80::TRP1 ura3::pGPD1-GAL4(848).ER::URA3/ura3::pGPD1-GAL4(848).ER::URA3 His3MX6:pGAL-Clb1-3V5:KanMX/His3MX6:pGAL-Clb1-3V5:KanMX kel2D::His3Mx6/kel2D::His3Mx6*
A26080	*MATa/alpha GAL-NDT80::TRP1/GAL-NDT80::TRP1 ura3::pGPD1-GAL4(848).ER::URA3/ura3::pGPD1-GAL4(848).ER::URA3 His3MX6:pGAL-Clb1-3V5:KanMX/His3MX6:pGAL-Clb1-3V5:KanMX pea2D::His3Mx6/pea2D::His3Mx6*
A26081	*MATa/alpha GAL-NDT80::TRP1/GAL-NDT80::TRP1 ura3::pGPD1-GAL4(848).ER::URA3/ura3::pGPD1-GAL4(848).ER::URA3 His3MX6:pGAL-Clb1-3V5:KanMX/His3MX6:pGAL-Clb1-3V5:KanMX bud6D::His3Mx6/bud6D::His3Mx6*
A26118	*MATa/alpha GAL-NDT80::TRP1/GAL-NDT80::TRP1 ura3::pGPD1-GAL4(848).ER::URA3/ura3::pGPD1-GAL4(848).ER::URA3 His3MX6:pGAL-Clb1-3V5:KanMX/His3MX6:pGAL-Clb1-3V5:KanMX kel1D::His3Mx6/kel1D::His3Mx6*

A26176	*MATa/alpha cdc20::pCLB2-CDC20::KanMX6/cdc20::pCLB2-CDC20::KanMX6 cdc5-as1 (cdc5L158G)/cdc5-as1 (cdc5L158G) Clb1-3V5:KanMX/Clb1-3V5:KanMX*

REFERENCES

Acosta, I., Ontoso, D., & San-Segundo, P.A. (2011). The budding yeast polo-like kinase Cdc5 regulates the Ndt80 branch of the meiotic recombination checkpoint pathway. *Mol Biol Cell, 22*(18), 3478-3490. doi: mbc.E11-06-0482 [pii]10.1091/mbc.E11-06-0482

Archambault, V., Chang, E.J., Drapkin, B.J., Cross, F.R., Chait, B.T., & Rout, M.P. (2004). Targeted proteomic study of the cyclin-Cdk module. *Mol Cell, 14*(6), 699-711. doi: 10.1016/j.molcel.2004.05.025S1097276504003272 [pii]

Benjamin, K.R., Zhang, C., Shokat, K.M., & Herskowitz, I. (2003). Control of landmark events in meiosis by the CDK Cdc28 and the meiosis-specific kinase Ime2. *Genes & development, 17*(12), 1524-1539. doi: 10.1101/gad.1101503

Bloom, J., & Cross, F.R. (2007). Multiple levels of cyclin specificity in cell-cycle control. *Nature reviews. Molecular cell biology, 8*(2), 149-160. doi: 10.1038/nrm2105

Burnette, W.N. (1981). "Western blotting": electrophoretic transfer of proteins from sodium dodecyl sulfate--polyacrylamide gels to unmodified nitrocellulose and radiographic detection with antibody and radioiodinated protein A. *Analytical biochemistry, 112*(2), 195-203.

Carlile, T.M., & Amon, A. (2008). Meiosis I is established through division-specific translational control of a cyclin. *Cell, 133*(2), 280-291. doi: S0092-8674(08)00283-3 [pii]10.1016/j.cell.2008.02.032

Clyne, R.K., Katis, V.L., Jessop, L., Benjamin, K.R., Herskowitz, I., Lichten, M. (2003). Polo-like kinase Cdc5 promotes chiasmata formation and cosegregation of sister centromeres at meiosis I. *Nature cell biology, 5*(5), 480-485. doi: 10.1038/ncb977

Dahmann, C., & Futcher, B. (1995). Specialization of B-type cyclins for mitosis or meiosis in S. cerevisiae. *Genetics, 140*(3), 957-963.

Dirick, L., Goetsch, L., Ammerer, G., & Byers, B. (1998). Regulation of meiotic S phase by Ime2 and a Clb5,6-associated kinase in Saccharomyces cerevisiae. *Science, 281*(5384), 1854-1857.

Fitch, I., Dahmann, C., Surana, U., Amon, A., Nasmyth, K., Goetsch, L. (1992). Characterization of four B-type cyclin genes of the budding yeast Saccharomyces cerevisiae. *Molecular biology of the cell, 3*(7), 805-818.

Furuno, N., Nishizawa, M., Okazaki, K., Tanaka, H., Iwashita, J., Nakajo, N. (1994). Suppression of DNA replication via Mos function during meiotic divisions in Xenopus oocytes. *EMBO J, 13*(10), 2399-2410.

Grandin, N., & Reed, S.I. (1993). Differential function and expression of Saccharomyces cerevisiae B-type cyclins in mitosis and meiosis. *Molecular and cellular biology, 13*(4), 2113-2125.

Hall, M.C., Jeong, D.E., Henderson, J.T., Choi, E., Bremmer, S.C., Iliuk, A.B. (2008). Cdc28 and Cdc14 control stability of the anaphase-promoting complex inhibitor Acm1. *J Biol Chem, 283*(16), 10396-10407. doi: M710011200 [pii]10.1074/jbc.M710011200

Henderson, K.A., Kee, K., Maleki, S., Santini, P.A., & Keeney, S. (2006). Cyclin-dependent kinase directly regulates initiation of meiotic recombination. *Cell, 125*(7), 1321-1332. doi: 10.1016/j.cell.2006.04.039

Holt, L.J., Hutti, J.E., Cantley, L.C., & Morgan, D.O. (2007). Evolution of Ime2 phosphorylation sites on Cdk1 substrates provides a mechanism to limit the effects of the phosphatase Cdc14 in meiosis. *Mol Cell, 25*(5), 689-702. doi: S1097-2765(07)00112-8 [pii]10.1016/j.molcel.2007.02.012

Iwabuchi, M., Ohsumi, K., Yamamoto, T.M., Sawada, W., & Kishimoto, T. (2000). Residual Cdc2 activity remaining at meiosis I exit is essential for meiotic M-M transition in Xenopus oocyte extracts. *EMBO J, 19*(17), 4513-4523. doi: 10.1093/emboj/19.17.4513

Izawa, D., Goto, M., Yamashita, A., Yamano, H., & Yamamoto, M. (2005). Fission yeast Mes1p ensures the onset of meiosis II by blocking degradation of cyclin Cdc13p. *Nature, 434*(7032), 529-533. doi: nature03406 [pii]10.1038/nature03406

Keaton, M.A., Bardes, E.S., Marquitz, A.R., Freel, C.D., Zyla, T.R., Rudolph, J. (2007). Differential susceptibility of yeast S and M phase CDK complexes to inhibitory tyrosine phosphorylation. *Curr Biol, 17*(14), 1181-1189. doi: S0960-9822(07)01509-6 [pii]10.1016/j.cub.2007.05.075

Kilmartin, J.V., & Adams, A.E. (1984). Structural rearrangements of tubulin and actin during the cell cycle of the yeast Saccharomyces. *The Journal of cell biology, 98*(3), 922-933.

Kimata, Y., Trickey, M., Izawa, D., Gannon, J., Yamamoto, M., & Yamano, H. (2008). A mutual inhibition between APC/C and its substrate Mes1 required for meiotic progression in fission yeast. *Dev Cell, 14*(3), 446-454. doi: S1534-5807(07)00487-X [pii]10.1016/j.devcel.2007.12.010

Laemmli, U.K. (1970). Cleavage of structural proteins during the assembly of the head of bacteriophage T4. *Nature, 227*(5259), 680-685.

Lee, B., & Amon, A. (2001). Meiosis: how to create a specialized cell cycle. *Curr Opin Cell Biol, 13*(6), 770-777. doi: S0955-0674(00)00282-9 [pii]

Longtine, M.S., McKenzie, A., 3rd, Demarini, D.J., Shah, N.G., Wach, A., Brachat, A. (1998). Additional modules for versatile and economical PCR-based gene deletion and modification in Saccharomyces cerevisiae. *Yeast, 14*(10), 953-961. doi: 10.1002/(SICI)1097-0061(199807)14:10<953::AID-YEA293>3.0.CO;2-U

Marston, A.L., & Amon, A. (2004). Meiosis: cell-cycle controls shuffle and deal. *Nature reviews. Molecular cell biology, 5*(12), 983-997. doi: 10.1038/nrm1526

Marston, A.L., Lee, B.H., & Amon, A. (2003). The Cdc14 phosphatase and the FEAR network control meiotic spindle disassembly and chromosome segregation. *Dev Cell, 4*(5), 711-726. doi: S1534580703001308 [pii]

Mendenhall, M.D., & Hodge, A.E. (1998). Regulation of Cdc28 cyclin-dependent protein kinase activity during the cell cycle of the yeast Saccharomyces cerevisiae. *Microbiology and molecular biology reviews : MMBR, 62*(4), 1191-1243.

Ostapenko, D., Burton, J.L., Wang, R., & Solomon, M.J. (2008). Pseudosubstrate inhibition of the anaphase-promoting complex by Acm1: regulation by proteolysis and Cdc28 phosphorylation. *Mol Cell Biol, 28*(15), 4653-4664. doi: MCB.00055-08 [pii]10.1128/MCB.00055-08

Park, H.O., & Bi, E. (2007). Central roles of small GTPases in the development of cell polarity in yeast and beyond. *Microbiol Mol Biol Rev, 71*(1), 48-96. doi: 71/1/48 [pii]10.1128/MMBR.00028-06

Peters, J.M. (2006). The anaphase promoting complex/cyclosome: a machine designed to destroy. *Nat Rev Mol Cell Biol, 7*(9), 644-656. doi: nrm1988 [pii]10.1038/nrm1988

Roeder, G.S., & Bailis, J.M. (2000). The pachytene checkpoint. *Trends Genet, 16*(9), 395-403. doi: S0168-9525(00)02080-1 [pii]

Schindler, K., & Winter, E. (2006). Phosphorylation of Ime2 regulates meiotic progression in Saccharomyces cerevisiae. *J Biol Chem, 281*(27), 18307-18316. doi: M602349200 [pii]10.1074/jbc.M602349200

Shuster, E.O., & Byers, B. (1989). Pachytene arrest and other meiotic effects of the start mutations in Saccharomyces cerevisiae. *Genetics, 123*(1), 29-43.

Stuart, D., & Wittenberg, C. (1998). CLB5 and CLB6 are required for premeiotic DNA replication and activation of the meiotic S/M checkpoint. *Genes & development, 12*(17), 2698-2710.

Towbin, H., Staehelin, T., & Gordon, J. (1979). Electrophoretic transfer of proteins from polyacrylamide gels to nitrocellulose sheets: procedure and some applications. *Proceedings of the National Academy of Sciences of the United States of America, 76*(9), 4350-4354.

Ubersax, J.A., Woodbury, E.L., Quang, P.N., Paraz, M., Blethrow, J.D., Shah, K. (2003). Targets of the cyclin-dependent kinase Cdk1. *Nature, 425*(6960), 859-864. doi: 10.1038/nature02062nature02062 [pii]

Unal, E., Kinde, B., & Amon, A. (2011). Gametogenesis eliminates age-induced cellular damage and resets life span in yeast. *Science, 332*(6037), 1554-1557. doi: 332/6037/1554 [pii]10.1126/science.1204349

Chapter 4:

Discussion and Future Directions

KEY CONCLUSIONS

Proper segregation of the genome during gametogenesis is critical for the proliferation of sexually reproducing species. The major engine of cellular division is the activity of cyclin-dependent kinases (CDKs). Proper regulation of CDKs is required to achieve the correct timing of events during cell division and to achieve accurate chromosome segregation during this process (Carlile & Amon, 2008). One of the key differences in transforming the mitotic cell division program to properly complete meiosis is the establishment of the specialized meiosis I chromosome segregation pattern. This requires multiple modifications to the cell cycle program and chromosome segregation machinery: (1) homologous chromosomes become linked through recombination to provide the linkages needed for their accurate segregation; (2) kinetochores of sister chromatids become cooriented or attach to microtubules from the same pole; and (3) sister-chromatid cohesion is removed from chromosomes arms thus allowing the segregation of homologs, but is maintained near centromeres to preserve the linkage required for accurate segregation of sister chromatids in meiosis II (reviewed in Marston & Amon, 2004). The work described in this thesis showed that an essential determinant of establishing the meiosis I chromosome segregation pattern is the temporal regulation of microtubule-kinetochore interactions (Chapter 2). Misexpression of a subset of cyclins, including Clb1 and Clb3, during premeiotic S phase and early prophase I causes premature microtubule-kinetochore interactions. These interactions disrupt both sister

kinetochore coorientation and protection of centromeric cohesin during meiosis I, resulting in a mitosis-like division. Thus, restricting microtubule-kinetochore interactions prior to meiosis I is a key determinant in establishing the meiosis I chromosome segregation pattern. This work also examined the mechanism by which Clb1-CDK activity is restricted to meiosis I (Chapter 3). A number of putative meiosis II Clb1-CDK binding partners were identified, however, each of the factors identified appear dispensable for the observed regulation suggesting they do not function in the regulation of Clb1-CDK during meiosis. The potential implications of this work, open questions and future directions are discussed below.

How do premature microtubule-kinetochore interactions disrupt meiosis I chromosome morphogenesis?

We found that misexpression of the cyclins, Clb1 and Clb3, prior to meiosis I transforms meiosis I into a mitosis-like division. We examined the consequences of premature *CLB3* expression in more detail. *CLB3* misexpression leads to premature microtubule-kinetochore interactions, prevents coorientation factors from associating with kinetochores and results in defects in the maintenance of centromeric cohesin at anaphase I onset. The observation that the transient disruption of microtubule-kinetochore interactions, either by inactivating the outer kinetochore or by microtubule depolymerization, allowed both coorientation factors to associate with kinetochores and the protection of centromeric cohesin, despite *CLB3* misexpression, led us to conclude that it is

the premature microtubule-kinetochore interactions that interfere with proper meiosis I chromosome segregation in cells prematurely expressing *CLB3*. Meiosis I chromosome morphogenesis, including the assembly of cohesin protective structures around centromeres and sister kinetochore coorientation, occurs during prophase I. We propose that when microtubules interact with kinetochores prior to completion of this remodeling process, they establish a default attachment, biorientation, which is incompatible with sister kinetochore coorientation and establishing a cohesin protective domain around centromeres (Figure 1). It is currently unclear how these premature microtubule-kinetochore interactions disrupt the proper chromosome architecture required for the meiosis I chromosome segregation pattern, however, some possibilities and further experiments are discussed below.

One key question is the nature of the microtubule-kinetochore attachments that result in chromosome morphogenesis defects. One possibility is that it is simply the attachment of microtubules to kinetochores that sterically blocks or occludes the binding of factors required to establish the meiosis I chromosome architecture. This seems plausible for the association of coorientation factors with kinetochores (discussed below). Another possibility is that defects arise due to the pulling forces exerted by stable microtubule-kinetochore interactions, and it is the tension between sister kinetochores that lead to the observed defects. The pulling forces could physically separate sister kinetochores, thus preventing coorientation factors from linking them as well as preventing the cohesin

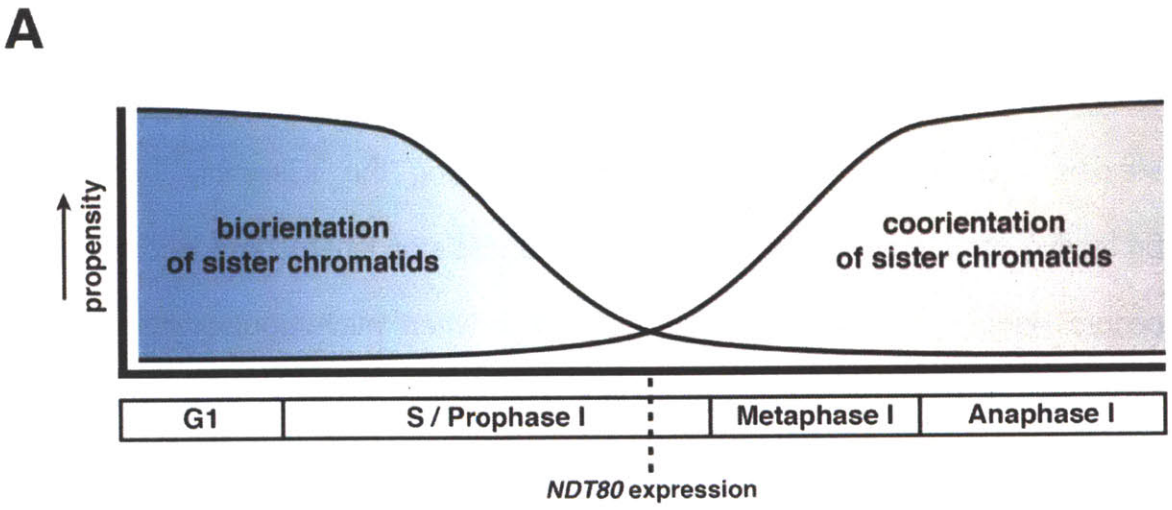
A
propensity
biorientation
of sister chromatids
coorientation
of sister chromatids
G1
S / Prophase I
Metaphase I
Anaphase I
NDT80 expression

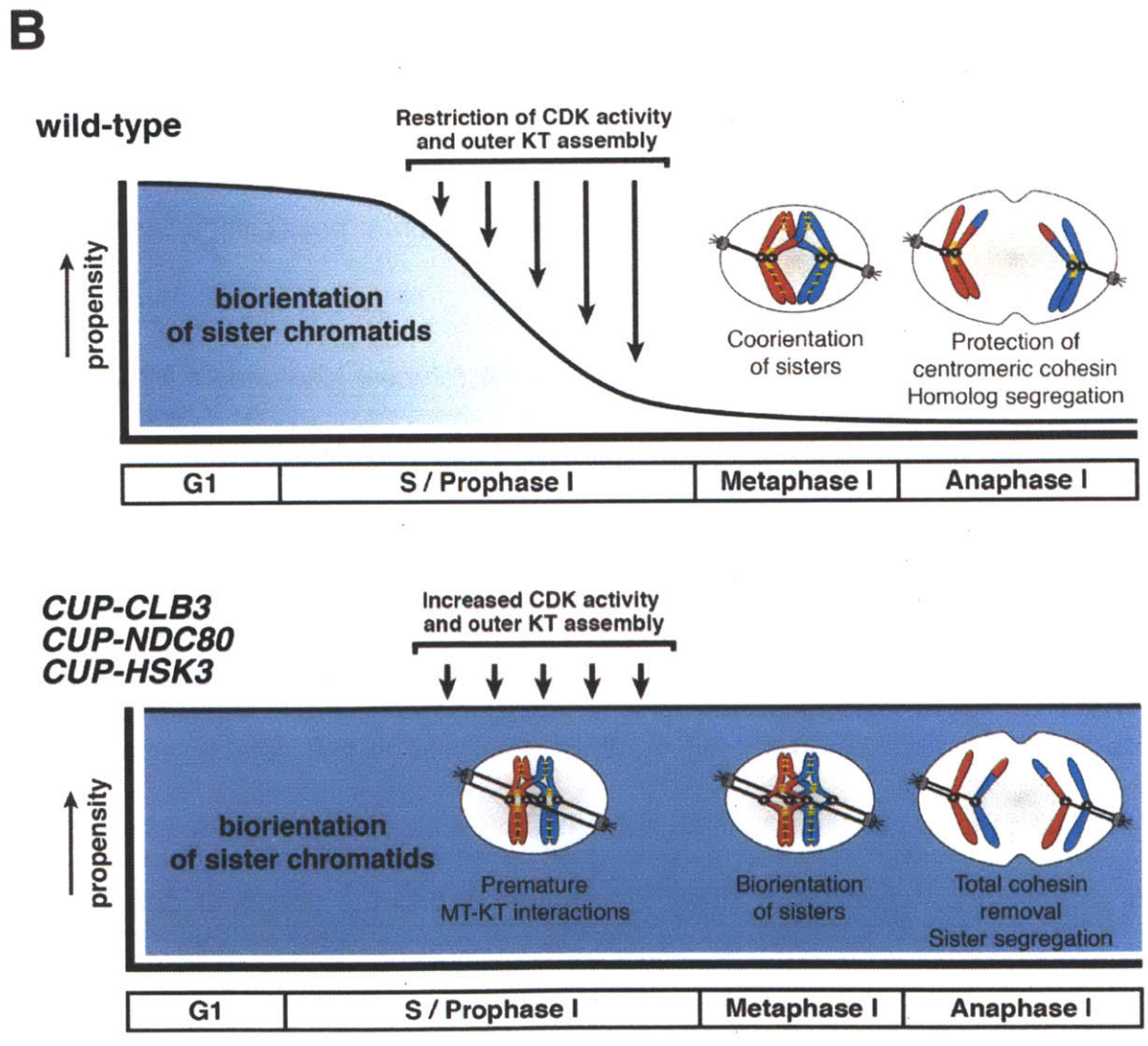
B
wild-type
Restriction of CDK activity
and outer KT assembly
propensity
biorientation
of sister chromatids
Coorientation
of sisters
Protection of
centromeric cohesin
Homolog segregation
G1
S / Prophase I
Metaphase I
Anaphase I
CUP-CLB3
CUP-NDC80
CUP-HSK3
Increased CDK activity
and outer KT assembly
propensity
biorientation
of sister chromatids
Premature
MT-KT interactions
Biorientation
of sisters
Total cohesin
removal
Sister segregation
G1
S / Prophase I
Metaphase I
Anaphase I

Figure 1. Model for temporal regulation of microtubule-kinetochore interactions during meiosis.

(A) As prophase I progresses, the propensity of sister chromatids to biorient decreases and the ability to coorient sister chromatids increases.

(B) Top panel: Inhibiting Clb-CDK activity and outer kinetochore (KT) assembly during prophase I establishes a meiosis I-specific chromosome segregation pattern by allowing sister kinetochore coorientation and protection of centromeric cohesin. Bottom panel: Disrupting the regulation of microtubule-kinetochore (MT-KT) interactions causes sister chromatid segregation in meiosis I.

protective machinery from acting on cohesin around centromeres. Alternatively, tension could alter the structure of the kinetochore and/or pericentromeric chromatin, resulting in defects in coorientation and centromeric cohesin protection (discussed below).

Another possibility is that premature microtubule-kinetochore attachments could provide the means for factors that could inhibit coorientation and centromeric cohesin protection to access the kinetochore (e.g. Clb-CDKs themselves or other factors). Such inhibitory factors may be associated with microtubules and could require their attachment to kinetochores for localization to centromeric and pericentromeric chromatin. This could explain the dependence on microtubule-kinetochore interactions for observed phenotypes. Distinguishing between these possibilities (i.e. occlusion, tension, or access to the kinetochore)

will be crucial to determine the mechanism by which premature microtubule-kinetochore interactions disrupt meiosis I chromosome morphogenesis. The next section will focus on the nature of the microtubule-kinetochores interactions that result in disruption of proper chromosome morphogenesis during meiosis. Then a discussion will follow that examines, in more detail, how these interactions could disrupt both the coorientation and the cohesin protective machinery.

First, it should be determined whether it is simply the attachment of microtubules with kinetochores, or the tension generated from these attachments that results in the defects observed. To address this question, it would be useful to examine meiosis I chromosome morphogenesis under conditions in which there are stable microtubule-kinetochore interactions but these interactions do not result in pulling forces. Unfortunately, the microtubule stabilizing drug taxol, does not stabilize microtubules in yeast (Gupta, Bode, Georg, & Himes, 2003), precluding its use to distinguish between these possibilities. Another possibility would be to use a conditional allele of *STU2,* a microtubule-associated protein of the XMAP215 family, which regulates microtubule dynamics during spindle orientation, and is required to form tension between sister kinetochores (Gillett, Espelin, & Sorger, 2004; Kosco et al., 2001). These experiments may be complicated by the fact that microtubules attachments may be transient under conditions in which Stu2 is inactive, constantly being turned over by the activity of the Aurora B kinase Ipl1. Thus, these attachments, while not forming tension, may not result in stable microtubule-kinetochore interactions, which may

complicate the interpretation of such analyses. Another possibility is to inhibit the activity of a kinetochore component (e.g. Ndc80) in combination with inactivating Ipl1. Inactivation of Ndc80 alone results in activation of the spindle assembly checkpoint and stabilization of Securin (Pds1), presumably due to the inability to form stable microtubule-kinetochore attachments and the constant destabilization of these interactions by Ipl1. Surprisingly, inactivation of Ipl1 in conjunction with Ndc80 silences the spindle assemble checkpoint (Pinsky, Kung, Shokat, & Biggins, 2006). These results suggest that under these conditions, stable microtubule-kinetochore attachments exist in the absence or with greatly reduced tension. One complication with these experiments will be that transient inactivation of Ipl1 may result in chromosome segregation defects, which again, may complicate the interpretation of analyses.

If the attachment of microtubules with kinetochores permits inhibitory factors to access the pericentric chromatin, then targeting such factors to these regions in the absence of microtubules should phenocopy premature microtubule-kinetochore attachments. One possibility for an inhibitory factor would be the centromeric localized activity of Clb-CDKs. First, it should be determined whether the various Clbs localize differentially to the centromeric chromatin under conditions with and without microtubule-kinetochore attachments. This can be accomplished, for example, by determining the chromatin localization of prematurely expressed Clb3, by chromatin immunoprecipitation, in *NDC80* and *ndc80-1* cells at the non-permissive

temperature. Second, ectopically targeting these cyclins to the centromere may result in defects in the absence of microtubule-kinetochore interactions. To this end, fusions between Clb3 and Sgo1 (or another similarly localized protein), which localizes to the pericentromere and is involved in the maintenance of centromeric cohesin, could be examined. These fusions should result in increased Clb-CDK activity at the centromere and could result in defects in coorientation and/or protection of centromeric cohesin. It would be interesting to also target Clb5 (whose misexpression does not result in chromosome morphogenesis defects) to centromeres as well to determine if simply increased cyclin-CDK activity at the centromere is sufficient to disrupt proper meiosis I chromosome morphogenesis. This may also serve as a control to ensure the function of the fusion Sgo1 protein in normal chromosome morphogenesis.

Another tool that may help distinguish between attachment versus tension causing the observed defects is the differences in phenotypes observed between *CLB3* and *CLB4* misexpression. Premature accumulation of both Clb3 or Clb4 results in premature bipolar spindle formation, however only *CLB3* misexpression results in microtubule-kinetochore attachments sufficient to generate tension between sister kinetochores and chromosome morphogenesis defects (Chapter 2). Determining the nature of the microtubule-kinetochore interactions when *CLB4* is misexpressed and mechanistically what is lacking for tension generation may provide another means to distinguish between these possibilities.

Finally, the hypothesis that premature microtubule-kinetochores interactions disrupt proper chromosome morphogenesis that occurs during prophase I, makes the prediction that once this remodeling process has taken place, misexpression of the cyclin, Clb3, and the limiting outer kinetochore component, Ndc80, will not affect meiosis I chromosome segregation. This appears to be the case. Cells that express *CLB3* and *NDC80* at the time of *NDT80* release exhibit a large meiosis I chromosome segregation defect (Chapter 2), however, cells induced to express *CLB3* and *NDC80* starting ~30min after release from an *NDT80* block properly segregate chromosome during meiosis I (Jingxun Chen, personal communication). These results are consistent with the notion that there is a window of sensitivity in which meiosis I chromosome morphogenesis can be disrupted by premature microtubule-kinetochore interactions. However, once this domain is established, its maintenance during meiosis I can no longer be disrupted by tension between sister kinetochores (Figure 1). This hypothesis is consistent with the observation that in cells lacking the coorientation factor *MAM1*, sister kinetochores come under tension in metaphase I, yet centromeric cohesin is not removed prematurely in these cells (Toth et al., 2000 and Chapter 2).

How do premature microtubule-kinetochore interactions disrupt the proper coorientation of sister chromatids?

In budding yeast, coorientation of sister chromatids is mediated by the monopolin complex. This complex binds directly to the kinetochore and is

believed to physically link the kinetochores of sister chromatids, effectively fusing them into a single microtubule-binding site (Corbett et al., 2010; Rabitsch et al., 2003). The monopolin complex, thus, forces sister chromatids to attach to microtubules emanating from the same spindle pole. The globular domains of Csm1 are believed to bind to the kinetochore component Dsn1, thus mediating localization of the complex to kinetochores (Corbett & Harrison, 2012; Chapter 1 - Figure 9). Another key question from our work is how premature microtubule-kinetochore interactions disrupt the localization of this complex. Precocious attachment of microtubules to kinetochores could physically occlude the monopolin complex from binding to kinetochores. Alternatively, tension between sister kinetochores generated from stable microtubule-kinetochore interactions could induce a conformational change at the kinetochore and/or pericentric chromatin such that coorientation factors can no longer associate with the kinetochore. Interestingly, a recent study examined the EM structure of purified yeast kinetochore particles in the presence or absence of taxol-stabilized microtubules (Gonen et al., 2012). This work revealed that the purified kinetochores adopt a different structure when bound to microtubules. It is possible that this structural change prevents the binding of the monopolin complex to the kinetochore. Thus, tension *per se*, may not be required to induce a conformational change of the kinetochore that prevents proper binding of the monopolin complex. It is possible that the kinetochore's altered conformation upon microtubule binding is sufficient to prevent monopolin complex association.

On the other hand, it is possible that the pulling forces exerted by stable microtubule-kinetochore interactions physically separate sister kinetochores preventing their linkage. We and others have shown that the monopolin complex can associate with a single, unpaired kinetochore. Cells that are depleted of the replication factor Cdc6, enter meiosis I without replicated chromosomes (and thus lack paired sister kinetochores), yet the monopolin complex properly localizes to kinetochores in these cells (data not shown and Matos et al., 2008). The physical separation of sister kinetochores, however, may still prevent their coorientation. With these results in mind, it is not clear how the simple physical separation of sister kinetochores would result in the monopolin localization defects that are observed when premature microtubule-kinetochore interactions exist. One way to distinguish between these possibilities would be to utilize the mitotic monopolin expression system described in (Monje-Casas, Prabhu, Lee, Boselli, & Amon, 2007) and in Chapter 2. Mitotic expression of the monopolin complex, by overexpressing *CDC5* and *MAM1*, results in coorientation of sister kinetochores and cosegregation of sister chromatids in mitotic anaphase. We found that preexisting microtubule-kinetochore interactions are sufficient to disrupt the function of the monopolin complex using this system (Chapter 2). Determining the localization of the monopolin complex under these conditions may shed light on the relevance of monopolin mislocalization with respect to coorientation dysfunction.

Another intriguing possibility is that the disassembly of the outer kinetochore that occurs during prophase I, including dissociation of the Ndc80 complex (see section below, Chapter 2 and Asakawa, Hayashi, Haraguchi, & Hiraoka, 2005)), is required to expose a monopolin complex binding site. The fact that both the Ndc80 and monopolin complex interact with the Mis12 complex to mediate kinetochore localization would be consistent with this hypothesis. However, expression of two limiting outer kinetochore components, *NDC80* and *HSK3*, during meiotic prophase I alone does not result in coorientation defects despite premature localization of Ndc80 to kinetochores (Chapter 2). Furthermore, mitotic expression of the monopolin complex in either G1 or metaphase (with depolymerized microtubules), conditions in which the kinetochore is believed to be fully assembled and functional, results in coorientation of sister chromatids. These results suggest that the fully assembled kinetochore is competent for monopolin binding and coorientation. Determining the exact mechanism by which premature microtubule-kinetochore interactions disrupt coorientation of sister kinetochores will be important for our understanding of the requirements needed for proper meiotic chromosome morphogenesis.

How do premature microtubule-kinetochore interactions disrupt centromeric cohesin maintenance?

During meiosis I, cleavage of cohesin distal to sites of crossovers allows homologs to disjoin (Buonomo et al., 2000). Accurate segregation of sister chromatids during meiosis II, however, requires that cohesin around centromeres

be protected from cleavage during meiosis I. Protection of centromeric cohesin is accomplished by preventing phosphorylation of the meiosis-specific kleisin subunit of the cohesin complex, Rec8. This is mediated, at least in part, by Sgo1 (MEI-S332)-dependent recruitment of the protein phosphatase PP2A to centromeric regions where it antagonizes Rec8 phosphorylation (Katis, Galova, Rabitsch, Gregan, & Nasmyth, 2004; Kerrebrock, Moore, Wu, & Orr-Weaver, 1995; Kitajima, Kawashima, & Watanabe, 2004; Kitajima et al., 2006; Riedel et al., 2006). Our findings suggest that premature microtubule-kinetochore interactions disrupt this process, at least in part, by affecting the ability of Sgo1-PP2A to counteract Rec8 phosphorylation (Chapter 2). *CUP-CLB3* cells show increased phosphorylation of Rec8 near centromeres relative to wild-type, albeit not to the same extent as cell depleted of the protective factor Sgo1. Interestingly, the localization of Sgo1-PP2A appears unperturbed under conditions of premature microtubule-kinetochore interactions, suggesting the localization of these factors is not sufficient to promote protection of cohesin from removal at anaphase I onset. As with coorientation defects, the inability to protect centromeric cohesin could arise from (1) the physical occlusion of a cohesin protective factor by microtubule attachment, (2) pulling forces causing a conformational change of the overall structure of the kinetochore or nearby chromatin or (3) by providing centromeric access of an inhibitory factor by way of the microtubule-kinetochore interaction.

The simplest explanation for how microtubules-kinetochore interactions disrupt the protection of centromeric cohesin is by preventing the centromeric association of the protective machinery (Sgo1-PP2A) or other factors implicated in cohesin protection (i.e. Spo13). This does not appear to be the case. Localization of Sgo1, the PP2A subunit Rts1, and Spo13 appear unperturbed in cells prematurely expressing *CLB3* (Chapter 2). It is possible that an unknown factor required for centromeric cohesin protection is occluded from binding to the kinetochore by preexisting microtubule interactions. In fact, the kinetochore components Iml3 and Chl4 are required for protection of centromeric cohesin. Cells lacking these factors do not properly maintain centromeric cohesin at anaphase I onset (Marston, Tham, Shah, & Amon, 2004). Iml3 and Chl4 may serve as docking sites (at the kinetochore) for the loading of protective factors to then spread throughout the pericentromeric region. It is possible that microtubules bound to kinetochores block these factors from loading. Unfortunately, it is not known if such factors exist and what role Iml3 and Chl4 play in protecting centromeric cohesin during meiosis I.

Another key factor in centromeric cohesin maintenance is the meiosis-specific protein Spo13. Cells lacking Spo13 do not maintain centromeric cohesin at anaphase I (B. H. Lee, Kiburz, & Amon, 2004; Shonn, McCarroll, & Murray, 2002). Additionally, overexpression of Spo13 during mitosis leads to the protection of both Rec8 and Scc1 (B. H. Lee et al., 2004; Shonn et al., 2002), suggesting a role in cohesin protection, however, its exact role in this process

during meiosis I is still unclear. Spo13 associates with centromeres to the same extent in wild-type and cells prematurely expressing *CLB3*, suggesting that the lack of cohesin protection is not due to defects in Spo13 localization.

Another possibility is that tension exerted from stable microtubule-kinetochore attachments perturbs the cohesin protective machinery. Two mechanisms have previously been proposed whereby tension modulates the activity of the cohesin protective machinery: (1) tension-dependent deformation of PP2A resulting in inhibition of catalytic activity (Grinthal, Adamovic, Weiner, Karplus, & Kleckner, 2010), and (2) tension-dependent spatial separation of centromeric cohesin from Sgo1-PP2A (J. Lee et al., 2008). However, it is not clear whether the pulling of sister kinetochores could physically separate pericentromeric cohesin from the protective machinery since the protected domain stretches ~50kb (Kiburz et al., 2005). Additionally, as discussed above, tension between sister kinetochores alone cannot explain the defect in centromeric cohesin protection since *mam1Δ* cells maintain centromeric cohesin during anaphase I (Toth et al., 2000). An open question is why the cohesin protective domain is sensitive to microtubule-kinetochore interactions during prophase I, but once it is established, its maintenance is unaffected by these interactions. Examining the factors that differentially associate with centromeres during the establishment phase (prophase I) compared to the maintenance phase (metaphase I) may provide insight into this question.

If tension modulates the cohesin protective machinery, it should be possible to find conditions in which centromeric cohesin is protected when it otherwise should be sensitive to removal. Again, it may be useful to turn to the mitotic cell cycle. Both Sgo1 and PP2A localize to centromeres during mitotic anaphase and, at least Sgo1, is required to sense lack of tension, promote biorientation of sister chromatids and mediate the spindle assembly checkpoint (Indjeian, Stern, & Murray, 2005). When Rec8 is expressed in mitosis, however, centromeric cohesin is not protected. It is possible that additional factors, such as Spo13, are required for maintenance of centromeric cohesin in mitotic anaphase (B. H. Lee et al., 2004; Shonn et al., 2002). An alternative hypothesis is that it is the difference in microtubule-kinetochore attachments during mitosis and meiosis that affects centromeric cohesin maintenance. In budding yeast, microtubules are bound to assembled kinetochores throughout the entire mitotic cell cycle, with the exception of a brief window during S-phase when the kinetochore is disassembled to allow DNA replication through the centromere (Guacci, Hogan, & Koshland, 1997; Jin, Fuchs, & Loidl, 2000; Tanaka et al., 2002; Winey & O'Toole, 2001). In contrast, microtubules are prevented from interacting with kinetochores during meiotic prophase I (Chapter 2). If microtubule-kinetochore interactions are a *bone fide* modulator of the cohesin protective machinery (e.g. Sgo1-PP2A activity), it will be interesting to determine whether modulating microtubule-kinetochore interactions during the mitotic cell cycle will influence the maintenance of centromeric Rec8-containing cohesin.

An alternative possibility is that the microtubule-kinetochore interactions provide a means for an inhibitor of centromeric cohesin maintenance to gain access to the centromeric chromatin. Again, targeting the various Clbs to the centromere may provide insight into this question if it is centromere localized CDK activity that disrupts the proper function of cohesin protection. If this is the case, determining the proteins that are phosphorylated by the different cyclin-CDKs may provide insight into the mechanism by which premature cyclin expression disrupts the cohesin protective machinery (see section below for further discussion).

Finally, it will be important to further investigate the mechanism of cohesin removal in cells prematurely expressing *CLB3*. *CUP-CLB3* cells prematurely remove cohesin from the entire chromosome during meiosis I, resulting in segregation of sister chromatids, however, counterintuitively Rec8 cleavage levels are lower in these cells compared to wild-type (Chapter 2). It is possible that *CUP-CLB3* cells rely more on an alternative cohesin removal pathway, such as the Separase-independent prophase pathway (Losada, Hirano, & Hirano, 2002; Sumara et al., 2002; Yu & Koshland, 2005). To this end, it will be useful to determine to what extent cohesin removal is dependent on Separase in *CUP-CLB3* cells, either using a conditional allele of *ESP1* or a non-cleavable allele of *REC8*.

What is the mechanism and relevance of outer kinetochore disassembly during prophase I?

Our findings demonstrate that restricting microtubule-kinetochore interactions prior to meiosis I is a key determinant of establishing the meiosis I chromosome segregation pattern. Given the importance of preventing premature microtubule-kinetochore interactions to meiosis I chromosome morphogenesis, it is not surprising that cells prevent premature microtubule-kinetochore interactions in two ways. Restriction of cyclin-CDK activity during premeiotic S phase and prophase I appears to be the major mechanism preventing premature microtubule-kinetochore interactions, but our data indicate that regulation of outer kinetochore assembly serves as an additional mechanism to prevent this from occurring.

In budding yeast, two essential components of the outer kinetochore, Ndc80 and Hsk3, are downregulated during prophase I. In *S. pombe*, Ndc80 and its binding partner Nuf2 dissociate from kinetochores in prophase I (Asakawa et al., 2005) raising the possibility that disassembly of the outer kinetochore is a conserved feature of meiotic prophase I. In fission yeast, the dissociation depends on the mating pheromone signaling pathway (Asakawa et al., 2005). It is not clear what the mechanism is by which the outer kinetochore is disassembled in budding yeast. In fact, the regulation of kinetochore assembly/disassembly has not been well studied in budding yeast since the kinetochore is assembled on centromeres for nearly the entire cell cycle. On the other hand, in mammalian cells, the kinetochore composition is dynamic

throughout the cell cycle, with some outer kinetochore components, such as Mis12 and KNL-1, not being recruited to the kinetochore until prophase (Cheeseman, Hori, Fukagawa, & Desai, 2008; Cheeseman et al., 2004).

A number of possibilities exist for the regulation of kinetochore assembly/disassembly during meiotic prophase I. Presumably the kinetochore must disassemble during premeiotic S-phase (as in premitotic S-phase) to allow DNA polymerase to pass through the centromere. It is possible that after the centromere has been replicated during premeiotic S-phase, the outer kinetochore is simply not reassembled, perhaps lacking the activity of a kinetochore assembly promoting factor in prophase I (e.g. cyclin-CDK activity). Alternatively, the outer kinetochore may reassemble after premeiotic S-phase but is then stripped off the inner kinetochore, perhaps by a protein degradation pathway. Another possibility is that in the absence of microtubule-kinetochore interactions, the outer kinetochore components are less stable and cannot remain associated with the inner kinetochore and thus dissociate and are ultimately targeted for degradation.

It will be important to distinguish between these possibilities. First, the stability of the outer kinetochore component Ndc80 should be examined in the presence or absence of microtubule attachments in both mitosis and meiosis. To this end, cells can be arrested in various cell cycle stages and then either treated with a microtubule depolymerizing drug (e.g. nocodazole or benomyl) or shifted to a non-permissive temperature in cells that harbor a conditional outer kinetochore allele (e.g. *dam1-1*). It will also be interesting to examine whether

premeiotic DNA replication is required to remove the outer kinetochore in meiotic prophase I. For these analyses, Ndc80 levels and localization can be examined in prophase I cells that are depleted of the replication factor Cdc6.

Interestingly, it was recently observed that expression of both *CLB3* and *CLB4* stabilize the outer kinetochore component Ndc80 in prophase I arrested cells (Jingxun Chen, personal communication). This stabilization was more dramatic with *CLB3* expression relative to *CLB4* expression. It will be interesting to examine whether the stabilization of Ndc80 in prophase I is due to microtubule attachments or due to increased CDK activity or even the activity of specific CDKs. Additionally, it will be important to determine whether the stabilized pool of Ndc80 is kinetochore bound or unbound.

Our work has shown that Ndc80 and Hsk3 are functionally limiting in late meiotic prophase I, but other outer kinetochore components also appear to be regulated at the level of synthesis (Chapter 2). It will be interesting to determine whether the expression of these other outer kinetochore components also modulates the microtubule-kinetochore interactions that occur upon cyclin misexpression.

The regulation of microtubule-kinetochore interactions appears to be a key factor in establishing the meiosis I chromosome segregation pattern. We propose that the regulated assembly/disassembly of the outer kinetochore is an additional conserved mechanism to prevent these interactions from occurring precociously. Intriguingly, fission yeast cells induced to undergo ectopic meiosis in the absence

of mating pheromone signaling (i.e. in *pat1* mutants) do not disassemble the outer kinetochore during prophase I. These mutants also segregate sister chromatids instead of homologous chromosomes in meiosis I (A. Yamamoto & Hiraoka, 2003; T. G. Yamamoto, Chikashige, Ozoe, Kawamukai, & Hiraoka, 2004). It is tempting to speculate that this change in the pattern of chromosome segregation in *pat1* mutants arises from premature microtubule-kinetochore interactions due to a defect in outer kinetochore disassembly.

Is there cyclin specificity with respect to promoting the biorientation of sister kinetochores?

An open question that remains in the field of cyclin-CDK regulation is why the cell encodes so many cyclins. It is unlikely that cyclin-specific targeting of CDK activity is essential, since each of the cyclins are individually dispensable for both mitosis and meiosis (Dahmann & Futcher, 1995; Grandin & Reed, 1993). However, there are experiments that suggest there is specificity among cyclin targets (Archambault et al., 2004; Cross & Jacobson, 2000; Cross, Yuste-Rojas, Gray, & Jacobson, 1999; Koivomagi et al., 2011; Loog & Morgan, 2005; Ubersax et al., 2003). We found that ectopic expression of *CLB1*, *CLB3*, or *CLB4* is sufficient to promote spindle pole body separation and bipolar spindle formation in prophase I arrested cells, while *CLB5* overexpression did not. This result was not entirely surprising given that Clb5-CDK is normally active during prophase I. Additionally, Clb5 was previously shown to be somewhat unique among the B-type cyclins in that a hydrophobic patch within the protein made it more efficiently

target particular substrates (Cross & Jacobson, 2000; Loog & Morgan, 2005; Ubersax et al., 2003).

However, the expression of *CLB1* and *CLB3*, but not *CLB4*, resulted in microtubule-kinetochore interactions stable enough to exert force and separate sister centromeres. Cyclin levels were expressed to similar levels in each case and these phenotypes did not correlate with in vitro kinase activity (Chapter 2). These results suggest that there exists cyclin specificity with respect to the ability to promote stable microtubule-kinetochore interactions that promote biorientation. This observed cyclin specificity could arise from differential subcellular localization of the various cyclin-CDKs or through inherent substrate specificity of the cyclin CDKs.

It will be interesting to identify the targets that are phosphorylated by the various cyclin CDKs using quantitative mass spectrometry. Preliminary studies comparing wild-type prophase I arrested cells to those expressing *CLB1*, *CLB3*, *CLB4*, *CLB5* or *CLB3 HSK3* and *NDC80* driven from the *CUP1* promoter has shown a number of differentially phosphorylated targets. Further work to optimize the tandem mass tag technique from samples harvested from sporulating cultures will help to increase the sensitivity of such analyses. Expected targets may be kinetochore components, microtubule associated proteins and/or motor proteins. Determining the mechanistic basis for the observed differences in sister kinetochore biorientation may yield insight into the role of cyclin-CDKs in

promoting microtubule-kinetochore attachments and/or the kinetochore assembly/disassembly cycle.

In addition, these analyses may also yield insight into the mechanism by which cyclin-CDK misexpression disrupts proper chromosome segregation in meiosis I. If the mechanism by which chromosome morphogenesis is disrupted in cells with premature microtubule-kinetochore interactions is by providing cyclin-CDK access to the centromere, then we would expect to find differentially phosphorylated factors in both the coorientation and cohesin protective machinery. Thus, these analyses may also offer insight into the role of CDKs in the regulation of the coorientation and cohesin protective machinery.

Conservation

The findings described in this thesis reveal a novel regulatory event that is essential for accurate meiosis I chromosome segregation and demonstrate that temporal restriction of microtubule-kinetochore interactions is instrumental in transforming mitosis into meiosis. Given the importance of preventing premature microtubule-kinetochore engagement to meiosis I chromosome morphogenesis, it is not surprising that cyclin-CDK activity is regulated at multiple levels in budding yeast; transcription of *CLB1, CLB3* and *CLB4* is not activated until cells exit pachytene (Chu & Herskowitz, 1998) and *CLB3* translation is restricted to meiosis II (Carlile & Amon, 2008).

Cyclin-CDK activity is also tightly regulated in other eukaryotes. Metazoan oocytes arrest for an extended period of time in prophase I. Multiple mechanisms keep cyclin-CDK activity low to maintain this arrest (reviewed in Von Stetina & Orr-Weaver, 2011). Similar regulation is observed in *D. melanogaster* and *C. elegans*. Remarkably, inappropriate activation of *Cyclin A* or cyclin E during prophase I in fruit flies and worms, respectively, results in a mitosis-like division (Biedermann et al., 2009; Sugimura & Lilly, 2006). Thus, restricting cyclin-CDK activity during premeiotic S phase and prophase I also appears to be required to establish a meiosis I-specific chromosome architecture in higher eukaryotes.

An additional regulatory mechanism to prevent premature microtubule-kinetochore interactions appears to be through regulation of outer kinetochore assembly. As discussed above, this appears to be a conserved mechanism during meiotic prophase I since in fission yeast, Ndc80 and its binding partner Nuf2 dissociate from kinetochores in prophase I (Asakawa et al., 2005). Interestingly, in mouse oocytes, the Ndc80 complex is recruited to chromosomes only after nuclear envelope breakdown (Sun, Zhang, Lee, Xu, & Kim, 2011), raising the possibility that outer kinetochore assembly is also prevented in meiotic prophase I in vertebrates.

As errors in meiotic chromosome segregation are the leading cause of birth defects and miscarriages in humans (Hassold & Hunt, 2001), further insight into the mechanistic basis by which cells properly orchestrate this process will be of great interest for future investigation. We discovered that the establishment of

a meiosis-specific chromosome segregation pattern depends on the regulation of microtubule-kinetochore interactions. This is accomplished by regulating cyclin-CDK activity as well as assembly of the outer kinetochore. It appears that similar regulatory events may be used across different organisms (Asakawa et al., 2005; Biedermann et al., 2009; Sugimura & Lilly, 2006; Von Stetina & Orr-Weaver, 2011), suggesting that temporal restriction of microtubule-kinetochore interactions is an evolutionarily conserved event required to execute proper meiotic chromosome segregation.

REFERENCES

Archambault, V., Chang, E.J., Drapkin, B.J., Cross, F.R., Chait, B.T., & Rout, M.P. (2004). Targeted proteomic study of the cyclin-Cdk module. *Mol Cell, 14*(6), 699-711. doi: 10.1016/j.molcel.2004.05.025S1097276504003272 [pii]

Asakawa, H., Hayashi, A., Haraguchi, T., & Hiraoka, Y. (2005). Dissociation of the Nuf2-Ndc80 complex releases centromeres from the spindle-pole body during meiotic prophase in fission yeast. *Molecular biology of the cell, 16*(5), 2325-2338. doi: 10.1091/mbc.E04-11-0996

Biedermann, B., Wright, J., Senften, M., Kalchhauser, I., Sarathy, G., Lee, M.H. (2009). Translational repression of cyclin E prevents precocious mitosis and embryonic gene activation during C. elegans meiosis. *Developmental cell, 17*(3), 355-364. doi: 10.1016/j.devcel.2009.08.003

Buonomo, S.B., Clyne, R.K., Fuchs, J., Loidl, J., Uhlmann, F., & Nasmyth, K. (2000). Disjunction of homologous chromosomes in meiosis I depends on proteolytic cleavage of the meiotic cohesin Rec8 by separin. *Cell, 103*(3), 387-398.

Carlile, T.M., & Amon, A. (2008). Meiosis I is established through division-specific translational control of a cyclin. *Cell, 133*(2), 280-291. doi: S0092-8674(08)00283-3 [pii]10.1016/j.cell.2008.02.032

Cheeseman, I.M., Hori, T., Fukagawa, T., & Desai, A. (2008). KNL1 and the CENP-H/I/K complex coordinately direct kinetochore assembly in vertebrates. *Mol Biol Cell, 19*(2), 587-594. doi: E07-10-1051 [pii]10.1091/mbc.E07-10-1051

Cheeseman, I.M., Niessen, S., Anderson, S., Hyndman, F., Yates, J.R., 3rd, Oegema, K. (2004). A conserved protein network controls assembly of the outer kinetochore and its ability to sustain tension. *Genes Dev, 18*(18), 2255-2268. doi: 10.1101/gad.123410418/18/2255 [pii]

Chu, S., & Herskowitz, I. (1998). Gametogenesis in yeast is regulated by a transcriptional cascade dependent on Ndt80. *Molecular cell, 1*(5), 685-696.

Corbett, K.D., & Harrison, S.C. (2012). Molecular architecture of the yeast monopolin complex. *Cell Rep, 1*(6), 583-589. doi: S2211-1247(12)00137-4 [pii]10.1016/j.celrep.2012.05.012

Corbett, K.D., Yip, C.K., Ee, L.S., Walz, T., Amon, A., & Harrison, S.C. (2010). The monopolin complex crosslinks kinetochore components to regulate chromosome-microtubule attachments. *Cell, 142*(4), 556-567. doi: 10.1016/j.cell.2010.07.017

Cross, F.R., & Jacobson, M.D. (2000). Conservation and function of a potential substrate-binding domain in the yeast Clb5 B-type cyclin. *Mol Cell Biol, 20*(13), 4782-4790.

Cross, F.R., Yuste-Rojas, M., Gray, S., & Jacobson, M.D. (1999). Specialization and targeting of B-type cyclins. *Mol Cell, 4*(1), 11-19. doi: S1097-2765(00)80183-5 [pii]

Dahmann, C., & Futcher, B. (1995). Specialization of B-type cyclins for mitosis or meiosis in S. cerevisiae. *Genetics, 140*(3), 957-963.

Gillett, E.S., Espelin, C.W., & Sorger, P.K. (2004). Spindle checkpoint proteins and chromosome-microtubule attachment in budding yeast. *J Cell Biol, 164*(4), 535-546. doi: 10.1083/jcb.200308100jcb.200308100 [pii]

Gonen, S., Akiyoshi, B., Iadanza, M.G., Shi, D., Duggan, N., Biggins, S. (2012). The structure of purified kinetochores reveals multiple microtubule-attachment sites. *Nat Struct Mol Biol, 19*(9), 925-929. doi: 10.1038/nsmb.2358nsmb.2358 [pii]

Grandin, N., & Reed, S.I. (1993). Differential function and expression of Saccharomyces cerevisiae B-type cyclins in mitosis and meiosis. *Molecular and cellular biology, 13*(4), 2113-2125.

Grinthal, A., Adamovic, I., Weiner, B., Karplus, M., & Kleckner, N. (2010). PR65, the HEAT-repeat scaffold of phosphatase PP2A, is an elastic connector that links force and catalysis. *Proc Natl Acad Sci U S A, 107*(6), 2467-2472. doi: 0914073107 [pii]10.1073/pnas.0914073107

Guacci, V., Hogan, E., & Koshland, D. (1997). Centromere position in budding yeast: evidence for anaphase A. *Mol Biol Cell, 8*(6), 957-972.

Gupta, M.L., Jr., Bode, C.J., Georg, G.I., & Himes, R.H. (2003). Understanding tubulin-Taxol interactions: mutations that impart Taxol binding to yeast tubulin. *Proc Natl Acad Sci U S A, 100*(11), 6394-6397. doi: 10.1073/pnas.1131967100 1131967100 [pii]

Hassold, T., & Hunt, P. (2001). To err (meiotically) is human: the genesis of human aneuploidy. *Nature reviews. Genetics, 2*(4), 280-291. doi: 10.1038/35066065

Indjeian, V.B., Stern, B.M., & Murray, A.W. (2005). The centromeric protein Sgo1 is required to sense lack of tension on mitotic chromosomes. *Science, 307*(5706), 130-133. doi: 307/5706/130 [pii]10.1126/science.1101366

Jin, Q.W., Fuchs, J., & Loidl, J. (2000). Centromere clustering is a major determinant of yeast interphase nuclear organization. *J Cell Sci, 113 (Pt 11)*, 1903-1912.

Katis, V.L., Galova, M., Rabitsch, K.P., Gregan, J., & Nasmyth, K. (2004). Maintenance of cohesin at centromeres after meiosis I in budding yeast requires a kinetochore-associated protein related to MEI-S332. *Current biology : CB, 14*(7), 560-572. doi: 10.1016/j.cub.2004.03.001

Kerrebrock, A.W., Moore, D.P., Wu, J.S., & Orr-Weaver, T.L. (1995). Mei-S332, a Drosophila protein required for sister-chromatid cohesion, can localize to meiotic centromere regions. *Cell, 83*(2), 247-256.

Kiburz, B.M., Reynolds, D.B., Megee, P.C., Marston, A.L., Lee, B.H., Lee, T.I. (2005). The core centromere and Sgo1 establish a 50-kb cohesin-protected domain around centromeres during meiosis I. *Genes Dev, 19*(24), 3017-3030. doi: 19/24/3017 [pii]10.1101/gad.1373005

Kitajima, T.S., Kawashima, S.A., & Watanabe, Y. (2004). The conserved kinetochore protein shugoshin protects centromeric cohesion during meiosis. *Nature, 427*(6974), 510-517. doi: 10.1038/nature02312

Kitajima, T.S., Sakuno, T., Ishiguro, K., Iemura, S., Natsume, T., Kawashima, S.A. (2006). Shugoshin collaborates with protein phosphatase 2A to protect cohesin. *Nature, 441*(7089), 46-52. doi: 10.1038/nature04663

Koivomagi, M., Valk, E., Venta, R., Iofik, A., Lepiku, M., Morgan, D.O. (2011). Dynamics of Cdk1 substrate specificity during the cell cycle. *Mol Cell, 42*(5), 610-623. doi: S1097-2765(11)00383-2 [pii]10.1016/j.molcel.2011.05.016

Kosco, K.A., Pearson, C.G., Maddox, P.S., Wang, P.J., Adams, I.R., Salmon, E.D. (2001). Control of microtubule dynamics by Stu2p is essential for spindle orientation and metaphase chromosome alignment in yeast. *Mol Biol Cell, 12*(9), 2870-2880.

Lee, B.H., Kiburz, B.M., & Amon, A. (2004). Spo13 maintains centromeric cohesion and kinetochore coorientation during meiosis I. *Current biology : CB, 14*(24), 2168-2182. doi: 10.1016/j.cub.2004.12.033

Lee, J., Kitajima, T.S., Tanno, Y., Yoshida, K., Morita, T., Miyano, T. (2008). Unified mode of centromeric protection by shugoshin in mammalian oocytes and somatic cells. *Nat Cell Biol, 10*(1), 42-52. doi: ncb1667 [pii]10.1038/ncb1667

Loog, M., & Morgan, D.O. (2005). Cyclin specificity in the phosphorylation of cyclin-dependent kinase substrates. *Nature, 434*(7029), 104-108. doi: 10.1038/nature03329

Losada, A., Hirano, M., & Hirano, T. (2002). Cohesin release is required for sister chromatid resolution, but not for condensin-mediated compaction, at the onset of mitosis. *Genes Dev, 16*(23), 3004-3016. doi: 10.1101/gad.249202

Marston, A.L., & Amon, A. (2004). Meiosis: cell-cycle controls shuffle and deal. *Nature reviews. Molecular cell biology, 5*(12), 983-997. doi: 10.1038/nrm1526

Marston, A.L., Tham, W.H., Shah, H., & Amon, A. (2004). A genome-wide screen identifies genes required for centromeric cohesion. *Science, 303*(5662), 1367-1370. doi: 10.1126/science.1094220

Matos, J., Lipp, J.J., Bogdanova, A., Guillot, S., Okaz, E., Junqueira, M. (2008). Dbf4-dependent CDC7 kinase links DNA replication to the segregation of homologous chromosomes in meiosis I. *Cell, 135*(4), 662-678. doi: 10.1016/j.cell.2008.10.026

Monje-Casas, F., Prabhu, V.R., Lee, B.H., Boselli, M., & Amon, A. (2007). Kinetochore orientation during meiosis is controlled by Aurora B and the monopolin complex. *Cell, 128*(3), 477-490. doi: 10.1016/j.cell.2006.12.040

Pinsky, B.A., Kung, C., Shokat, K.M., & Biggins, S. (2006). The Ipl1-Aurora protein kinase activates the spindle checkpoint by creating unattached kinetochores. *Nat Cell Biol, 8*(1), 78-83. doi: ncb1341 [pii]10.1038/ncb1341

Rabitsch, K.P., Petronczki, M., Javerzat, J.P., Genier, S., Chwalla, B., Schleiffer, A. (2003). Kinetochore recruitment of two nucleolar proteins is required for homolog segregation in meiosis I. *Developmental cell, 4*(4), 535-548.

Riedel, C.G., Katis, V.L., Katou, Y., Mori, S., Itoh, T., Helmhart, W. (2006). Protein phosphatase 2A protects centromeric sister chromatid cohesion during meiosis I. *Nature, 441*(7089), 53-61. doi: 10.1038/nature04664

Shonn, M.A., McCarroll, R., & Murray, A.W. (2002). Spo13 protects meiotic cohesin at centromeres in meiosis I. *Genes Dev, 16*(13), 1659-1671. doi: 10.1101/gad.975802

Sugimura, I., & Lilly, M.A. (2006). Bruno inhibits the expression of mitotic cyclins during the prophase I meiotic arrest of Drosophila oocytes. *Developmental cell, 10*(1), 127-135. doi: 10.1016/j.devcel.2005.10.018

Sumara, I., Vorlaufer, E., Stukenberg, P.T., Kelm, O., Redemann, N., Nigg, E.A. (2002). The dissociation of cohesin from chromosomes in prophase is regulated by Polo-like kinase. *Mol Cell, 9*(3), 515-525. doi: S1097276502004732 [pii]

Sun, S.C., Zhang, D.X., Lee, S.E., Xu, Y.N., & Kim, N.H. (2011). Ndc80 regulates meiotic spindle organization, chromosome alignment, and cell cycle progression in mouse oocytes. *Microscopy and microanalysis : the official journal of Microscopy Society of America, Microbeam Analysis Society, Microscopical Society of Canada, 17*(3), 431-439. doi: 10.1017/S1431927611000274

Tanaka, T.U., Rachidi, N., Janke, C., Pereira, G., Galova, M., Schiebel, E. (2002). Evidence that the Ipl1-Sli15 (Aurora kinase-INCENP) complex promotes chromosome bi-orientation by altering kinetochore-spindle pole connections. *Cell, 108*(3), 317-329. doi: S0092867402006335 [pii]

Toth, A., Rabitsch, K.P., Galova, M., Schleiffer, A., Buonomo, S.B., & Nasmyth, K. (2000). Functional genomics identifies monopolin: a kinetochore protein required for segregation of homologs during meiosis i. *Cell, 103*(7), 1155-1168.

Ubersax, J.A., Woodbury, E.L., Quang, P.N., Paraz, M., Blethrow, J.D., Shah, K. (2003). Targets of the cyclin-dependent kinase Cdk1. *Nature, 425*(6960), 859-864. doi: 10.1038/nature02062nature02062 [pii]

Von Stetina, J.R., & Orr-Weaver, T.L. (2011). Developmental control of oocyte maturation and egg activation in metazoan models. *Cold Spring Harbor perspectives in biology, 3*(10), a005553. doi: 10.1101/cshperspect.a005553

Winey, M., & O'Toole, E.T. (2001). The spindle cycle in budding yeast. *Nat Cell Biol, 3*(1), E23-27. doi: 10.1038/35050663

Yamamoto, A., & Hiraoka, Y. (2003). Monopolar spindle attachment of sister chromatids is ensured by two distinct mechanisms at the first meiotic division in fission yeast. *The EMBO journal, 22*(9), 2284-2296. doi: 10.1093/emboj/cdg222

Yamamoto, T.G., Chikashige, Y., Ozoe, F., Kawamukai, M., & Hiraoka, Y. (2004). Activation of the pheromone-responsive MAP kinase drives haploid cells to undergo ectopic meiosis with normal telomere clustering and sister chromatid segregation in fission yeast. *Journal of cell science, 117*(Pt 17), 3875-3886. doi: 10.1242/jcs.01248

Yu, H.G., & Koshland, D. (2005). Chromosome morphogenesis: condensin-dependent cohesin removal during meiosis. *Cell, 123*(3), 397-407. doi: 10.1016/j.cell.2005.09.014

Appendix A:

Role of Polo-like kinase Cdc5 in Meiosis II

INTRODUCTION

Meiosis is a unique type of cell division in which a single round of DNA replication is followed by two rounds of nuclear division (termed meiosis I and meiosis II). In the first meiotic division, homologous chromosomes segregate to opposite poles while during the second meiotic division, sister chromatids segregate, thus generating haploid gametes (Marston & Amon, 2004). One of the key differences in transforming the mitotic cell division program to properly complete meiosis is the establishment of the specialized meiosis I chromosome segregation pattern. This requires multiple modifications to the chromosome segregation machinery: (1) reciprocal recombination between homologous chromosomes provide the linkage to promote their segregation; (2) kinetochores of sister chromatids attach to microtubules from the same pole; (3) sister-chromatid cohesion is removed from chromosomes arms to allow segregation of homologs, but maintained near centromeres to retain linkages between sister chromatids required for accurate segregation in meiosis II; and (4) microtubule-kinetochore interactions are prevented prior to meiosis I to allow the establishment of a centromeric chromosome architecture that dictates the chromosome segregation pattern in meiosis I. These changes permit the unique meiosis I chromosome segregation pattern and are required for the production of viable gametes.

Along with cyclin-CDK activity, another major regulator of both mitosis and meiosis is the Polo-like kinase (Lee & Amon, 2003a; Nigg, 1998). In mitosis,

Polo-like kinase promotes centrosome duplication and spindle elongation (Lane & Nigg, 1996; Sunkel & Glover, 1988), removal of cohesin from chromosomes (Alexandru, Uhlmann, Mechtler, Poupart, & Nasmyth, 2001; Sumara et al., 2002), activation of the ubiquitin ligase anaphase promoting complex/cyclosome (APC/C) and anaphase onset (Charles et al., 1998; Shirayama, Zachariae, Ciosk, & Nasmyth, 1998), exit from mitosis (Stegmeier, Visintin, & Amon, 2002; Visintin et al., 1998) as well as cytokinesis (Bahler et al., 1998; Carmena et al., 1998; Song & Lee, 2001).

Polo-like kinase is believed to fulfill a similar role in the analogous events during meiosis (Nigg, 1998). In budding yeast, Cdc5 (Polo-like kinase) also plays a large role in establishing the meiosis I chromosome segregation pattern. Cdc5 promotes this unique division is a number of ways: (1) Cdc5 promotes double Holliday junction resolution and exit from the pachytene stage of prophase I (Clyne et al., 2003; Sourirajan & Lichten, 2008); (2) Cdc5 regulates coorientation of sister chromatids by promoting the release of Lrs4 and Csm1 from the nucleolus and assembly of the monopolin complex at kinetochores (Clyne et al., 2003; Lee & Amon, 2003b; Matos et al., 2008); (3) Cdc5 is required for phosphorylation of the cohesin subunit Rec8, and promotes the removal of cohesin from chromosome arms at the onset of anaphase I (Clyne et al., 2003; Lee & Amon, 2003b); and (4) Cdc5 is a component of the Cdc14 early anaphase release (FEAR) network, which is required to promote the release of Cdc14 from

the nucleolus and is required for exit from meiosis I (Buonomo et al., 2003; Lee & Amon, 2003b; Marston, Lee, & Amon, 2003).

The role of Cdc5 in promoting the events that occur in meiosis II has not been investigated in great detail. This appendix will describe experiments aimed at determining whether Cdc5 function is required during meiosis II in budding yeast.

RESULTS

Phosphorylation of some Cdc5 targets is restricted to meiosis I.

Through our work to investigate the mechanisms by which Clb1-CDK activity is restricted to meiosis I, we determined that Clb1 is phosphorylated in a Cdc5-dependent manner and that this phosphorylation occurs only during meiosis I (Chapter 3 and Figure 1). Since this modification did not correlate with Clb1-CDK activity, we speculated that Clb1 phosphorylation might be a readout for Cdc5 activity during meiosis.

We first chose to examine the levels of Cdc5 as cell progress through meiosis. To this end, we tagged Cdc5 with a 13x myc epitope and determined protein levels during a synchronous meiosis, using the previously described *GAL-NDT80* block-release system (Carlile & Amon, 2008). In this system, expression of *NDT80* is controlled by the *GAL1-10* promoter, which is regulated by an estrogen-inducible Gal4-ER fusion (Benjamin, Zhang, Shokat, & Herskowitz, 2003; Carlile & Amon, 2008). We induced *GAL-NDT80 GAL4.ER* cells to

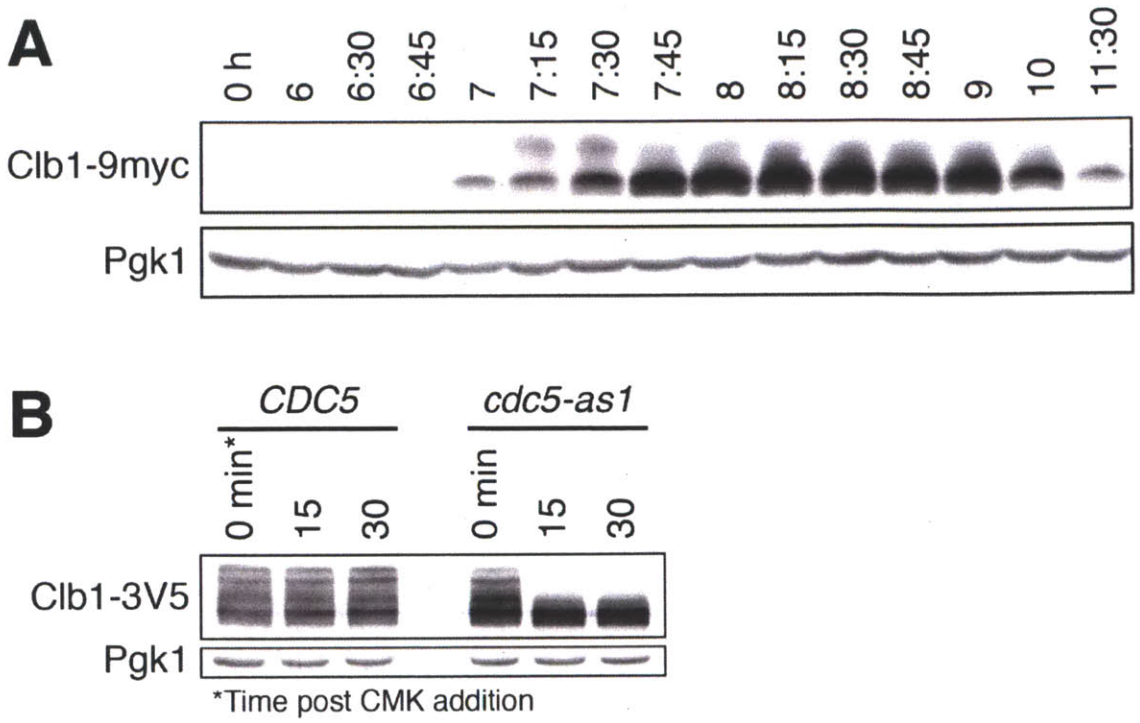

Figure 1. Meiosis I specific phosphorylation of Clb1 is dependent on Cdc5.

(A) Cells carrying the *GAL4-ER*, *GAL-NDT80* and *CLB1-9myc* fusions (A15591) were induced to sporulate. Cells were released from the *NDT80* block at 6h post transfer to sporulation medium. Samples were taken at indicated time points to analyze Clb1-9myc levels and mobility shift by Western blot. Pgk1 was used as a loading control.

(B) Wild-type (A24207) or *cdc5-as1* (A26176) cells carrying the *CLB1-3V5* fusion and also harboring a Cdc20 depletion allele (*cdc20-mn*) were induced to sporulate and arrested in metaphase I due to depletion of Cdc20. 8h after induction of sporulation when the majority of cells had arrested in metaphase I, cells were treated with 5 μM CMK. Samples were taken at indicated time points to analyze Clb1-3V5 levels and mobility shift by Western blot. Pgk1 was used as a loading control.

---

sporulate and subsequently arrest in pachytene of prophase I due to lack of *NDT80* expression. Once the majority of cells had arrested in pachytene, 6h after

sporulation induction, estrogen was added to induce *NDT80* expression and to allow cells to synchronously proceed through the meiotic divisions. We observed that Cdc5 levels are low during the *NDT80* block and increased as cells enter the meiotic divisions (Figure 2A). These results are consistent with *CDC5* being a target of *NDT80* as well as required for many events in meiosis I (Chu et al., 1998; Chu & Herskowitz, 1998). Cdc5 levels increased further as cells entered meiosis II (Figure 2A), suggesting that the decreased Cdc5-dependent phosphorylation of Clb1 in meiosis II is not due to decreased levels of Cdc5.

We next wished to examine the phosphorylation of other known Cdc5 targets using the *NDT80*-block/release system. We chose to examine the mobility shift of Lrs4, the nucleolar protein and component of the monopolin complex, and Nud1, a scaffold protein of the spindle pole body and component of the Mitotic Exit Network (Clyne et al., 2003; Lee & Amon, 2003b; Maekawa, Priest, Lechner, Pereira, & Schiebel, 2007; Park et al., 2008). We observed that Lrs4-13myc showed a hyper-mobility shift as cells entered meiosis I that was largely absent as cells progressed into meiosis II (Figure 2B). This is consistent with phosphorylation promoting the release of Lrs4 from the nucleolus to promote coorientation of sister chromatids, however, the maximum shift was observed just prior to anaphase I onset, a time when coorientation of sister chromatids should have already occurred. These results are also consistent with the notion that Cdc5 activity may be restricted to meiosis I.

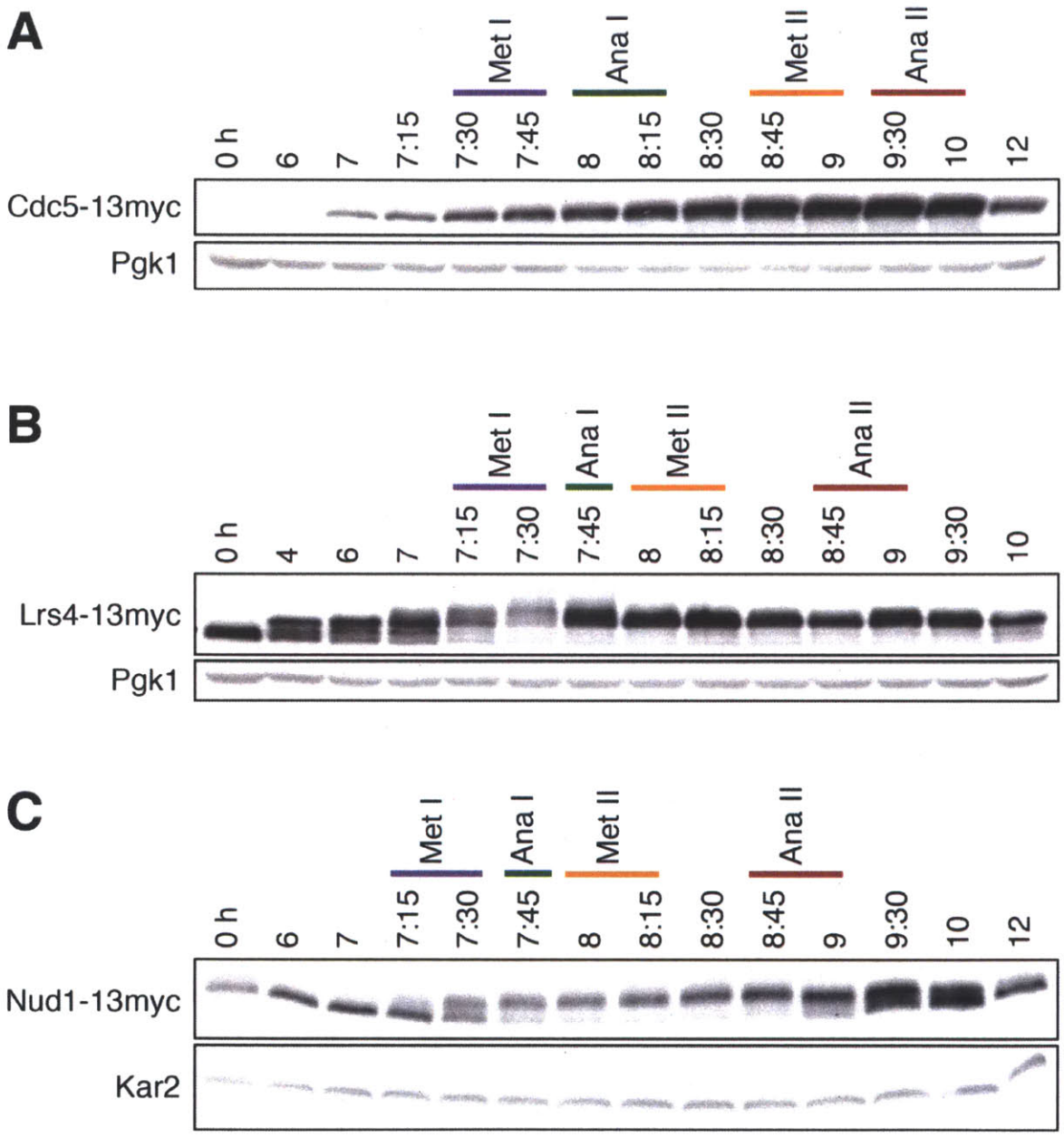

Figure 2. Levels and gel mobility of Cdc5, Lrs4 and Nud1 during synchronous meiosis.

(A) Cells carrying the *GAL4-ER*, *GAL-NDT80* and *CDC5-13myc* fusions (A24758) were induced to sporulate. Cells were released from the *NDT80* block at 6h post transfer to sporulation medium. Samples were taken at indicated time points to analyze Cdc5-13myc levels and mobility shift by Western blot. Pgk1 was used as a loading control.

(B) Cells carrying the *GAL4-ER*, *GAL-NDT80* and *LRS4-13myc* fusions (A24760) were induced to sporulate. Cells were released from the *NDT80* block at 6h post transfer to sporulation medium. Samples were taken at indicated time points to analyze Lrs4-13myc levels and mobility shift by Western blot. Pgk1 was used as a loading control.

(C) Cells carrying the *GAL4-ER*, *GAL-NDT80* and *NUD1-13myc* fusions (A19443) were induced to sporulate. Cells were released from the *NDT80* block at 6h post transfer to sporulation medium. Samples were taken at indicated time points to analyze Nud1-13myc levels and mobility shift by Western blot. Kar2 was used as a loading control.

Nud1-13myc also showed a mobility shift that increased as cells entered the meiotic divisions (Figure 2C). This mobility shift was not restricted to meiosis I and persisted as cells entered meiosis II. In addition to Cdc5, however, CDK and other kinases are known to phosphorylate Nud1 confounding the interpretation of these results. The nature of the observed mobility shifts of Lrs4-13myc and Nud1-13myc will need to be further examined, however, these results raise the possibility that Cdc5 activity is restricted to meiosis I.

Cdc5 activity is required for meiosis I but not meiosis II.

To address whether the activity of Cdc5 is required during meiosis II, we utilized the analog sensitive allele *cdc5-as1* to inhibit Cdc5 activity at different times during meiotic progression. Using the *NDT80* block system, wild-type or *cdc5-as1* cells were induced to sporulate and synchronously progress through

the meiotic divisions. After cells had arrested in the *NDT80* block, 6h after sporulation induction, cells were released to undergo the meiotic divisions. At 7h, 7:45h or 8h after sporulation induction cells were either treated with 5 μM CMK or DMSO (Figure 3). Under these conditions, 7h corresponded to a time point just prior to entry into metaphase I, while 7:45 and 8h corresponded to time points just prior to or during metaphase II. Thus, *cdc5-as1* activity was inhibited during either meiosis I or during meiosis II. Wild-type cells treated with either DMSO or 5 μM CMK progressed through both meiotic divisions with very similar kinetics (Figure 3 and Figure 4). Cells carrying the *cdc5-as1* allele also progressed through both meiotic divisions when treated with DMSO, albeit with slightly delayed kinetics relative to wild-type (Figure 4). These results suggest that the *cdc5-as1* allele is hypomorphic.

Interestingly, *cdc5-as1* cells treated with 5 μM CMK prior to metaphase I (7h) arrested in metaphase I consistent with phenotypes observed in meiotic depletions of *CDC5* (Clyne et al., 2003; Lee & Amon, 2003b). In contrast, *cdc5-as1* cells treated with 5 μM CMK just prior to or during metaphase II did not arrest during meiosis II, and in fact, completed both meiotic divisions with kinetics similar to the DMSO treated control (Figure 4). These results suggest that Cdc5 activity is not required to remove centromeric cohesin during meiosis II or for exit from meiosis II. However, Cdc5 activity may be required for spore wall formation as *cdc5-as1* cells treated with 5 μM CMK did not produce spores (data not shown). More detailed analyses, including execution point studies with greater

temporal resolution, will be required to determine the exact stages of meiosis that require Cdc5 activity.

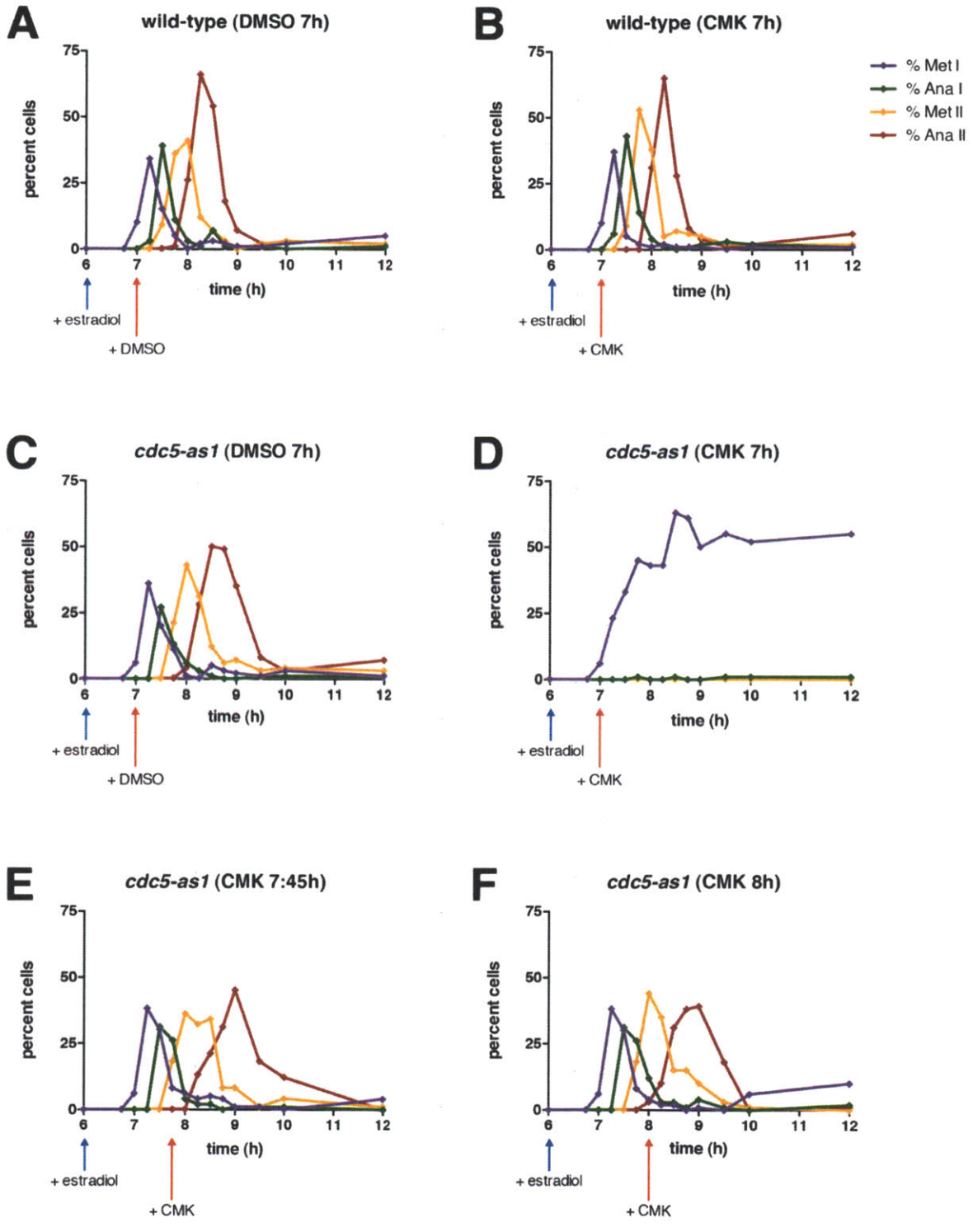

Figure 3. Cdc5 activity required for metaphase I-anaphase I transition but not for meiosis II.

For **(A)** and **(B)**: Cells carrying the *GAL4-ER* and *GAL-NDT80* fusions in addition to a wild-type *CDC5* allele (A14201) were induced to sporulate. Cells were released from the *NDT80* block at 6h post transfer to sporulation medium by addition of estradiol. Cells were treated with DMSO **(A)** or 5 μM CMK **(B)** at 7h post sporulation induction.

For **(C)**-**(F)**: Cells carrying the *GAL4-ER* and *GAL-NDT80* fusions in addition to an analog sensitive *cdc5-as1* allele (A24899) were induced to sporulate. Cells were released from the *NDT80* block at 6h post transfer to sporulation medium by addition of estradiol. Cells were treated with DMSO **(C)** or 5 μM CMK **(D)** at 7h post sporulation induction or with 5 μM CMK at 7:45h **(E)** or 8h **(F)** post sporulation induction.

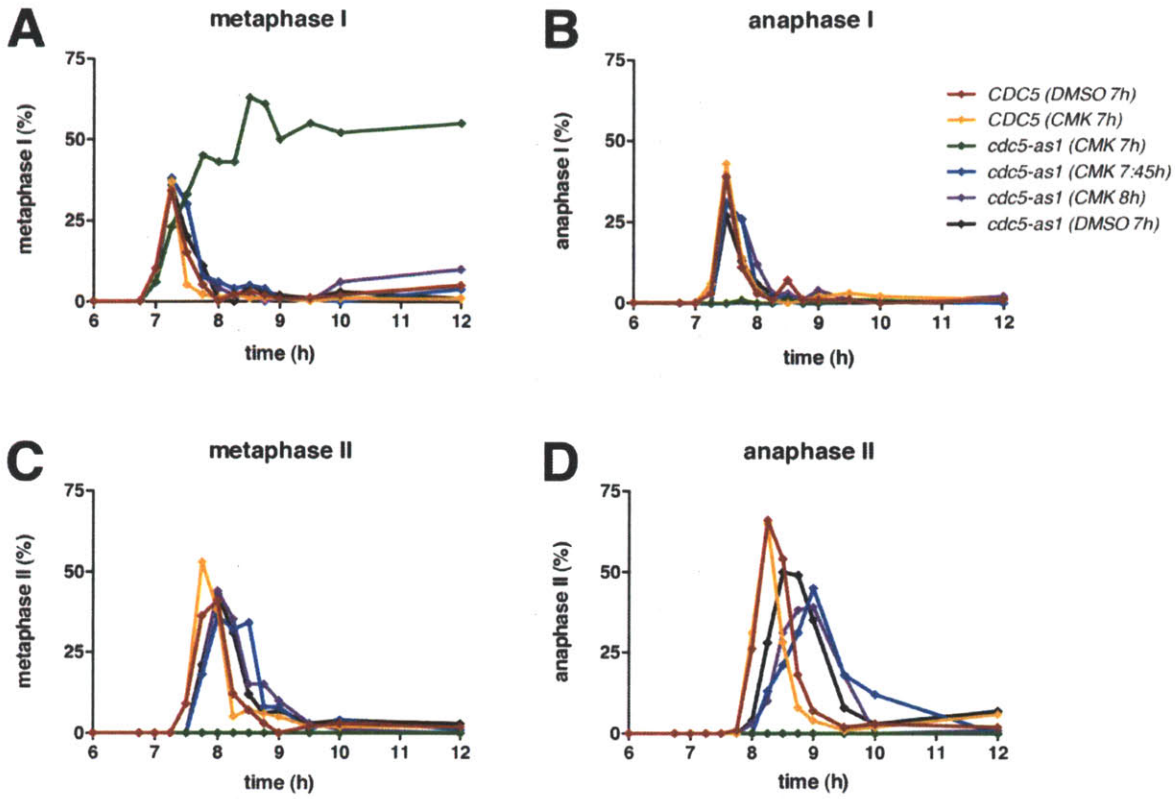

Figure 4. Cdc5 activity required for metaphase I-anaphase I transition but not for meiosis II.

Percent cells with metaphase I **(A)**, anaphase I **(B)**, metaphase II **(C)**, or anaphase II **(D)** spindles plotted for strains and experiment described in Figure 3.

DISCUSSION

The role of Cdc5 in promoting the meiosis I chromosome segregation pattern has been well established, however, its role in promoting analogous events in meiosis II has not been examined in great detail. This is largely due to a lack of tools to specifically inhibit Cdc5 activity in meiosis II. The use of the *cdc5-as1* allele in combination with the *NDT80* block system provides an experimental system to examine these questions.

Cdc5 activity plays a number of roles in promoting meiosis I chromosome segregation. Double Holliday junction resolution as well as coorientation of sister chromatids both depend on Cdc5 function. These events are specific to meiosis I, however, and as such, there is not an analogous event in meiosis II. In contrast, cohesin removal and exit from meiosis I, both require Cdc5 function and the role of Cdc5 in regulating the analogous events in meiosis II is not clear. Our results suggest that both centromeric cohesin removal at anaphase II onset and exit from meiosis II occur independent of Cdc5 activity.

During anaphase I onset, Cdc5 it is absolutely required for cleavage of Rec8 (Clyne et al., 2003; Lee & Amon, 2003b). Phosphorylation of Rec8 is also required as the expression of an allele of Rec8, in which 29 in vivo phosphorylated residues are mutated to the nonphosphorylatable residue alanine (*rec8-29A*), results in a large metaphase I delay (Brar, Hochwagen, Ee, & Amon, 2009). The finding that an allele of Rec8 in which four phosphorylated residues are mutated to the phosphomimetic aspartic acid (*rec8-4D*) leads to premature

cohesin removal in meiosis I, suggests that phosphorylation of Rec8 results in improving Rec8 as a substrate for Separase (Katis et al., 2010). However, cohesin is also thought to be removed by a Separase-independent pathway in prophase I, and the role of this pathway in removing cohesin during the meiotic divisions is not well defined (Yu & Koshland, 2005). The fact that Cdc5 activity does not appear to be required for removal of cohesin at anaphase II onset is consistent with observations that *rec8-29A spo11Δ* cells (which bypass the requirement for cohesin removal in meiosis I due to lack of crossovers) do not show a metaphase II arrest (Brar et al., 2006). Further work will be required to fully understand the role of Cdc5 in cohesin removal during meiosis I and II, however, it appears that these processes occur by different mechanisms.

Exit from meiosis I requires the release of Cdc14 from the nucleolus and is governed by Cdc5 through its role in the Cdc14 early anaphase release (FEAR) network (Buonomo et al., 2003; Lee & Amon, 2003b; Marston et al., 2003). A different pathway that promotes Cdc14 release and is required for exit from mitosis (mitotic exit network or MEN), also requires Cdc5 activity (Shou et al., 1999; Visintin et al., 1998; Visintin, Hwang, & Amon, 1999). This pathway plays a role in spindle disassembly during meiosis II but is not required for exit from meiosis I (Attner & Amon, 2012). The fact that Cdc5 activity is dispensable for exit from meiosis II, raises the possibility that both FEAR and MEN activity are not required for exit from meiosis II. How the cell coordinates nuclear division with downregulation of cyclin-CDK activity to exit from meiosis II remains to be

determined, however, it appears that the major cell cycle regulator, Cdc5, is not required for this process.

MATERIAL AND METHODS

Strains and plasmids

Strains used in this chapter are described in Table 1 and are derivatives of SK1. *GAL-NDT80* and *GAL4.ER* constructs are described in (Benjamin et al., 2003). Strains were constructed by PCR-based methods described in (Longtine et al., 1998). 3V5 tagging plasmids were provided by Vincent Guacci.

Sporulation conditions

Strains were grown to saturation in YPD at room temperature, diluted in BYTA (1% yeast extract, 2% tryptone, 1% potassium acetate, 50mM potassium phthalate) to OD_{600} = 0.25, and grown overnight at 30°C. Cells were resuspended in sporulation medium (0.3% potassium acetate [pH 7], 0.02% raffinose) to OD_{600} = 1.85 and sporulated at 30°C unless otherwise indicated. *GAL-NDT80 GAL4.ER* strains were released from the *NDT80* block by the addition of 1 μM β-estradiol (5 mM stock in ethanol, Sigma E2758-1G) at 6hr unless otherwise indicated.

Indirect immunofluorescence

Indirect immunofluorescence was performed as described in (Kilmartin & Adams, 1984). Spindle morphologies were classified as follows: Metaphase I were defined as a short, bipolar spindle spanning a single DAPI mass. Anaphase I

spindles were defined as an elongated spindle spanning two distinct DAPI masses. Metaphase II spindles were defined as two short, bipolar spindles, each spanning a DAPI mass. Anaphase II spindles were defined as two elongated spindles, each spanning two distinct DAPI masses (four DAPI masses total).

Western blot analysis

For immunoblot analysis, ~10 OD_{600} units of cells were harvested and treated with 5% trichloroacetic acid for at least 10min at 4°C. The acid was washed away with acetone and the cell pellet was subsequently dried. The cell pellet was pulverized with glass beads in 100µL of lysis buffer (50mM Tris-Cl at pH 7.5, 1mM EDTA, 2.75mM DTT, complete protease inhibitor cocktail [Roche]) using a bead-beater (Biospec Products, Inc. Bartlesville, OK). 3X SDS Sample buffer was added and the cell homogenates were boiled. Standard procedures for sodium dodecyl sulfate-polyacrylamide gel electrophoresis (SDS-PAGE) and Western blotting were followed (Burnette, 1981; Laemmli, 1970; Towbin, Staehelin, & Gordon, 1979). A nitrocellulose membrane (VWR) was used to transfer proteins from polyacrylamide gels. Antibody dilutions are described in the Antibody section.

Antibodies

Indirect immunofluorescence

Spindle morphology was determined using a rat anti-tubulin antibody (Oxford Biotechnology) used at a dilution of 1:100, and anti-rat FITC antibodies (Jackson) used at a dilution of 1:100-200.

Western blotting

Clb1-9myc, Cdc5-13myc, Lrs4-13myc and Nud1-13myc were detected using a mouse anti-Myc antibody (Covance) at a 1:500 dilution. Clb1-3V5 was detected using a mouse anti-V5 antibody (Invitrogen) at a 1:2000 dilution. Pgk1 was detected using a mouse anti-Pgk1 antibody (Molecular Probes) at a 1:10000 dilution. Kar2 was detected using a rabbit anti-Kar2 antibody (kindly provided by Mark Rose) at a 1:200,000 dilution. The secondary antibodies used were a sheep anti-mouse antibody conjugated to horseradish peroxidase (HRP) (GE Biosciences) at a 1:5000 dilution or a donkey anti-rabbit antibody conjugated to HRP (GE Biosciences) at a 1:5000 dilution. Antibodies were detected using the SuperSignal West Pico Chemiluminescent Substrate (Thermo Scientific).

STRAINS USED

Table 1. Strains used in this appendix.

strain	Relevant Genotype
SK1 (diploid)	*MATa/MATalpha ho::LYS2/ho::LYS2 lys2/lys2 ura3/ura3 leu2::hisG/leu2::hisG his3::hisG/his3::hisG trp1::hisG/trp1::hisG*
A14201	*MATa/alpha GAL-NDT80::TRP1/GAL-NDT80::TRP1 ura3::pGPD1-GAL4(848).ER::URA3/ura3::pGPD1-GAL4(848).ER::URA3*
A15591	*MATa/alpha GAL-NDT80::TRP1/GAL-NDT80::TRP1 ura3::pGPD1-GAL4(848).ER::URA3/ura3::pGPD1-GAL4(848).ER::URA3 CLB1-9Myc::TRP1*
A19443	*MATa/alpha GAL-NDT80::TRP1/GAL-NDT80::TRP1 ura3::pGPD1-GAL4(848).ER::URA3/ura3::pGPD1-GAL4(848).ER::URA3 NUD1-13MYC:KanMX6/NUD1-13MYC:KanMX6*
A24207	*MATa/alpha cdc20::pCLB2-CDC20::KanMX6/cdc20::pCLB2-CDC20::KanMX6 Clb1-3V5:KanMX/Clb1-3V5:KanMX*
A24758	*MATa/alpha GAL-NDT80::TRP1/GAL-NDT80::TRP1 ura3::pGPD1-GAL4(848).ER::URA3/ura3::pGPD1-GAL4(848).ER::URA3 cdc5::CDC5-13MYC::kanMX6/cdc5::CDC5-13MYC::kanMX6*
A24760	*MATa/alpha GAL-NDT80::TRP1/GAL-NDT80::TRP1 ura3::pGPD1-GAL4(848).ER::URA3/ura3::pGPD1-GAL4(848).ER::URA3 LRS4-13MYC::KanMX6/LRS4-13MYC::KanMX6*
A24899	*MATa/alpha GAL-NDT80::TRP1/GAL-NDT80::TRP1 ura3::pGPD1-GAL4(848).ER::URA3/ura3::pGPD1-GAL4(848).ER::URA3 cdc5-as1(cdc5L158G)/cdc5-as1(cdc5L158G)*
A26176	*MATa/alpha cdc20::pCLB2-CDC20::KanMX6/cdc20::pCLB2-CDC20::KanMX6 cdc5-as1(cdc5L158G)/cdc5-as1(cdc5L158G) Clb1-3V5:KanMX/Clb1-3V5:KanMX*

REFERENCES

Alexandru, G., Uhlmann, F., Mechtler, K., Poupart, M.A., & Nasmyth, K. (2001). Phosphorylation of the cohesin subunit Scc1 by Polo/Cdc5 kinase regulates sister chromatid separation in yeast. *Cell, 105*(4), 459-472. doi: S0092-8674(01)00362-2 [pii]

Attner, M.A., & Amon, A. (2012). Control of the mitotic exit network during meiosis. *Mol Biol Cell, 23*(16), 3122-3132. doi: 10.1091/mbc.E12-03-0235mbc.E12-03-0235 [pii]

Bahler, J., Steever, A.B., Wheatley, S., Wang, Y., Pringle, J.R., Gould, K.L. (1998). Role of polo kinase and Mid1p in determining the site of cell division in fission yeast. *J Cell Biol, 143*(6), 1603-1616.

Benjamin, K.R., Zhang, C., Shokat, K.M., & Herskowitz, I. (2003). Control of landmark events in meiosis by the CDK Cdc28 and the meiosis-specific kinase Ime2. *Genes & development, 17*(12), 1524-1539. doi: 10.1101/gad.1101503

Brar, G.A., Hochwagen, A., Ee, L.S., & Amon, A. (2009). The multiple roles of cohesin in meiotic chromosome morphogenesis and pairing. *Molecular biology of the cell, 20*(3), 1030-1047. doi: 10.1091/mbc.E08-06-0637

Brar, G.A., Kiburz, B.M., Zhang, Y., Kim, J.E., White, F., & Amon, A. (2006). Rec8 phosphorylation and recombination promote the step-wise loss of cohesins in meiosis. *Nature, 441*(7092), 532-536. doi: 10.1038/nature04794

Buonomo, S.B., Rabitsch, K.P., Fuchs, J., Gruber, S., Sullivan, M., Uhlmann, F. (2003). Division of the nucleolus and its release of CDC14 during anaphase of meiosis I depends on separase, SPO12, and SLK19. *Dev Cell, 4*(5), 727-739. doi: S1534580703001291 [pii]

Burnette, W.N. (1981). "Western blotting": electrophoretic transfer of proteins from sodium dodecyl sulfate--polyacrylamide gels to unmodified nitrocellulose and radiographic detection with antibody and radioiodinated protein A. *Analytical biochemistry, 112*(2), 195-203.

Carlile, T.M., & Amon, A. (2008). Meiosis I is established through division-specific translational control of a cyclin. *Cell, 133*(2), 280-291. doi: S0092-8674(08)00283-3 [pii]10.1016/j.cell.2008.02.032

Carmena, M., Riparbelli, M.G., Minestrini, G., Tavares, A.M., Adams, R., Callaini, G. (1998). Drosophila polo kinase is required for cytokinesis. *J Cell Biol, 143*(3), 659-671.

Charles, J.F., Jaspersen, S.L., Tinker-Kulberg, R.L., Hwang, L., Szidon, A., & Morgan, D.O. (1998). The Polo-related kinase Cdc5 activates and is destroyed by the mitotic cyclin destruction machinery in S. cerevisiae. *Curr Biol, 8*(9), 497-507. doi: S0960-9822(98)70201-5 [pii]

Chu, S., DeRisi, J., Eisen, M., Mulholland, J., Botstein, D., Brown, P.O. (1998). The transcriptional program of sporulation in budding yeast. *Science, 282*(5389), 699-705.

Chu, S., & Herskowitz, I. (1998). Gametogenesis in yeast is regulated by a transcriptional cascade dependent on Ndt80. *Molecular cell, 1*(5), 685-696.

Clyne, R.K., Katis, V.L., Jessop, L., Benjamin, K.R., Herskowitz, I., Lichten, M. (2003). Polo-like kinase Cdc5 promotes chiasmata formation and cosegregation of sister centromeres at meiosis I. *Nature cell biology, 5*(5), 480-485. doi: 10.1038/ncb977

Katis, V.L., Lipp, J.J., Imre, R., Bogdanova, A., Okaz, E., Habermann, B. (2010). Rec8 phosphorylation by casein kinase 1 and Cdc7-Dbf4 kinase regulates cohesin cleavage by separase during meiosis. *Developmental cell, 18*(3), 397-409. doi: 10.1016/j.devcel.2010.01.014

Kilmartin, J.V., & Adams, A.E. (1984). Structural rearrangements of tubulin and actin during the cell cycle of the yeast Saccharomyces. *The Journal of cell biology, 98*(3), 922-933.

Laemmli, U.K. (1970). Cleavage of structural proteins during the assembly of the head of bacteriophage T4. *Nature, 227*(5259), 680-685.

Lane, H.A., & Nigg, E.A. (1996). Antibody microinjection reveals an essential role for human polo-like kinase 1 (Plk1) in the functional maturation of mitotic centrosomes. *J Cell Biol, 135*(6 Pt 2), 1701-1713.

Lee, B.H., & Amon, A. (2003a). Polo kinase--meiotic cell cycle coordinator. *Cell Cycle, 2*(5), 400-402. doi: 475 [pii]

Lee, B.H., & Amon, A. (2003b). Role of Polo-like kinase CDC5 in programming meiosis I chromosome segregation. *Science, 300*(5618), 482-486. doi: 10.1126/science.10818461081846 [pii]

Longtine, M.S., McKenzie, A., 3rd, Demarini, D.J., Shah, N.G., Wach, A., Brachat, A. (1998). Additional modules for versatile and economical PCR-based gene deletion and modification in Saccharomyces cerevisiae. *Yeast, 14*(10), 953-961. doi: 10.1002/(SICI)1097-0061(199807)14:10<953::AID-YEA293>3.0.CO;2-U

Maekawa, H., Priest, C., Lechner, J., Pereira, G., & Schiebel, E. (2007). The yeast centrosome translates the positional information of the anaphase spindle into a cell cycle signal. *J Cell Biol, 179*(3), 423-436. doi: jcb.200705197 [pii]10.1083/jcb.200705197

Marston, A.L., & Amon, A. (2004). Meiosis: cell-cycle controls shuffle and deal. *Nature reviews. Molecular cell biology, 5*(12), 983-997. doi: 10.1038/nrm1526

Marston, A.L., Lee, B.H., & Amon, A. (2003). The Cdc14 phosphatase and the FEAR network control meiotic spindle disassembly and chromosome segregation. *Dev Cell, 4*(5), 711-726. doi: S1534580703001308 [pii]

Matos, J., Lipp, J.J., Bogdanova, A., Guillot, S., Okaz, E., Junqueira, M. (2008). Dbf4-dependent CDC7 kinase links DNA replication to the segregation of homologous chromosomes in meiosis I. *Cell, 135*(4), 662-678. doi: 10.1016/j.cell.2008.10.026

Nigg, E.A. (1998). Polo-like kinases: positive regulators of cell division from start to finish. *Curr Opin Cell Biol, 10*(6), 776-783. doi: S0955-0674(98)80121-X [pii]

Park, C.J., Park, J.E., Karpova, T.S., Soung, N.K., Yu, L.R., Song, S. (2008). Requirement for the budding yeast polo kinase Cdc5 in proper microtubule growth and dynamics. *Eukaryot Cell, 7*(3), 444-453. doi: EC.00283-07 [pii]10.1128/EC.00283-07

Shirayama, M., Zachariae, W., Ciosk, R., & Nasmyth, K. (1998). The Polo-like kinase Cdc5p and the WD-repeat protein Cdc20p/fizzy are regulators and substrates of the anaphase promoting complex in Saccharomyces cerevisiae. *EMBO J, 17*(5), 1336-1349. doi: 10.1093/emboj/17.5.1336

Shou, W., Seol, J.H., Shevchenko, A., Baskerville, C., Moazed, D., Chen, Z.W. (1999). Exit from mitosis is triggered by Tem1-dependent release of the protein phosphatase Cdc14 from nucleolar RENT complex. *Cell, 97*(2), 233-244. doi: S0092-8674(00)80733-3 [pii]

Song, S., & Lee, K.S. (2001). A novel function of Saccharomyces cerevisiae CDC5 in cytokinesis. *J Cell Biol, 152*(3), 451-469.

Sourirajan, A., & Lichten, M. (2008). Polo-like kinase Cdc5 drives exit from pachytene during budding yeast meiosis. *Genes Dev, 22*(19), 2627-2632. doi: 22/19/2627 [pii]10.1101/gad.1711408

Stegmeier, F., Visintin, R., & Amon, A. (2002). Separase, polo kinase, the kinetochore protein Slk19, and Spo12 function in a network that controls Cdc14 localization during early anaphase. *Cell, 108*(2), 207-220. doi: S0092867402006189 [pii]

Sumara, I., Vorlaufer, E., Stukenberg, P.T., Kelm, O., Redemann, N., Nigg, E.A. (2002). The dissociation of cohesin from chromosomes in prophase is regulated by Polo-like kinase. *Mol Cell, 9*(3), 515-525. doi: S1097276502004732 [pii]

Sunkel, C.E., & Glover, D.M. (1988). polo, a mitotic mutant of Drosophila displaying abnormal spindle poles. *J Cell Sci, 89 (Pt 1)*, 25-38.

Towbin, H., Staehelin, T., & Gordon, J. (1979). Electrophoretic transfer of proteins from polyacrylamide gels to nitrocellulose sheets: procedure and some applications. *Proceedings of the National Academy of Sciences of the United States of America, 76*(9), 4350-4354.

Visintin, R., Craig, K., Hwang, E.S., Prinz, S., Tyers, M., & Amon, A. (1998). The phosphatase Cdc14 triggers mitotic exit by reversal of Cdk-dependent phosphorylation. *Mol Cell, 2*(6), 709-718. doi: S1097-2765(00)80286-5 [pii]

Visintin, R., Hwang, E.S., & Amon, A. (1999). Cfi1 prevents premature exit from mitosis by anchoring Cdc14 phosphatase in the nucleolus. *Nature, 398*(6730), 818-823. doi: 10.1038/19775

Yu, H.G., & Koshland, D. (2005). Chromosome morphogenesis: condensin-dependent cohesin removal during meiosis. *Cell, 123*(3), 397-407. doi: 10.1016/j.cell.2005.09.014